INORGANIC SYNTHESIS

A Manual for Laboratory Experiments

NIKOLAY GERASIMCHUK

SERGIY TYUKHTENKO

Inorganic Synthesis

Inorganic Synthesis:

A Manual for Laboratory Experiments

By

Nikolay Gerasimchuk
and Sergiy Tyukhtenko

CONTENTS

PREFACE

This laboratory manual originated from eighteen years of teaching the class *Inorganic Preparations,* which follows the *Descriptive Inorganic Chemistry* course in the Inorganic Chemistry curriculum of Missouri State University (USA). Both courses are designed for chemistry majors. They represent a logical progression and harmonic combination of theoretical background in the discipline at first, with enhancement and retention of gained knowledge during following experimental laboratory work. This course is designed for lab sessions of four hours each.

The book provides an extensive and necessary introduction for students to typical glassware and lab equipment (labware) which are normally used in the synthetic chemistry laboratory. This introduction is followed by a brief description of the main laboratory procedures and operations that are essential for safe and productive laboratory work. These were limited to: filtration, extraction, distillation and reflux, work with vacuum, anaerobic/moisture free procedures, flash column and preparative thin-layer chromatography, and products recovery from solutions. In this context it is very important to note that *this laboratory manual is neither intended to promote or advertise any of the equipment brands and their manufacturers, nor it is intended to show off, or brag about the laboratory capabilities that exist at the authors' institutions!* In fact, the glassware, apparatuses and equipment used in this book fit very well into the average teaching and research facilities typical of numerous institutions of higher education around the world. Moreover, during the description of laboratory glassware, hardware and laboratory methods at the beginning of this manual, special attention is drawn to inexpensive alternative solutions when building equipment for common procedures, as well as to cost-saving lab techniques.

All preparative experiments are designed for the synthesis of grams' quantities of compounds. This ensures students' satisfaction with the whole process of the synthesis, work-up procedures and post-lab handling of substances, many of which will be further studied. This manual is heavily illustrated with 224 figures, 12 schemes and 20 tables, to aid students in carrying out all experiments and to help them learn laboratory

techniques. The main purpose of such an illustrative approach is to go in step with a new and younger generation of *visual learners,* who, in the digital age of the internet and mobile devises, truly value the old sentiment that 'a picture is better than a thousand words'. Almost all illustrative material was produced by the authors, taking photographs from actual lab equipment and setups, or making drawings using freely available software.

Before the description of many experiments and characterizations of the obtained compounds, there are brief and condensed sections of theoretical background information. These allow the reader to get familiar with the topic that follows. Thus, the following physical methods and techniques are presented in these short introductory sections:

- thermal analysis,
- X-ray diffraction methods,
- molecular weight determination - cryoscopic measurements,
- cyclic voltammetry measurements in solutions,
- solutions electrical conductivity measurements,
- magnetochemistry in solid state and in solution,
- spectroscopy (vibrational, electronic, ^{1}H and ^{13}C NMR).

The concept of indirect learning has been used by authors for many years. In our academic settings, that means splitting a class of students into two equal groups, both of which conduct the same kind of experimental preparations, but use different compounds and some alternative work-up and samples handling details. There are laboratory exercises with extensions A, B, or C. Being in the same laboratory for four hours, students, in an indirect way, learn what their peers in the other group are working on. All experiments are presented in clear, step-by-step fashion to help students to carry out particular syntheses, conduct important procedures, and accomplish necessary measurements. All sections in the book are supplied with appropriate literature references for the reader interested in further learning.

During the course of these lab experiments, suitable single crystals of several compounds were grown by students, and subsequently characterized using the X-ray analysis. The main results of this work are presented and discussed in this manual, with all CIFs for five determined structures deposited into the Cambridge Crystallographic Data Center (CCDC).

Therefore, a combination of specially selected series' of experiments, with alternative lab work, accompanied with paragraphs of short and

concise theoretical background, and detailed examples of calculations, make this book truly unique in the modern academic environment. This book also can be a useful reference for other synthetic chemists not limited to the inorganic/coordination chemistry field, who will be interested in the *interpretation* of vibrational, electronic, and - more importantly – 1D and 2D NMR spectra.

      In summary, according to numerous students' feedback and evaluations, it is engaging, very intense, and yet likeable, and is considered to be a useful class. It has been a popular laboratory course, with 120+ chemistry majors who have enjoyed taking it, thus far.

ACKNOWLEDGMENTS

INTRODUCTION

This laboratory course is designed to develop important practical skills for chemistry majors interested in synthetic chemistry overall, not just inorganic chemistry. Students will learn proper techniques for preparation and handling of a variety of inorganic and coordination compounds. Thus, students will conduct:

- thermal decomposition reactions,
- preparation of moderately air-sensitive compounds,
- multistep synthesis/composition reactions,
- preparation and handling of moisture-sensitive compounds,
- synthesis, isolation and purification of coordination compounds,
- characterization of the obtained metal complexes using a variety of commonly available physical methods.

This course is structured in the following way:

I) The first part, which is reflected in experiments **1** – **4**, contains preparations of typical inorganic compounds with all relevant experimental details. Characterization of these compounds includes application of thermal analysis.

II) The second part, consisting of experiments **5** – **13**, comprises the synthesis and isolation of the two specially selected coordination compounds of kinetically inert transition trivalent metal ions – Cr and Co. These complexes' purification and subsequent characterization, using several spectroscopic and physical methods such as UV-visible, IR, and NMR (^{1}H, ^{13}C) spectroscopy, solutions electrical conductivity, and magnetochemistry (the Evans method for solutions and the Gouy method for solid samples), takes considerable laboratory time and effort.

Both these metal centers are selected for the following reasons:

1. Co(III) complexes are intensely colored, neutral and diamagnetic, which makes them suitable for extensive studies by the NMR method, along with conventional spectroscopic methods.
2. Cr(III) complex is also colored, but represents an anionic paramagnetic compound which brings to its characterization other techniques: solutions' electrical conductivity and magnetism.

Therefore, investigations of both complexes invoke complimentary physical methods that are often used in synthetic inorganic chemistry.

Overall, the number of synthesized or studied compounds is not large – only eleven compounds: Cu_2O, $FeSO_4\cdot 7H_2O$, PbSe, PbTe, $CdCO_3$, $NiCl_2$, $CoCl_2$, $SnCl_2$ including two neutral Co(III) isomeric complexes and one anionic Cr(III) complex. Two other simple inorganic compounds ($KMnO_4$ and $Mn(NO_3)_2\cdot xH_2O$), were investigated using their thermal transformations. However, for a one-semester laboratory course in preparative chemistry, it is completely sufficient, counting the time spent on chromatographic purification, obtaining what is necessary for the characterization of different spectra, thermogramms, volammogramms, and powder XRD patterns.

One of the most important components of this laboratory course is not only recording, but also *interpreting,* spectra of synthesized coordination compounds. Thus, interpretation of traditional IR- and electronic spectra of complexes of Co(III) and Cr(III) is entirely delegated to students provided with respective literature citations. However, the interpretation of the NMR spectra of seemingly simple Co-complexes *was not trivial* at all. It is presented in the laboratory manual in necessary detail for educational and training purposes.

The Student's Responsibilities

1) Come to the laboratory session prepared. This means reading and forming a conceptual understanding of the experimental procedures before the class. An explanation of details will be provided by the class instructor in a pre-lab discussion, at the beginning of the laboratory period. Nevertheless, students must come prepared for the experiment, as an understanding of the procedures, and the concepts behind them, will extend the time actually spent in performing them, and will provide safer operations in general.
2) Maintain a safe environment during laboratory experiments. While in the lab, always wear approved safety goggles, rubber gloves, and lab coat. Double check that you are placing the proper waste into the proper container; mixing organic and inorganic waste can generate explosive combinations and can cause injury or even death. Above all, use common sense and caution during all lab procedures. Absolutely no goofing or horseplay is allowed.
3) Use chemicals, solvents, and compressed gases, wisely.

4) Clean the lab after the experiments. This includes washing glassware, returning all containers, vials, and bottles to their proper places, and cleaning all workspaces (bench tops, hoods, sinks, and balance room).
   • Chemicals go in the cabinets beneath the hoods.
   • Acids and bases go in their respective cabinets, below the hoods as well.
   • Non-flammable solvents belong in the cabinet to the left of the chemicals.
   • Flammable solvents go in the yellow, flammable cabinet at the front of the room.
5) Students are expected to actively participate in data collection, recording spectra, and their understanding and interpretation, following detailed examples provided in the laboratory manual.
6) Compose and submit, in a timely manner, lab reports that include all details of the work performed: specifics of the procedure (including any deviations from the directions contained herein); chemical equations; quantities of the compounds used, in grams and moles; observations made during the course of the experiment; yield of the desired compound; and some plausible sources of its loss.
7) Stock all the obtained compounds in ampoules, or tightly closed and parafilmed vials, in a dedicated safe place. Attach a label to an ampoule, or vial and write the compound's formula, amount, date, and the author's name.
8) Segregate waste (organic *vs* inorganic), and properly dispose of used chemicals and solvents.

CHAPTER 1

EXPERIMENTAL METHODS AND LABWARE IN INORGANIC SYNTHESIS

## 1.1. Commonly Used Glassware and Hardware

1.1.1 Types of laboratory glass, glass joints, greases

Glass is an amorphous solid material, obtained in an oven at a high temperature. Different oxides, such as SiO_2, Na_2O, B_2O_3 and others, being melted and thoroughly homogenized, form glass for variable applications depending on the purpose. Laboratory glassware is made of four different types of glass: 1) fused silica, or quartz, SiO_2; 2) borosilicate Pyrex©-type/Kimax, etc.; 3) 'molybdenum glass'; and 4) soda-lime green glass. There is a very significant difference in their thermal expansion coefficients and chemical composition. The most thermally stable (with the lowest expansion coefficient) is quartz; pure SiO_2. 'Molybdenum glass' is indispensable when an electric feed through is required; the Mo-wire has the same thermal expansion coefficient and the glass-metal junction is vacuum-tight. However, the need for such a specific type of glass is far less common in synthetic chemical laboratory use, as opposed to electrochemical, physical chemistry, or physical laboratories. Therefore, in this manual we will focus on only three types of glass, the physical properties of which are summarized in Table 1.

Glass joints are used for the quick, tight, and convenient connection of different pieces of glassware during a variety of laboratory operations. Glass joints are conical (tapered), spherical, and flat O-ring, as displayed in Figures 1–5. Among tapered joints, there are clear, non-ground joints (made by pressing hot glass into high precision molds), and ground joints. Spherical joints are always ground, while flat O-ring joints are always clear. Tapered and spherical joints have two distinctive parts; inner (**F**, female type), and outer (**M**, male type), which, being connected, provide secure junctions of different pieces of glassware. In order to provide continuous connection of joints during work, plastic clips are used (Figure

Table 1. The most commonly used types of laboratory glass and their physical and chemical properties.

Glass type / Property	Quartz	Borosilicate	Soda-lime (green)
Point of annealing, °C	~1120	~550	~520
Softening, °C	1710	820	700
Working T,°C	1850	1240	1050
Coeff. expansion, ppm	0.6	3.3	9.3
Density, g/cm^3	2.65	2.23	2.51
Chemical stability	unstable to bases	medium	relatively stable
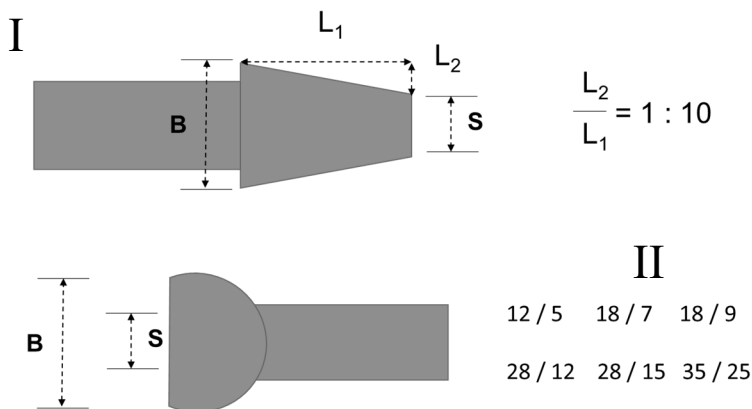
Figure 1. **I**: Tapered/conical glass joints were standardized to have 1:10 conicity (the cone angle) regardless of the joint's length. The **M** type of joint (outer) is shown as an example. **II**: Spherical ground glass joint, and the most commonly used sizes in chemical laboratories'. The **F** type (inner) is shown.

8), while for spherical and flat O-ring joints, metal clamps are used (Figures 4, 5). The diameters of portions of the joint are labeled B (big) and S (small), respectively, and used for the joints' size marking. An adoption of the same set of standard sizes throughout the scientific community around the world has allowed joints to be mutually interchangeable and replaceable, independent of the state or method of their manufacturing (Figure 1). For spherical joints, their size is determined by the diameter of ball size and the inside diameter of the joint (glass tube part), with all numbers being in millimeters.

Thus, a tapered joint #24/40 reads as largest diameter of 24mm, and the length is 40mm. For a spherical joint #28/15, the reading is ball diameter 28mm, while the opening, the tube diameter, is 15mm.
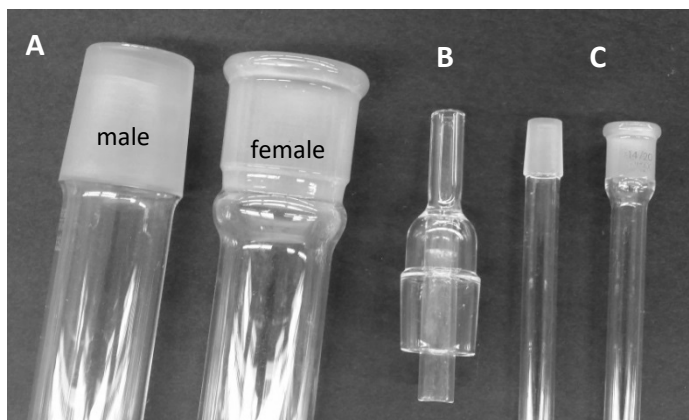
Figure 2. Unlubricated tapered 'short' glass joints; grounded Pyrex joints (**A,C**), and hot-pressed clear glass joint (**B,** by Vicor®).
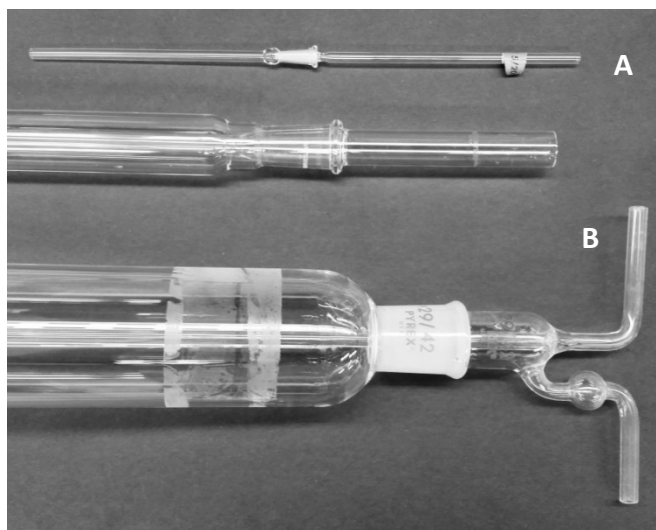
Figure 3. Unlubricated tapered full-length glass joints; grounded Pyrex joints (5/20 - **A**, and 29/42 - **C**), and hot-pressed clear glass joint (19/38 – **B**, by Vicor®).
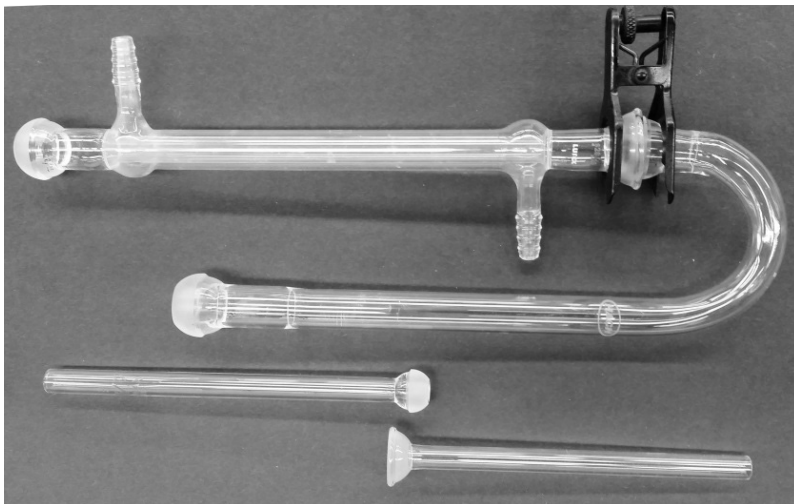
Figure 4. Unlubricated spherical grounded glass joints of different sizes. A small amount of grease and a metal clamp are required to keep joints tight.
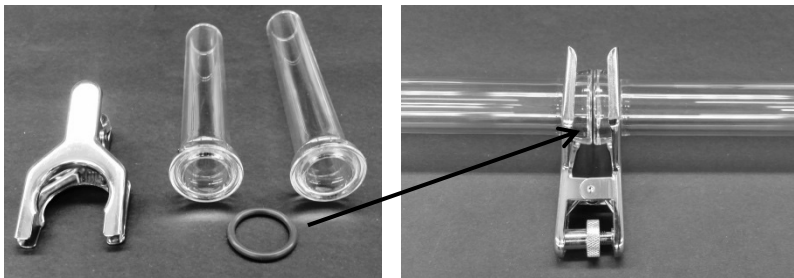
Figure 5. Flat, polished, clear, O-ring glass joints. A metal clamp is required to keep joints tight. No grease is necessary to provide vacuum-tight connection.

Quartz is the least chemically stable glass, but has excellent thermal stability. A great variety of test tubes, flasks, beakers, and evaporating dishes are made from quartz. Because of its intrinsic chemical purity (just SiO_2), quartzware is widely used in analytical chemistry for the analysis of special purity materials, used for instance, in electronics, when possible leaching of boron, as well as Ca, Mg and Na ions, is undesirable. Quartz is also transparent for the visible and NIR regions of the electromagnetic spectrum, and for UV-radiation down to 190nm. Thus, it

is used in windows' materials and cuvettes for numerous photochemical and optical spectroscopy applications.

Pyrex/Kimax/Duran borosilicate glass is the dominant material for the manufacturing of modern laboratory glassware. It is also relatively stable to temperature gradients of almost 250°C without cracking, whereas 'green glass' is the most stable to etching by bases in solutions, but has very low tolerance for heat shock.

All types of glass, and glassware made from it, are highly sensitive to fluoride anion, because of the fast formation of gaseous SiF_4, which leaves the system and etches, or weakens, the glass:

$$SiO_2 + 4\ HF = 2\ H_2O + SiF_4\uparrow \quad \text{or} \quad SiO_2 + 4\ F^- = SiF_4\uparrow + 2\ O^{2-}$$
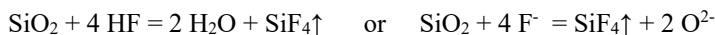
Therefore, special care should be taken to avoid even short contact of any glass with HF, its solutions and salts, even those not soluble in water. Plastic bottles and plastic-ware are necessary for the work and handling of fluorine-containing ionic inorganic compounds.

Tapered joints in common laboratory settings can be easily connected and held in place by color-coded plastic clamps (Figures 8, 9).

Table 2. The most common tapered joint sizes used in synthetic laboratories. All sizes are in mm; the small end diameter is notated in parenthesis as Θ.

'Shorty' (Θ)		Medium length (Θ)		Full length (Θ)	
14/10	(13.5)	14/20	(12.5)	14/35	(11.0)
19/10	(17.8)	19/22	(16.6)	19/38	(15.0)
24/12	(22.8)	24/25	(21.5)	24/40	(20.0)
29/12	(28.0)	29/26	(26.6)	29/42	(25.0)
34/12	(33.3)	34/28	(31.7)	34/45	(30.0)
45/12	(43.8)	n/a		45/50	(40.0)

Threaded glass items are a recent addition to the ways of connecting different glass pieces. One of the methods is to make a thread on a glass by stamping molten glass into the cast form, as introduced by some companies making laboratory glassware (Aldrich, Figure 6), and stopcocks (Kontes, Ace, Figure 7). Stopcock plugs are commonly made of highly chemically-resistant Teflon, and silicon rubber O-rings, making a tight fit which does not require lubrication. The latter makes stopcocks very suitable for both vacuum applications, and in addition of chemicals in

laboratory procedures, makes funnels that are capable of controlled delivery of very aggressive liquids and solutions such as nitric acid, bromine, *etc*.
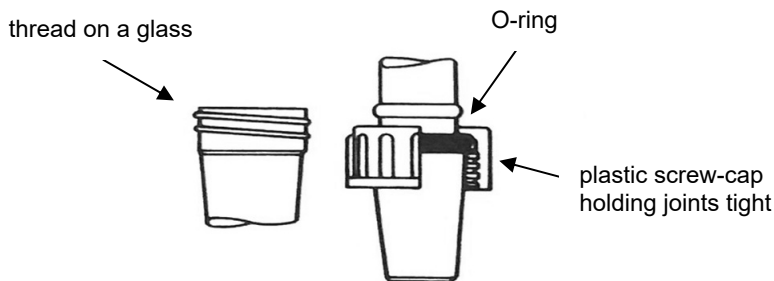

Figure 6. Two lines outer thread on a tapered glass joint designed by Aldrich.
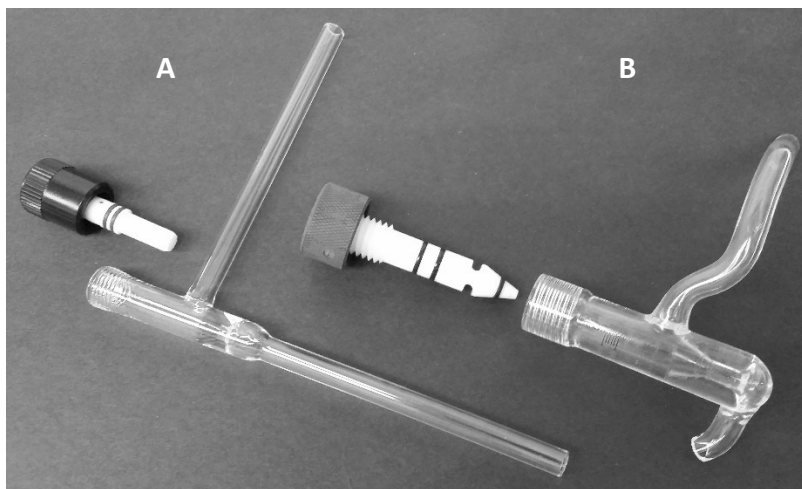
Figure 7. Two vacuum stopcocks with threads on glass: *outer*, **A** (manufactured by Kontes, ChemGlass and others), and *inner*, **B** (pioneered by Ace Glass Inc.).

Figure 8. Plastic clamps (Keck clips) for the secure connection of the most common joints from left to right: #14 (yellow), #19 (blue), #24 (green), #29 (red), and #34 (orange).

Greases. All joints are made to fit the purpose which is to provide the tight connection of different pieces of glassware during a variety of laboratory procedures. One of the most important properties is vacuum tightness, followed by solvent/solution tightness. Normal ground joints (both tapered and spherical) are not tight or leaking, unless grease is used to lubricate both *F* and *M* type of joints (Figures 2, 4). Vacuum-tight yellow color greases are made of petroleum products (Apiezon-type) and are readily available, albeit pricy. More economical versions are clear silicon greases. Both can be applied on joints, as a thin layer at room temperature or, slightly heated, which is better for providing complete lubrication; an air/vacuum-tight pair of joints is transparent and has no streaks or discontinuity (Figure 9). Both of these greases can be safely used during work with aqueous solutions, alcohols, acetonitrile, and acetic acid.

Both petroleum and silicon greases should be removed prior to glassware storage and cleaning using hydrocarbons, such as heptane or hexanes soaked into a cotton ball. All these procedures must be conducted wearing protective gloves (to avoid skin damage), under the ventilation hood, and in complete absence of an open flame to avoid fire. Clear glass joints do not require lubrication for normal operations, because of their intrinsic tightness achieved during manufacturing, but these joints are considerably pricier and rarely used in chemical laboratories.

Because of the solubility of petroleum-based greases in hydrocarbons, other types of starch-glycerol based greases, which are not soluble in the former, are used [1,2].
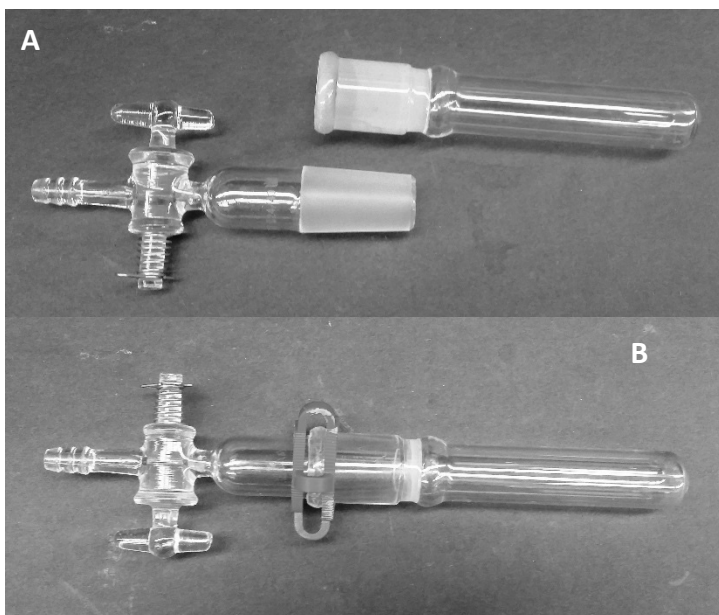
Figure 9. A pair of full length #24/40 tapered joints: **A** – unlubricated, and **B** – greased with Apiezon M, and secured together with Keck plastic clamps.

Figure 10. Petroleum-based vacuum greases in aluminum foil tubes.

1.1.2 Glassware for common laboratory procedures and operations

Vessels for carrying out chemical reactions in open air

These pieces of glassware are beakers, flasks, and test-tubes. They all exist in a great variety of sizes. Below, you may find pictures and short descriptions of all these items with some comments.

Figure 11. Pyrex beakers of variable sizes (**A**), and jacketed beaker (**B**).

Beakers are known to be made of flint glass (green glass), Pyrex/Kimax glass, and quartz, all in variable sizes (Figure 11 A). A set of the most usual volumes of beaker ranges from 10mL to 2L capacity. Marks indicate approximate volume and can't be used for accurate measurements. A special kind of beaker – a jacketed one – is used for carrying chemical reactions, or crystallizations at controlled temperatures by circulating hot (or cold) fluid from the thermostat (Figure 11 B)[see Section 1.1.3 below].

Flasks can be round-bottomed, or flat-bottomed, with the latter group providing the convenience of being able to stand unsupported on level flat surfaces, such as benchtops, hotplates, and ventilation hoods (Figure 12). The top end of a flask can be just fire-polished, or with a tapered ground joint. Also, flasks can have more than one end (called a *neck* in this category of glassware). Two or three-neck round flasks are widely used in the lab (Figure 13), although four and five-neck flasks are known, but rare, and mostly used in laboratories carrying out chemistry procedures in the field of natural products synthesis, medicinal chemistry, organic/heterocyclic chemistry, and polymers chemistry. These flasks are commonly named as *reactors*. As beakers, flasks have a variety of sizes, and in the chemical laboratory, the most useful volumes range from 25mL to 2L. All the flasks

mentioned here are made of thermally stable glass, such as Pyrex/Kimax, or quartz (single neck only), because their main purpose is to carry out reactions which, most of the time, involve heating.

Figure 12. Flasks: round flat-bottomed, round, and pear-shaped.
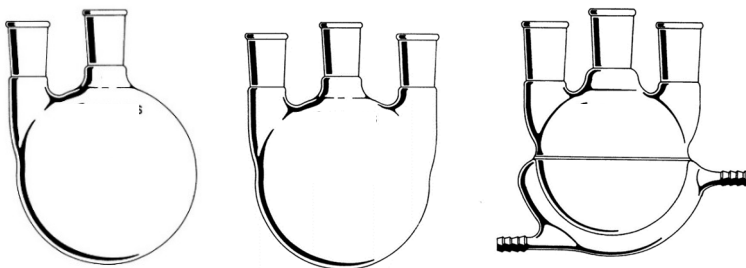
Figure 13. Two-neck reaction flask, and three-neck reaction flasks, including jacketed flask.

The extra necks are there to accommodate connection to additional funnels, such as gas tubes to deliver gases, reflux condensers, or thermometers, which are needed to carry out certain chemical reactions. Jacketed reactors are very convenient for low-temperature procedures, or in conditions when heating of the vessel should be confined into a small place, and the use of a hot plate is not desirable, or possible.

        Another type of flask widely used in the synthetic laboratory is the flat-bottomed conical flask – Erlenmeyer flask – which is made in a large variety of sizes and types of glass. There are flint glass, Pyrex/Kimax, and quartz flasks, with volumes for the first two types of glass ranging from 10mL to 4L. Typical sets of these flasks are shown in Figure 14.
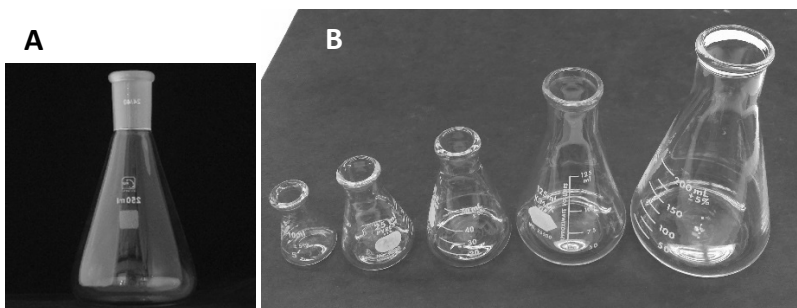
Figure 14. Conical (Erlenmeyer) flasks with ground taper joint (**A**), and with fire-polished rim end (**B**).
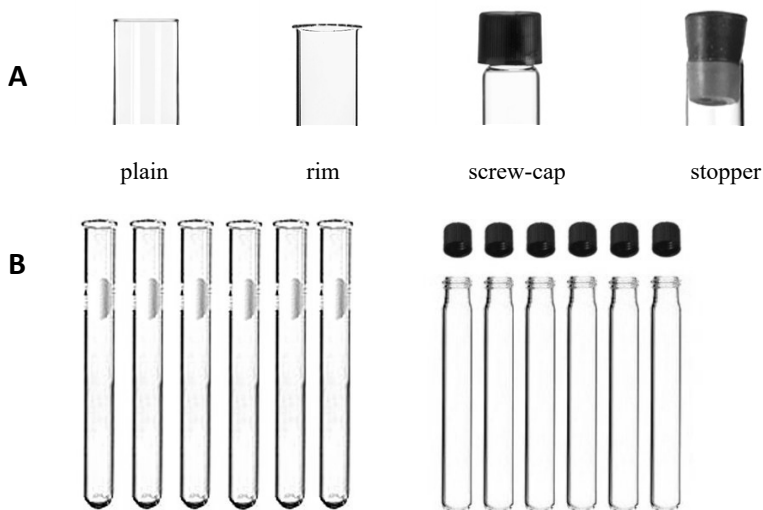
Figure 15. Types of test tubes' ends (**A**), and sets of the most commonly used test tubes in the laboratory (**B**).

Test tubes. Large varieties are available for common laboratory work, both by size/diameter, and by the type of test tube end, as shown in Figure 15. Depending on the type of laboratory work, test tubes can be made of plastic or glass of different kinds; green borosilicate, Pyrex/Kimax, or quartz. Typical glass-made representatives are shown here.

Glassware for laboratory processes

Addition of gases to the reaction mixture can be achieved by direct bubbling using a gas conditioning bottle (Figure 16**A**), or via adapters, either straight, or angled, with multiple ports, when more than one gas is needed (Figure 16**B**). For example, the washing bottle allows drying of the gas, or monitoring the rate of gas addition by counting bubbles. When the number of inlets into the reaction vessel is limited, a multiple port adaptor is a convenient piece of glassware, where, for instance, an inert gas and a gas for the reaction (H_2S, CO_2, NH_3, etc.) can be added simultaneously, at different rates (Figure 16**B**).
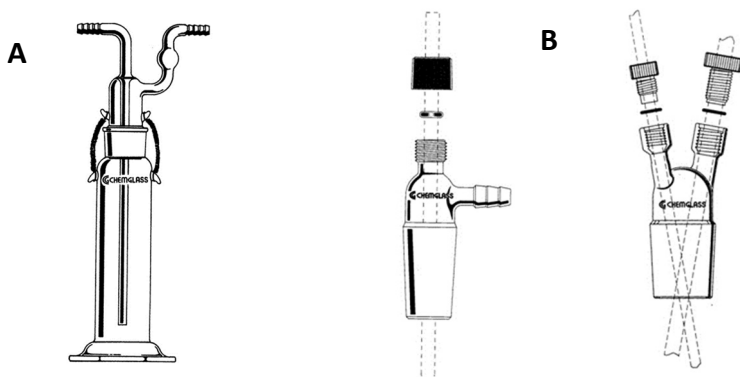
Figure 16. Bottle that allows gas conditioning and monitoring (**A**) and straight, single tube, single and multiple port adapters (**B**).

Adding liquids and solids to the reaction mixture (or transfer of these materials) can be accomplished using additional glassware funnels, shown in Figure 17. Fast, unregulated addition/mixing can be achieved using these funnels.

As depicted in Figure 18, the addition of liquids (**A**), or solids (**B**), can be done in a dropwise or stepwise fashion, over a controlled, prolonged time. In all these cases, ingredients can be added under vacuum, or an inert gas blanket, due to the side bypass tube indicated by the arrow. The tube allows for keeping the same pressure above and below the stopcock. As shown in Figure 18, funnels are available in a variety of sizes, but made exclusively from thermally stable Pyrex/Kimax glass.
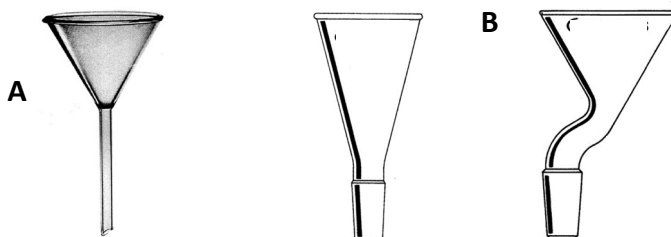
Figure 17. Transfer of liquids (**A**) and addition of solids using straight or curved adapters for the reactors with multiple necks, when space around them is often limited (**B**).
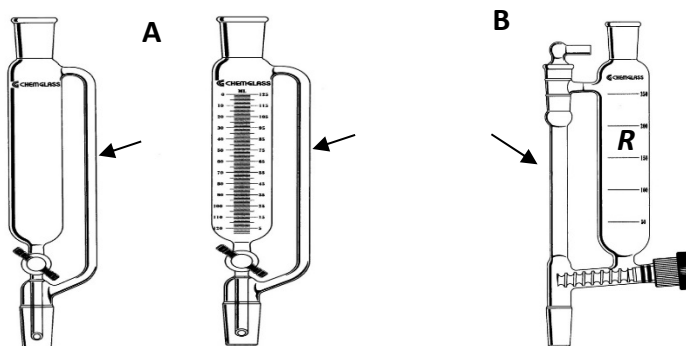
Figure 18. Funnels for regulated addition of liquids (**A**) and solids (**B**) to the reaction mixture. The latter funnel has a Teflon-made screw turning, which allows advancing of solid material from the main reservoir **R** to the vessel below.

Addition of small quantities of liquids by pipettes. For qualitative, quick, and convenient addition of solutions and solvents, two types of pipette are widely used in the synthetic chemical laboratory; disposable variable length glass pipettes, and disposable plastic pipettes (Figure 19).
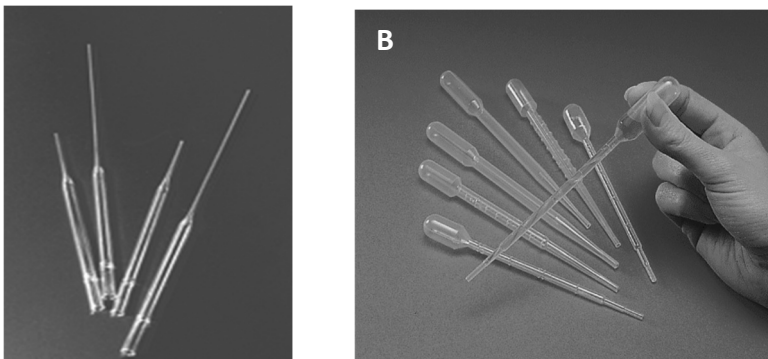
Figure 19. Disposable glass (**A**) and plastic pipettes (**B**).

Glass pipettes are made of flint (green) glass, and require a small rubber bulb for use. Their total capacity is ~3mL, and they are only for delivery/transfer of liquids, since they don't have graduated marks. Plastic pipettes are made of thin polyethylene or polypropylene, appear as translucent devices in several sizes, and can deliver from 5mL to 25mL of liquid. Marks on plastic pipettes are not very accurate, and these pipettes are only for delivery/transfer of approximate (±5%) quantities. Both types of pipette are resistant to corrosive substances in ambient conditions such as acids and bases (for several minutes at least), work well with the majority of common organic solvents/solutions, and, therefore, have gained popularity in laboratory practice over the last two decades.

Compounds' storage

Chemical compounds that require storage without contact with moisture or air can be kept in vacuumed desiccators charged with drying agents. These are typically P_2O_5 in a porcelain or glass dish, activated (preheated under vacuum – see Figure 35 in the next section) with granulated silicagel, anhydrous salts such as $CaCl_2$, $CaSO_4$, or concentrated H_2SO_4, placed inside the Erlenmeyer flask inside the desiccator (Figure 20). Most desiccators these days are equipped with stopcocks, to provide a vacuum which can be pumped within a minute or two, to speed up the drying of material in these very useful pieces of glassware. Glass desiccators (Figure 20**A**) require a thin layer of lubricating grease to keep the vacuum inside, while plastic desiccators need to have a soft rubber O-ring for the same purpose (Figure 20**C**). In desiccators, compounds can be stored in vials of different kinds, beakers, flasks, or bottles made of clear or amber glass, or

plastic. If dryness is a concern, then the most convenient way of storage is the use of dry cabinets (Figure 20**B**) filled with solid absorbents; drierite®, or blue, indicating silicagel (with $CoCl_2$ as the color-changing ingredient).
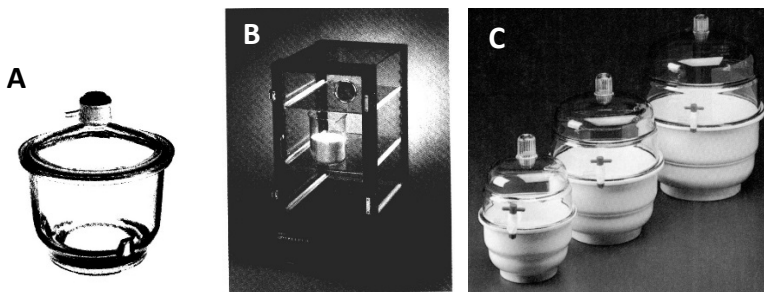
Figure 20. Desiccator (**A**), plastic dry cabinet (**B**), and plastic vacuum desiccators (**C**).

Important auxiliary glassware: gas washing bottles, drying tubes, gas drying towers, and porcelain-ware

Typical examples of these pieces are presented in Figures 21-23. The **gas washing bottles** have a fritted (coarse grade) ending at the end of the inner tube, which provides much larger numbers of small bubbles coming through the washing liquid, for better efficiency. Often, this is concentrated H_2SO_4 or H_3PO_4 used for gas drying, but frequently, concentrated solutions of baking soda, or bases, are used to trap acidic impurities, such as gaseous HCl or mist of the acids above. The layer of liquid inside the bottle is normally kept ~2cm above the upper end of the frit to avoid a significant inner pressure build-up. Plastic clips or metal springs are often used to keep both parts of washing bottles tight, because of the presence of some small extra pressure normally encountered during work with these devices. **Drying towers** are normally filled with blue-indicating SiO_2, granulated anhydrous $CaCl_2$, glass/ceramic/porcelain beads, mixed with P_2O_5. The first agent has a very large static capacity to absorb moisture, while the last agent is the most efficient, albeit messy, during its replacing. Two cotton balls (or compacted glass-wool balls) on the top and the bottom of the tower are necessary to contain the drying content inside.
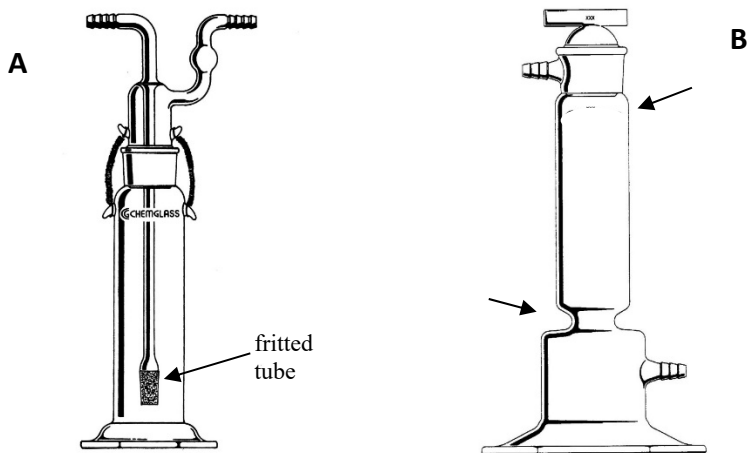
Figure 21. The washing bottle with a fused coarse glass frit (**A**), and the drying tower (**B**). Arrows indicate where cotton/glass-wool balls should be placed to prevent motion of drying agents during work or handling the tower in the lab.
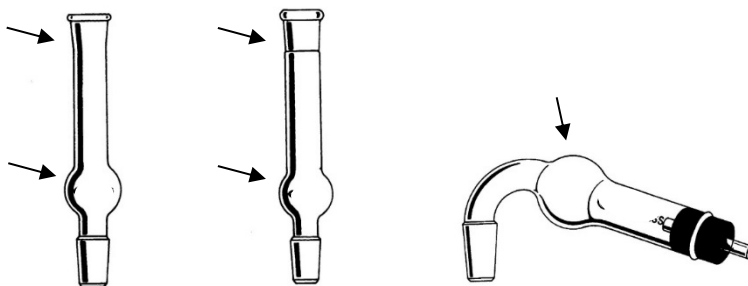
Figure 22. Drying tubes (to be filled with a desiccant) to prevent moisture entering distillation equipment, or freshly distilled solvents, or reaction mixtures. Arrows indicate where cotton/glass-wool balls should be placed to keep drying agents in place.

Drying tubes normally have tapered joints for connection with the condenser, or other parts of distillation equipment, to which they are attached by plastic clamps (Figure 22). It is very important to keep free passage of air through these tubes and avoid clogging, because of the absorbed moisture! Failure to maintain this working condition may lead to whole reflux or distillation equipment breakdown, due to pressure buildup.

Porcelain-ware is shown in Figure 23. Dishes and crucibles (Figure 23**A**, **B**) are used for elevated temperature processes, such as evaporation of solutions, or strong heating of solids (calcination), up to 1500ºC. These pieces of labware are remarkably thermally stable, absolutely tolerant to heat shock, and possess significantly greater mechanical stability than glass. Crucibles should always have matching covers to prevent spills/sputtering of heated material inside. Porcelain mortar-and-pestle combinations (Figure 23**C**) come in a variety of matching sizes, and are widely used in synthetic laboratories.

Figure 23. Examples of the porcelain-ware used in laboratories.

Measuring devices

Graduated cylinders are made of thermally stable Pyrex/Kimax glass, or translucent plastic for the obvious reason – non-breakability. Being tall, and glass-made, graduated cylinders frequently become victims of unintentional, accidental tip over. Some manufacturers even offer movable plastic collars to prevent cylinders' breakage during a sideways fall on a benchtop. Graduated cylinders are available in variable sizes, ranging from 10mL to 2L capacity, and provide delivery accurate to ±3-5 % volumes of measuring liquids (Figure 24). Plastic cylinders are made of relatively chemically inert, opaque, high-density polyethylene or polypropylene, capable of withstanding the majority of organic solvents for extended periods of time (hours), as well as acids and bases.

Figure 24. Glass (**A**) and plastic (**B**) graduated cylinders.

Pipettes. There are two types of these measuring devices which are widely used in synthetic laboratories; calibrated glass pipettes, and automated hand-held plastic pipettes, with disposable tips made of chemically resistant polyethylene (Figure 25). The first kind – glass pipettes – has two variables: those with a fixed volume of delivered liquids (Moore pipettes), or graduated pipettes that require a rubber bulb for their proper use (Figure 25**A**-**C**). Automated pipettes with variable deliverable volumes have different capacities; from 1000µL to 20µL, and require different sizes of disposable plastic tips (Figure 25**D**). The required volume can be entered by dialing the top screw or ring with a set of numbers in the pipette body.

Volumetric flasks. These pieces of laboratory equipment can also be made of glass (clear or amber, as shown below in Figure 26), or plastic (for work with HF or fluoride-containing solutions). Short, tapered, female-type ground joints in specifically designated sizes (e.g. #13, #15, #17, #23, #27) are normally found at the ends of these flasks, and require same-size stoppers, made of glass, Teflon, or polypropylene. Glass-made volumetric flasks are manufactured of either flint (green) glass, or Pyrex/Kimax glass.
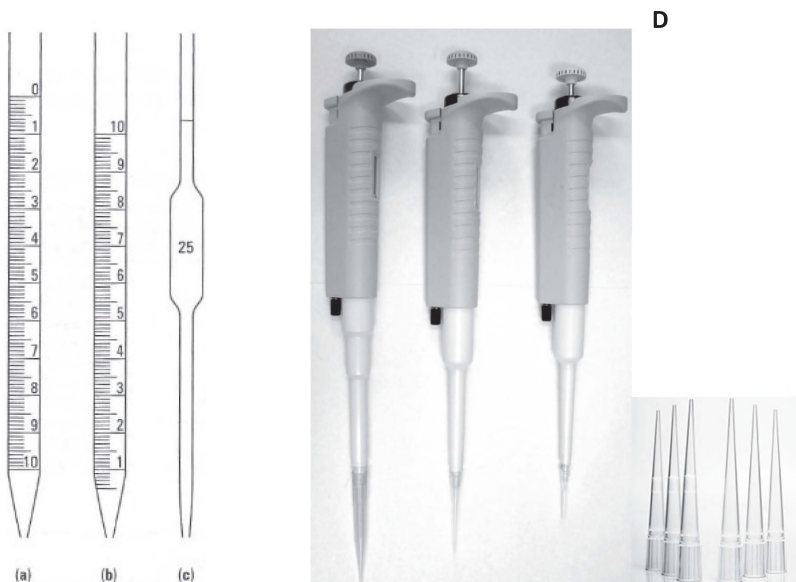
Figure 25. Glass (**A-C**) and variable capacity plastic pipettes with tips (**D**).
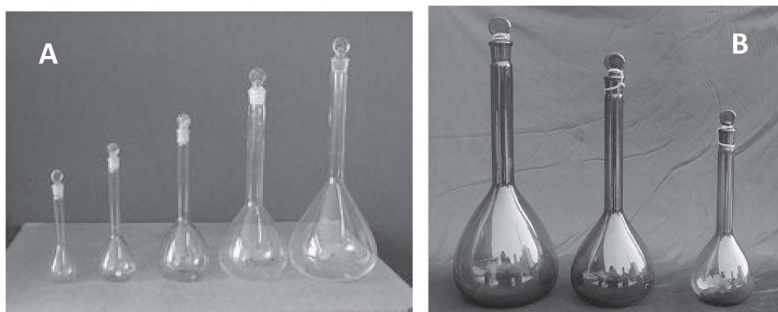
Figure 26. A set of common glass flasks with stoppers (**A**), and special flasks for light-sensitive solutions (**B**), such as those containing Ag^+ compounds, or iodide solutions, or halo-hydrocarbons prone to photo-degradation.

1.1.3 Simple Labware
Solids handling and stirring; bars, stirrers

A variety of metallic spatulas of variable shapes for convenient samples' treatment is readily available. Most of them represent stainless steel, although common iron, or more corrosion resistant Ni / Co-plated spatulas are used as well (Figure 27). Glass spatulas are very useful and convenient, albeit fragile, especially when handling wet or corrosive samples. Normally these spatulas have two different ends; one flat for solids pick-up, and the opposite end having a compressed, wider part, useful for compacting precipitates during the filtration procedure (Figures **44-46** below). Another good use of glass spatulas is checking on samples in 'air dried' conditions; which means that there will be no adhesion of a solid sample to the glass.
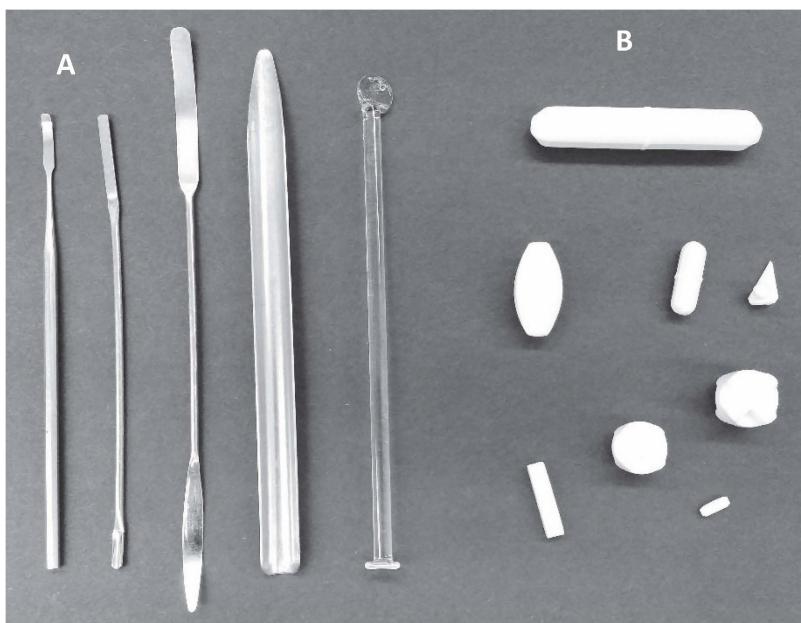
Figure 27. Metal and glass spatulas for solid samples handling (**A**), and stirbars in Teflon casing (**B**).

Stirring bars are small pieces of iron (or magnetic steel) encased in Teflon. A large variety of sizes and shapes is available for lab use. It should be noted, that the size of the stirbar should reasonably match the vessel and

purpose of use. Large stirbars develop significantly larger force upon contact with magnetic stirrers, and, thus, can break an inappropriate glass container, or even jump out of it, causing spills and possible safety violations.

The process of stirring of solutions and reaction mixtures can be accomplished by using: a) a vibrating pad creating the vortex; b) magnetic stirrers; or c) mechanical stirrers driven via electric motor. The vibrating plate machine (vortex mixer), with the ability to set and maintain desired speed and the time for the action, and a mechanical stirrer, are shown in Figure 28. The latter requires a variable voltage transformer (called a *variak,* Figure 28**A**), to be able to regulate the speed of the stirrer. The end of the stirring rod that goes into the solution is made of glass or Teflon, while the stirring blade is normally made of chemically inert and mechanically robust Teflon plate (Figure 29**B**).
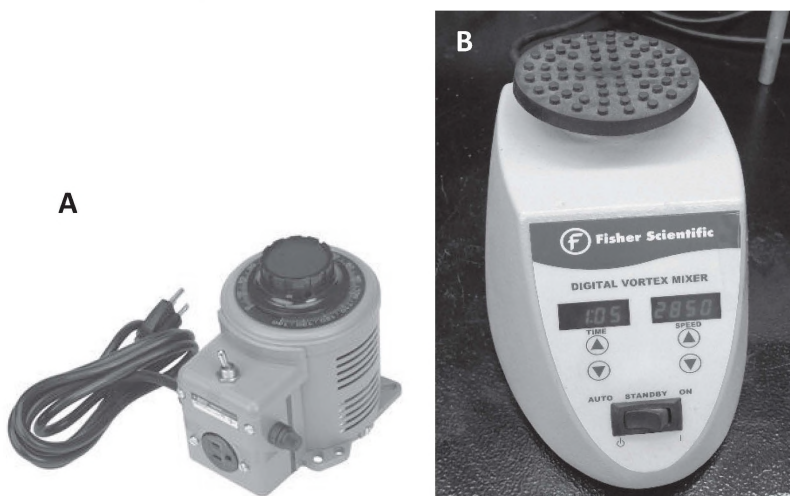
Figure 28. The variak (**A**) and the vortex mixer (**B**).

The most commonly used laboratory devices are magnetic mixers which are also coupled with a heating element (hot plate) (Figure 30). There is a constant bar-magnet under the plate attached to the electric motor axis, and the speed of rotation is regulated via the knob in the front panel. Another very useful piece of multi-purpose laboratory hardware, which is very often used for the mixing of components during the reaction, is the ultrasound bath (called a *sonicator*) (Figure 29**A**).
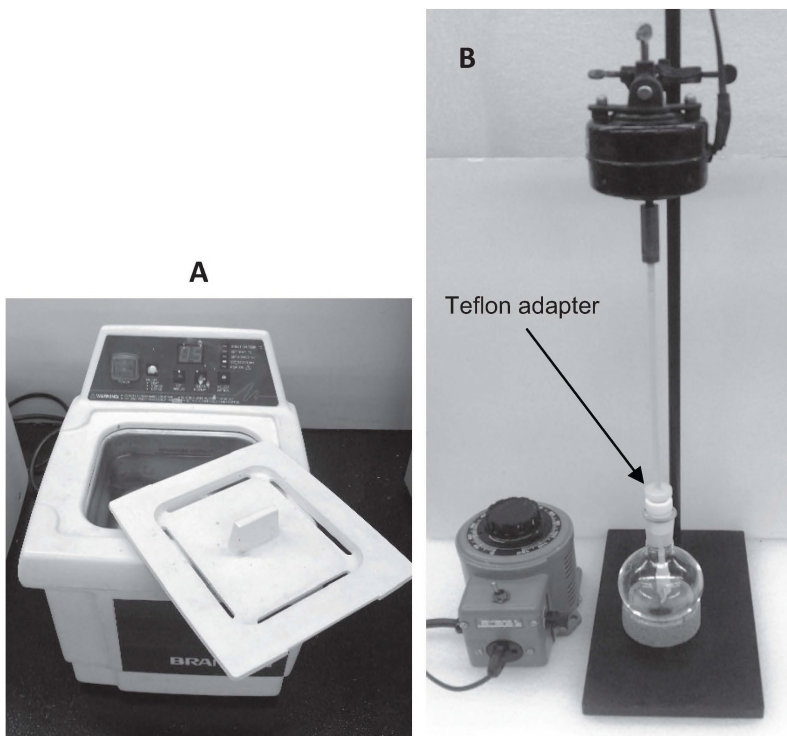
Figure 29. The 'sonicator' – an ultrasound mixer (**A**), and the mechanical mixer; electric motor connected to the variak, Teflon stirring rod with stirring plates, and adapter (**B**).

1.1.4 Heating and cooling devices

Heaters. Sand baths and heating mantles (Figure 31) require a variable voltage transformer (a *variak*, shown in Figure 28**A**). The most common heating devices in a modern chemical laboratory are hot-plates, or *combos* (Figure 30), which are available in variety of sizes and have the ability to deliver the required temperature. Being used under the ventilation hood, these devices, because of the draft, need to be shielded by wrapping in aluminum foil or heat-conserving blankets. A submersible heater (Figure 30**B**) requires the variak to provide controllable heating to the liquid bath, or to be connected to a temperature controller. Otherwise it will boil the liquid it is in. Also, special care should be taken during work with this very convenient and efficient submersible heater; it should be depowered

(switched off) prior to removal from the water or oil bath. Being left turned on after removal from the bath can cause burns on touch, or create a fire hazard.
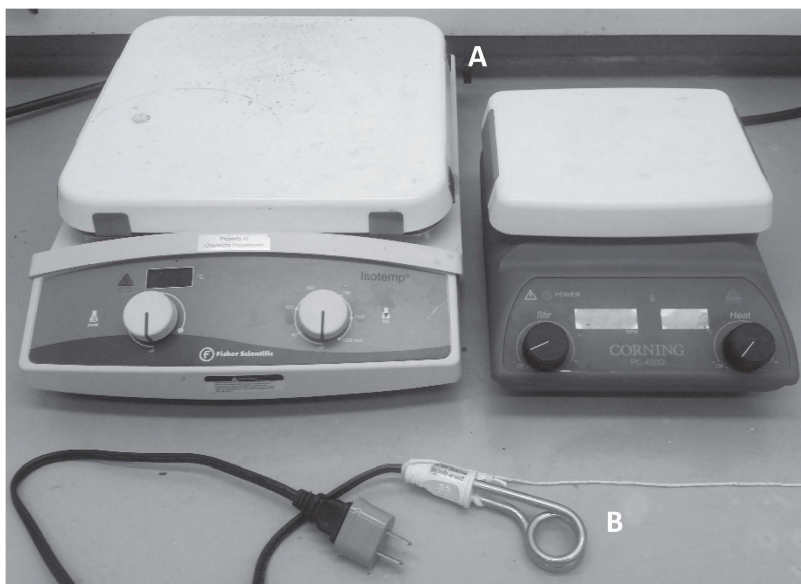
Figure 30. The hot plates and stirrers (combos) for the bench-top chemical operations (**A**), and submersible heater for water baths, Dewar flasks, etc. (**B**).

Other heaters involve water solutions, such as water baths and thermostats (Figures 32,33). An inexpensive water bath is just a simple metal container or jar that can be heated on a hot plate (or via submersible heater, see Figure 30**B**), or has a built-in heating element (Figure 32). In the latter case, there is a rough temperature control/regulation as well, but the accuracy is ±5°C. The use of thermostats is as follows: a) a vessel is inserted into the thermostat cavity; and b) heated water is carried via hoses to the reaction site or instrument operating at variable temperatures (for instance, spectrometers). Both thermostats and thermostat/chillers have an electric motor inside, which may provide external circulation of the heating/cooling liquid via hoses. Appropriate heat insulation for these hoses is required to avoid condensation of water on cold hoses, or to make delivery of heated liquids more efficient and less time-consuming in attaining the desired temperature.
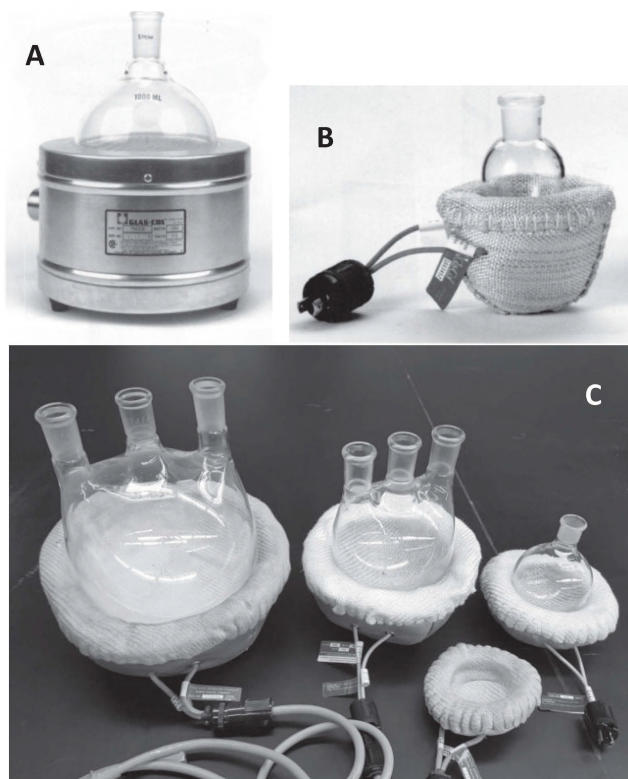
Figure 31. The sand bath (**A**) and heating mantles; microscale (**B**), and general use, from 2L to 200mL flask capacity (**C**).
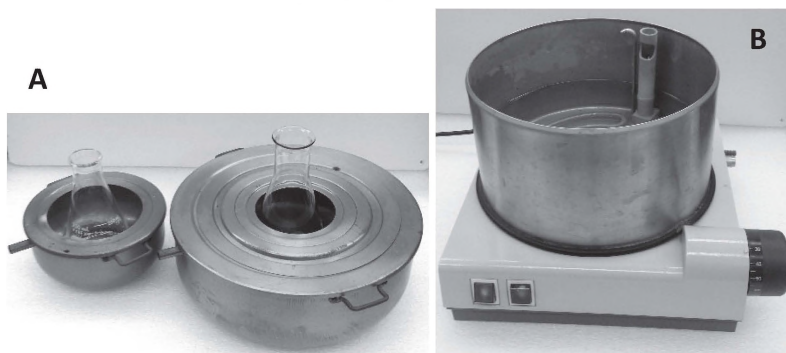
Figure 32. Water baths: **A** - metal containers with required external heater, **B** – with the heater and simple analog thermo-controller.

An air gun provides a controllable flow of warm/hot air (Figure 34), and is widely used in synthetic laboratories, especially those using thin layer chromatography (later abbreviated as TLC).
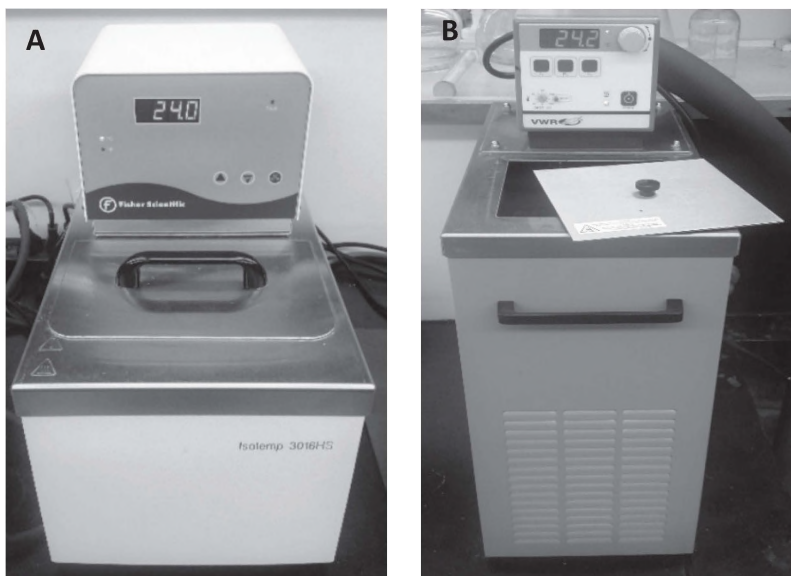
Figure 33. Thermostat for heating (**A**), and universal heating/cooling thermostat with small built-in refrigeration machine (**B**).

Finally, drying ovens – either ambient pressure or vacuum – are used in chemical laboratories for glassware drying or desiccation of salts, making them anhydrous and suitable for drying solutions in organic solvents, or desiccants for drying cabinets and desiccators (Figure 20 above). These salts are typically Na_2SO_4, $MgSO_4$, and $CaCl_2$ which, in hydrated stage, contain 12, 7, and 6 crystallized water molecules respectively. Drying agents are normally granulated silica gel SiO_2, or of Drierite® $CaSO_4$, which are colored with traces of anhydrous blue $CoCl_2$. When the color changes to pink, it is time to re-activate the desiccant by heating in the oven at ~150ºC. Two typical drying ovens are shown in Figure 35. The vacuum oven makes the process of activation much faster. It is important to note that a drying tower has to be connected to a vacuum oven; when the process is completed, dry air must fill the chamber to keep the materials inside dry. Aside from the aforementioned drying needs, ovens are also used as heated cabinets, in which reactions can be carried out,

either in common glassware, or in sealed ampoules in protective capsules during hydrothermal syntheses. Temperature control in heating ovens is maintained via either analogous, or more frequently today, digital devices.
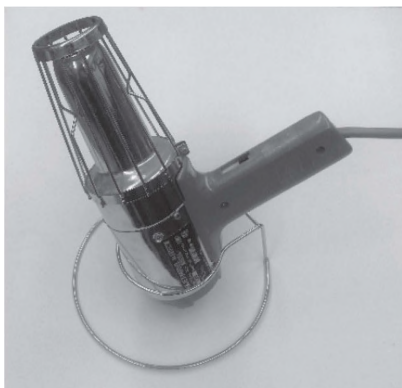
Figure 34. An air gun on its support.
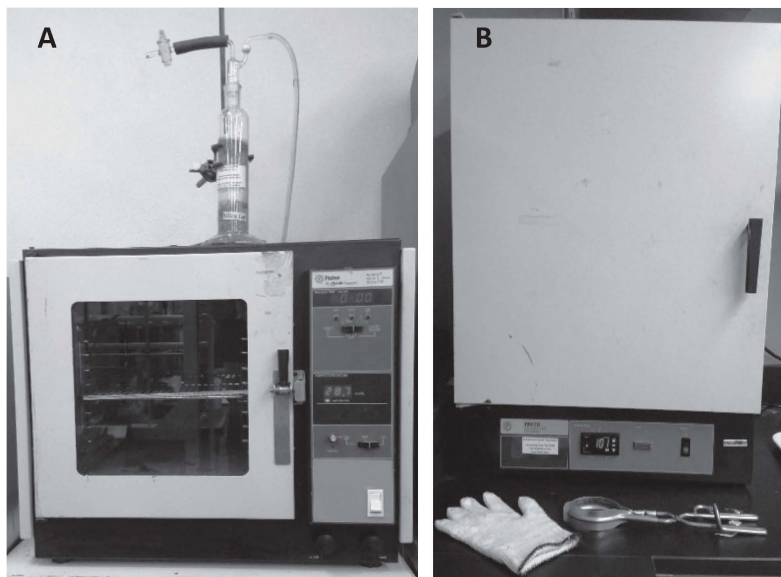
Figure 35. Drying ovens: vacuum (**A**), and glassware drying oven (**B**)

Coolers. Thermostats with refrigeration capabilities (Figure 33**B**) can easily be used to cool reaction vessels which are inserted into them, to -20ºC. Lesser temperatures, normally around -5 – 0ºC can be delivered to cuvettes or other instruments' accessories, via heat-insulated hoses. However, temperatures below -20ºC can be maintained relatively easily in the Dewar's flask (Figure 36). This vacuumed flask was named after James Dewar, who invented it in 1891 to keep liquefied oxygen and air. A liquid N_2 filled Dewar allows the user to get roughly -180ºC, while using only dry ice inside the Dewar provides -75ºC. Nevertheless, mixtures of dry ice with some common organic solvents have managed to achieve the following temperatures (in ºC) [**2**]:

ethanol/CO_2	-72
chloroform/CO_2	-61
acetonitrile/CO_2	-42
CCl_4/CO_2	-23
ethylenglycole/CO_2	-15

Dry ice should be added to the Dewar ~1/2 filled by volume with organic solvent, until the system becomes viscous. These vacuum-jacketed flasks can be made of borosilicate glass, or metals such as Cu, its alloys, or stainless steel. Both metal and glass Dewars are widely used in chemical synthetic laboratories to keep hot and cold liquids/solutions for extended periods of time.
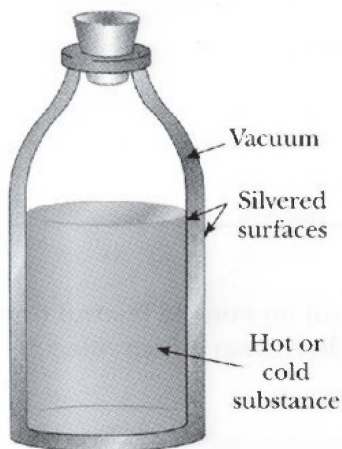
Figure 36. The physical principle behind the Dewar's flask (vacuumed flask), and examples of variable sizes of device, which are widely used in chemical laboratories.

Another method of achieving subzero temperatures for chemical benchtop reactions is using crushed ice and adding salt to make a salt bath, which needs to be prepared and kept in heat-insulating containers, such as thick Styrofoam buckets or boxes. Below, we present several inexpensive ice/salt mixtures (in grams per 100g of ice), and attainable temperatures [1].

KCl, on ice	30g	-10ºC
NH_4NO_3, on ice	45g	-16ºC
NaCl, on ice	33g	-20ºC
$CaCl_2 \cdot 6H_2O$, on ice	123g	-40ºC

It must be noted that all operations with these low temperature mixtures must be conducted wearing special insulating gloves to avoid dangerous frostbite. Working with liquid N_2 and vacuumed flasks absolutely requires a face-protecting shield, due to possible implosion of these devices, or spilling of cryogenic fluid.

Measuring temperature is conducted in the preparative chemical laboratory in two ways, using glass Hg-free thermometers, and digital hand-held meters equipped with thermocouples of J or K types (Figure 37). The latter vary in size, precision, and function, but can be found to suit any budget.
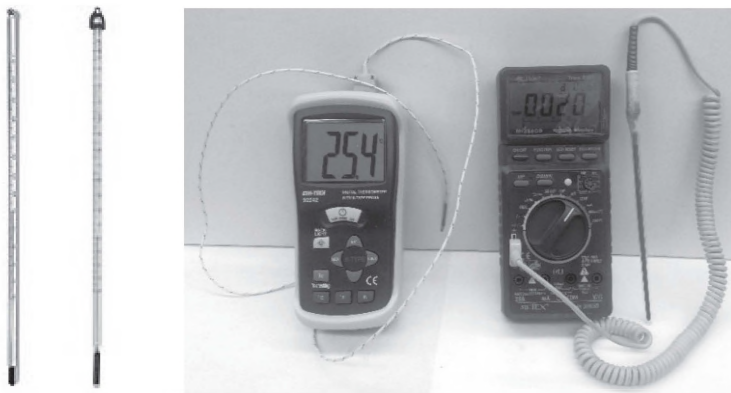
Figure 37. Variable accuracy and size glass thermometers and digital devices.

1.1.5 Other important auxiliary equipment

Other pieces necessary for normal synthetic laboratory operations include: a) metal lab stands, supports, and holding clamps; b) elevating/descending lab jacks; c) circular flask-supporting corks; d) glassware cleaning brushes; e) magnetic stirbar retrievers; f) UV-lamp for the TLC developing/visualizing; and g) melting temperature measuring devices. Examples of this auxiliary equipment are displayed in Figures 38–42. There are many other useful devices that make laboratory work convenient, but we believe that the items listed in this section are crucial for safe and productive syntheses.
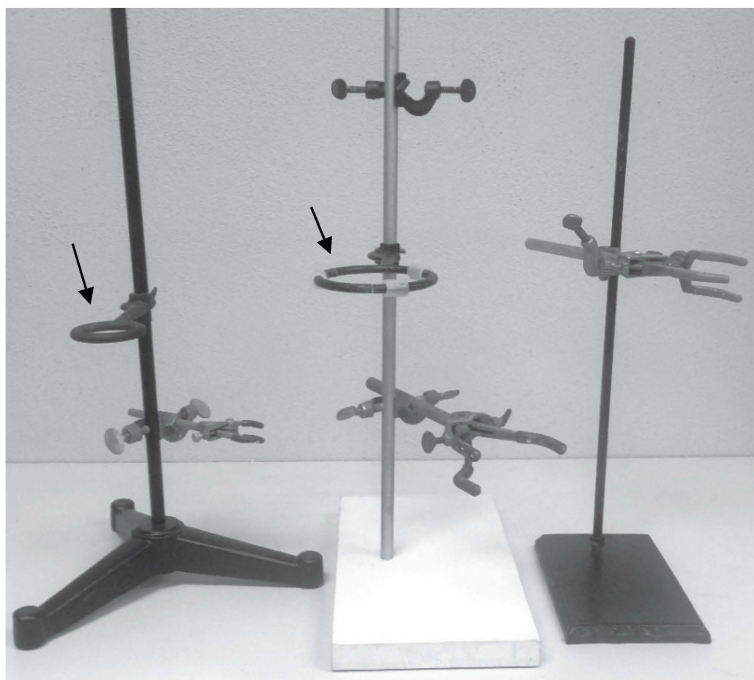
Figure 38. Types of lab stand with clamps commonly used in synthetic laboratories for the support of different glassware and hardware. Arrows indicate O-ring clamps designed to support gravity filtration funnels and separation funnels.
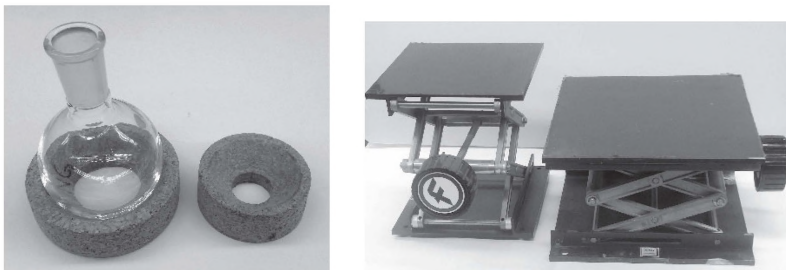
Figure 39. Variable sizes of circular cork for benchtop flask support, and lab jacks.
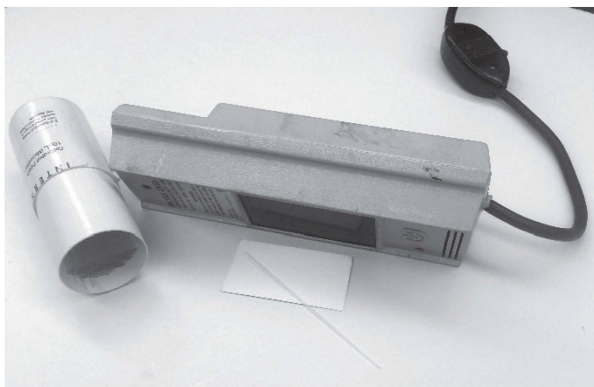
Figure 40. The TLC capillaries and the UV-lamp for viewing of the TLC plates.
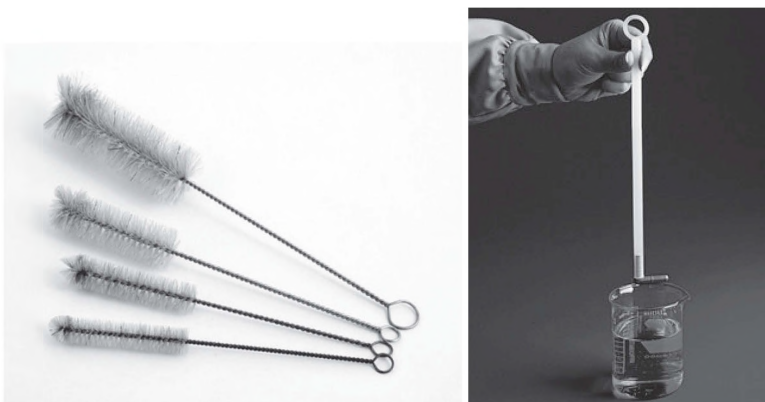
Figure 41. Variable size glassware brushes and magnetic stirbar retriever.

Figure 42. Apparatus for measurement of the melting/decomposition points of chemical compounds. Shown are Pyrex glass capillaries for samples packing.

Cited References

1. A. Gordon, R. Ford. *Chemist's Companion*: A Handbook of Practical Data, Techniques and References. Wiley Interscience Publication; New-York – London – Toronto – Sydney, 1972.
2. H. Lux. *Anorganisch-chemische Experimentierkunst*. 2nd Ed. by J. A. Barth (Verlag), Leipzig, 679 pp., 358 figs. 1959.

1.2. Important Laboratory Procedures and Techniques

1.2.1 Filtration and filterware

Mixtures that have a clearly defined phase separation surface area are: 1) suspensions – solid/liquid interface or solid/gas interface; 2) emulsions – liquid/liquid interface; and 3) aerosols – liquid/gas interface. Systems can be multicomponent, but the essential feature is immiscibility of two (rarely three) phases which define the physical state of matter; solid, liquid, and gas.

Separation by filtration.

Filtration is a process of separation of a condensed phase (solid or liquid) from solutions, or gases, respectively.
        The most common laboratory procedure is the filtration of solids from solutions. For that purpose, a variety of filtering devices and filters are widely used. Paper filters of different porocity and diameter are still in use in numerous laboratory operations involving aqueous solutions with pH close to neutral. An appropriate-size paper filter has to be folded to form a funnel, as shown in Figure 43, and then fitted into the glass funnel for a gravity filtration. Slight moisturizing of the filter with a few drops of water (or solvent from the mixture to be filtered) is needed to assure a tight fit to the funnel's wall.

fold paper filter
four times

place wet
on filter
funnel
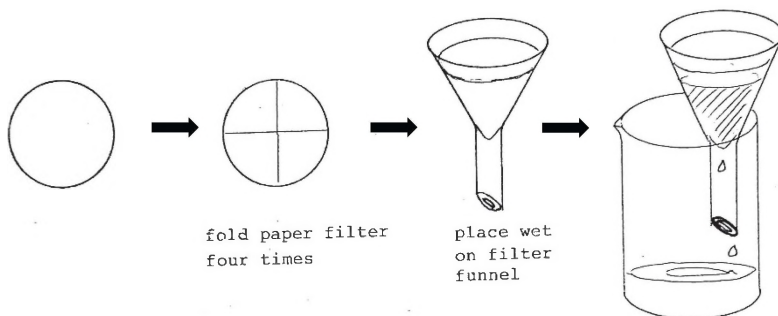
Figure 43. Paper filter and its adjustment for gravity filtration.

The funnel can be supported with the O-ring clamp (Figure 38). The one unpleasant problem with this method of filtration is the limitation of the size of the funnel and filter, plus the fragility of the wet filter with precipitate that may perforate the paper.

Another widely-used method of paper filtration in the chemical laboratory is the application of the Büchner funnel and Büchner flask method [**1, 2**], shown in Figure 44 below.
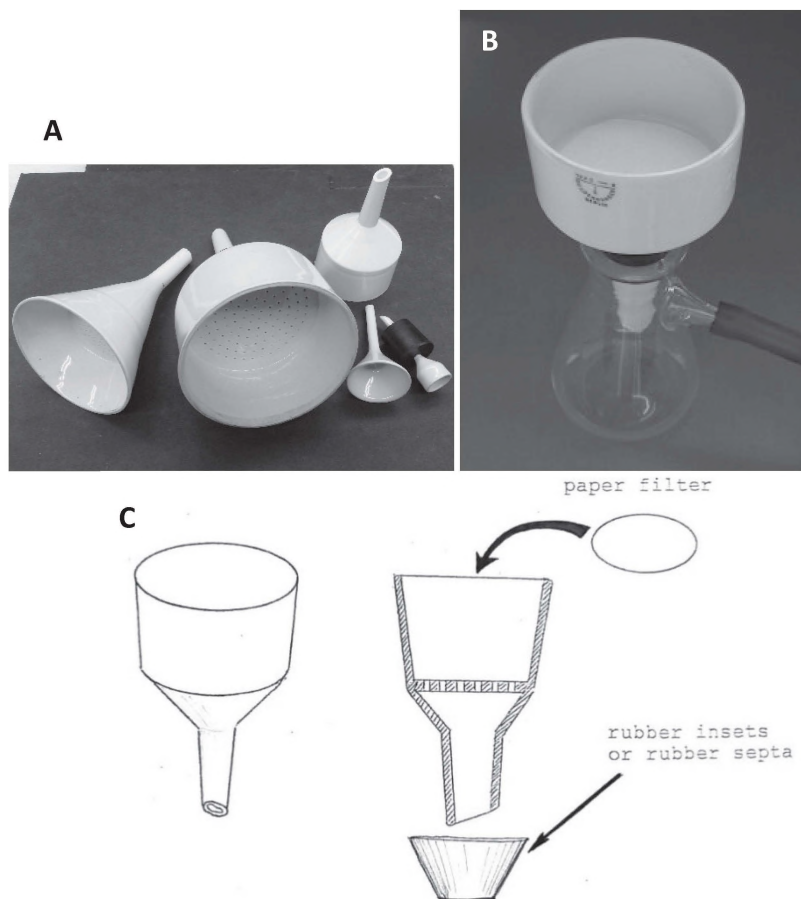
Figure 44. A variety of ceramic Büchner filter funnels (**A**), sketch of the funnel and paper filter (**B**), and assembled filtration system connected to vacuum source (**C**).
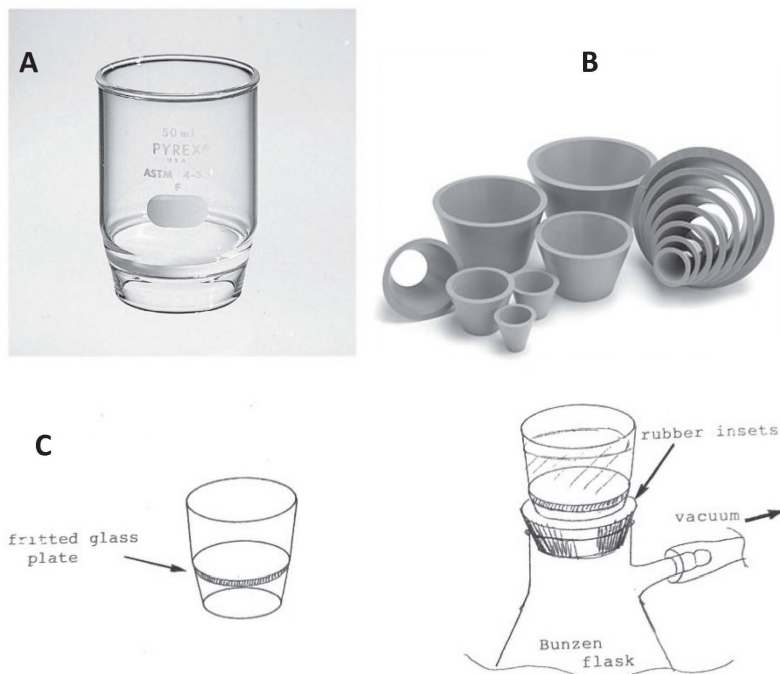
Figure 45. The Gooch filter (**A**), soft rubber inserts used together with the filter (**B**), and sketch of assembled filtration system with the Büchner flask (**C**).

For non-aqueous solutions, the most popular are glass frits, which are sintered glass discs, welded into the filter funnel body. These disks are made of sifted glass particles of the same size, fused upon heating, between graphite plates at glass-softening temperature (Figure 45). These frits normally have gradation C, M and F, which reflects their porocity and their ability to retain particles of the precipitate of a respective size. These are: coarse (**C**), with 40-60µm pore size; medium (**M**), with 10-15µm pore size; and fine (**F**), 4-5.5µm pore size. Other, but seldom used, sizes are extra-coarse (**EC**, 170-220µm), very fine (**VF**, 2-2.5µm), and ultra-fine (**UF**, 0.9-1.4µm) filters. Some of the glass fritted filters are shown in Figure 46. The 'side-arm flask', named after the industrial chemist Ernst Büchner, is the most convenient vessel to accumulate the filtrate (often called mother liquor) during the filtration process (Figure 46). The Büchner flasks can have the top end as a rim, or a tapered glass joint, to accommodate glass filters with the joint (Figure 47).
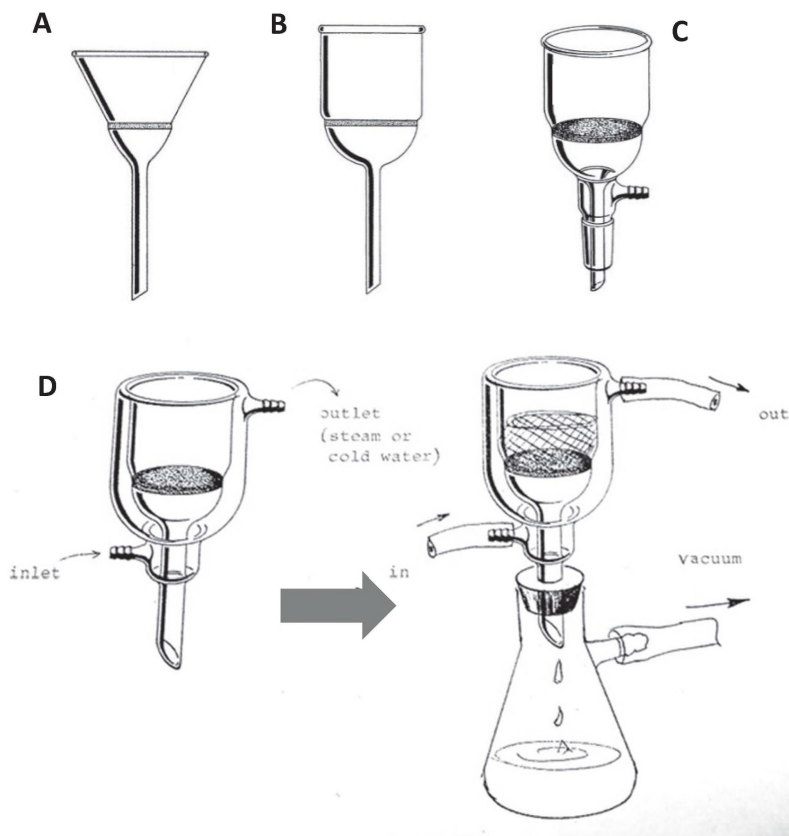
Figure 46. Normal glass frit filters (**A**,**B**), a glass filter with the joint and a suction tip (**C**), and jacketed filter for hot or cold filtration accompanied with the full assembly sketch (**D**).

Finally, the separation of fine solid materials, such as charcoal Norit® [**3**] from solutions can be achieved using quick 'plug filtration', depicted in Figure 48, below. This high surface area charcoal sorbent is widely used in synthetic laboratories for solutions' decolorizing and impurities absorption. Thus, an elongated fritted glass filter **A** is loaded with Celite® [**4**], or fine powder of $MgSO_4$, and the reaction mixture is filtered using either gravity (Figure 48**B**), or vacuum suction (Figure 48**C**). This type of filtration is often used during work with metallo-porphyrins, phtalocyanins or similar conjugated cyclic systems that are sensitive to acids. In that case, chlorohydrocarbon solvents such as CH_2Cl_2, $CHCl_3$,

$CHBr_3$, CCl_4 which, being exposed to the laboratory light, always contain traces of HCl or HBr, are quickly filtered through a plug of a dry K_2CO_3.

Figure 47. Büchner flasks for filtration. Barbed suction ends (side arms) are designed for tight soft rubber vacuum hose connection.
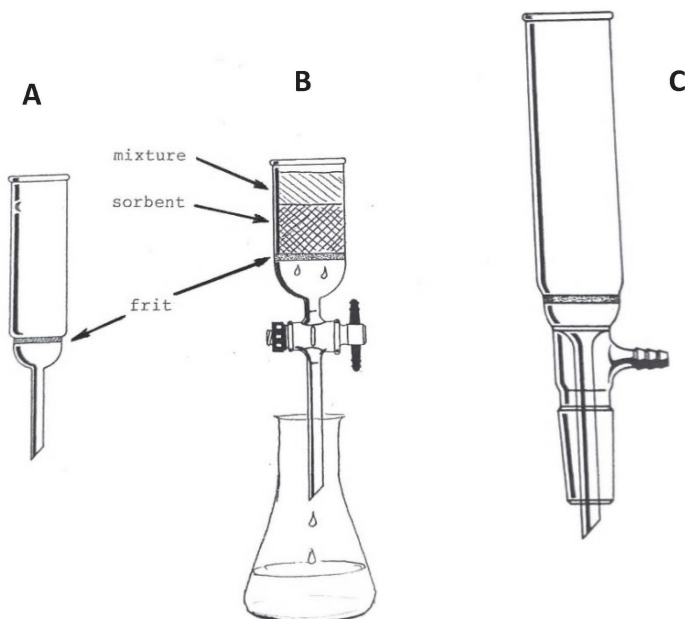
Figure 48. Types of glass filters for 'plug filtration': regular (**A**), with the stopcock (**B**), and with the joint and vacuum suction end (**C**).

Separation of compounds by extraction

In many cases, compounds of interest do not form saturated solutions, or just the opposite – precipitate out of it. Therefore, an extraction procedure is needed. An extraction is a laboratory operation that is based on the solubility difference of a compound of interest in two immiscible solvents placed in one container. This leads to the distribution of the substance of interest between two layers, and partitioning when equilibrium is attained. The extraction is performed with fresh portions of immiscible solvent until all product of interest is removed from the reaction mixture.

Technically, there are two different sets of glassware which have to be used to perform an extraction of solids/liquids from mixtures. One set is designed for manual procedures, while the other one is for an automated, continuous operation. Figure 49 contains images of the separation funnels most commonly used in the laboratory.
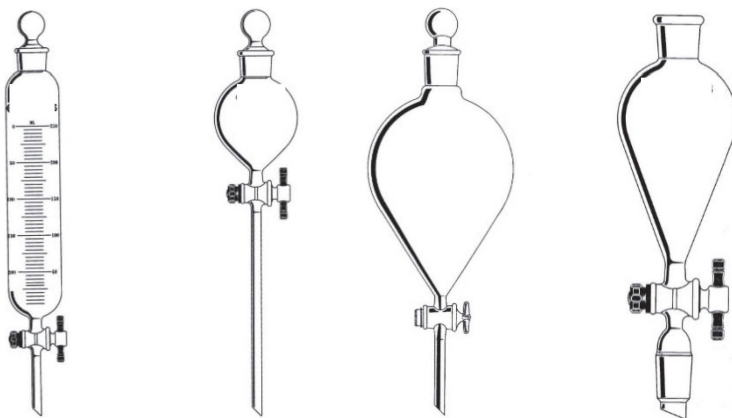
Figure 49. Shapes of commonly used separatory funnel: graduated funnel, small round with a long stem, large, pear-shaped, and that with joint.

All of these must have a stopcock for draining depleted or enriched solutions. When a solvent in which the compound needing to be separated and isolated is accumulated has density greater than that of water, it will be collected at the bottom of the funnel and can be easily drained. For example, these are systems such as water-CH_2Cl_2, water-$CHCl_3$, water-$CHBr_3$, water-CCl_4, and water-C_2Cl_4. When a solvent has density lighter than water, it is collected on top of the mixture, and the aqueous layer has to be drained, leaving the valuable solution in the separatory funnel. For

instance, these systems are water-ether, water-ethylacetate, water-toluene, water-hexane, etc. Glass-bodied stopcocks must be thinly lubricated with grease to prevent dissolution into organic solvents, and to keep contamination of the solution of the product of interest, to the minimum. For work with hydrocarbons, a special grease based on a carbohydrates/glycerol mixture should be employed [**5**].

An extraction apparatus (Soxhlet) for continuous solid-to-liquid extraction is shown in Figure 50. It was invented in 1879 by Franz von Soxhlet [**6**], and this apparatus is ideal for unmanaged and unattended extraction of a compound of interest (regardless of its physical shape – liquid, or solid!) from solids. These could be natural materials, such as bark, seeds, leaves, etc., or sorbents, after column or preparatory chromatography, which contain absorbed/separated desired compounds. A thimble with solid material is placed inside the main Soxhlet apparatus body, and the solvent, in which the compound of interest is soluble, is washed out in a continuous fashion.

glass thimble (to be filled with a solid for extraction)

large joint condenser

and

large mouse Soxhlet body attached to a flask with the solvent for extraction
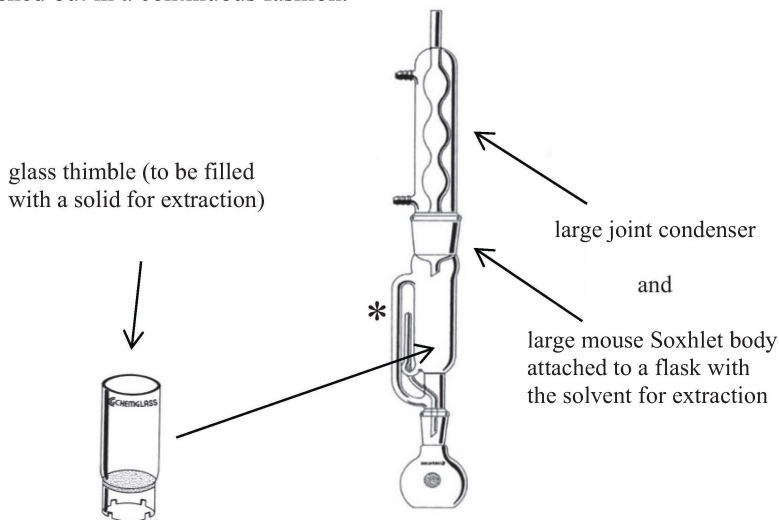
Figure 50. The Soxhlet apparatus assembly.

When a liquid is extracted from a liquid, a different type of apparatus for continuous liquid-to-liquid extraction is used (Figure 51). The main feature of both types of continuous flow extractor is a drainage pipe that works as a syphon, allowing an overflow liquid to escape from the chamber where solid and solvent, or two immiscible liquids, are located.

The Soxhlet apparatus is widely used in synthetic laboratories in different areas of chemistry, while liquid-to-liquid extractors are mostly used in medicinal chemistry, natural products chemistry, or in the petroleum industry.
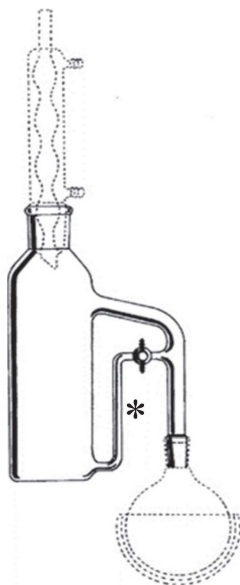
Figure 51. The assembly of a typical liquid-to-liquid extractor.

1.2.2 Sources of vacuum, measuring vacuum, and cold traps

The term 'vacuum' reflects conditions when pressure in the system is less than atmospheric. The pressure is customarily expressed in torrs (mm of Hg, named after Evangelista Torrichelli, an inventor of the barometer [7]), or, in the SI system, in Bars (1 torr = 0.00131 bar = 0.0013 atm). Vacuum is roughly divided into three categories: a) low vacuum (700 – 1 torr); b) medium vacuum (1 – 1·10^{-3} torr); and c) high vacuum (> 0.1·10^{-3} torr). There are several types of vacuum pumps normally used in the synthetic chemical laboratory for different purposes. They can be categorized by their main principle of action as:

1)   *Mechanical pumps* (most types use oil). These are forepumps, roughing pumps, and membrane pumps. All have vanes and intake/exhaust valves. They normally deliver vacuum in the range

of 0.1 to $5 \cdot 10^{-4}$ torr. A basic schematic of how mechanical oil-laden pumps work is shown in Figure 52.
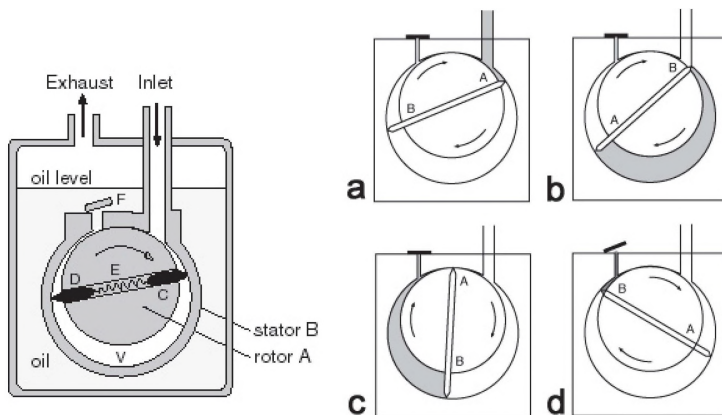
Figure 52. Principal components of the mechanical pump (left), and four stages of its action during generation of vacuum (right panel), with shaded areas here indicating movement of air during intake (a), and final exhaust (d).

Mechanical oil-containing pumps always contain an electric motor that makes pumps work. The latter are typically belt driven, or have direct drive connection to the motor (Figure 53). Good advice is to keep these rather heavy and vibrating machines on a cushioning pad (Figure 53**A**), and to keep oil from eventually seeping out of pumps in a shallow pan (Figure 53**B**). The latter is an inexpensive piece of household kitchenware, but is very useful for keeping the lab clean.

An oil that is normally used in such pumps must keep low vapor pressure at all times, even during long hours of work when it gets warm. Therefore, good quality and homogeneity of oil is essential, and that provides the necessity for traps, which prevent moisture or organic solvent from pump oil contamination. Thermal cracking of oil during operations at elevated temperatures (because of the friction of the pump's mechanical parts) provides the need for oil change when it changes color, from clear off-white to brown, sometimes with a significant turbidity.
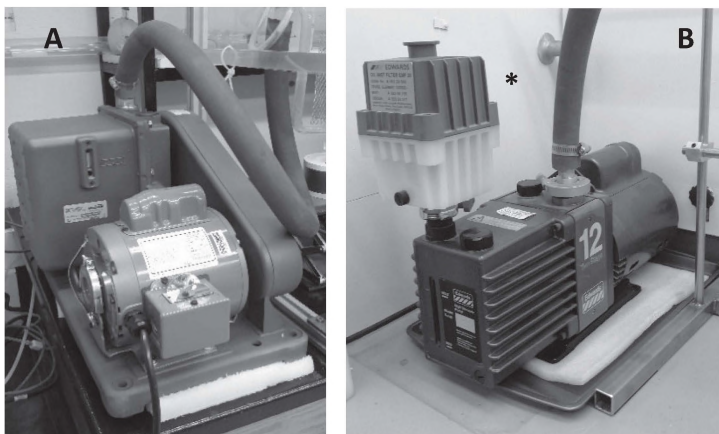
Figure 53. The belt-driven (**A**), and direct-drive (**B**), oil-containing vacuum pumps. Styrofoam cushioning is shown by arrows, while the mist trap is indicated as *.

2)   *Entrainment pumps*: diffusion pumps and turbomolecular pumps.

The most widely used entrainment pumps in the laboratory are water pumps, or aspirators, which can easily deliver vacuum from 750 to 25 torr, in controlled fashion. The lowest limit is, of course, tight to the water vapor pressure at a particular lab temperature. A typical aspirator is depicted in Figure 54. An intense water flow is required for the pump's proper operation. Attention should be paid to: a) the possibility of the pump clogging by solid particles accidentally sucked through the main hose; and b) the possibility of flooding if the outer hose is dislodged (popped-up) from the drain, because of water pressure oscillations during the day.

Diffusion oil pumps, however, can generate high vacuum beyond $1 \cdot 10^{-4}$ torr, whereas turbomolecular pumps create even better vacuum; one order of magnitude better. Before this last kind of pump can efficiently work, a pre-vacuum less than 0.1 torr must be created. A basic principle of operation of the oil-filled high vacuum pump is presented in Figure 55.

Figure 54. Actual photograph of a plastic-made aspirator under the ventilation hood.
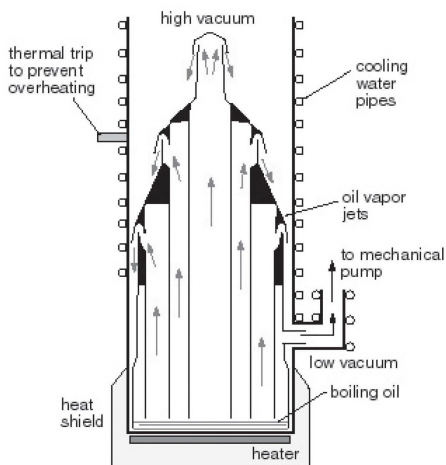
Figure 55. Schematic diagram/cross-section of an oil diffusion pump. Arrows indicate the flow of oil vapors. The top of the picture is the place where the pump is attached to the system and where the highest vacuum is generated.

3)   *Entrapment pumps* remove gas particles from the system in several ways: a) by deep cooling – cryopumps; b) by gas sorption using molecular sieves; and c) by gases' chemical reactions. For example, remains of N_2 and O_2 are reacted with hot Ti, or other suitable pure metal vapors (Ba). These pumps can achieve up to $1 \cdot 10^{-7}$ torr

pressure, but in order to be able to do that, a pre-vacuum from an oil diffusion pump must be delivered first.

All pumps described here have their own specific productivity, which is expressed as speed in L/sec, at the maximum delivered vacuum.

Vacuum can be measured in several ways. The most common way of measurement in the laboratory is the use of electronic gadgets which have completely replaced the old-fashioned, liquid mercury-filled McLeod vacuum meters [8], which, if broken, were one of the main sources of premises contamination by Hg. These meters are thermocouple or ionization gauges (Figure 56). The first one utilizes the principle of heat dissipation by surrounding gas; the less gas around the sensor (good vacuum), the hotter the filament, and the higher the temperature measured by the thermocouple. The ionization gauge works differently; in a poor vacuum, plenty of gas molecules can be ionized by the high voltage in a special tube, and some electric current can be determined. Upon pumping and vacuum improvement, the amount of gas in the electronic tube gets smaller and smaller, and the amount of ionization current traces it, following the same trend.
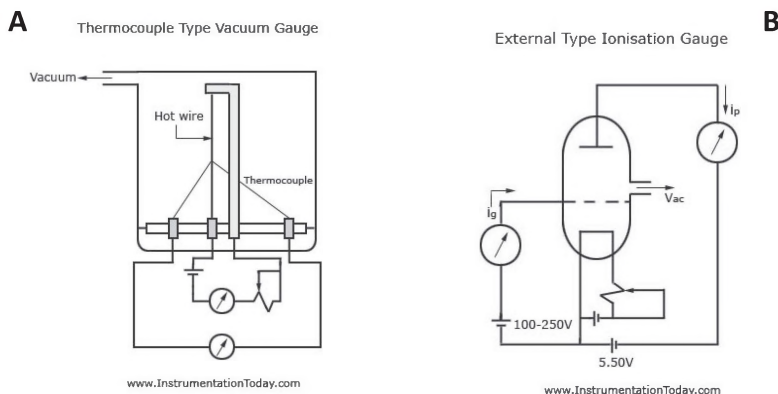
Figure 56. Schematic representation of the principles of the work of thermocouple (**A**) and ionization (**B**) vacuum meters.

Vacuum regulation is a more complex and difficult topic, and requires a special, electronically-controlled valve system which maintains the desired vacuum. Some high-end rotary evaporators have built-in analogous or

digital vacuum regulators [**9**]. This subject, however, is out of the scope of this current manual, and can be explored in detail in other references [**10**].

Cold traps are pieces of labware, made of glass or metal, designed to prevent volatile compounds from solids, solutions, or reaction mixtures entering oil-based vacuum pumps upon drying. Glass-made cold traps have a variety of sizes, but are all made of Pyrex/Kimax-type, thermally stable, glass, for obvious reasons; while in operation they will be inserted into Dewar's flasks filled with cryogenic mixtures/liquids. Typical glass cold traps are shown in Figure 57. There are separable, easy-to-clean, cold traps with large-size tapered joints (Figure 57**A**), and non-separable traps (Figure 57**B-D**). The latter tend to maintain a better vacuum during operation. Traps **A-C** are for outer cooling, while trap **D** is for inner cooling, and is also designed for convenient drainage of the condensate during prolonged operation. A lower, barbed outlet is for connection to the system, while the upper outlet is to be connected to the vacuum pump.
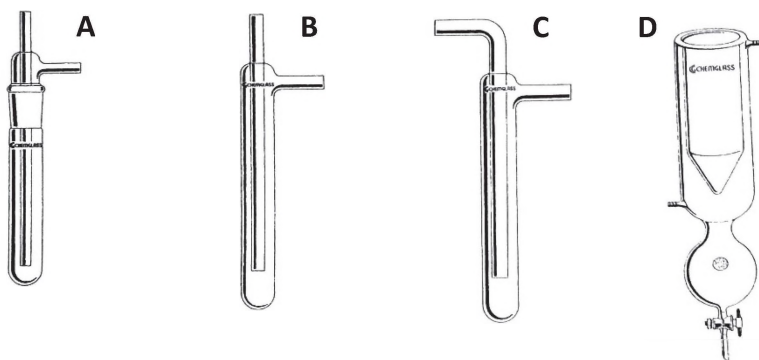
Figure 57. Commonly used glass cold traps: **A** – separable, **B-D** – non-separable.

A schematic drawing of a setup for vacuuming flasks, sublimators, etc., is shown in Figure 58. There are two high-vacuum stopcocks – 2-way and 3-way – which are necessary to separate the oil pump from the system in order to manipulate safely, and to be able to change objects, or refresh the cold trap.
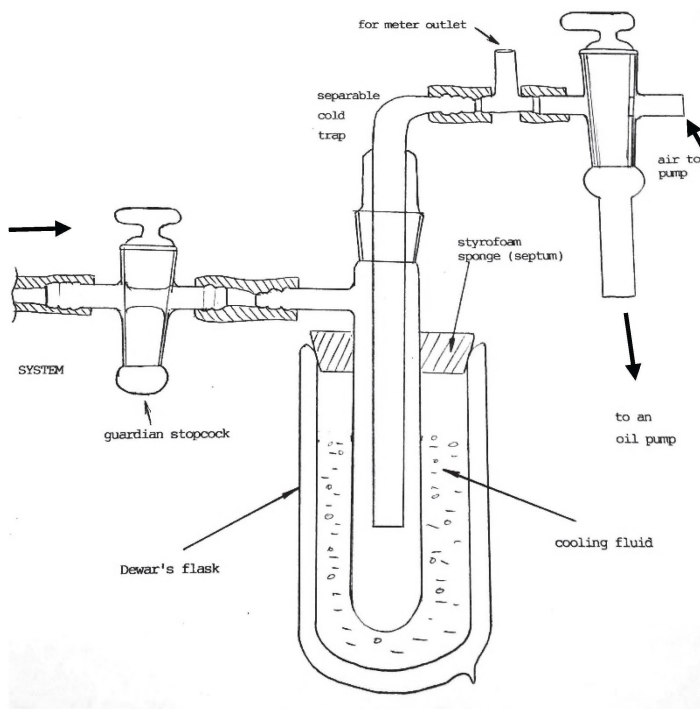
Figure 58. Schematic drawing of a proper setup for using the cold trap and vacuum stopcocks in the chemical laboratory.

High-vacuum glass stopcocks are shown in Figure 59. A thin layer of petroleum-based lubricant is required for their proper use. Despite centuries of laboratory use in different fields of science, they have several disadvantages: 1) if they are not used often, the grease thickens and sometimes plugs get seized; and 2) the glass plug may be lost, due to the system pressure changes in Schlenk lines or manifolds (the plug pops-up). In order to keep these vacuum stopcocks operational for a long time, periodic rotation or re-lubrication is necessary. Also, a loose fabric strand can be placed around the stopcock assembly, to prevent accidental popping out of the glass barrel.

Recently a new system of grease-free high vacuum stopcocks, with glass-threaded Teflon plugs was developed, and gained popularity in synthetic laboratories (Figure 60). Two types, with outer (**A**), and inner (**B**) glass

threads, are very common in manifolds and Schlenk lines these days (Figure 60).

Figure 59. High vacuum stopcocks; 2- and 3-way, with hollow plugs.
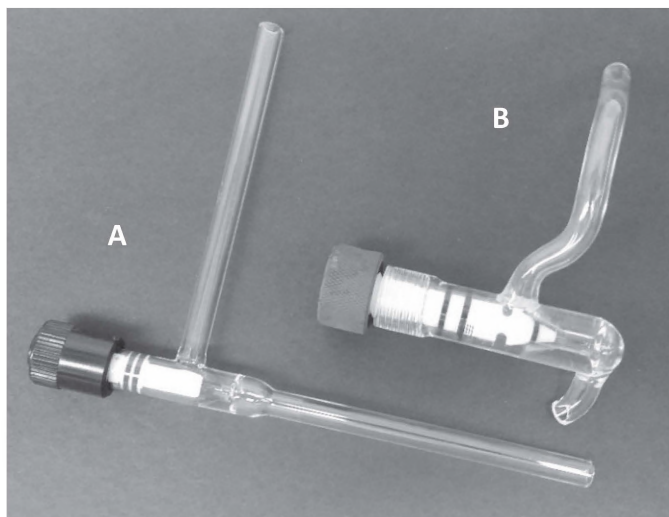
Figure 60. High vacuum 2-way ventils with glass thread and Teflon plugs. Multiple rubber O-rings provide tightness.

Cited References

1. a) https://glossary.periodni.com/glossary.php?en=Buchner+funnel;
   b) http://www2.ohlone.edu/people/jklent/labs/101b_labs/buchner.pdf
2. a) https://www.camlab.co.uk/buchner-flasks-glass-p17457.aspx;
   b) https://www.deviantart.com/theinvertedtower/art/Chemistry-Laboratory-Equipment-Buchner-Flask-442107885
3. a) Norit® http://www.cabotcorp.com/solutions/products-plus/activated-carbon;
   b) https://www.sigmaaldrich.com/catalog/substance/
   activatedcharcoalnorit1201744044011?lang=en&region=US
4. a) Celite® :
   http://umich.edu/~chemh215/W14HTML/SSG1/SSG1.2/Celite.html
   b) https://www.youtube.com/watch?v=oAzScPuZqjU;
   c) https://www.fishersci.com/shop/products/celite-545-filter-aid-powder-fisher-chemical-3/p-31544
5. A. Gordon, R. Ford. *Chemist's Companion: A Handbook of Practical Data, Techniques and References*. Wiley Interscience Publication; New-York – London – Toronto – Sydney, 1972.
6. a) Soxhlet, F.: Die gewichtsanalytische Bestimmung des Milchfettes, *Poly technisches J.* (Dingler's) 1879, *232*, 461;
   b) Rommel, Otto: Franz von Soxhlet Münchener. *Medizinische Wochenschrift* . 1926, *73*, 994–995
7. Jervis-Smith, Frederick John (1908). *Evangelista Torricelli*. Oxford University Press. p. 9. ISBN 9781286262184.
8. McLeod, Herbert. "Apparatus for measurement of low pressures of gas". *Philosophical Magazine*. xlviii: 1874, 110–113.
9. http://www.buchi.com/us-en/products/laboratory-evaporation/rotavapor-r-300?gclid=EAIaIQobChMIqJmR0bm82AIVgSWBCh0tVANPEAAYASAAEgKKnfD_BwE
10. a) http://www.acrossinternational.com/JKEM-DVR-200-Digital-Vacuum-Regulator-DVR-200.htm;
    b) https://www.thomassci.com/Equipment/Viscometers/_/DVR-1000-DIGITAL-VACUUM-REGULATORS

1.2.3 Distillation and reflux

Reflux is a process of heating and boiling a solvent or reaction mixture, at conditions when evaporating liquid gets returned back into the vessel (flask, vial, reactor, etc.), due to the condensation of vapors in condenser placed on top of the system.

Typical apparatus for reflux includes a flask, condenser, and drying tube (end tube), as shown in Figure 61. This setup is commonly used when a reflux procedure is designed for purification of the solvent when it boils over an appropriate chemical agent. Thus, alkali metals (Na, K, or their alloy) are present during deep dehydration of ethers, and aromatic and normal hydrocarbons. At the same time, P_2O_5 is used when dry CH_3CN, benzene, or CH_2Cl_2, is needed. The CaO is used for the drying of alcohols prior to their distillation. Sources of heat are hotplates, hearing mantles, or oil/water baths. The drying tube must be attached to the top of the condenser, to prevent moisture entering the system.

The reflux procedure is very often used during chemical synthesis procedures. Both two- and three-neck reactors are commonly used (Figure 63). In the latter case, either purging gas (N_2, argon), or the addition of a reactive gas (Cl_2, CO_2, CO, H_2S, etc.) is achieved using the third neck.

To provide efficient solvents' vapor condensation into liquid, an efficient condenser is needed. There are two types of continuous flow condensers in use for the reflux and for the distillation; straight, or Liebig condensers (Figure 62**A**). Reflux condensers, in turn, can be further classified by the boiling point of the solvent; low boiling point/high vapor pressure solvents (below $+70^oC$) require very efficient devices with a large cooling surface area for safe operations, achieved by the use of coils (Graham and Dimroth condensers), or 'barbed' inner tubes (Allihn and Friedrichs condensers) (Figure 62**A**). In many cases, however, it is not good enough, and double water-jacketed condensers are used (Figure 62**B**). The cooling water flow in condensers always goes from the bottom to the top of the glassware. Finally, instead of tap water, a cooling liquid from the refrigerator/thermostat, with an operating temperature below the freezing point of water, is often used. In such cases, insulated cooling water lines are needed (see Figure 33**B**, Part 1.1), and those systems are especially effective during work with highly volatile solvents, such as CS_2, CH_2Cl_2, CH_3Cl, CH_3Br, methyl-ethyl ether, etc.

Reflux operation is also possible for liquids and solvents with boiling temperatures below $+20^oC$. These are, for example, liquid at ambient conditions, NH_3, SO_2, CH_3NH_2, $(CH_3)_2NH$, trimethylamine. A special type of inexpensive top-filled condenser is needed, and an example

of the experimental setup is shown in Figure 64. The most economical cooling mixtures are: 1) ice/salts (Part 1.1., in the section titled "Heating/Cooling Devices"); and 2) dry ice, widely available everywhere. The drying tube in this setup is much larger, and is a convenient, U-shaped tube which has to be clamped near the reflux system. Typical drying agents are granulated SiO_2 (for work with SO_2, SO_3), or NaOH pellets during work with amines.

The absolute necessity of a free gas/air passage through the tube should be emphasized! A clogged drying tube of any shape creates unsafe conditions for operations, and may lead to over-pressuring the system, and possible explosion.
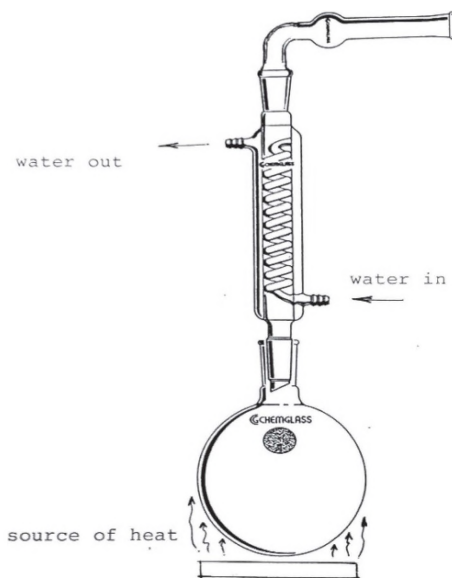
Figure 61. Principal setup for the reflux operation.
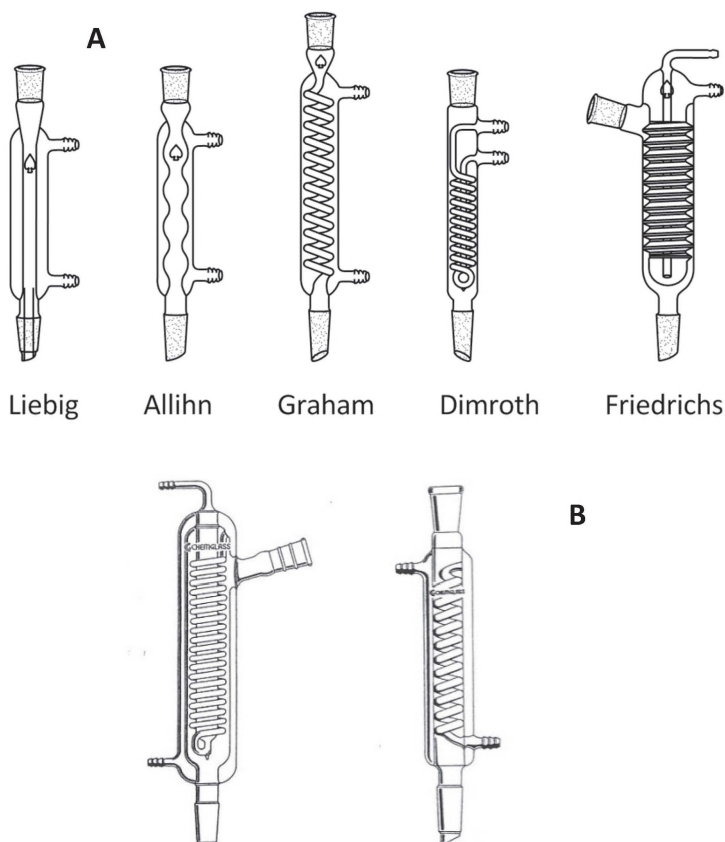
Figure 62. The reflux and distillation (Liebig, straight) condensers (**A**), and the most efficient double-jacketed condensers (**B**).

Finally, reflux operations are widely used in synthetic laboratories dealing with preparation and studies of organometallic compounds, and more specifically in numerous 'stills' (Figure 65). These are continuous-work glassware devices, comprised of the still-head and condenser, and a positive pressure of protective inert gas (dry N_2 or Ar) is constantly maintained through the system as a slow, continuous flow of these gases. The beauty and advantage of the use of stills is access to a freshly distilled, pure, and anhydrous solvent. Many varieties of still-heads are designed and manufactured by major glassware companies, and the chemist may select the type that is the best fit for the work intended.
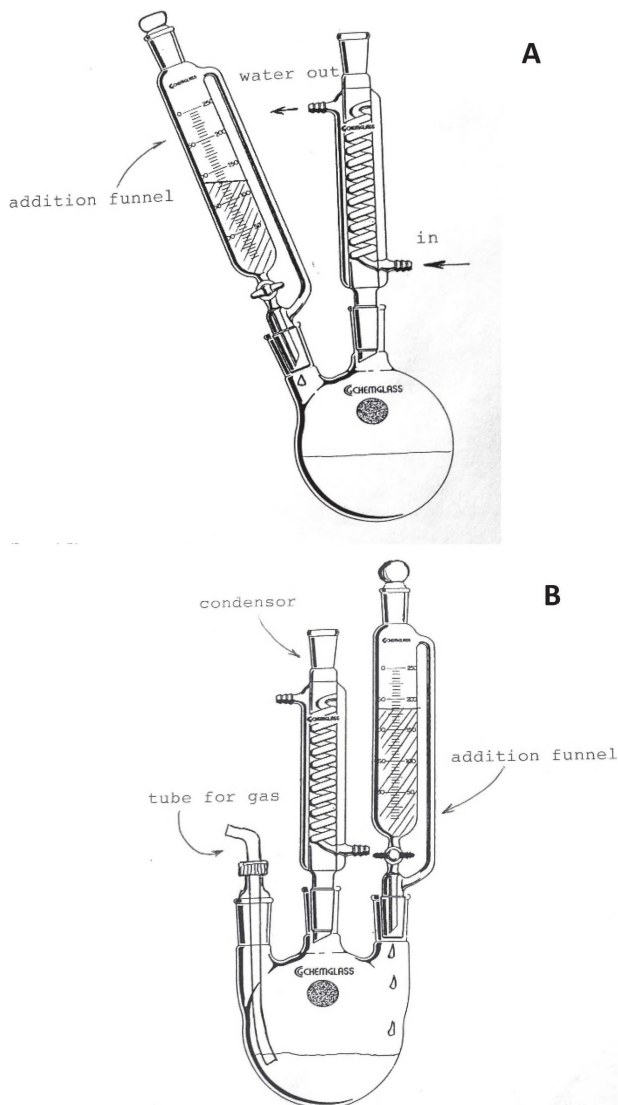
Figure 63. Examples of common setup for reflux, using two-neck (**A**) and three-neck (**B**) reactors.
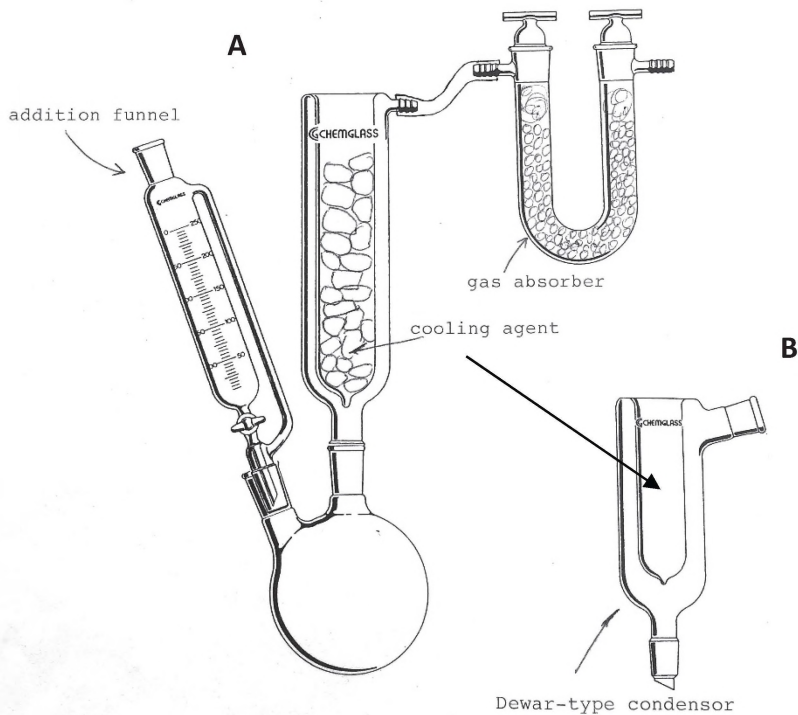
Figure 64. Reflux apparatus for below-room temperature solvents (**A**), and condenser with the top joint for connection to other glassware pieces (**B**).
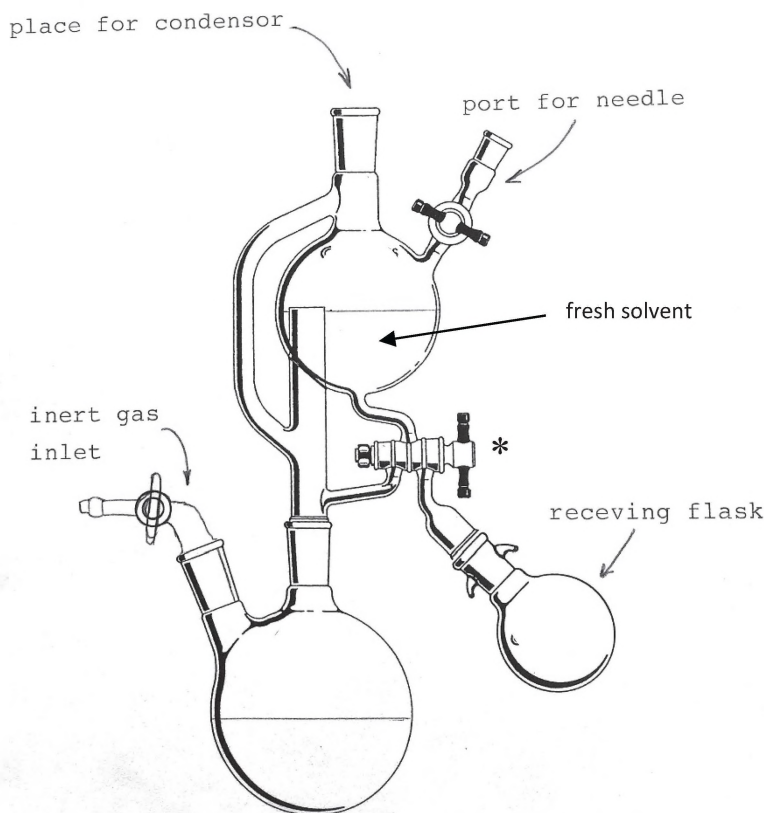
Figure 65. A still-head apparatus principal scheme. An asterisk identifies a three-way stopcock that allows either return of the solvent back to reflux, or allows its drainage into the receiving flask.

Distillation is a process of separation of a liquid mixture into its components on the basis of differences in boiling points. That is, the volatilization or evaporation of a liquid and subsequent condensation of it into another vessel. The principal components of a simple distillation apparatus are depicted in Figure 66. Attention should be paid to the position of the thermometer; it should be next to the opening of the distilling adapter of the condenser, to reflect properly the process' temperature! A lower or higher position of the measuring part of a

thermometer will give inaccurate readings which will affect the fractional distillation process.
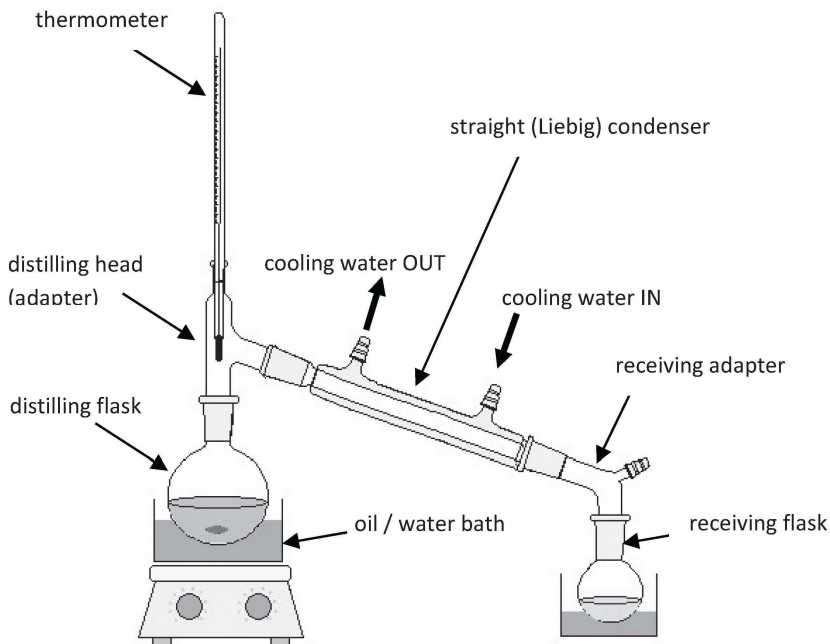
Figure 66. Schematic drawing of the distillation process, with indication of all necessary glassware components (6!) in this classical setup.

Shown in Figure 66, the system has several taper joints that require proper alignment to alleviate the strain in the assembled apparatus. Although this multicomponent system is very inexpensive, it is somewhat cumbersome to assemble. Hence, numerous other designs have emerged, and have been introduced into laboratory practice. There, we have several components fused into one piece, as shown in Figure 67. Thus, one-piece distillation assembly made work much more convenient, but added a concern about the fragility of such devices, especially during the cleanup procedure. An elongation with inward-pointed glass barbs on the distillation head adapter is called a *dephlegmator* (Figure 67**A** and **C**). This is a device that has a large surface area due to barbs, and provides partial condensation of a

multicomponent vapors stream. The vapor stream flows vertically upwards, and the condensate (condensed vapor) runs back down under the influence of gravity. The vapor stream and condensate thus move counter-currently, and are in direct contact with each other. In addition to heat transfer between the vapor stream and cooling medium, mass is transferred between the rising vapor and falling condensate. Vapor leaving the device has become concentrated in the more volatile components, while the condensate is richer in the less volatile components. This is an important basis for a *fractional distillation,* at which individual components of the liquid mixture can be successfully separated, based on the boiling points difference (assuming the absence of the *azeotrope* – see below).
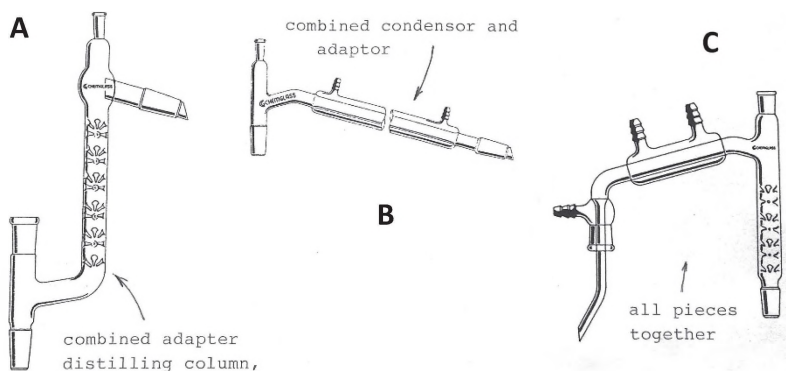
Figure 67. Different types of fused, one-piece components of distillation setup.

In order to segregate fractions upon such distillation, a special distributing adapter was invented with a set of two (also called a 'cow adapter'), shown in Figure 68. Simple rotation of this adapter around either a straight or a bent adapter (Figure 68) allows easy separation of individual fractions, which are segregated by different boiling points, into individual flasks.

straight receiving
adapter

bent receiving
adapter

distributing adapter
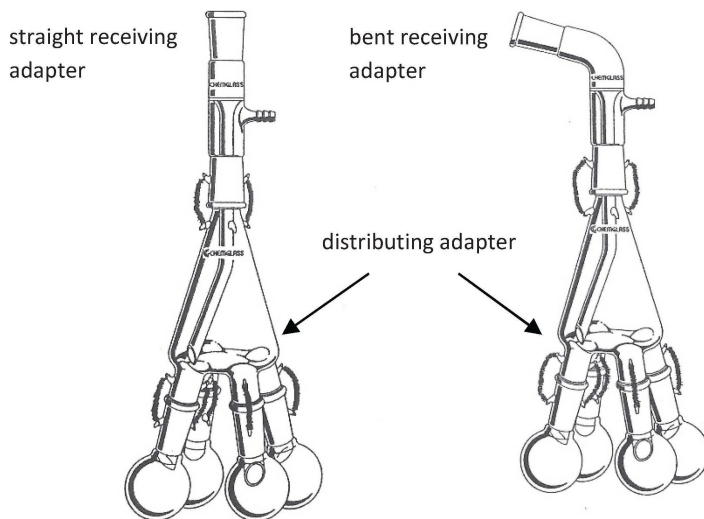
Figure 68. Receiving adapter connected with fractional distribution adapter, with attached flasks for individual fractions.

A special case of distillation shows the use of rotary evaporators, also called *rotovaps*. The introduction of this device truly revolutionized synthetic chemistry, especially organic and medicinal, because it dramatically increased the productivity of work in a laboratory. The most common setup is presented in Figure 69. It is a relatively complex system, consisting of a temperature-regulated water bath, a support that holds a large and efficient water-cooled condenser, and an electric motor with a spinning device. It allows a rotation of the flask with the reaction mixture, out of which a solvent has to be evaporated, through a special vacuum-seal gasket. An aspirator pump is typically used, and the created vacuum allows fast removal of the solvent from the mixture, leaving solid material in the evaporation flask for further processing (Figure 69). Even a low-grade vacuum allows solvents to boil at much lower temperatures. A membrane pump is often used instead of the aspirator. The refrigerating thermostat is used to cool the condenser, low enough to liquefy vapors of ether, CH_2Cl_2, acetone, etc., into the receiving flask. The latter is also often cooled with ice, for more efficient solvent(s) condensation.

In order to cut the cost of laboratory operations, collected individual solvents after the use of the *rotovap* are reprocessed and reconditioned for future work. In fact, this practice of solvent recovery has been used for many years in the author's research laboratory. It provides a valuable teaching and learning tool for students involved in the research process.
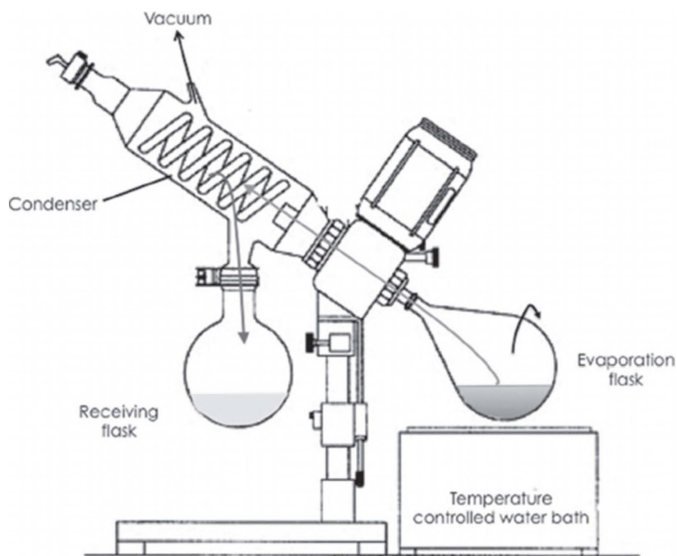
Figure 69. Principal scheme of the *rotovap* – rotary evaporator.

1.2.4 Azeotropes

When processes of reflux and distillation are discussed, it is impossible to skip the topic of azeotropes. The word comes from the Greek language, meaning '*azeos tropos*' – αζεοσ τροποσ – 'boiling without separation'. An azeotrope is a mixture that exhibits the same composition in the vapor phase and the liquid phase. If the mixture forms an azeotrope, the vapor and the liquid phase have the same percentage composition of components. Therefore, a separation via distillation is not possible. There are *positive* and *negative* azeotropes. A positive azeotrope boils at a lower temperature than any other ratio of its constituents. Similarly, a negative azeotrope boils at higher temperature than the mixture. Examples of some azeotropes are given in Table 3.

Azeotropes play an important role in synthetic chemistry, especially in industrial manufacturing. There are several important applications:

1) The most important benefit of an azeotrope is the unexpected ability to mix flammable and nonflammable ingredients to produce a stable nonflammable mixture.
2) Another benefit of azeotropes is that they are very easy to distill and recover, and the solvent can be boiled and recycled. Meanwhile, the contamination — the non-azeotropic material, such as powders, fluxes, oils, water, etc., stays 'trapped' in the evaporating flask. In effect, using azeotropic solvent mixtures allows the separation of contamination using distillation, instead of more energy-demanding processes, such as press-filtration and membranes.
3) The formation of an azeotrope is essential during the production of active pharmaceutical ingredients (later abbreviated as API), because it allows the removal of unwanted or toxic solvents (which are trapped in microcrystalline powders, or adsorbed on the surface), used in manufacturing these compounds. Thus, an addition of a small quantity of another appropriate, non-toxic solvent, which is able to form an azeotrope, provides conditions for the evaporation of both.
4) Most azeotropes are positive, and, therefore, it is an energy-efficient and cost-efficient way of removing solvents by evaporation.

Table 3. Some selected azeotropes useful for synthetic laboratory work. Boiling points are in °C.

Solvents	Composition, v %	mixture b.p.	individual solvent b.p.
Double azeotropes:			
acetone	59	*50*	56.2
n-hexane	41		69
benzene	68	*68*	80.1
ethanol	32		78.3
benzene	61	*58*	80.1
methanol	39		64.5
chloroform	93	*59*	61.7
ethanol	7		78.3
chloroform	87	*53*	61.7
methanol	13		64.5
acetic acid	51	*138**	118.1
pyridine	49		115.6
Triple azeotropes:			
chloroform	91	*78*	61.7
ethanol	5		78.3
water	4		100
chloroform	81	*53*	61.7
methanol	15		64.5
water	4		100
ethanol	12	*56*	78.3
n-hexane	85		69
water	3		100
ethanol	37	*74*	78.3
toluene	51		110.6
water	12		100

*- negative azeotrope

1.2.5 Air-free operations: related glassware and hardware

Laboratory work in anaerobic conditions can be done in two ways: a) inside the glove box; and b) using the benchtop Schlenk line and respective glassware. In numerous laboratories, when such experiments are necessary, both methods are employed due to their complementarity.

The glove boxes are expensive pieces of hardware, and require other auxiliary equipment, such as O_2-sensors, moisture sensors, sorbents regenerators, pumps/foot pedals, and controllers, etc. Thick protective rubber gloves are uncomfortable for work, and they become quite moist inside, because of the operators' work in them. However, inside the glove box, a normal set of glassware and hardware (which we described earlier) can be easily employed. The biggest advantage of the glove box is the ability to accurately weigh samples for chemical reactions, and to press pellets for the IR-spectroscopic studies. Detailed description of glove boxes and their operation is out of the scope of this book, but can be found in several other sources [1].

The Schlenk line represents a set of specialty glassware used for the complete isolation of reactants and products from the harmful conditions of open-atmosphere work. The name for the system came after the legendary work of German chemist Wilhelm Schlenk [2], who first designed sophisticated and elaborate pieces of glassware for safe work with compounds which are unstable in ambient conditions. Details of operations using this specialty glassware are beyond the scope of this book, but can be learned from several laboratory manuals specifically designed to present numerous syntheses of air sensitive compounds [3-5]. In this book, we outline only the basic principles of operation, and will show the most important pieces of this kind of glassware. Also, we offer a brief pictorial description of basic air-free operations with Schlenk-ware to interested readers, in *Appendix 1.*

The main principles behind the design and subsequent operations of anaerobic glassware are the complete avoidance of contact of solids and solutions, with atmosphere, and with the joints' grease that helps to connect pieces of glassware.
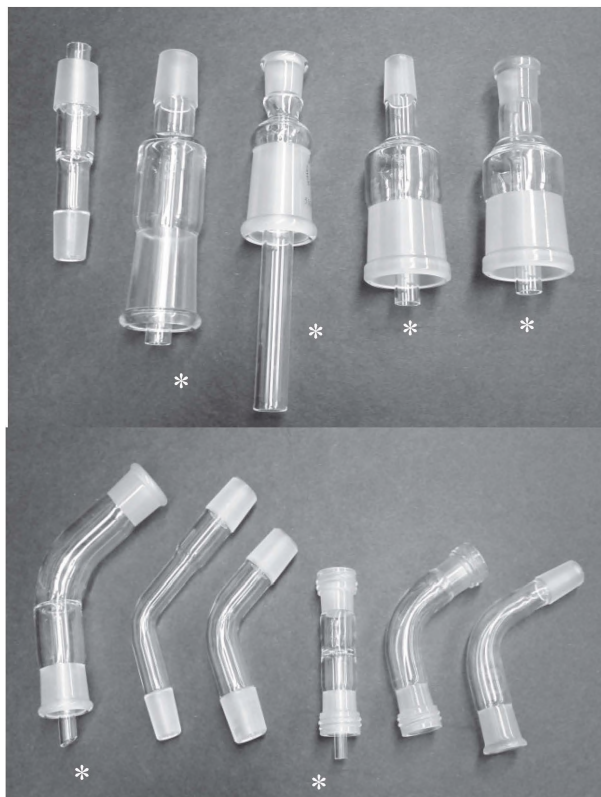
Figure 70. Reducing/enlarging joints adapters (top), and transfer adapters (bottom). Asterisks show inner tubes for substances' safe transfer.
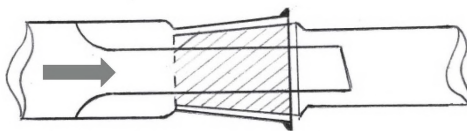
Figure 71. A pair of taper joints with inner tube for proper air-free glassware design. The direction of a flow of materials is indicated by the arrow.

The first one is addressed by the application of special adapters (Figure 70), while the second one results in using outer (male) joints and inner

tubes for compounds' transfer in all equipment (Figure 70, indicated by asterisks). In such cases, the absence of contact between solids or solutions with joints is guaranteed (Figure 71).

Adapters connect Schlenk flasks (Figure 72**A**), and tubes (Figure 72**B**). These can have both inner and outer joints, but attention should be paid to choosing a proper adapter that excludes possible contact between moving chemicals with joints, and, respectively, grease.

Lastly, stainless steel 2mm diameter cannulas pierced through rubber septa can be used for connection of pieces of glassware and safe transfer of solutions of air-sensitive compounds.
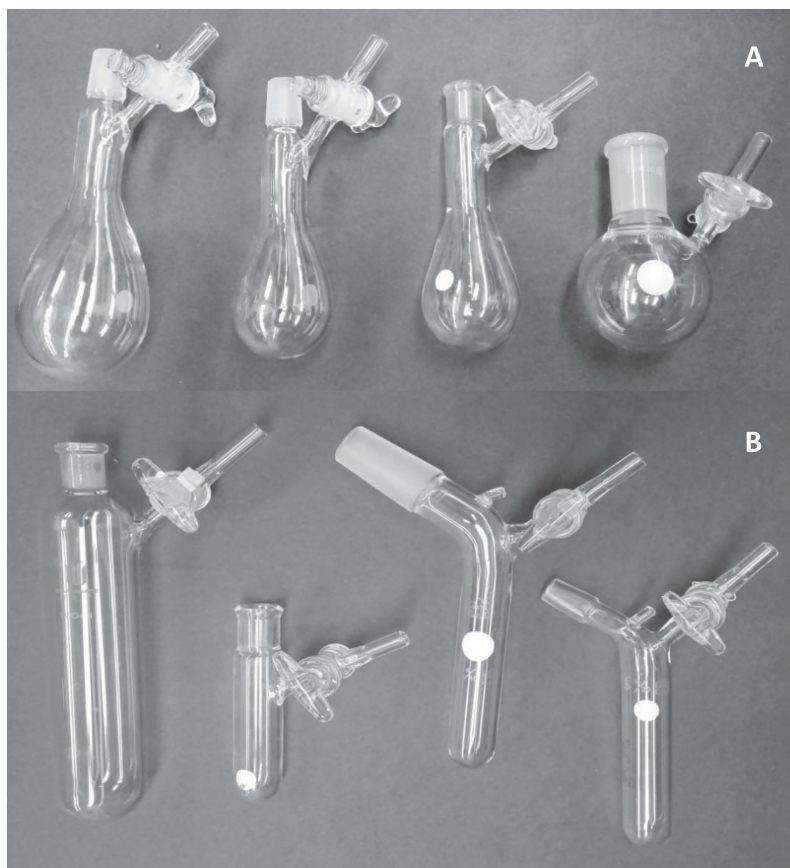
Figure 72. Schlenk flasks (**A**) and Schlenk tubes (**B**) with inner (female) and outer (male) joints.

Filtration also requires special filters that exclude contact with air and moisture (Figure 73). Details of the filtration procedure are given in *Appendix 1*.
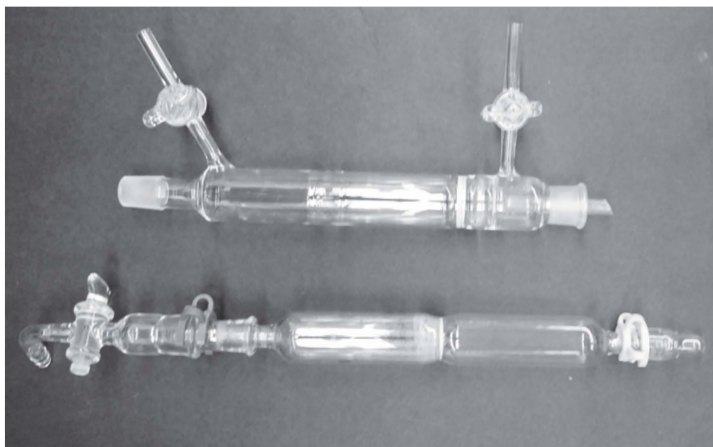
Figure 73.   Schlenk filters for anaerobic filtration.
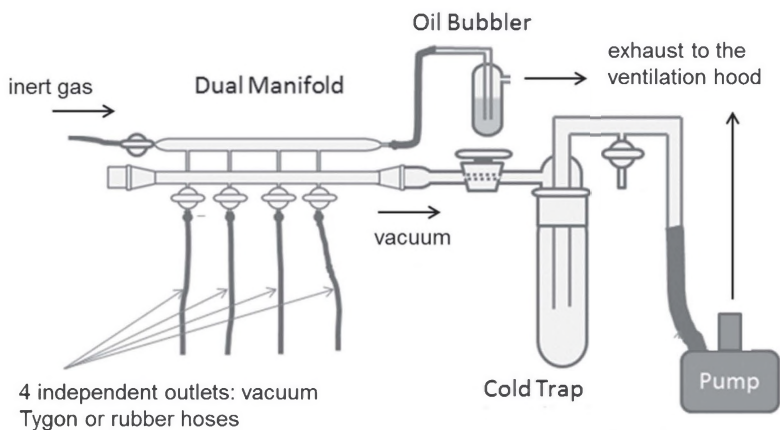
Figure 74. Principal diagram of the Schlenk line and its components.

In general, a system that provides insulation of the compounds of interest and guarantees air-free procedures, is depicted in Figure 74. The main advantage of such apparatus is convenience of use of several independent

outlets, that provide a flow of an inert protective gas (N_2 or Ar), and vacuum, on demand, by just turning specially designed stopcocks (Figure 75). Argon is much better for a protective atmosphere than nitrogen, because it is denser. Normally, an oil pump is used in Schlenk lines, as well as liquid N_2 filled cold traps to insure proper vacuum (typically ~10^{-2} torr) and extend the pump's lifetime. An oil bubbler is a useful piece which visualizes the flow of a protective gas.
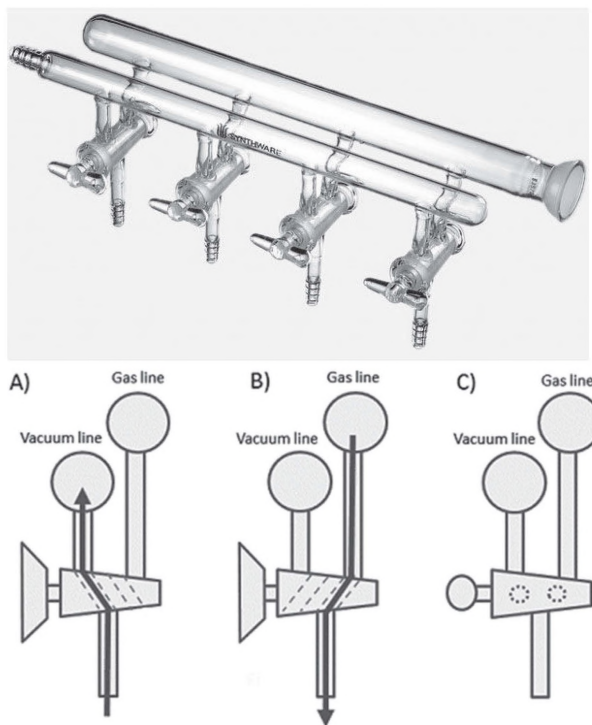
Figure 75. Glass 4-port manifold (**top**), its main feature of a three-way stopcock, and 'how it works' (bottom): **A** – vacuuming the system, **B** – filling with an inert gas, **C** - closed.

Finally, a series of anaerobic operations to isolate by drying, and work with the obtained solids, is presented in Figure 76. One of the authors has designed a set of air-free glassware, which was commercialized by Aldrich Chemical Co. some years ago [**6**].
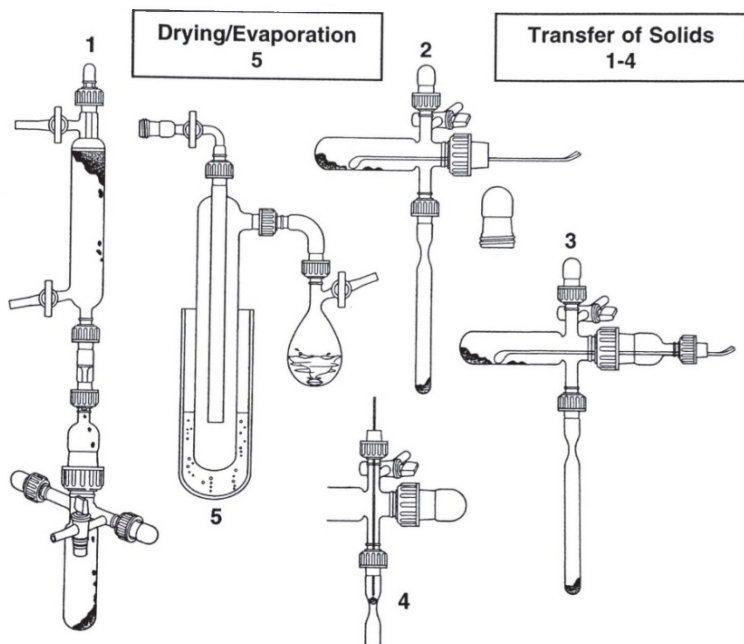
Figure 76. Schematic representation of the most common manipulations with air/moisture sensitive compounds.

Cited References

1. Glove boxes: Glove boxes:
    https://www.terrauniversal.com/glove-boxes/chambers-x.php
2. Thomas T. Tidwell "Wilhelm Schlenk: The Man Behind the Flask" *Agnew. Chem. Int. Ed.* 2001, 40, *2*, 331-337.
3. Andrea Wayda, Marcetta Darensburg "*Experimental Organometallic Chemistry*" ACS Symposium Series 357, Washington DC, 1987.
4. Duward F. Shriver, M. A. Drezdzon. *"The Manipulation of Air-Sensitive Compounds"*, 2nd Edition; Wiley, 1986.
5. R. J. Angelici. "*Synthesis and technique in inorganic chemistry*", W.B. Saunders Company, 1977.
6. a) *Aldrich 1991: new Products*. Brochure and mini-catalog, p.68-70; Aldrich Chemical Co, 1001 West St. Paul Ave., Milwaukee, WI 53233;
    b) Subsequent listing in all *Aldrich catalog*; for instance, in 2005-2006 catalog on E19-21, E26 in the glassware section and in other newer catalogs in the same section of "Air-free glassware".

1.2.6 Methods of generation of small quantities of common gases

Many gaseous substances can be obtained as products of thermal decomposition, dehydration, or composition reactions of inorganic salts and mixtures. For example, chemically pure gases such as N_2, N_2O, NO, NO_2, SO_2, H_2S, H_2Se, CO, CO_2, HCl, HBr, Cl_2 and O_2, in laboratory quantities (0.1–5 M, or hundreds of milliliters to dekaliters), can be conveniently obtained from these systems respectively:

1. $(NH_4)_2Cr_2O_7 \overset{+t}{=} N_2\uparrow * + 4\ H_2O + Cr_2O_3$

2. $NH_4NO_3 \overset{+t}{=} N_2O \uparrow + H_2O$

3. $2\ Pb(NO_3)_2 \overset{+t}{=} 2\ PbO + 4\ NO_2\uparrow + O_2\uparrow$ ***d, mixture***

4. $Cu + 2\ H_2SO_{4(conc)} \overset{+t}{=} CuSO_4 + SO_2\uparrow + 2\ H_2O **$ ***d***

5. $S + paraffin \overset{+t,\ \sim300^oC}{=} H_2S \uparrow$ ***d***

6. $Se + paraffin \overset{+t,\ \sim300^oC}{=} H_2Se \uparrow$ ***d***

7. $CH_2O \overset{+ H_2SO_{4(conc)}}{=} CO\uparrow + H_2O *$ ***d***

8. $2\ NaCl + H_2SO_{4(conc)} = Na_2SO_4 + 2\ HCl \uparrow$ ***d***

9. $2\ KBr + H_3PO_{4(conc)} = K_2HPO_4 + 2\ HBr \uparrow$ ***d***

10. $NaI + H_3PO_{4(conc)} = Na_2HPO_4 + 2\ HI \uparrow$ ***d***

11. $2\ Na_2SO_3 + H_3PO_{4(conc)} = Na_2HPO_4 + 2\ H_2O + SO_2\uparrow$

12. $2\ KClO_3 \overset{+t,\ \sim200^oC}{=} 2\ KCl + 3\ O_2 \uparrow$ ***d***

13. $\quad 2\,KMnO_4 \overset{+t,\ \sim250^oC}{=} K_2MnO_4 + MnO_2 + O_2 \uparrow$ $\quad\quad\quad\quad\quad$ d

14. $\quad CaC_2\ +\ 2\,H_2O\ = Ca(OH)_2 + C_2H_2 \uparrow$

15. $\quad Al_4C_3 + H_2O = Al(OH)_3 + CH_4 \uparrow$

16. $\quad 2\,H_2O_2 \overset{MnO_2}{=} 2\,H_2O + O_2 \uparrow$

17. $\quad ROH + NaNO_2 + H_2SO_4 = Na_2SO_4 + H_2O + R\text{-}ONO \uparrow$
    $\quad (R = CH_3,\ C_2H_5)$

18. $\quad 2\,KMnO_4 + 16\,HCl = 2\,MnCl_2 + 2KCl + 8\,H_2O + 5\,Cl_2 \uparrow$

19. $\quad FeS + 2\,HCl = FeCl_2 + H_2S \uparrow$

20. $\quad NH_4OH\ (\text{30\% solution}) \overset{NaOH\ pellets}{=} H_2O + NH_3 \uparrow$ $\quad\quad\quad$ d

*- Small arrows in the reactions above, and further in the book, indicate either formation of poorly soluble species, or gases, for reader convenience.
** dehydration reaction, or concentrated acid used as water retaining agent.

These small-scale reactions of the preparation cited above, pure, and in many cases dry, gaseous substances, have serious advantages over receiving these gases in compressed metal cylinders and tanks. Dry gases in preparations above are indicated by the *d* notation. Thus, thermal decomposition reactions are cost-effective in generating small quantities, as compared to pressurized gases in stainless steel cylinders which frequently need special and quite expensive gas regulators (for instance for HCl, Cl$_2$, CO$_2$, etc.). Typically, chemicals and glass/hardware required for thermal decomposition reactions are readily available and inexpensive. Also, all chemical generations of gases are carried out at ambient pressure, contrary to elevated pressures in gas cylinders. The latter itself poses certain safety risks, and frequently requires expensive specialized glassware.

The temperatures of decomposition reactions are commonly less than 300°C. Therefore, simple Bunsen gas burners or hotplates can be

conveniently used. Further details of simple methods of generation of the above gases, and also their detection, are described below.

Other widely-used useful laboratory reactions:

21. $Zn + 2\ HCl_{(dil)} = ZnCl_2 + H_2\uparrow$
22. $CaCO_3$ (marble chunks/chips) $+ 2\ HCl_{(dil)} = CaCl_2 + CO_2\uparrow + H_2O$
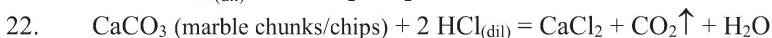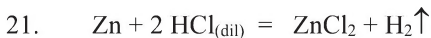
        Gases obtained in such way are wet, and require passing through drying towers over a drying agent, such as $CaCl_{2(anh)}$, $H_2SO_{4(conc)}$, or freshly activated silicagel SiO_2, as described in section 1.1.2 above (Figure 21). When there is interaction between solid substance and liquid/solution, the most quick and convenient experimental setup, using an addition funnel, is shown below in Figure 77.
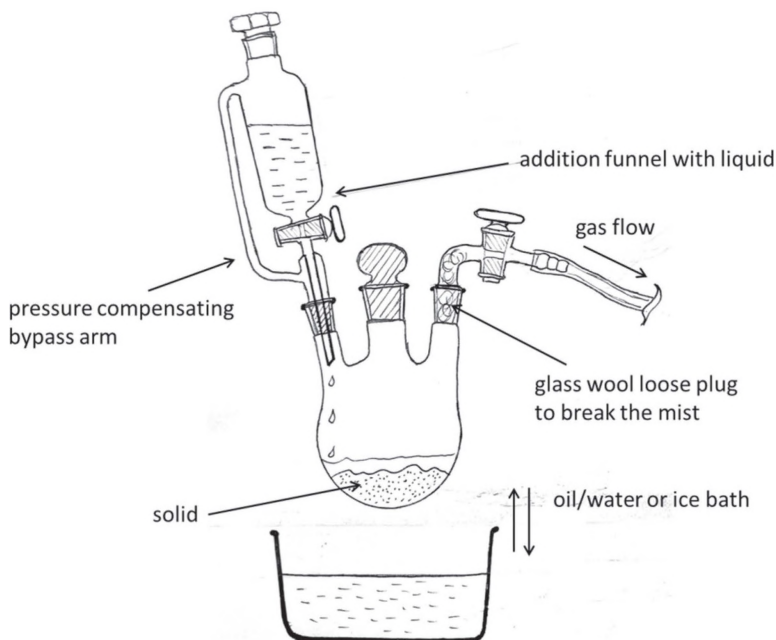
Figure 77. Simple method of generation of small quantities of gases during interaction between solids and liquids.

The rate of gas evolution in this setup is regulated only by the speed of addition of liquid (solution), and care should be taken not to over-pressurize the system. This method works very well for reactions **7**–**11**, **14**–**16**, and **20,** shown above, and was tested numerous times in the author's teaching and research laboratories.

The Kipp generator (Figure 78) was named after the Dutch pharmacist Jacobus Kipp, who invented it in 1844. This is an apparatus designed for preparation of small volumes of gases; 5–50L. It is still widely used in analytical (for the generation of CO_2 and H_2S), and synthetic chemical laboratories (for the generation of H_2 and HCl). With closed stopcock, the extra pressure of generated gas pushes liquid back to the upper globe until equilibrium is attained. Pressure release by opening the stopcock leads to gas escape and liquid flooding the middle globe, and the reaction of a gas generation continues. The most suitable reactions for the use of the Kipp apparatus are reactions **14**, **19**, **21**, and **22,** because of the availability of solids in large enough chunks/blocks to be loaded into the middle globe of the generator.
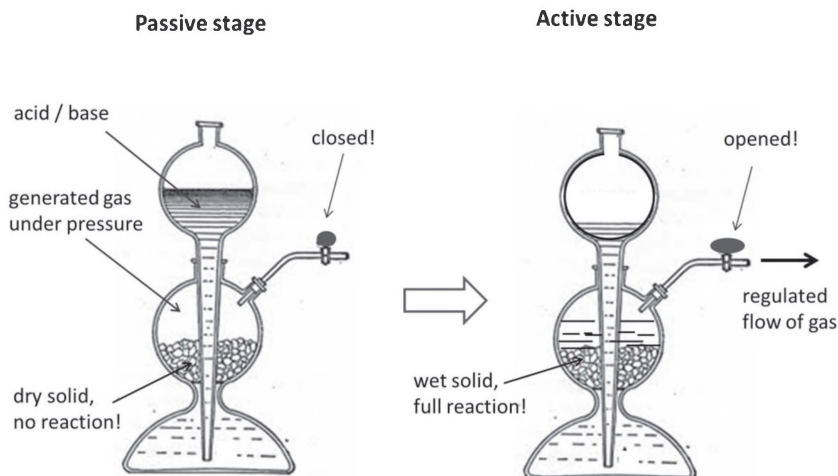
Figure 78. The Kipp apparatus; principal scheme of operation.
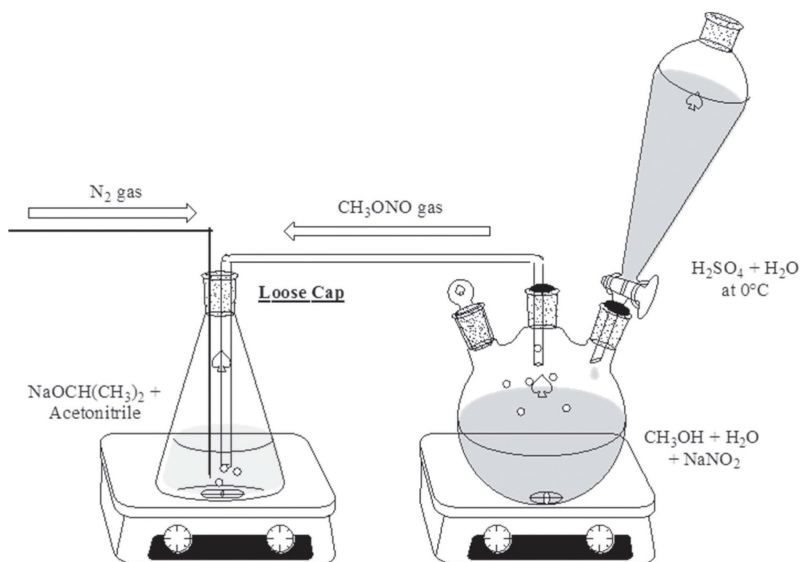
Figure 79. Schematic diagram for generation of gaseous light alkyl-nitrites; an example of the oximes formation reactions (the nitrosation reaction).

A simple and elegant method of generation of gaseous alkyl-nitrites R-ONO (R = CH_3, C_2H_5) is used for the preparation of oximes – excellent ligands for inorganic and organometallic chemistry [1-3]. The way of making these heavy gases is shown in Figure 79, and was recently included into the patent [4]. The basic solution of the precursor – organic acetonitrile – is open to the air to avoid over-pressurizing the system. Typical volumes of these nitrites, which can be generated using this method, are from 1L to 10L. Also, this technique allows the use of the multiple consecutive flasks, connected in 'daisy chain' fashion, to maximize the use of the gas. In such a scenario, only the last in the chain of Erlenmeyer flasks has a loose cap.

In summary, the methods of generation of gases described here provide quick, easy, and *economical* solutions for the needed gases, and are *complementary* to large quantities of gases supplied in still tanks, when the gas consumption is high, or elevated pressures are required.

Cited References

1. N.N. Gerasimchuk, K. Bowman-James. "Mixed Donor Ligands." (Chapter in Encyclopedia of Inorganic Chemistry; Ed. B. King), v.5, p.2254-2269, 1994. John Wiley & Sons, England.
2. A.A. Mokhir, K.V. Domasevich, N.Kent Dalley, Xiaolan Kou, N.N. Gerasimchuk, O.A. Gerasimchuk. "Syntheses, crystal structures and coordination compounds of some 2-hetarylcyanoximes." *Inorg. Chim. Acta.* 1999, *284*, 85-98.
3. Gerasimchuk, N.; Guzei, I.; Sipos, P. "Structural Peculiarities of Cyanoximes and their Anions: Co-crystallization of Two Diastereomers and Formation of Acid-salts" *Curr. Inorg. Chem.*, 2015, *5*(1), 38-63.
4. US patent 7,727,967 B2, 2010 "*Cyanoxime Inhibitors of Carbonyl Reductase and methods of Using Said Inhibitors in Treatments Involving Antracyclines*" Henry Charlier, Nikolay Gerasimchuk.

CHAPTER 2

PREPARATION AND CHARACTERIZATION OF INORGANIC COMPOUNDS

2.1. Types of Chemical Reaction

Before we begin the description of the laboratory experiments in this book, it is important to provide some necessary background information for the reader regarding the main topic – chemical reactions. There are two major categories of chemical reaction commonly used in inorganic chemistry: 1) reactions in which the oxidation states of involved elements do not change; and 2) reactions in which there is a change in the oxidation states (Scheme 1). The first large group is normally called *acids-bases reactions,* with some of the examples of reactivity displayed below. The second, no less voluminous, group is frequently called *redox reactions*. Detailed explanation of both categories is out of the scope of this book, and can be found in more specific sources, such as general chemistry textbooks, or numerous web-based publications [**1**]**.** In this laboratory manual, however, we will cover general aspects of chemical reactivity and show major classes of inorganic compounds.

The manifestation of the fact that the chemical reaction indeed has occurred is normally visible by:

a) The reaction mixture's color changes;
b) The heat is evolved (most commonly, the reaction mixture warms up), or consumed from the environment (fairly rare);
c) Light is emitted (luminescence);
d) The precipitate formation is observed;
e) The precipitate or solid substance is dissolved;
f) The gas formation is observed.

The chemical reaction is always going from the reactants to the products, often spontaneously, if there is the possibility for the following:

I)   The formation of the precipitate:

$$CuSO_4 + 2\ KOH = Cu(OH)_2 \downarrow + K_2SO_4$$
$$Na_2SiO_3 + 2\ HBr = SiO_2 \cdot H_2O \downarrow + 2\ NaBr$$
$$FeSO_4 + (NH_4)_2S = FeS \downarrow + (NH_4)_2SO_4$$

II)   The formation of a gaseous product, or more volatile product:

$$NH_4Cl + LiOH = NH_3 \uparrow + LiCl + H_2O$$
$$CaS + HCl = CaCl_2 + H_2S \uparrow$$
$$2\ NaCl + H_2SO_4\ (conc.)\ =\ Na_2SO_4\ +\ 2\ HCl \uparrow$$

III)   The formation of water (neutralization reaction):

$$Ba(OH)_2 + 2\ HNO_3 = Ba(NO_3)_2 + 2\ H_2O$$
$$CaO + 2\ HI = CaI_2 + H_2O$$
$$2\ NaOH + CO_2 = Na_2CO_3 + H_2O$$

IV)   The formation of a complex particle (weak electrolyte):

$$Zn + 2\ KOH + H_2O = K_2[Zn(OH)_4] + H_2 \uparrow$$
$$HgI_2 + 2\ NH_4I = (NH_4)_2[HgI_4]$$
$$Al(OH)_3 \downarrow + 3\ NaOH = Na_3[Al(OH)_6]$$

Small arrows in the reactions above, and further in the book, indicate, for readers' convenience, the formation of either poorly soluble species, or gases. The most common gases evolving in chemical reactions, procedures, and methods, used in preparative inorganic chemistry, are H_2, O_2, CO_2, CO, N_2, NH_3, SO_2, $HHal$ (Hal = F, Cl, Br) and H_2S. Their evolution shifts the equilibrium quickly to the right part of the equation, and these reactions are very facile and complete [**2, 3**]. The *Solubility Chart,* reflecting the most common precipitating solid products of chemical reactions employed in inorganic chemistry, can be found in *Appendix 2,* at the end of the book.

Among the vast number of redox reactions, the *disproportionation* and *comproportionation* take special place because of their unusual character. Two examples are shown below.

$3\ Br_2 + 6\ NaOH = 5\ NaBr + NaBrO_3 + 3\ H_2O$; here is the split in oxidation state of bromine, (0) to -1 in bromide, and +5 in bromate; it is the *disproportionation* reaction.

$SO_2 + H_2S = 3\ S + H_2O$; here is the 'compromise' between the two oxidation states of sulfur; -2 in hydrogen sulfide, and +4 in sulfur dioxide

that leads to the formation of elemental sulfur; this is the *comproportionation* reaction.
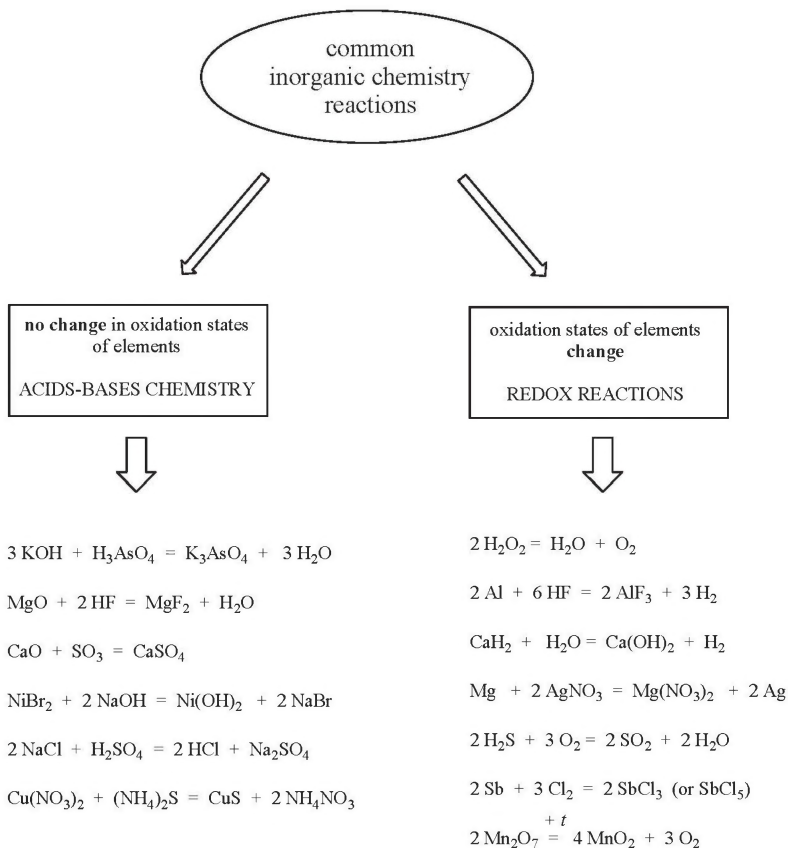
Scheme 1. Types of inorganic chemical reactions.

By the character of changes that occur during the chemical reaction, these maybe further classified as:

1)   Combination (composition) reactions
            $NH_3 + HBr = NH_4Br$
            $Se + 2 F_2 = SeF_4$
2)   Decomposition reactions
            $2 NaHCO_3 = Na_2CO_3 + H_2O + CO_2 \uparrow$
            $2 Cl_2O_7 = 4 ClO_2 + 3 O_2$

3)   Combustion reactions [redox type only!]
            $2 N_2O + C = 2 N_2 + CO_2$
            $S + O_2 = SO_2$
            $12 P + 10 O_3 = 3 P_4O_{10}$

4)   Displacement reactions [redox type only!]
$Al + 3 AgNO_3 = Al(NO_3)_3 + 3 Ag \downarrow$; $2 KI + Br_2 = KBr + I_2 \downarrow$

5)   Double displacement (metathesis, or exchange) reactions [acid-base type only!]

$Ni(NO_3)_2 + 2 NaOH = 2 NaNO_3 + Ni(OH)_2 \downarrow$
$K_2SiO_3 + 2 HCl = 2 KCl + H_2SiO_3 \downarrow$
$AgNO_3 + LiI = LiNO_3 + AgI \downarrow$

In this book, the most typical reactions involved in synthesis of inorganic compounds are used. These are decomposition, displacement, and composition reactions.

Cited Literature

1.   (a) Ebbing, D.D.; Gammon, S.D. *General Chemistry*; 8th Ed, Houghton Mifflin Co, New York-Boston, 2005; (b) Tro, N.J. *Chemistry: a molecular approach*; 2nd Ed, Pearson, 2011.
2.   Robertson, D., Barnes, C., Gerasimchuk, N. *J. Coord. Chem.* 2004, 57, (*14*), 1205-1216.
3.   Brouwer, H. *J. Chem. Educ.*, 1995, 72 (*5*), p A100.

2.2. Thermal decomposition reactions

Decomposition reactions are the most efficient when obtaining a metal oxide is a goal. Just simple heating of a solid finely ground sample, as needed, for complete reaction temperature is normally sufficient. However, stirring of the reaction mixture is difficult. Rotation of the reaction vessel provides better homogeneity and purity of the product, and can be achieved, for example using rotating furnace.

Metal carbonates and nitrates are excellent initial compounds for thermal decomposition reaction. Carbonates typically require higher temperatures for the process, but reaction is a bit cleaner, since many carbonates don't contain crystallization water. Nitrates, however, are the best choice, because of the much greater variety of products that can be obtained after their decomposition. Thus, three rules for the decomposition of nitrates were empirically established, during examination of a large group of metal nitrates.

Rule #1. Nitrates are formed by metal cation, which has a corresponding, water-soluble, strong base, which generates appropriate nitrite and oxygen during the decomposition reaction.

$$2\ NH_4NO_3 = 2\ NH_4NO_2 + O_2\uparrow$$

$$NH_4NO_3 = N_2O\uparrow + 2\ H_2O$$

The list of those metal cations is short, and comprises main groups I and II: Li, Na, K, Rb, Cs, Ca, Sr, Ba and Tl^+ (main group III). Ammonium nitrate decomposes upon heating through two pathways, the choice of which depends on specific conditions, or presence of the catalyst:

a) $NH_4NO_3 = NH_4NO_2 + O_2\uparrow$ and b) $NH_4NO_3 = N_2O\uparrow + H_2O$
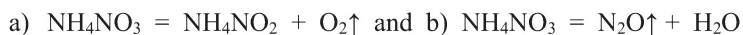
Reactions are carried out at 250 - 400ºC temperatures. For some of the above metal cations it is the only way of obtaining respective *nitrites*.

Rule #2. Nitrates formed by metal cations that form weak and water-insoluble bases upon heating, decompose to metal oxide and gaseous nitrogen dioxide and oxygen:

$Cu(NO_3)_2 \cdot 4H_2O = CuO + NO_2\uparrow + O_2\uparrow + 4\ H_2O$

$2\ Pb(NO_3)_2 = 2\ PbO + 4NO_2\uparrow + O_2\uparrow$

$4\ Tl(NO_3)_3 = 2\ Tl_2O_3 + 12\ NO_2\uparrow + 3\ O_2\uparrow$
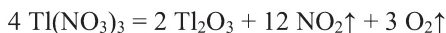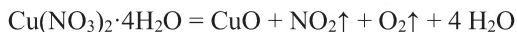
The vast majority of metals nitrates in the Periodic Table decompose according this rule. Indeed, those form weak, sparingly soluble bases; main groups III, IV and V metals, 3d-, 4d- transition metals, lanthanides, and actinides.

There are two exceptions: bivalent Mn and Fe nitrates decompose to the metal oxides in more positive oxidation states; MnO_2 and Fe_2O_3. In reality, the MnO and FeO are formed, but quickly oxidize to MnO_2 and Fe_2O_3 in the presence of oxygen at elevated temperatures.

Rule #3. Nitrates that are formed by low reactive or noble metals that either don't have respective hydroxides, or have those which are unstable, decompose to pure metal and gaseous nitrogen dioxide and oxygen:

$2\ Cu(NO_3)_2 \cdot 4H_2O = 2\ CuO + 4\ NO_2\uparrow + O2\uparrow + 8\ H_2O$

$2\ AgNO_3 = 2\ Ag + 2\ NO_2\uparrow + O_2\uparrow$

$2\ Ir(NO_3)_3\ xH_2O = 2\ Ir + 6\ NO_2\uparrow + 3\ O_2\uparrow + x\ H_2O$
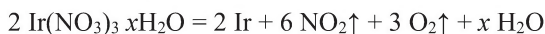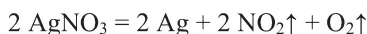
For several metals, this method is preferable, when a deposition of thin layer of metal or formation of a mirror is sought.

2.2.1. Theoretical Background: Thermal analysis (TA) and Differential Scanning Calorimetry (DSC)

The instrument called a thermal analyzer (shown in Figure 80, below), allows for the simultaneous accurate determination of the heat flow from, and to, the sample, with monitoring of its weight upon heating. There are several specialized companies that produce such equipment, for numerous industrial and academic uses. In our teaching/research park, we happen to have a Q-600 from TA Instruments, but there are other similar instruments readily available.

The DSC/TG analyzer provides the linear sample's temperature increase and detects heat effects (exo-/endothermic reactions) that accompany its thermal decomposition under anaerobic conditions. A

sample of compound or substance (not necessarily a solid!) is placed in a small crucible made of pure Pt or alumina. Measurements are normally carried out under pure N_2 flow, although other purging gases such as air, argon, or helium, can be used as well. Gaseous products of thermal decomposition can be trapped, and, using a gas-chromatograph/mass-spectrometer, analyzed further. Weight loss is measured simultaneously with temperature and a heat flow, and is expressed in mass %, while the heat flow is given in Watts/g. The normal operating range of the DSC/TG analyzer is from +25 to +1500ºC. The rate of heating can vary from 1º to 20º/min, and different operation modes can be employed. These are: 1) steady temperature ramping with continuous heat at constant rate; 2) stepwise heat with plateau periods, the lengths of which are programmable; 3) cyclic mode, when continuous heat follows monitored cooling to a desired temperature.

        In this laboratory exercise we use the most commonly used method; steady ramping of temperature from room to +1200ºC. The typical thermogram of wet '$Mn(NO_3)_2 \cdot 6H_2O$' decomposition is shown in Figure 86**A,** with data analysis presented in Table 4. A stepwise curve of the weight loss provides valuable information about the amount of sample remaining in the crucible, and the sign of heat flow allows detection of the *exo-* or *endothermic* reactions that occur during thermal decomposition (Figure 86**B**). It contains values of the calculated sample's weight loss, which is very useful for elucidating the path of its thermal decomposition. Using that information, the chemist can calculate expected, theoretical weight loss from the studied sample, and compare it with that determined experimentally, using the TG/DSC traces. Therefore, the method of thermal analysis provides very useful information about the compound's purity and chemical composition, and also establishes the path of its decomposition upon heating.
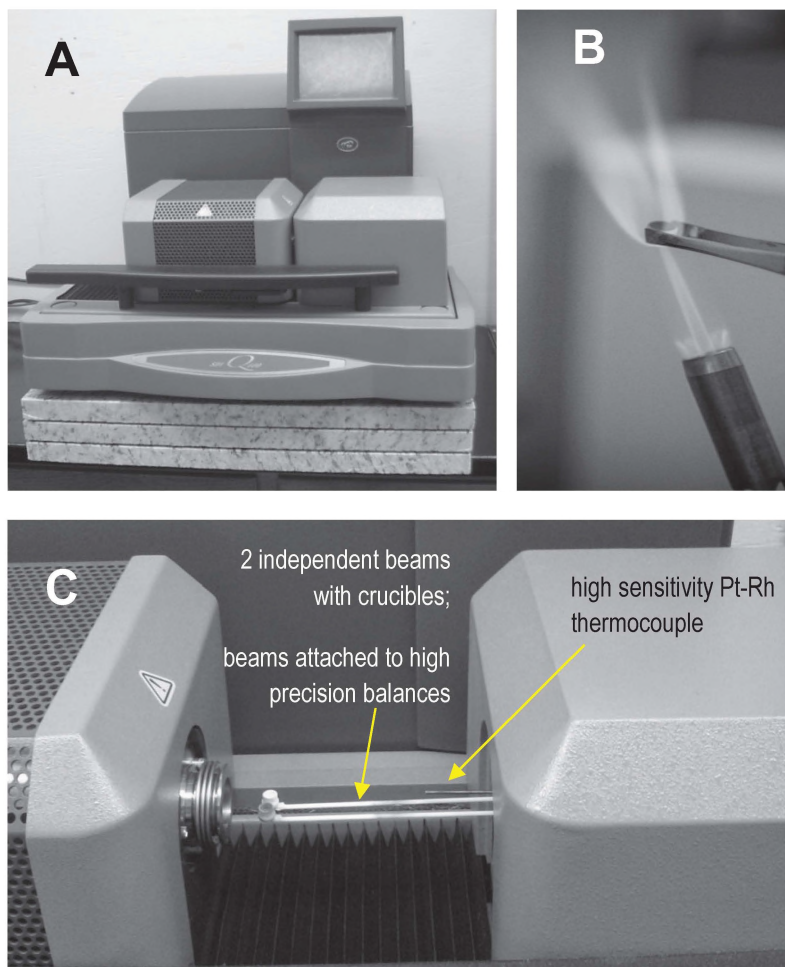
Figure 80. **A** – general view of the thermal analyzer showing blow torch for crucible cleaning and tools; **B** – cleaning of alumina crucible with flame; **C** – opened furnace view showing two beams with alumina crucibles for differential analysis (darkened for sample, lighter (empty) for control)).

2.3. Experiment 1A: Preparation of Manganese Dioxide from Manganese(II) Nitrate

Manganese dioxide, MnO_2, is an important compound with a large variety of practical applications. It is an active component of cylindrical batteries, an oxidizer for numerous industrial processes for manufacturing some organic compounds, and is also used as a catalyst. The amount of manganese dioxide produced is estimated in thousands of tons annually, and the vast majority of it comes from processing the mineral called β-pyrolusite. In small amounts, MnO_2 is produced from respective Mn(II) nitrate by thermal decomposition. This process usually leads to substantially better quality dioxide. This is due to the larger surface area of MnO_2 obtained from $Mn(NO_3)_2$, and also the fact that the dioxide does not require activation if the compound is intended for use as an oxidant or catalyst.

The main objective of this experiment is to learn a technique for the thermal decomposition of inorganic salts which can be used in laboratory practice for the preparation of different compounds. *Pure Fe₂O₃, PbO and CuO can be obtained in a similar fashion from respective nitrates.*

Equation for the reaction:

$$Mn(NO_3)_2 \times 6\,H_2O \quad \rightarrow \quad MnO_2 \quad + \quad 2\,NO_2 \quad + \quad 6\,H_2O$$
286.9 g   86.9 g   92.0 g   108.0 g
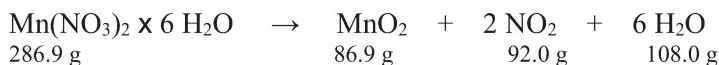
Chemicals: Manganese(II) nitrate, hexahydrate;
Nitric acid (1:6) diluted by water from concentrated acid.

Equipment: Analytical balance;
Sand bath (two kinds can be used; electrically heated or gas heated);
Digital thermometer (thermocouple);
Ceramic evaporating dish, 100mL capacity;
Ceramic mortar and pestle, small size;
Spatula;
Vial with a screw-cap.

Figure 81. Typical setup for $Mn(NO_3)_2$ decomposition using electrically heated sand bath powered through the *variak* (see Chapter 1, Figures 28, 29; a heating mantle is another option for an intense and controllable heating).

Procedure: *(will be carried out in groups, with two students per group)*:

This experiment is carried out exclusively under the ventilation hood!

      The typical appearance of hydrated manganese(II) nitrate is either as a 'wet solid', or viscous pink solution. These differences do not affect the reaction. Thus, 10g of the salt is placed in a medium-sized ceramic evaporating dish. The dish is placed on a sand bath for heating. Attain a temperature of ~190ºC, and maintain this temperature until the reaction is over. Alternative heating can be achieved using an electrically heated sand bath connected to the laboratory auto-transformer, better known as a *variac* (Figure 28**A**, Chapter 1). If your starting manganese(II) nitrate is solid, then it will melt into a pink viscous liquid prior to decomposition. Different stages of reaction are shown in Figures 81-85.
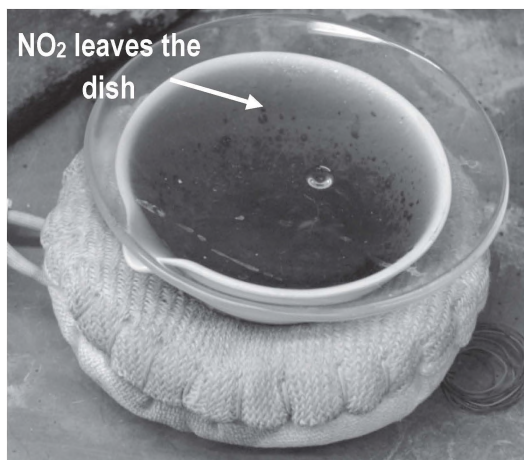
Figure 82. A porcelain dish with the reaction mixture, covered with a watch glass to prevent sputtering.

Figure 83. The decomposition is complete.

Figure 84. Boiling of MnO_2 with nitric acid to assure completeness of Mn(II) nitrate decomposition.
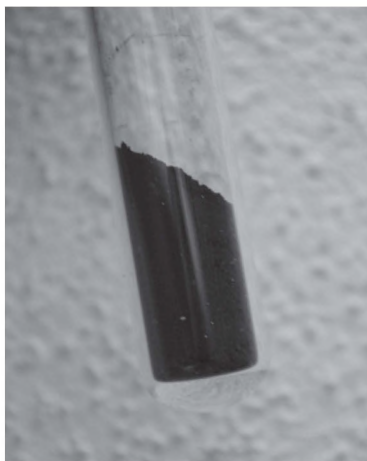
Figure 85. Final product packed in the screw-cap vial.

Thermal decomposition of $Mn(NO_3)_2$ is accomplished with the color change from pink to dark-brown, and the evolution of nitrogen dioxide, NO_2, which is a toxic, yellow-brown heavy gas with an unpleasant smell. The reaction is over when there is no gas coming off the dark-colored solid residue upon continuous heating for at least five

minutes. When the decomposition is complete, the porcelain dish is removed from the sand bath and placed onto a ceramic pad under the hood to cool.

The dark-brown solid residue is removed from the dish using a metallic spatula and placed into the mortar to be ground. *This step is performed **only** if the solid residue represents hard lumps of material.* Afterwards, the ground, powdered, dark-brown MnO_2 is placed back into the original porcelain dish, and ~ 50mL of diluted nitric acid (1:6 by volume) is added at once to the solid. Manganese dioxide is not soluble in acid.

The mixture is heated again, this time to boiling, on a sand bath or hot plate. Boiling of the MnO_2 mixture continues for 30 minutes, and during this time, one new portion of the acid solution is added as the liquid evaporates. After another 30 minutes, the temperature is elevated to ~150°C, and all liquid is completely evaporated. Dry solid residue, which at this point represents exclusively MnO_2, is continued heating at this temperature for ~20 more minutes. The porcelain dish with the manganese dioxide is removed from the heating device and left to cool off under the hood, to room temperature. The final product is weighed using weighing paper or a weighing boat, and then packed into the vial.

The reaction usually leads to 100% conversion of the nitrate into MnO_2. Therefore, it is possible to determine the hydrate composition of the starting $Mn(NO_3)_2$.

A sample of the initial Mn(II) nitrate, crystallohydrate, will be analyzed with the help of the differential scanning calorimeter/thermal analyzer pictured in Figure 80. Necessary background information on the method of thermal analysis and an example of the analysis of the thermogram are presented after this laboratory exercise.

Properties of MnO₂: a black powder, insoluble in water and organic solvents, soluble in concentrated HCl with generation of Cl_2 and $MnCl_2$, and soluble in hot, strong, basic solutions with formation of manganites – MnO_3^{2-} - salts. Density: 5.026 g/cm³; the crystal system orthorhombic, a = 4.418, b = 9.510, c = 2.811 Å.

Goals of this laboratory experiment and expected accomplishments:

1) Perform thermal decomposition of Mn(II) nitrate, crystallohydrate according to provided procedure;
2) Calculate yield and determine water content in the sample using the final weight of your compound;

3) Record DSC/TG traces for a small sample (~20mg) of the 'Mn(NO$_3$)$_2$·6H$_2$O' under N$_2$ flow using available thermo-analyzer;
4) Carry out data analysis similar to that shown in Table 4, and present it with your lab report on the next laboratory session;
5) Provide explanation for sequential simplification of manganese oxides from MnO$_2$ to MnO upon heating, and include it in the lab report.

Make a printed paper label for your compound! The number of the experiment, date, and author of the reaction, and the total amount of the obtained compound should be written on the label. The label will be attached to the vial with the product.

The compound will be accepted (or declined) for storage, after careful inspection. The homogeneity of the MnO$_2$ and its color are major criteria for the decision; a) the compound should represent a homogeneous powder without foreign inclusions; b) the color should be black with some metallic shine.

Potential hazards:

1) Hot surfaces of hardware;
2) Nitric acid, which may cause severe burns if it comes into contact with skin for more than 30 seconds; even very brief exposure to HNO$_3$ leaves yellow stains on the skin for a couple of weeks. Therefore, wearing latex gloves during operations with the acid is highly recommended.

Always wear eye protection during the lab work!

Cited Literature

1. Brauer, G. *Handbuch der Praparativen Anotganishen Chemie*. Dritte umgearbeitete Auflage; Ferdinand Enke, Verlag Stuttgart, 1975.

2.3.1 Analysis of the TG/DSC Traces from Manganese(II) Nitrate Decomposition
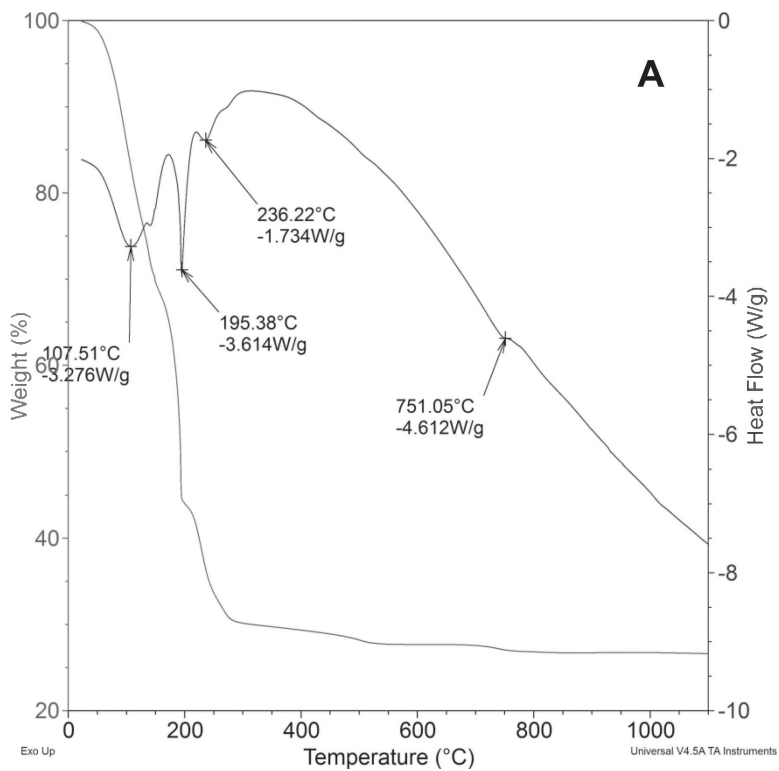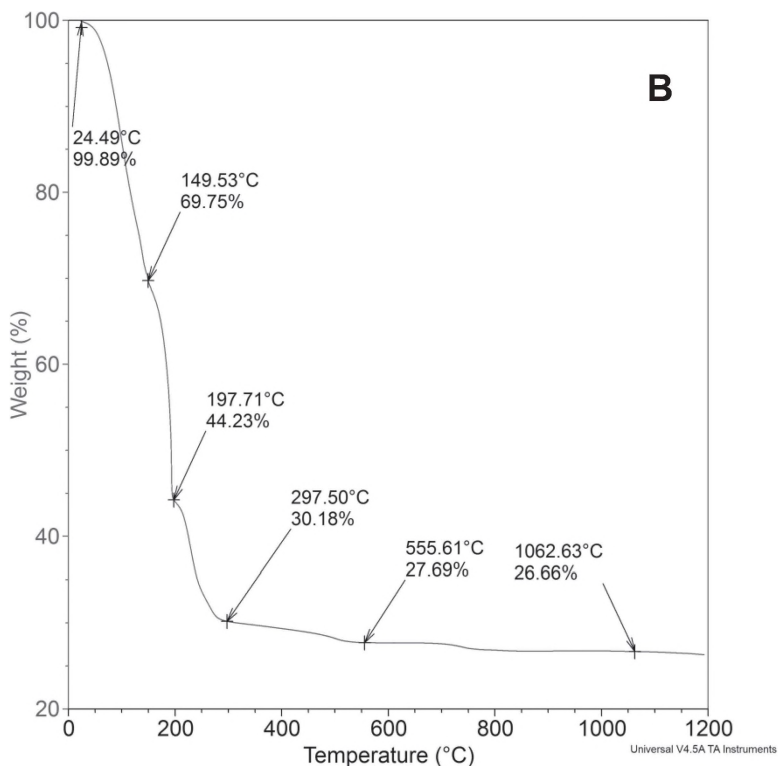
Figure 86. Typical combined DSC/TG traces for panoramic view (**A**), and weight loss trace for compound analysis (**B**).

Table 4. Results of thermal analysis studies of decomposition of wet "$Mn(NO_3)_2 \cdot 6H_2O$" under pure N_2 atmosphere (Figures 86**A** and **B**).

Compound	Process*	Product	Weight losses, % calculated (*found*)	Error %
$Mn(NO_3)_2 \cdot 6H_2O$	-5H_2O	$Mn(NO_3)_2 \cdot H_2O$	68.61 (*69.75*)	-1.14
$Mn(NO_3)_2 \cdot H_2O$	-H_2O,-NO_2,-O_2	MnO_2	30.28 (*30.18*)	+0.10
MnO_2	-O_2	Mn_3O_4**	26.56 (*27.69*)	-1.13
Mn_3O_4	-O_2	MnO***	25.76 (*26.66*)	-0.90

*- all these processes are endothermic
**- the reaction of MnO_2 decomposition is: $MnO_2 \rightarrow Mn_3O_4 + O_2 \uparrow$
***- mixed oxide Mn_3O_4 decomposes further; $Mn_3O_4 \rightarrow MnO + O_2 \uparrow$

2.4. Experiment 1B: Thermal Decomposition of Potassium Permanganate

The **goal** of this laboratory exercise is to generate gaseous dioxygen, as the product of a thermal decomposition reaction of a solid salt ($KMnO_4$), and to study one of the most important chemical properties of dioxygen, supported by the burning of other elements as proof of O_2 oxidizing ability.

The following objectives will be achieved in this work:

1) Learning the proper technique of gas collection under water;
2) Observation of the burning of elemental sulfur (or red phosphorous*) in an oxygen atmosphere;
3) Observation of the dissolution of the product of sulfur (or red phosphorous) combustion in water, and its chemical reactivity;
4) Calculation of the completeness of the conversion of the initial salt into products.

Equation for the reaction:

$$2\ KMnO_4\ \rightarrow\ MnO_2\ +\ K_2MnO_4\ +\ O_2\uparrow$$

2 x 158.1 g   86.9 g   197.1 g   32.0 g
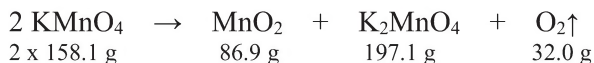
Chemicals:	Potassium permanganate, elemental sulfur (or red phosphorous), solutions of $BaCl_2$ and $CuCl_2$, solution of the methyl orange indicator (or litmus indicator), or paper strips containing acid-base indicators.
Equipment:	Analytical balance;
	Wide mouth Pyrex test tube;
	Cotton ball;
	Rubber septum with rubber gas tube and glass tip;
	500mL - capacity glass column with stopcock;
	Two lab stands with two clamps: wide and normal grip plastic jar;
	Metal spatula and metal spoon for burning combustible substances.

Procedure: *(will be carried out by each student)*:

This experiment can be carried out on the bench top. Wear eye protection and a lab coat!

Please follow the pictorial description and explanation of this laboratory experiment provided below, as schemes. For your convenience, stick diagrams are used for making unobstructed views.

Step 1.
Place approximately 3g of the potassium permanganate (±0.2g) on the bottom of a wide mouth test tube. A cotton ball is carefully advanced into the tube opening (Scheme 2). Weigh the test tube with the salt and cotton ball to the second decimal point, using the balances. Write the mass into your lab report. The test tube should be kept at a low angle, close to a horizontal position, to avoid spill/loss of $KMnO_4$, or its contact with the cotton ball. The cotton ball should not tightly close the tube!

Scheme 2 $KMnO_4$ loose cotton ball
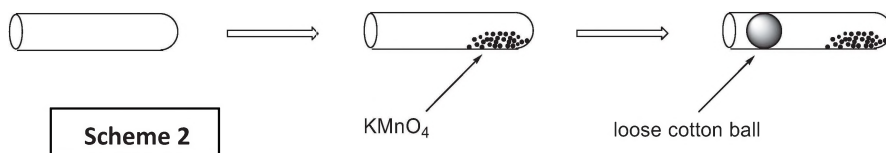
Step 2.
Close the test tube with the rubber septum, connected to a hose with the glass tip at the end of it (Scheme 3). Check the equipment for tightness (hermeticity). This can be done by immersing the glass tip into the beaker with water, and gently heating the test tube with your palm while you are holding it. If the system is hermetic, then one or two bubbles of air will escape from the glass tip into the beaker, thus proving the system's tightness.

rubber septum with the gas tube
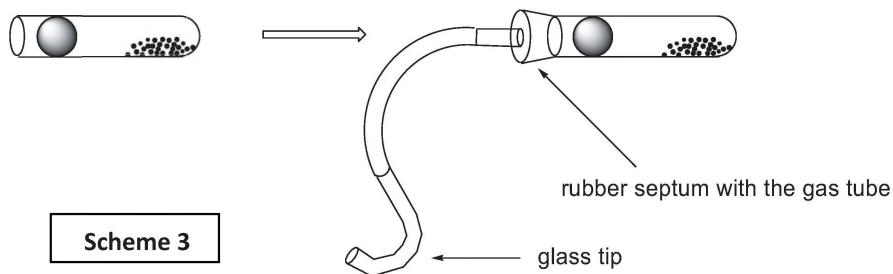
Scheme 3

glass tip

Step 3.
Place the large lab stand and the wide grip clamp close together, and add water to the plastic jar to approximately ¾ of its capacity (see Scheme 4 below). We will collect O_2 using water substitution from the glass column by incoming gas.

wide grip clamp

plastic jar

large lab stand
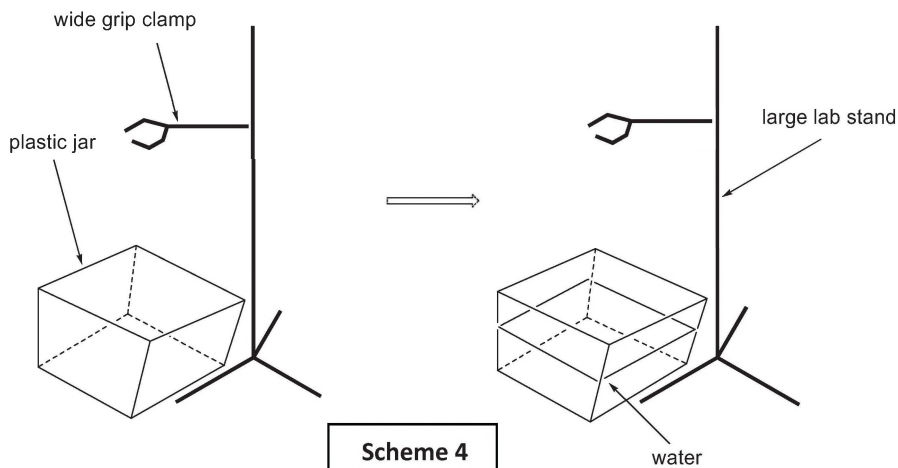
Scheme 4

water

Step 4.
Fill the glass column with distilled water to the top. Close the column with the rubber septum, in such way that there will be no air bubbles left trapped inside the system. Flip the closed column upside down, as shown (Scheme 5). Carefully immerse the column into the plastic jar with the water, and secure the vertical position of the column on the large lab stand, using the wide grip clamp. Remove the rubber septum from the column and let it float nearby in the jar. No water should escape from the flipped upside-down column at this point!

rubber septum

water
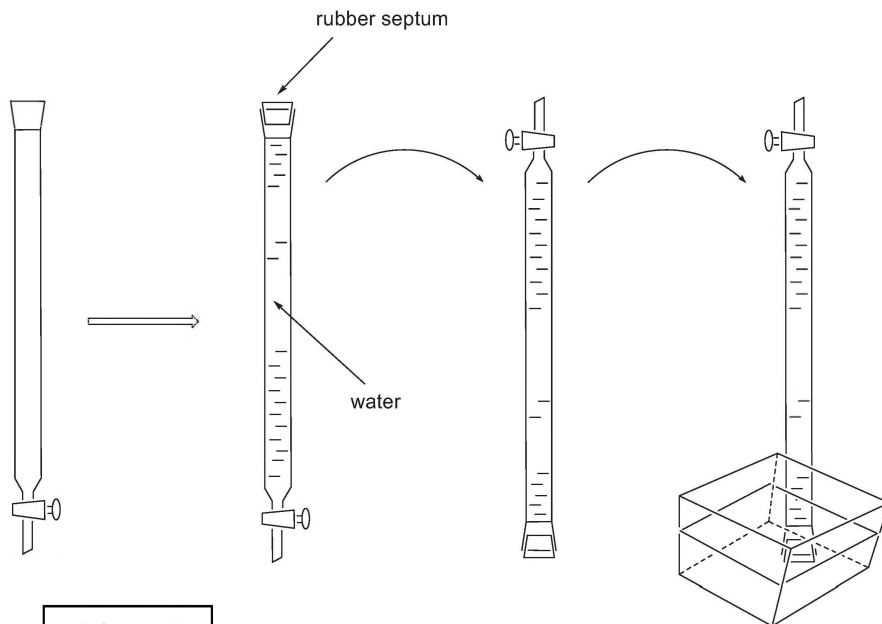
Scheme 5

Step 5.

Use the smaller lab stand to clamp the assembled hermetic test tube system with $KMnO_4$ (from step 2) almost horizontally. At this point you should be able to insert the rubber hose glass tip into the glass column, without stretching. Move this setup close to the large lab stand. Begin to gently heat the test tube with a small flame (~2 inches tall), to remove air from the test tube and the hose (Scheme 6). This gentle heating is done only to warm the test tube, to avoid the heat shock. Again, a glass tip should be <u>off</u> the column, and air bubbles should be able to escape into the atmosphere freely. *Do not heat the solid salt inside the test tube* at this point! This is the final preparation to collect the pure O_2 under water.

Scheme 6

air bubbles

Bunzen burner
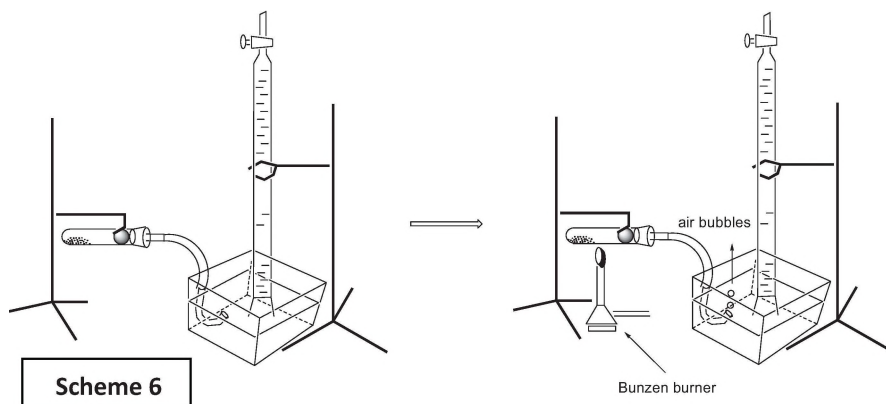
Step 6.
When air is removed from the test tube with salt, carefully and quickly insert the glass tip into the opening of the glass column filled with water, and prepare to collect the pure O_2. Start gently heating the test tube, but this time in the area of the $KMnO_4$ location (Scheme 7). ***Avoid heating the rubber septum area***! Observe the O_2 evolution, and control the process by moving the burner on and off the test tube. Collect all the gas evolved (this will take ~1 or 2 minutes). A photograph of the experiment is shown in Figure 87. *A small alcohol burner can replace the Bunsen burner in labs not equipped with a natural gas source, as explained in Figure 88.*

O_2

Scheme 7
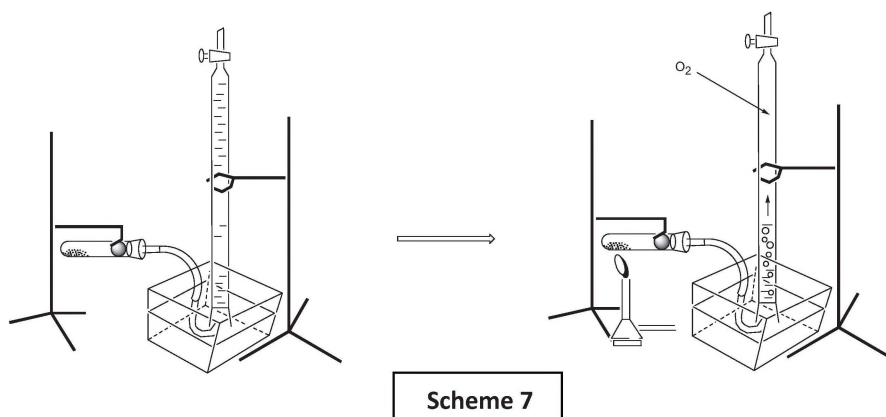
Step 7.

When no more O_2 bubbles appear, quickly turn the burner off and open the test tube. Remove the septum with the rubber hose and place it close by. Wait until the system cools off. The final stage of your work with the test tube should look as shown below (Scheme 8). Using the rubber septum floating nearby, close the opening of the glass column partially filled with O_2 and containing water.

Scheme 8

trapped O_2

water
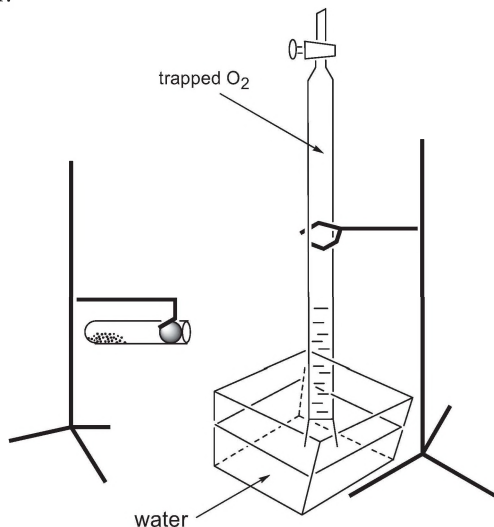
Step 8.

Weigh the cold test tube, which contains the cotton ball and decomposition products (MnO_2 + K_2MnO_4), on the balances, to two decimal points. The mass difference between is the amount of O_2 evolved. Write the number in your notebook. Calculate the degree of completeness of $KMnO_4$ decomposition using the chemical equation at the beginning of this laboratory experiment. Record all observations into your lab notebook.

Step 9.

Make sure that the glass column filled with water/O_2 is tightly closed. Flip the column upside down again to its normal position (Figure 89**A**). Clamp the column to the lab stand and move it under the ventilation hood.

Take a spatula, place a small amount of elemental sulfur (or *red phosphorous: this depends on the instructor's decision) in it, and ignite it using the nearby Bunsen burner (or alcohol-filled portable burner, Figure 88). *These operations MUST be carried out under the hood! This is to*

protect students from exposure of SO$_2$ and P$_2$O$_5$ and formed mist of respective acids! Quickly remove the rubber septum from the top of the glass column and insert burning sulfur (or phosphorous) into the column, paying close attention to what is happening (Figure 89**B**). When the flame subsides completely, remove the spatula from the glass column and close it again with the rubber septum. Write your observations into the laboratory notebook. Provide an appropriate equation of the chemical reaction.
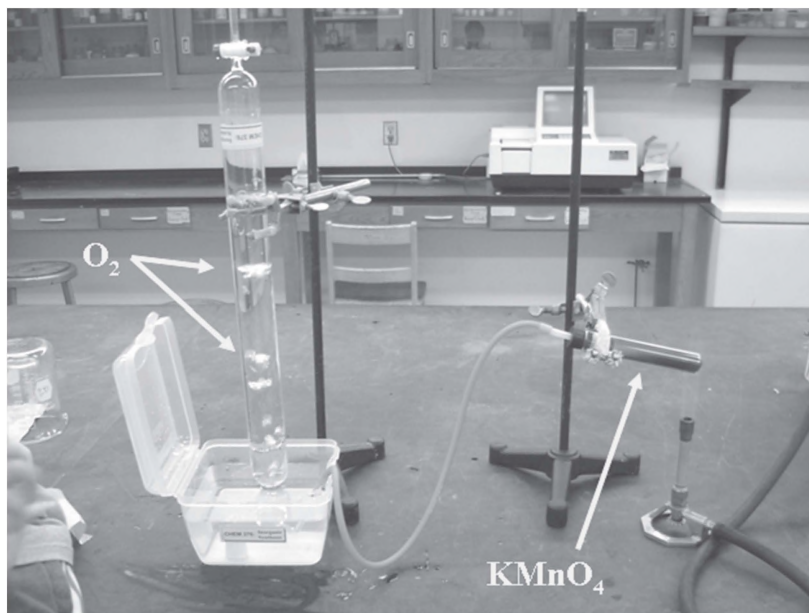
Figure 87. Experimental setup used for decomposition of potassium permanganate.
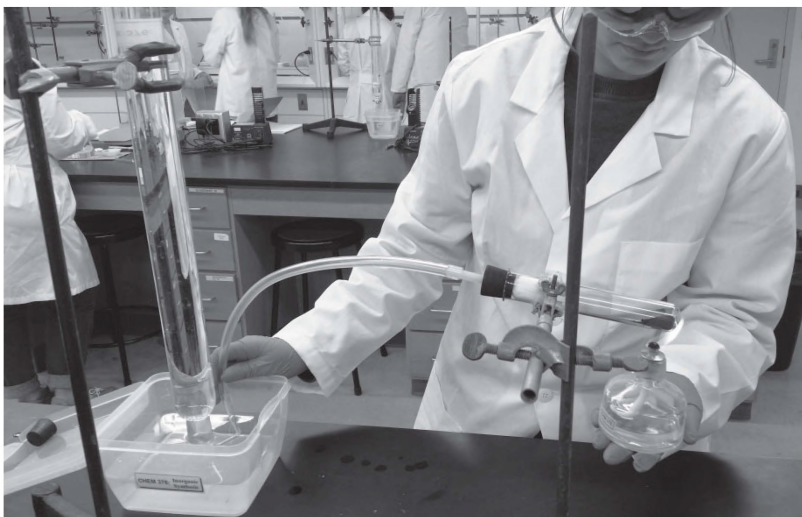
Figure 88. Experimental setup for thermal decomposition of a salt using an alternative heat source – alcohol filled burner.
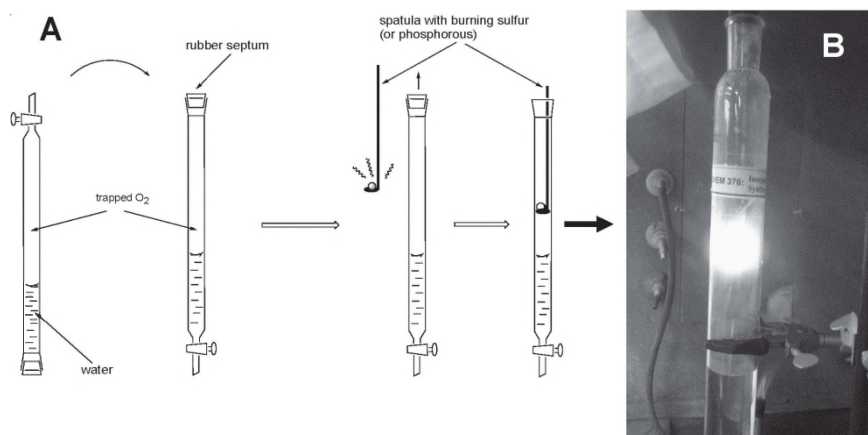
Figure 89. Manipulations with the glass column filled with O_2 prior to insertion of molten sulfur (**A**), and bright burning of non-metals S_8 or $(P_4)_n$ in oxygen (**B**).

Step 10.
Take the column from the lab stand and shake it well several times to let the gas inside be absorbed by the water. This is seen when the misty/foggy residue in the column slowly disappears and a clear solution is formed.

Using the stopcock at the bottom of the column, drain a few mL of solution from the column and test it with a paper strip with universal pH indicator (or litmus, or methyl-orange paper strips). Write your observations into the lab notebook.

Step 11.
If you observed burning of S_8 in pure oxygen, add several mL of the $BaCl_2$ solution made prior to the experiment, into the column. Write your observations and an appropriate equation of the chemical reaction into your lab report.

If you observed burning red phosphorous* $(P_4)_n$ then add a few mL of drained solution to small portions of solid baking soda, to roughly neutralize the solution to pH ~6-7. After that, add $CuCl_2$ solution and make your observations, accompanied by the writing of an appropriate chemical equation, into your lab report.

Step 11.
Disassemble all pieces of equipment used in this experiment. Collect solids into a special container. Wash all glassware with soap and water, then rinse it with distilled water, and let it dry in the oven or on the lab stand. Clean the lab for the next lab session.

Step 12.
Prove the formation of potassium manganate in solid residue after the decomposition reaction, by taking a small amount of a dark-brown/black powder and placing it into the test tube. Add 2-5mL of dilute NaOH (or KOH) solution and stir the mixture using the Vortex (Figure 28**B**). Let precipitate collect at the bottom of the test tube and record your observations.

Properties of K_2MnO_4 (F.W. = 197.13): represents a dark green powder, density = 2.78 g/cm^3, with melting point of 190°C. Solid salt forms adopts orthorhombic crystal system with a = 4.418, b = 9.510, c = 2.811 Å.
The salt is soluble in water with the formation of a dark emerald green solution that quickly fades, unless solution is caustic. Under neutral conditions, manganate ion MnO_4^{2-} disproportionates according to reaction:

$$3 K_2MnO_4 + 2 H_2O = 4 KOH + MnO_2 + 2 KMnO_4$$

After some time, solutions of manganates in water gain purple color, characteristic of permanganate ions. Solid compound reacts vigorously with concentrated HCl with generation of Cl_2 and $MnCl_2$.

Expected accomplishments:

1) Perform thermal decomposition of $KMnO_4$, collect gaseous O_2 and investigate process of sulfur (*red phosphorous) burning in it;
2) Qualitatively study products of both reactions;
3) Calculate yield of O_2 and % of permanganate decomposition;
4) Prepare detailed lab report with all observations, discussion of results and conclusions; your lab report will be due at the next laboratory session.

Potential hazards:
1) Flame, and hot surfaces of glassware, burning sulfur (*or red phosphorous);
2) Solid permanganate leaves yellow burns on the skin and paper, therefore, caution should be taken while handling this oxidizer;
3) Burning sulfur (or red phosphorous) emits irritating gas that may cause extensive coughing when inhaled!

---

*- *your lab instructor will specify which of the nonmetals will be used by each student*

2.5. Manipulations with Moderately Air Sensitive Compounds

Background information

The great majority of chemical reactions which are normally carried out in the laboratory for teaching and research activities take place at ambient conditions, including open air. At the same time, there are many reactions that require isolation of the whole synthetic procedure from air and/or moisture. Detailed description of those processes is beyond the scope of this book, but can be found in several laboratory manuals specifically designed to present numerous syntheses of air-sensitive compounds [**1-4**]. Nevertheless, as stated above in Chapter 1, some of these procedures are outlined in *Appendix 1,* for interested readers.

Here, we present two simple laboratory exercises describing operations with wet being moderately sensitive to air compounds – $FeSO_4 \cdot 7H_2O$ and Cu_2O. Purging the initial solutions with an inert gas (N_2 or Ar), or providing a protective blanket using heavy gas (CO_2), are the main methods which keep air oxidation of the ferrous (Fe^{2+}) and cuprous (Cu^{1+}) ions to a minimum. Both are susceptible for oxidation to Fe^{3+} and Cu^{2+} species, being wet solids that have precipitated from aqueous solutions.

2.6. Experiment 2a: Preparation of Ferrous Sulfate, Heptahydrate, $FeSO_4 \cdot 7H_2O$

Ferrous sulfate, $FeSO_4$, is a useful water-soluble, starting salt for the synthesis of numerous iron-containing compounds. In addition, it has some unique applications in laboratory practice. Thus, $FeSO_4$ is used, for example, as the scavenger of hydroperoxides from common organic ethers such as tetrahydrofuran (THF), diethyl- and dipropyl- ethers. This is an important safety issue, since the above hydroperoxides are very prone to explosion. These substances have caused numerous incidents, both in chemistry labs and in industry. Concentrated aqueous solutions of ferrous sulfate represent soft and effective hydroperoxide neutralizers. As with the majority of Fe(II) inorganic salts, ferrous sulfate is air-sensitive, and slowly undergoes oxidation to its respective, partially hydrolyzed, ferric(III) salts. Therefore, preparing and handling iron(II) compounds requires certain practical skills.

Goals of this laboratory experiment and expected accomplishments:

1) Carry out preparation of Fe(II) sulfate, heptahydrate according to provided procedure;
2) Dry your sample, pack in the ampoule (made during the lab), and calculate yield;
3) Record DSC/TG traces for a small sample (10–20mg) of the $FeSO_4 \cdot 7H_2O$ under N_2 flow using available thermo-analyzer;
4) Carry out data analysis and present them, with your lab report at the next laboratory session;
5) Prepare a detailed lab report with all observations, discussion of results, and conclusions; your lab report will be due at the next laboratory session.

Equation for the reaction:

$$\text{Fe} \quad + \quad \text{H}_2\text{SO}_4 \quad \xrightarrow{\text{H}_2\text{O, +t}} \quad \text{FeSO}_4 \cdot 7\,\text{H}_2\text{O} \quad + \quad \text{H}_2 \uparrow$$

$$\quad\; 56\,\text{g} \qquad\quad 98\,\text{g} \qquad\qquad\qquad 278\,\text{g} \qquad\quad\; 2\,\text{g}$$
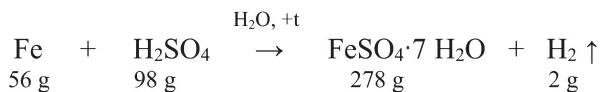
Chemicals: Rusted iron pieces, fillings, etc., sulfuric acid (concentrated; d=1.96 g/ml);
Distilled water (DI), ethyl alcohol, 96.5%.

Equipment: Analytical balance;
Water bath (600mL beaker);
Immersion thermometer;
Ceramic (or porcelain) evaporating dish of medium (100ml) capacity;
Flask for filtration – side arm flask (Bunsen flask);
Two glass fritted filters (Schott filter);
Large glass gravity funnel;
Several spatulas, rubber hoses, cotton balls;
Ampoules (test tube blanks);
Blow torch with glassblowing accessories;
Gas tank with compressed argon;
Gas tank with compressed N_2;
Universal pH indicator (paper strips).

Procedure: *(will be carried out in groups, with two students per group)*:

Step 1.
Place ~5g of the raw iron pieces (provided by instructor) into a 125mL Erlenmeyer flask. Add slowly, but all at once, 10.0g of concentrated sulfuric acid to 40mL of distilled water, to form a 20% solution of H_2SO_4. Pour this solution at once into the flask, with the metallic iron, and place it for heating in a water bath, or on the hot plate. Maintain the temperature of the water bath at boiling during the dissolution of iron and generation of hydrogen. The dissolution process is usually accomplished with a minor amount of toxic gaseous phosphines and silanes being released, since raw metallic iron contains impurities, usually phosphorus and silicon. Although the amount of these gases is small, they produce a foul smell upon evolution. Therefore, the dissolution process should be carried out *under the hood!* Also, pay attention to *foaming* of the flask's contents, and prevent it from spilling over, by manual stirring with a glass rod.

Step 2.
Observe complete, or almost complete, stop of H_2 evolution, which signals that the dissolution of all of available iron metal is over. The ferrous salts in an acidic solution are more stable towards oxidation in open air than in neutral or basic solutions. The resulting solution is filtered using the Schott glass filter and Bunsen side-arm flask, which was filled with carbon dioxide prior to filtration (Figure 90). This is an important step to prevent Fe(II) air oxidation in warm solution. At pH~4 there is no iron(II) carbonate formation, but since CO_2 is a heavy gas (F.W. = 44), it helps to maintain a protective atmosphere in the system.

Step 3.
Check the clear filtrate for the Fe(III) impurity using the KNCS method! This method includes the reaction of a solution of potassium thiocyanate in the test tube with one drop of $FeSO_4$ filtrate solution. If everything is done correctly and carefully, the solution will remain colorless, or the color of the mixture in the test tube will be pale pink-orange. When substantial oxidation of Fe(II) to Fe(III) occurs, the solution in the test tube will immediately turn blood-red, due to the formation of the $[Fe(NCS)_6]^{3-}$ complex anion. If the KNCS test for Fe(III) in the filtrate turns out positive, add ~0.3g of iron powder and 5mL of 20% H_2SO_4 to the flask with the filtered solution, to reduce Fe(III) to its intended bivalent state. Practically, this is a repetition of the above dissolution procedure.

Step 4.
Transfer the solution of $FeSO_4$ into the porcelain dish, place the dish on a steam bath, and cover it with the large glass funnel connected to the Argon tank through the hose. Maintain the flow of Argon and start heating the dish with steam (Figure 91). This is a water evaporation step, which may take 15-30 minutes. As soon as the first crystals of a light-blue salt appear on the wall of the dish, immediately remove it from the steam bath and place on ice for crystallization, while using argon gas for protection during both heating and cooling (Figure 92).

Step 5.
Filter the precipitate $FeSO_4 \cdot 7H_2O$ using the glass **C**-grade filter (Schott filter, coarse grade), gently pack it on the filter to remove the mother liquor. Without using the vacuum, thoroughly wash the solid with ~15mL of ethanol. Dry the precipitate on the filter, and then remove it from the filter and press between the sheets of filter paper for complete drying. The solid salt is lightly air-sensitive and can be handled safely in the open air for 10-15 minutes. The dry, light blue-green salt should no longer stick to a glass rod. Take a small sample (~20mg) of your compound and record its DSC/TG traces on an available thermal analyzer. Typical DCS curves of the iron(II) sulfate, heptahydrate, are shown in Figure 94.

You will need to match *your* freshly recorded TG/DSC traces with one displayed in Figure 94 below, and *your* data, with appropriate interpretation, should be included in the lab report.
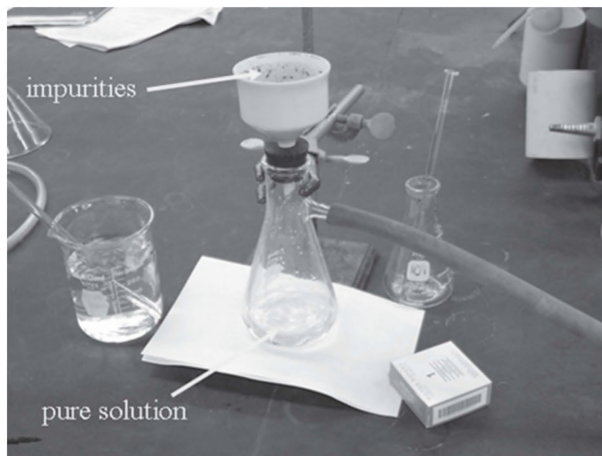
Figure 90. Filtration of hot $FeSO_4$ solution from impurities.

Step 6.

Weigh the premade empty ampoule (Figure 93**A**), carefully place inside air-dried solid $FeSO_4 \cdot 7H_2O$, clear the ampoule's neck, purge it with an inert gas available (CO_2, N_2 or Ar), and then seal it using the blow torch* (Figure 93). Wait until the ampoule's neck cools off, and then weigh two pieces together; an ampoule and its leftover after sealing. The weight of pure ferrous sulfate heptahydrate is the difference between the mass of an empty ampoule and two pieces obtained above. An example of the final product sealed in ampoules is shown in Figure 93**C**.
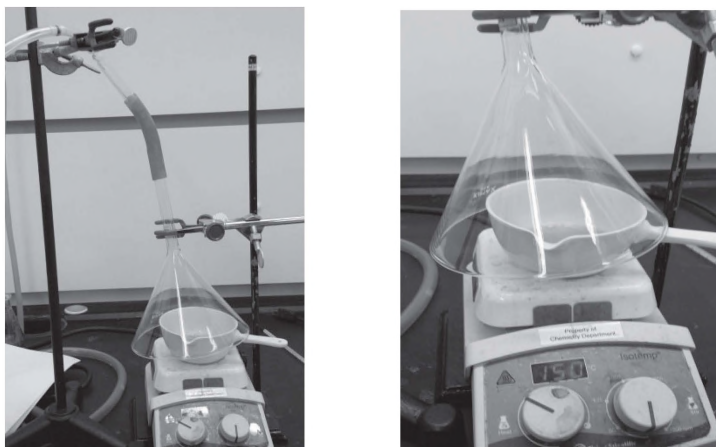
Figure 91. Evaporation of water from the $FeSO_4$ solution, under an umbrella with a blanket from protective gas.
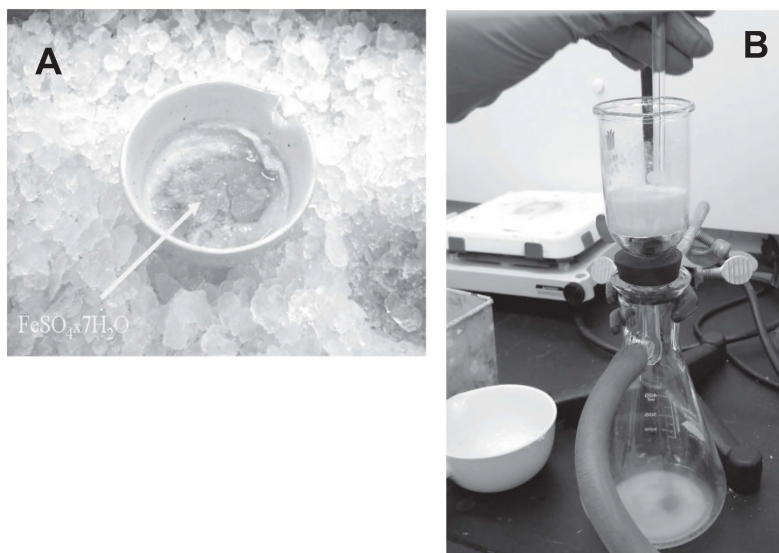
Figure 92. Crystallization of FeSO$_4$ heptahydrate on an ice bath (**A**) and filtration of the salt (**B**). See centerfold for this image in colour.
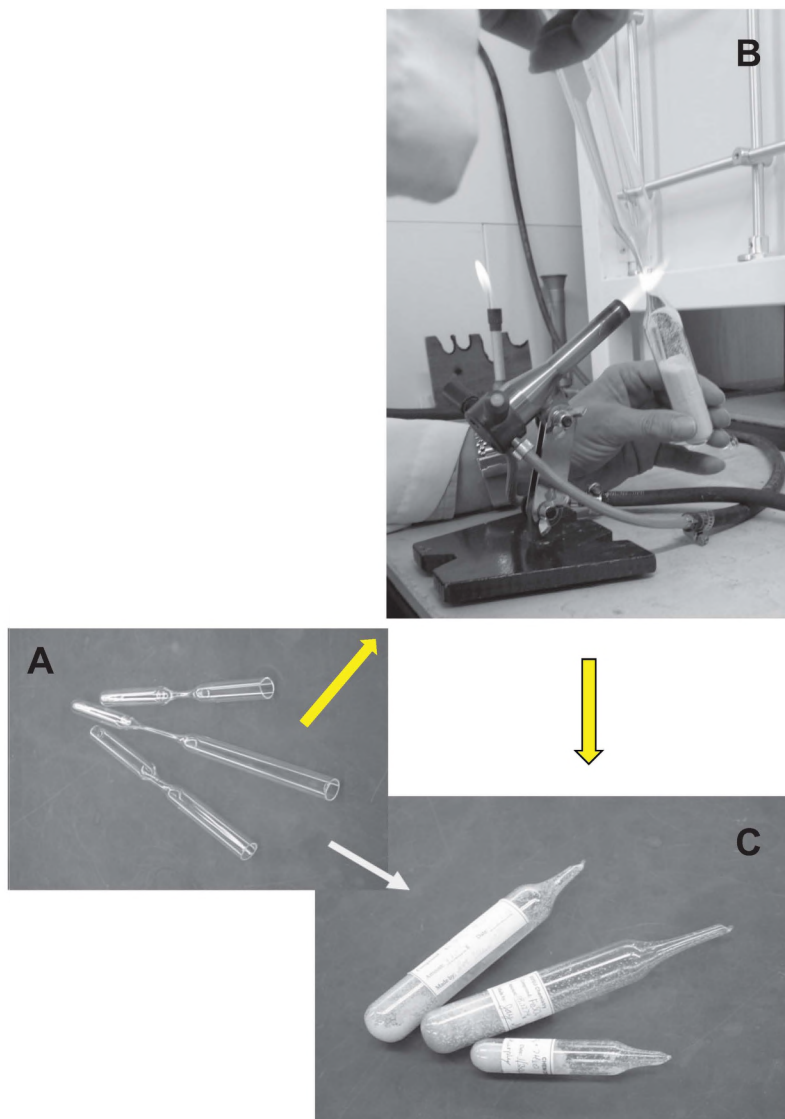
Figure 93.   Pre-made blank ampoules (**A**), blow torch sealing of air sensitive compound (**B**), and sealed under nitrogen iron(II) sulfate heptahydrate (**C**).

*- the basic skills of using a blow torch will be practiced while waiting for the evaporation of the FeSO₄ solution; a propane torch may be employed as well, if thin glass pipes are used.

2.6.1 Thermal analysis results

After recording an air-dried, freshly-made sample of $FeSO_4 \cdot 7H_2O$, students should match it with TG/DSC traces, shown above in Figure 94. Also, students should build their own table of calculated/found weight losses, and include all the materials included in the lab report.

It is expected that students will provide explanation for the thermal decomposition pattern of the target compound $FeSO_4 \cdot 7H_2O$, and especially account for the formation of Fe(III) and S(IV) species. Appropriate reactions should be included in the lab report.
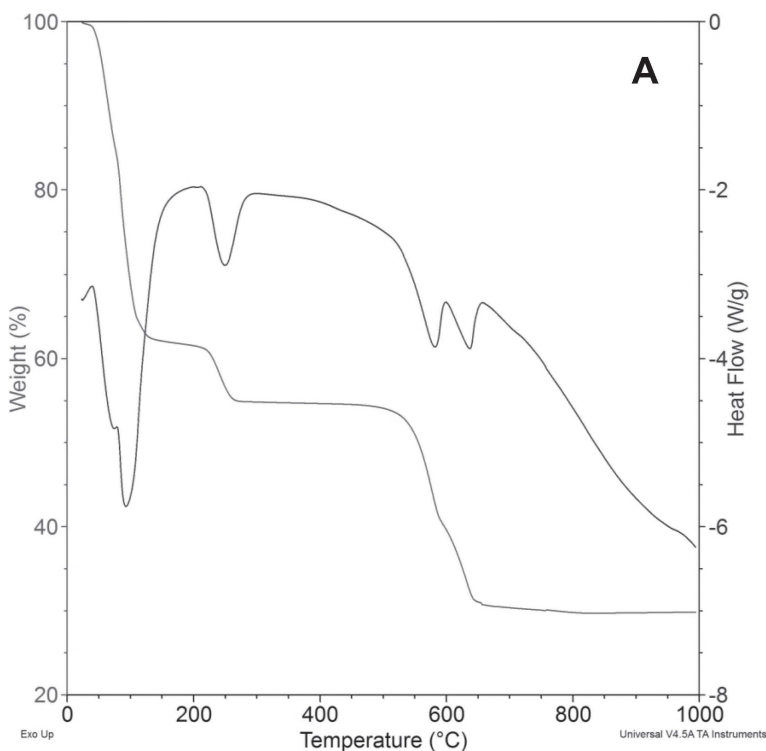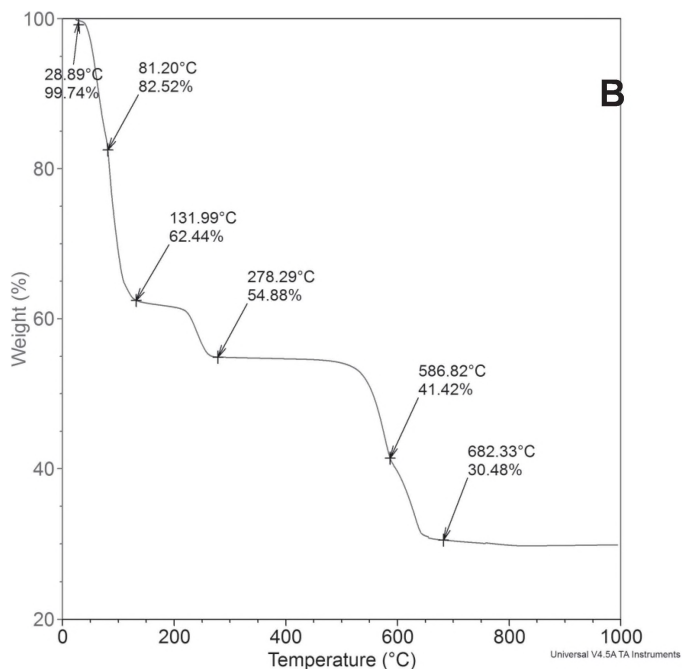
Figure 94. Typical combined DSC/TG traces for the panoramic view (**A**), and weight loss trace for the FeSO$_4$·7H$_2$O thermogravimetric analysis (**B**).

Table 5. Results of thermal analysis studies of decomposition of FeSO$_4$·7H$_2$O under pure N$_2$ atmosphere (Figures 94**A** and **B**).

Compound	Process*	Product	Weight losses, % calculated (*found*)	Error, %
FeSO$_4$·7H$_2$O	-3H$_2$O	FeSO$_4$·4H$_2$O	80.56 (*82.52*)	-1.96
FeSO$_4$·4H$_2$O	-3H$_2$O	FeSO$_4$·H$_2$O	61.15 (*62.44*)	-1.29
FeSO$_4$·H$_2$O	-H$_2$O	FeSO$_4$	54.68 (*54.88*)	-0.20
6 FeSO$_4$	Fe$_2$(SO$_4$)$_3$,2Fe$_2$O$_3$, -2SO$_2$	Fe$_2$(SO$_4$)$_3$,		
		Fe$_2$O$_3$, SO$_2$	40.29 (*41.22*)	-1.13
2 Fe$_2$(SO$_4$)$_3$	2Fe$_2$O$_3$, -6SO$_2$, -3O$_2$			
		Fe$_2$O$_3$, SO$_2$, O$_2$	28.27 (*30.48*)	-2.21

* all these processes are endothermic [**5**].

Properties of the obtained compound:

F.W of $FeSO_4 \cdot 7H_2O$ is 278g/m; monoclinic crystal system, density is $1.899g/cm^3$; solubility in cold water is 15.7g /100g, in hot water (50^oC) 48.6g /100g. The compound represents prismatic blue-greenish crystals, that oxidize in the air within an hour to a familiar respective, yellow-brown, Fe(III) hydroxo-derivative. The target $FeSO_4 \cdot 7H_2O$ salt is insoluble in alcohols, ether, and benzene. Ferrous sulfate heptahydrate is thermally unstable, and begins losing crystallization water when exposed, even to the slightest heat above 70^oC. Established steps of dehydrations are shown below, in the compound's thermogram on Figure 94.

Potential hazards:
1) Sulfuric acid, which may cause severe burns to skin;
2) Hot surfaces of porcelain ware, glassware, hot plates, and a steam bath;
3) Compressed gases in argon and N_2 tanks; therefore, caution should be taken while working with them;
4) Attention should be maintained all the time while working with a blow torch; hot glass from manipulations with ampoules may cause burns.

Wear eye protection at all times during the lab!

Cited Literature

1. Thomas T. Tidwell "Wilhelm Schlenk: The Man Behind the Flask" *Angew. Chem. Int. Ed.* 2001, 40, *2*, 331-337.
2. Andrea Wayda, Marcetta Darensburg *"Experimental Organometallic Chemistry"* ACS Symposium Series 357, Washington DC, 1987.
3. Duward F. Shriver, M. A. Drezdzon. *"The Manipulation of Air-Sensitive Compounds"*, 2nd Edition; Wiley, 1986.
4. R. J. Angelici. *"Synthesis and technique in inorganic chemistry"*, W.B. Saunders Company, 1977.
5. Masset, P.; Poinso, J.Y.; Poignet, J.C. *J. Therm. Anal. Calorim.* 2006, *83* (2), 457-462.

2.7. Experiment 2B: Preparation of Cuprous Oxide, Cu_2O

Cuprous oxide, Cu_2O, is the simplest derivative of monovalent copper. This compound is used in laboratory practice as a soft reducing agent in a variety of organic reactions. Cuprous oxide reacts under anaerobic conditions with concentrated inorganic acids, such as HF, HCl, HBr and HI, to yield respective Cu(I) salts. However, the dissolution in oxygen-containing inorganic and organic acids leads to the formation of metallic copper and respective Cu(II) salts, due to the disproportionation reaction. Cuprous oxide, Cu_2O, is soluble in concentrated ammonia solution, and is also noticeably soluble in base solutions, such as NaOH, LiOH, KOH, demonstrating amphoteric properties.

Cuprous oxide is only slightly air-sensitive, but the best way to store it is still in sealed ampoules. Therefore, the main objective of this experiment is to learn a typical technique for the chemical reduction of metal ions by an inorganic reducing agent, such as hydrazine. Learning simple glassblowing operations, such as making ampoules, and sealing synthesized compounds in them, is also essential.

Goals of this laboratory experiment and expected accomplishments:
1)   Perform synthesis of Cu_2O according to the procedure provided;
2)   Filter and dry your sample; yield of the product will be calculated after its complete dryness;
3)   Packing the oxide in an ampoule will be done when the oxide is totally dry on the next lab session;
3)   Record DSC/TG traces for a small sample (~20mg) of the Cu_2O under N_2 flow using available thermo-analyzer;
4)   Carry out data analysis and present them in your lab report, which is due at the next laboratory session;

Equation for the reaction:

$$4Cu(CH_3COO)_2 \cdot H_2O + N_2H_4 \cdot H_2O \rightarrow 2Cu_2O + N_2 + 8CH_3COOH + 3H_2O$$
     4 x 199.54 g   50.60 g   286.16 g
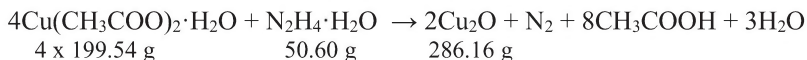
Chemicals:	Copper acetate, monohydrate: $Cu(CH_3COO)_2 \cdot H_2O$;
	Hydrazine monohydrate, $N_2H_4 \cdot H_2O$;
	Ethyl alcohol, C_2H_5OH.

Equipment:	Thermometer;
	Buchner flask with the glass filter, coarse porosity;
	Volumetric cylinder;

Pipettes (Pasteur and volumetric);
Spatula;
Ampoules blanks for sealing the final product;
Blow torch with oxygen tank;
Magnetic stirring plate with the stirbar.

Procedure: (*will be carried out in groups, with two students per group*):

Step 1.

The amount of cupric acetate, monohydrate of ~8.0g, is dissolved in 135mL of water upon slight heating of the mixture to ~40-50ºC. It is necessary to purge the obtained solution with nitrogen for ~10 minutes, and let it cool off to room temperature. The resulting solution is shown in Figure 95.
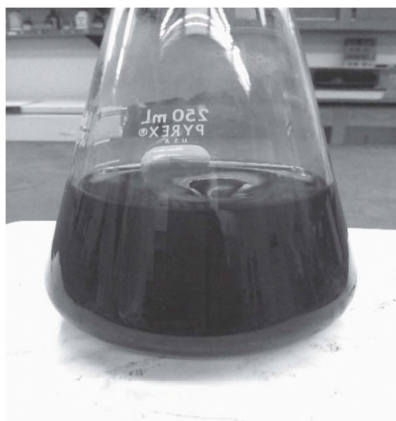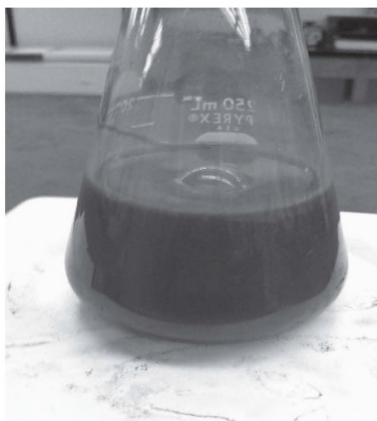
Figure 95. Initial solution of Cu^{2+} acetate.   **Figure 96.** The reaction mixture after addition of hydrazine hydrate, purged with N_2 and cooled to room temperature.

See centerfold for these images in colour.

Step 2.

A stoichiometric amount of 20% solution (by weight) of $N_2H_4 \cdot H_2O$ from the equation above will be added to a solution of $Cu(CH_3COO)_2 \cdot H_2O$ in DI water at room temperature. This is a dropwise addition that is carried out using a pipette and accomplished under intensive stirring. The typical time for addition is 5-7 minutes.

The stoichiometry should be obeyed, since the excess of hydrazine may lead to the formation of metallic copper powder. In other words, the reduction of Cu(II) can go farther than the oxidation state of Cu(I). At this point, the color of the reaction mixture will change, from blue to dark blue-purple, then to green, and gaseous nitrogen will evolve. When all the N_2 has evolved, the flask needs to be closed and placed aside for some time. After standing at room temperature for one hour, a yellow, fine powdery precipitate of Cu_2O will form in the flask in abundance (Figure 96).

Step 3.
The precipitate is then filtered, washed with room-temperature water (50mL), then with 25mL of ethyl alcohol, and, finally, with 25mL of diethyl ether. If the precipitate is too fine, and passes through the filter (glass frit or paper), then it should be centrifuged using a standard lab centrifuge with 5mL-capacity plastic test tubes. In such cases, the supernatant will be discarded, and precipitate of Cu_2O washed with water three times from acetic acid, hydrazonium salts, remains of Cu^{2+} and its unreduced complex with N_2H_4. Each time, the centrifugation is required to settle Cu_2O at the bottom of the test-tube. Washing the precipitate is necessary to remove electrolytes which prevent particles of cuprous oxide from coagulation and aggregation, making the filtration process lengthy. The filtrate solution should be colorless at this point. After washing the precipitate in several test-tubes, an additional ~10mL of water is added, and Cu_2O is re-suspended for paper filtration using the Vortex apparatus (Figure 28**B**, Chapter 1). Typical arrangements of test tubes and filtration setup are displayed in Figures 97 and 98.

Figure 97. Test tubes with Cu₂O precipitate after first centrifugation.
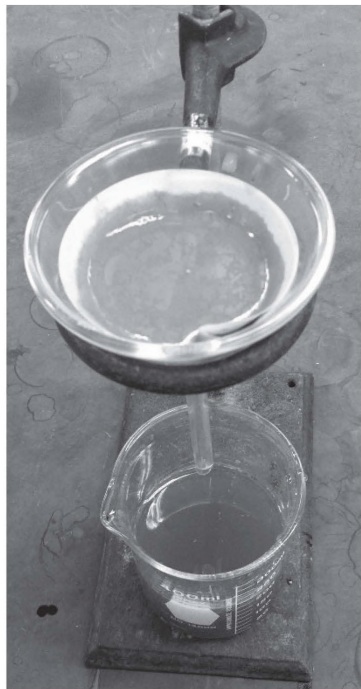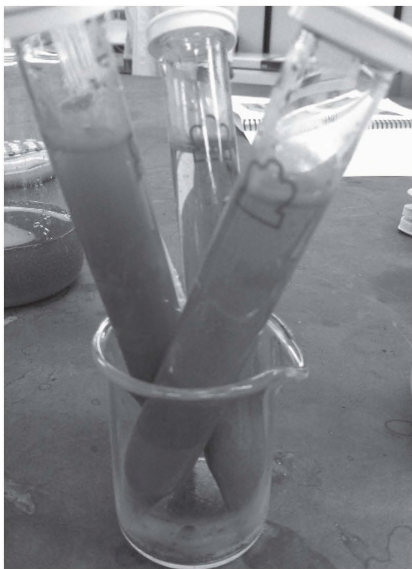
Figure 98. Gravity filtration of the reaction mixture using dense and thick paper filter.

See centerfold for these images in colour.

Step 4.

The air-dried precipitate is removed from the filter, and weighed for calculation of the yield. After all procedures, cuprous oxide should be packed in an ampoule and then sealed under nitrogen, using a blow torch. The number of the experiment, date, author of the reaction, and total amount of the obtained compound, must be written on the label. The label should be attached to the sealed ampoule with the target compound.

Step 5.

The quality of Cu₂O can be verified using a DSC/TG instrument. The color of this dried solid substance, generally speaking, depends on the size of the particles. In this experiment, some of the oxide obtained may even be a brownish-reddish color, which is an indication of smaller sized particles, compared to yellow precipitate (Figure 99).

Figure 99. Two batches of dried Cu₂O samples obtained from the same reaction: red-colored precipitate (on the left) filtered first, within an hour, followed by golden-colored (on the right) filtered second.

Step 6.

A sample should not demonstrate any significant (over 5%) weight loss, but should show phase transition (melting) of the oxide on the heat flow graph. Students should analyze their recorded thermogram, provide an explanation to weight trace, and comment on the observed phase transition temperature, as compared to that cited in the literature. All gained observations and conclusions should be included in the lab report.

Typical TG/DSC traces for good quality, differently colored, samples of cuprous oxides are shown in Figure 100.

Physical properties of cuprous oxide: yellow color, m.p.=1235°C (under vacuum, or an inert gas protection), density is 6.01g/mL at 20°C. Crystal system cubic, space group Pn3m; a=4.268 Å. Cuprous oxide dissolves in HHal (Hal = F, Cl, Br) acids under an inert gas protection to form respective Cu(I) halides. Similarly, dissolution in non-oxidizing acids, in standard conditions, such as acetic, other carboxylic acids, and sulfuric acid, leads to respective cuprous salts that are air-sensitive. However, generally speaking, in solutions Cu(I), species are prone to disproportionation reactions:

$$2\ Cu^+\ \rightarrow\ Cu^{(0)}+\ Cu^{(2+)}$$

Divalent species are easily detected by their blue/green color and presence of an intense signals in the EPR spectrum.
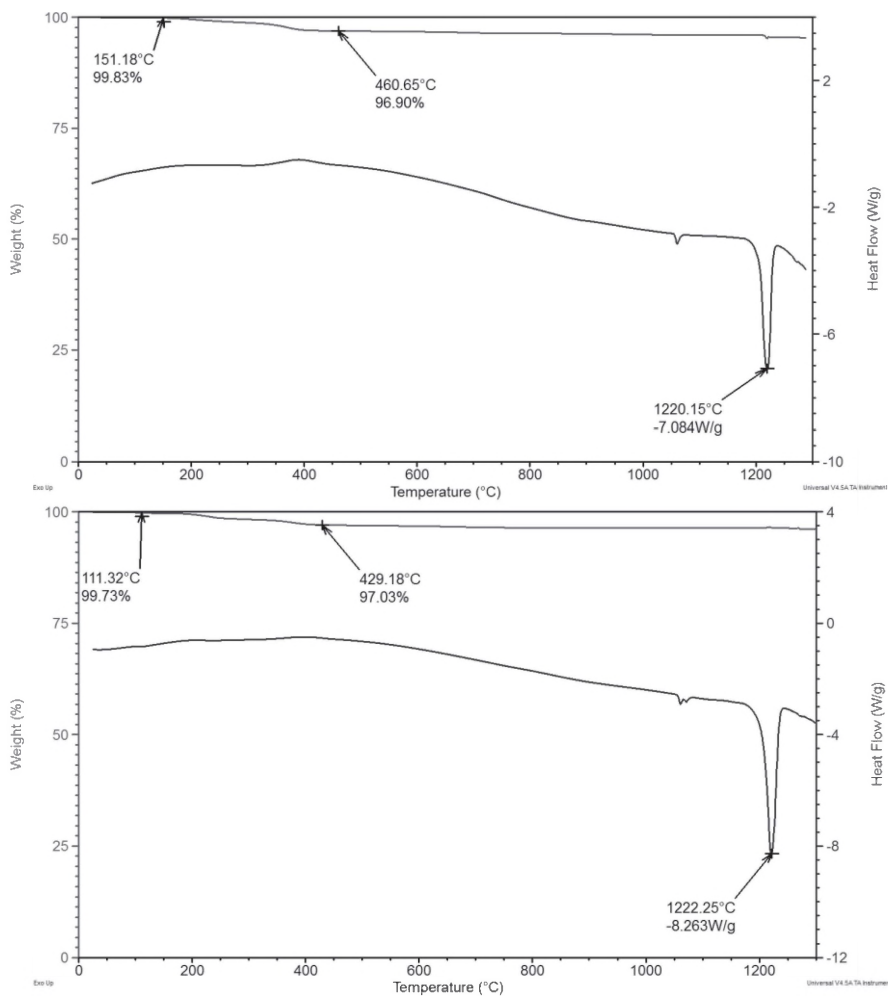
Figure 100. Typical thermograms for the yellow-colored Cu_2O (top panel), and the red-colored cuprous oxide (bottom panel).

Potential hazards:
1) Hydrazine hydrate (toxic substance);
2) Vacuum (possibility for glassware implosion).

Wear eye protection at all times during the lab!

2.8. Multistep Inorganic Reactions

The next two laboratory experiments are dedicated to the preparation of simple inorganic salts in several consecutive steps. Typically, two or more solutions are prepared, and then mixed together in a certain order for the desired reaction. There is a reason why these syntheses have to be carried out in such a way, instead of just simple one-step preparations. One of the examples is making *stoichiometric* binary compounds. Here, direct reactions between components (oxygen for oxides, halcogens for halcogenides, pnictogens [1] for pnictides, etc.) lead to non-stoichiometric, defective phases of variable compositions [2].

The solution to this problem is 'preassembly' of needed stoichiometry in some intermediate product which can be easily converted into the final product with fixed composition. The best way to prepare the stoichiometric binary halcogenides of heavy metals is the indirect, multistep reaction described below. For example, two components containing a chalcogene part and heavy metal part are mixed together to form *selenites* or *tellurites* - salts of $MSeO_3$ or $MTeO_3$ composition (M = Cd, Zn, Cu, Pb, Co), in which the ratio between the metal and halcogene is already preset to be exactly one-to-one. Both halcogens in these salts are in their tetravalent oxidation state, and have no bonding to the heavy metal part. Thus, interaction between M^{2+} cations and SeO_3^{2-} or TeO_3^{2-} anions has a purely ionic character and requires precise stoichiometry to balance the charge: +2 to -2. Then the reduction of $MHalcO_3$ leads to the desired MHalc (M = metal ions above; Halc = Se, Te) compounds of 1:1 stoichiometry in the binary halcogenide.

Two experiments on that subject are offered below.

2.9. Experiment 3A: "Preparation of Lead Telluride, PbTe"

There are several binary chalcogene-containing compounds that have essential practical significance. These are sulfides (ZnS, PbS, CdS, CuS, HgS), selenides (ZnSe, CdSe, PbSe), and tellurides (ZnTe, CdTe, PbTe), which have specific applications as semiconductors and photoelectric

elements. Thus, ZnS is the major component of luminophore in TV or monitor screens, while CdSe and CdS are widely used as thermistors. Both lead selenide and telluride are employed in IR-sensitive devices, including heat cameras and night vision equipment. Both polycrystalline materials and monocrystals are used for the above applications. Certainly, monocrystals of binary compounds are obtained from high purity polycrystalline substances upon slow and controlled cooling [3].

Preparation of binary compounds is not synthetically challenging. Nonetheless, it is known that, for this type of binary compound, it is very difficult to obtain high purity materials using direct reactions between elements. Those are normally carried out in a crucible, or in a quartz ampoule under vacuum. However, there is no exact stoichiometric ratio (1:1 or 1:2, etc.) between elements in such preparations. For example, typically obtainable phases in the Pb-Se, Pb-Te, Cd-Se systems are $Pb_{1.05}Se_{0.95}$, and similar for others, or in V-O systems, it is $VO_{1.8-1.95}$ instead of expected VO_2 composition [2]. It turns out that the composition depends on the method of synthesis of these compounds [4]. Clearly, the inconsistency of composition of the above and analogous binary systems creates big problems with consistency and reproducibility of electrophysical characteristics in such phases.

In this laboratory preparation we will use a multistep approach outlined above, and pre-assemble in one stoichiometric compound; lead and tellurium at 1:1 ratio. Thus, in the case of the lead telluride, PbTe, the reaction pathway is the following:

1) Solution #1: $2 Te + 8 HNO_3 = 2 H_2TeO_3 + 8 NO_2 + 2 H_2O$

2) Solution #2: $PbO + 2 HNO_3 = Pb(NO_3)_2 + H_2O$
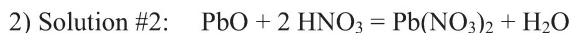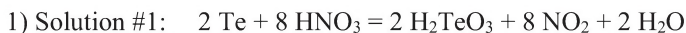
3) Mixing both solutions leads to the formation of lead selenite, $PbTeO_3$:

$$H_2TeO_3 + Pb(NO_3)_2 = PbTeO_3 + 2 HNO_3$$
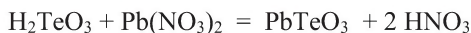
4) Reducing the lead selenite with hydrazine hydrate to lead selenide:

$$2 PbSeO_3 + 3 N_2H_4 = 2 PbSe + 3 N_2\uparrow + 6 H_2O$$

There are several redox reactions in this preparation. They are balanced, explained and displayed below.

For the dissolution of tellurium and lead during the preparation of initial and separate solutions:

Te^0 - 4e = Te^{4+} reducer, but gets oxidized
N^{5+} + e = N^{4+} oxidizer, but gets reduced
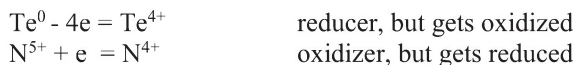
For the reduction of lead tellurite to lead telluride:

Te^{4+} + 6e = Te^{2-} (from tellurite)
$2N^{2-}$ - 4e = $2N^0 \rightarrow N^2$ (from hydrazine)
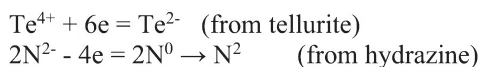
There are two other important ingredients in this synthesis; ammonia and tartaric acid. Both are introduced only for the purpose of keeping lead(II) cations in solution by the formation of stable complex particles, in given conditions.

The main goal of this experiment is to learn a typical technique of multistep inorganic synthesis.

The objectives of this laboratory exercise include: a) preparing several separate solutions for the reaction; b) controlled mixing of the ingredients; c) prolonged heating of the reaction mixture; d) work-up procedures involving filtration, washing of the precipitate, and drying; and e) packaging of a target compound in the glass ampoule (or tightly closed vial) for storage.

Equations for the preparation:

Solution #1: $Te + 4\ HNO_3 = H_2TeO_3 + 4\ NO_2 + H_2O$

Solution #2: $PbO + 2\ HNO_3 = Pb(NO_3)_2 + H_2O$

Mixing the two solutions:
        $Pb(NO_3)_2 + H_2TeO_3 = PbTeO_3\downarrow + HNO_3$

Main reaction: $2\ PbTeO_3 + 3\ N_2H_4 = 2\ PbTe\downarrow + 3N_2\uparrow + 6\ H_2O$
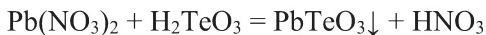
Chemicals: Tellurium powder, Te;
        Lead oxide powder, PbO (or lead carbonate, $PbCO_3$ if PbO is not available);
        Nitric acid, concentrated HNO_3 (40%);
        Hydrochloric acid concentrated, HCl;
        Hydrazine hydrate solution;

Tartaric acid;
Ammonia, concentrated solution;
Ethanol for washing the precipitate;
Methanol.

Equipment: Analytical balance;
Four little beakers, 50mL capacity;
Hotplate (combo) as a heat source;
Volumetric cylinders;
Magnetic stirrer and stir bar;
Beaker, 300 - 500mL capacity;
Spatulas;
Ampoule blanks with stretched neck for sealing;
Propane or blow torch with oxygen tank and accessories.

Procedure: *(will be carried out in groups, with two students per group)*:
Follow the pictorial description in the Figures below, and the explanations
of this laboratory experiment.

Step 1.
Place a preparation of solution #1: 0.638g of elemental tellurium in a small
beaker, and in a separate small beaker, mix 1 volume (7mL) of concentrated
HCl and 1 volume (7mL) of concentrated nitric acid, to form 14mL of
aqua regia*. Under the hood, add *aqua regia* to the beaker containing Te
particles. A brown gas (NO_2) is evolved, and tellurium powder dissolves
during this step (Figure 101).

---

*- the *aqua regia* is the Latin name for the mixture of acids HCl and HNO_3 = 4:1
that was known to alchemists to be the only liquid capable of dissolving metallic
gold; silver is not soluble in HCl, but dissolves in HNO_3.
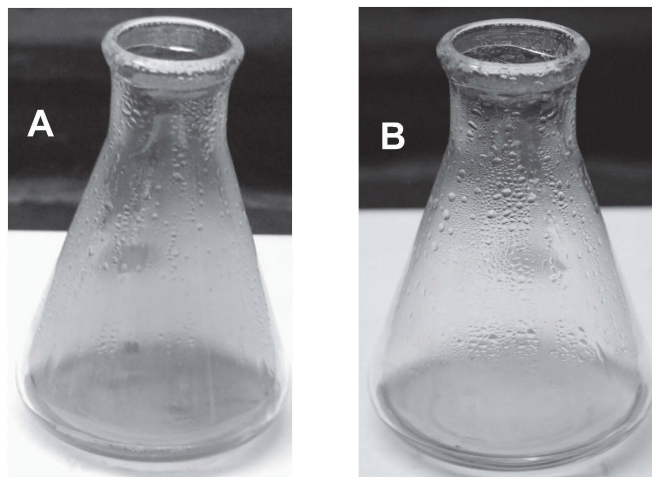
Figure 101. Dissolution of tellurium powder in nitric acid: **A** – beginning of the reaction and intense NO_2 evolution, **B** – final appearance of yellowish transparent H_2TeO_3 solution.

Step 2.
Place a preparation of solution #2: 1.116g of lead oxide powder (PbO) (5×10-3 moles) in a small beaker, and dissolve in 4mL of concentrated nitric acid. Then add 4 drops of DI water. After dissolving all of the lead oxide, dilute the obtained solution with 8mL of water. If PbO is not available, then you may use 1.336g of the lead carbonate $PbCO_3$, and the same amount of acid.

Step 3.
Place a preparation of solution #3: 2g of tartaric acid in a bigger beaker. Dissolve the solid in 5mL of water, and then mix with 15mL of concentrated ammonia, and with 25mL of hydrazine hydrate.

Step 4: **Combination of solutions**.
While solution #3 is under intensive stirring at room temperature under the hood, add solution #2 dropwise, quickly, using a disposable plastic pipette (Figure 102). Extreme care should be taken at this point, since an acidic solution is being mixed with a very basic solution! Wearing protective goggles and carrying out the whole procedure under the hood is absolutely necessary.
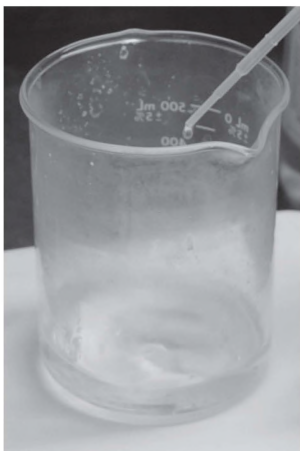
Figure 102. Dropwise addition of solution of NH_3 to a solution of $Pb(NO_3)_2$.
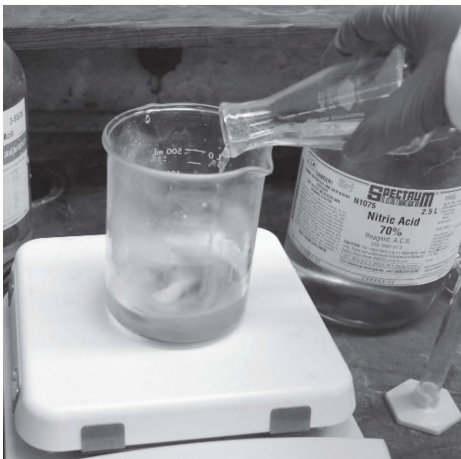
Figure 103. Rapid mixing of H_2TeO_3 with solution of the $[Pb(NH_3)_6](NO_3)_2$ complex leads to a formation of white $PbTeO_3$.

Step 5: Reduction reaction.

Solution #1 is added at once to the mixture in step 4, under intensive stirring, at room temperature (Figure 103). The mixture has a grey lumpy appearance, and consists primarily of $PbTeO_3$, which is white, and some of the black PbTe that has already formed. At this point, everything is added together and stays in a larger beaker, while being heated on a hot plate. The reaction mixture is boiled for ~60 minutes, during which the lead telluride will gradually appear as a black precipitate (Figure 104). This precipitate tends to form on the beaker's wall, and needs to be washed down with water. Also, you may use a stirring rod to help move the precipitate back into the solution.

Step 6: Work-up.

The precipitate of PbTe is filtered using a glass fritted filter (Figure 105). Let the reaction mixture sit in the fritted filter before turning on the vacuum. Apply a slight vacuum, to make sure the precipitate is not lost in filtration, once the precipitate settles on the bottom of the filter. Then wash with 100mL of water (be sure to rinse the beaker used for heating to obtain the highest yield of product), and then with 25mL of ethanol, C_2H_5OH, and 25mL of methanol, and wash the precipitate for the last time with CH_3OH. For each washing, be sure to suspend the precipitate in the solution and wait for the precipitate to settle before re-applying a slight

vacuum. The precipitate should be completely air-dried (or in the desiccator over P_2O_5) before sealing in an ampoule (Figure 106). The yield is usually close to 100%.
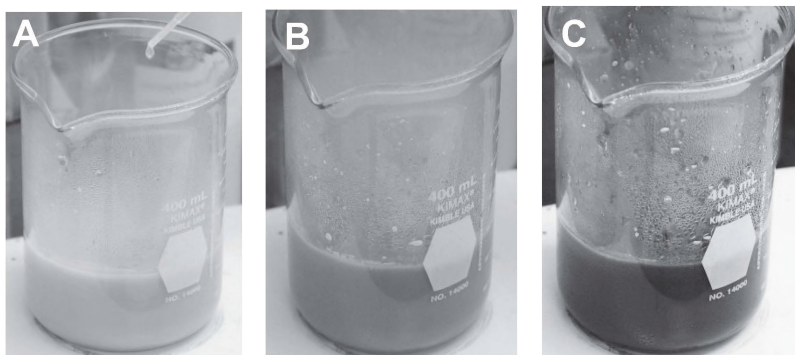
Figure 104. Progressive reduction of $PbTeO_3$ to PbTe during heating of the reaction mixture; **A** – beginning, **B** – after ~10 min, **C** – after 30 min.

The target compound can be stored in a tightly closed vial. However, in order to preserve its quality and completely avoid slow hydrolysis, the best method of storage is in a sealed ampoule (Figure 106).
The number of the experiment, date, authors of the preparation, and total amount of the obtained compound, with its yield, must be written on the label. The label should be attached to the sealed ampoule with the target compound.

Physical properties of lead telluride, PbTe: black microcrystalline powder, F.W. = 334.82g/M; m.p.=914°C (in vacuum); a cubic crystal system, d = 8.16g/cm^3. The compound exhibits semiconductor properties. Being heated in air, lead telluride at ~900°C undergoes oxidative decomposition with the formation of white TeO_2.
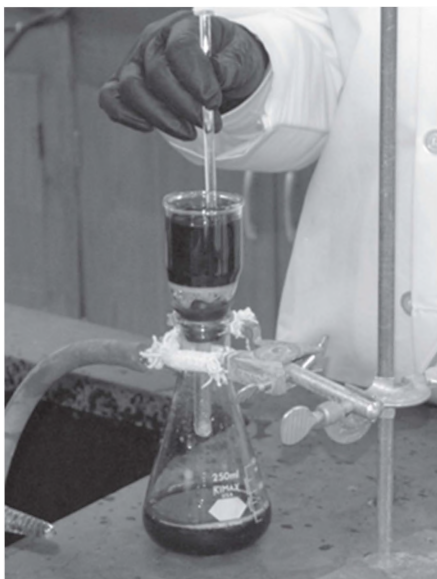
Figure 105. Filtration and then washing of PbTe using Büchner flask and *M*-grade fritted glass filter.

Figure 106. Dry lead(II) halcogenides sealed in glass ampoules under nitrogen for storage.

Potential hazards:

1) Elemental lead is a toxic substance; be careful with it.
2) Tellurium compounds have a distinctive smell, and are toxic as Well.
3) Concentrated HCl and HNO_3 are strong acids, and the latter is an oxidizer. If handled improperly, they can cause severe and painful burns to bare skin. Therefore, all operations with acids should be carried out using protective gloves and under the ventilation hood.
4) Concentrated ammonia solution is caustic, and vapors have a sharp and extremely unpleasant odor; all operations with NH_3 have to be carried out under the hood.
5) Sealing a compound that is not completely dried into an ampoule may cause its rupture due to pressure build-up. This may cause bodily injuries.

Wear eye protection during the lab work at all times!

Note: The lead selenide, PbSe, can be prepared in exactly the same way, using elemental selenium instead of tellurium as a source of halcogene.

Solution #1:

$$2\ Se + 8\ HNO_3\ \rightarrow\ 2\ H_2SeO_3\ +\ 8\ NO_2\ +\ 2\ H_2O$$
   78.96 g   63.01 g   128.97 g   46.01 g   18.01 g
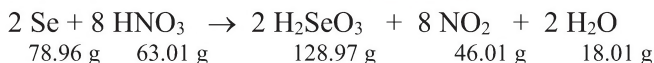
Oxidation of selenium and reduction of nitric acid:
$$Se^0 - 4\ e = Se^{4+}$$
$$N^{5+} +\ \ e = N^{4+}$$

Solution #2:

$$PbO\ \ +\ \ 2\ HNO_3\ \rightarrow\ Pb(NO_3)_2\ +\ \ H_2O$$
223.2 g   63.01 g   331.2 g   18.01 g

Mixing of solutions:

$$H_2SeO_3\ \ +\ \ Pb(NO_3)_2\ \rightarrow\ PbSeO_3\ \ +\ \ 2\ HNO_3$$
129.0 g   331.2   334.2 g   63.01 g
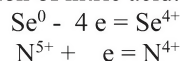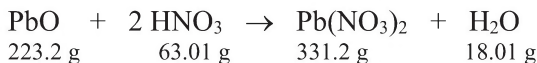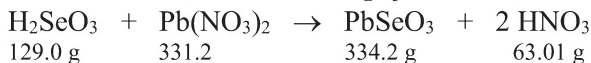
Reduction of selenite and formation of the product:

$$2\ PbSeO_3 + 3\ N_2H_4\ \rightarrow\ \ 2\ PbSe\ \ +\ \ 3\ N_2 \uparrow\ \ +\ \ 6\ H_2O$$
   334.1 g   32.05 g   286.2 g   28.00 g   18.01 g

$$Se^{4+} + 6\ e = Se^{2-}$$
$$2N^{2-} - 4\ e = 2N^0 \rightarrow N_2$$
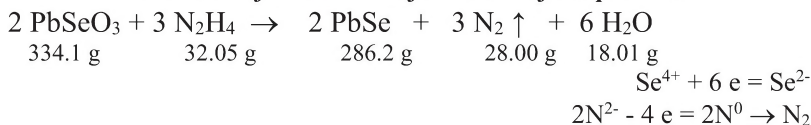
Used amounts of compounds in the above reactions are the following:

Se: 1.005g;
PbO: 1.116g of a yellow lead oxide powder. Added 4mL of
             concentrated nitric acid first, and then after heating to ~60°C
             added 4 drops of water to a complete dissolution;
$C_4H_6O_6$ (*d,l*-tartaric acid): 2.00g in 5mL of water;
NH_3:   15mL of concentrated ammonia solution;
N_2H_4: 25mL hydrazine hydrate.

Physical properties of lead selenide, PbSe: black microcrystalline powder, F.W. = 286.17g/Mol; m.p.= 1080.7°C (in vacuum); a cubic crystal system, a = 6.124 Å; d = 7.99g/cm^3. The compound exhibits semiconductor properties. Being heated in air, lead selenide decomposes with emission of red vapors of elemental selenium. Compound is not water soluble, but dissolves in HCl and HNO_3 with chemical reaction.

Cited Literature

1. Raynar-Canham, G.; Overton, T. *Descriptive Inorganic Chemistry*, 6th Ed.; W.H. Freeman & Company, 2015.
2. Shriver, D.F.; Atkins, P. *Inorganic Chemistry*. 3rd Ed., W.H. Freeman & Company, New York; 1999.
3. a) Trivedi, S. (Brimrose Technology Corporation) "*Mercurous Halide Crystals for Optoelectronic Applications*" presentation on The 3rd Collaborative Conference on Crystal Growth; San Sebastian, Spain, September 4-8, 2016; b) Barta, C.; Barta, Jr. *Materials Science Forum*, 1990, *61*, pp 93-150 (doi: 10.4028/www.scientific.net/MSF.6193)
4. Cotton, A.F.; Wilkinson, G.; Murillo, C.A.; Bochmann, M. *Advanced Inorganic Chemistry*. 6th Ed., Wiley Interscience Publication, 1999.

2.10. Experiment 3B: "Preparation of Cadmium Carbonate, CdCO₃"

This preparation is an alternative to Experiment 3A describing multistep inorganic synthesis, and is similar to the preparation of the lead(II) telluride PbTe, which required preparation of several solutions which were mixed in a certain sequence, and led to the final product. The synthesis of $CdCO_3$ will be carried out *in situ**. In this case, however, there are small differences in the preparation which will be seen during the synthesis description.

The objectives of this laboratory exercise include: a) preparing two separate solutions for the reaction; b) mixing the ingredients; c) controlling a prolonged heating of the reaction mixture; d) working-up procedures involving filtration, washing of the precipitate, and drying; and e) packing a target compound for storage, using either glass ampoule, or tightly closed screw-cap vial.

Goals of this laboratory experiment:
1) Perform multistep preparation of $CdCO_3$ according to given procedure.
2) Filter and dry your sample; yield of the product will be calculated after its complete dryness prior to, or at the next lab session.
3) Packing of $CdCO_3$ in an ampoule will be done when the oxide is totally dry, at the next lab session.

Procedure: *(will be carried out in groups, with two students per group)*:

Chemicals: Elemental Cd (as thin foil);
                      Gas tank with CO_2;
                      Nitric acid concentrated, HNO_3;
                      Ammonium carbonate, $(NH_4)_2CO_3$;
                      Ammonia, concentrated solution;
                      Methanol, technical grade, to wash the precipitate;

_____

*- *in situ* – Latin, 'in one pot', or without isolation of intermediate products.

Equipment: Analytical balance;
                      Two beakers of 100mL capacity;
                      Erlenmeyer flask of 125mL capacity;
                      Magnetic stirrer/hotplate combo and a stirbar;
                      Spatulas;
                      Lab stand with clamp and ring stand;
                      Filter paper;
                      Rubber hose with glass pipe tip;
                      Ampoule blank, or vial.

Step 1: Preparation of the metal salt solution.

$$Cd \quad + \quad 4\,HNO_3 \quad = \quad Cd(NO_3)_2 \quad + 2\,H_2O + NO_2\uparrow$$
112.4 g   4 x 63 g   236.42 g
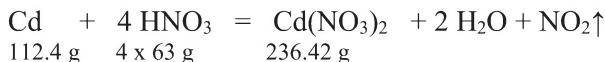
Place 2g of metallic cadmium turnings (or filings) into a ~100mL capacity glass beaker and add at once an equivalent amount of concentrated HNO_3, according to the reaction above. Observe the brown gas evolution (NO_2) and heating of the reaction mixture (Figure 107**A**). After all metal pieces dissolve, cool the beaker to room temperature and proceed to step #2. The solution should appear clear and colorless (Figure 107**B**). Solid $Cd(NO_3)_2$ will not be isolated at this stage, and another reactant will be added to it in the next step.

Step 2: Formation of the complex with required stoichiometry.

$$Cd(NO_3)_2 + (NH_4)_2CO_3 + 4\,NH_3 \quad = [Cd(NH_3)_4]CO_3 + 2\,NH_4NO_3$$
236.42 g   96.1 g   dropwise added   240.5 g   80.02 g
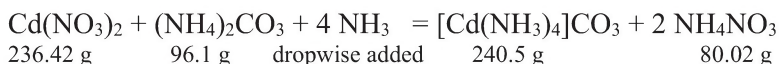
Prepare a solution of 1.71g of ammonium carbonate, $(NH_4)_2CO_3$ in 50mL of water at room temperature. When the salt dissolves, add this solution at once to the beaker with the solution of $Cd(NO_3)_2$ under stirring. It is required that a mid-sized stirbar be placed into the beaker with the latter, prior to the addition of the carbonate solution. The beaker must be placed on the hotplate/stirrer combo as well. A precipitate of several cadmium carbonates that are sparingly soluble will form in the beaker upon mixing. The precipitate must be carefully dissolved by the dropwise addition of a concentrated ammonium solution at room temperature. The addition of the neutral ligand – NH_3 – assures the formation of the stoichiometric Cd(II) complex, with a 1:1 metal-to-carbonate stiochiometry: $[Cd(NH_3)_4]CO_3$, which is necessary for the next reaction. Coordinated ammonia is a

convenient ligand, since upon heating it leaves the metal center, allowing the outer-sphere carbonate anion to bind cadmium at the exact stoichiometry.
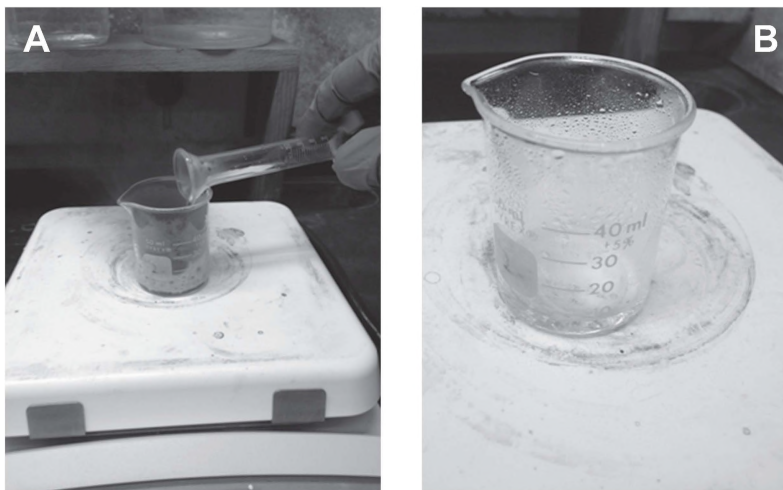
Figure 107. The dissolution of metallic cadmium in nitric acid with intense brown NO_2 gas evolution (**A**), and **B** – final clear solution of $Cd(NO_3)_2$.

Step 3: Thermal decomposition of the complex and formation of the product.

When the precipitate in step #2 dissolves, begin heating the reaction mixture in the beaker (or Erlenmeyer flask if the previous step was carried out in it), on a hot plate (Figure 108). The stoichiometric cadmium(II) carbonate begins to form according to the equation below:

$$[Cd(NH_3)_4]CO_3 \quad = \quad CdCO_3\downarrow + 4\ NH_3\uparrow$$
240.5 g   172.4 g   68.1 g
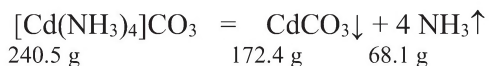
When the precipitate stops forming, remove the beaker from the hotplate, and let its contents cool at ambient conditions.
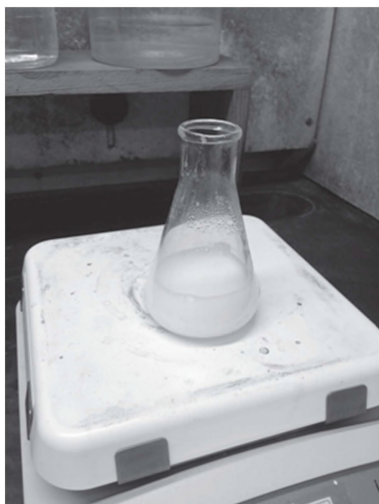
Figure 108. The formation of $CdCO_3$ precipitate upon heating of the reaction mixture**.**

Figure 109. The filtration procedure.

Step 4:   Work up.

Filter the precipitate of $CdCO_3$ using dense and thick paper filter (Figure 109), wash it with methanol, and thoroughly air-dry between paper towels in the open air. Being exposed to CO_2 and moisture, cadmium carbonate slowly converts into water soluble $Cd(HCO_3)_2$, which appears as wet slimy sugar and tends to penetrate paper towels or filter paper, leading to a significant yield drop. The best way of getting $CdCO_3$ out of the filter paper is its thorough drying in a vacuum desiccator over H_2SO_4 for several days (Chapter 1). The weighing and packing compound procedure can be accomplished prior to, or during, the next lab session. The target compound can be stored in a tightly closed vial. However, in order to preserve its quality, the best method of storage is in a sealed ampoule. Thus, pack the dry product without any smell of methanol into the ampoule blank, clean the ampoule's neck with a piece of cotton, and seal it, using the blow torch.

The number of the experiment, date, authors of the reaction, and total amount of the obtained compound, with its yield, must be written on the label as shown below (Figure 110). The label should be attached to the sealed ampoule (or tightly closed screw-cap vial) with the target compound.
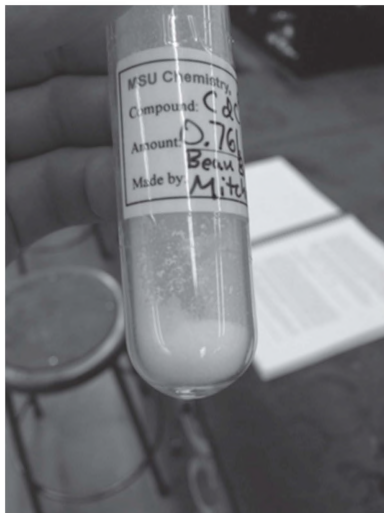
Figure 110. Sealed ampoule with dried cadmium carbonate.

Properties of cadmium carbonate, CdCO₃: the compound represents a white crystalline material, F.W.= 172.4g/M; structure – hexagonal, R-3c space group (a=4.920 Å, c=16.298 Å). The compound is slightly soluble in water, but readily dissolves in mineral and organic acids with the formation of respective Cd(II) salts.

Cadmium carbonate is a precursor for the cadmium oxide, which is valuable transparent and electricity conducting compound.

Potential hazards:
1) Elemental cadmium is a toxic substance.
2) Concentrated HNO_3 is a strong acid, and is an oxidizer. If handled improperly, it can cause severe and painful burns to bare skin as well, coloring it yellow, which will stay for 2-3 weeks. Therefore, all operations with acids should be carried out using protective gloves and under the ventilation hood.
3) Concentrated ammonia solution has a sharp smell, and accidental inhalation of its vapors is not pleasant, and is dangerous.

Wear gloves and eye protection at all times during the labwork!

2.11. Dehydration of Inorganic Salts: Reflux, Distillation

Background information

Preparing anhydrous metal salts is an important part of industrial chemical manufacturing. Chlorides, bromides, sulfates, phosphates and nitrates are the most common compounds of this series.

Some of the salts (for instance, Na_2SO_4, $MgSO_4$, $CaSO_4$, $Mg(ClO_4)_2$), are employed as drying agents in laboratory practice. The water-consuming action of these salts is based on the formation of stable hydrates with multiple molecules of crystallization water:

$$Na_2SO_4 + 10\,H_2O \quad \rightarrow \quad Na_2SO_4 \cdot 10H_2O$$
$$MgSO_4 \; + \; 7\,H_2O \qquad \rightarrow \quad MgSO_4 \cdot 7H_2O$$
$$Mg(ClO_4)_2 \; + \; 4\,H_2O \rightarrow \quad Mg(ClO_4)_2 \cdot 4H_2O$$
$$CaSO_4 + 2\,H_2O \qquad \rightarrow \quad CaSO_4 \cdot 2H_2O$$
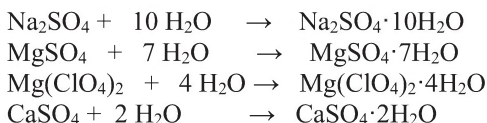
With the exception of magnesium perchlorate, all the aforementioned salts can be regenerated to their anhydrous state by heating them to ~150°C at ambient pressure, or under vacuum. The $Mg(ClO_4)_2 \cdot 4H_2O$ cannot be heated because of its poorly controllable response to such an action, which may lead to an explosion, especially in the presence of traces of organic compounds and residual amount of organic solvents [1]. This salt slowly fades away from the arsenal of efficient desiccators.

Another group of the anhydrous inorganic compounds has a different area of application. These salts are used as catalysts in numerous multi-ton organic and organometallic syntheses. Typical examples of such salts are halogenides of Al(III) and Fe(III) (Friedel-Krafts catalysts for electrophilic substitution), $CoCl_2$, $SnCl_4$, $SiCl_4$ and many, many other compounds. It appears that hydrates of those, and many other salts made of metal cations (which form weak bases and hydrolyze in aqueous solutions) is seemingly simple. Unfortunately, these salts cannot be obtained from their easily-accessible hydrated analogs upon heating. This is due to the fast and irreversible reactions of hydrolysis and oxo-salts formation at elevated temperatures. Commonly observed processes for some salts are shown below.

heat
$$FeCl_3 \cdot 6H_2O \quad \rightarrow \quad FeOCl + 5\,H_2O + 2HCl,$$
(and also, a mixture with $Fe(OH)Cl_2$, $Fe(OH)_2Cl$ instead of $FeCl_3$)

$$\underset{}{\overset{heat}{\text{CoBr}_2 \cdot 6\text{H}_2\text{O} \quad \rightarrow}} \quad \text{Co(OH)Br} \; + \; 5 \; \text{H}_2\text{O} \; + \; \text{HBr},$$
(instead of expected CoBr$_2$)

$$\underset{}{\overset{heat}{\text{AlCl}_3 \cdot 6\text{H}_2\text{O} \quad \rightarrow}} \quad \text{Al(OH)}_2\text{Cl} + 4 \; \text{H}_2\text{O} + 2 \; \text{HCl},$$
(and also, Al(OH)Cl$_2$, AlOCl instead of expected AlCl$_3$)
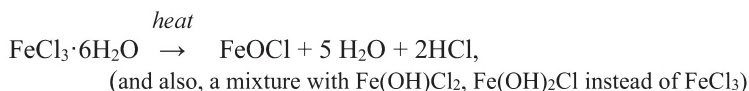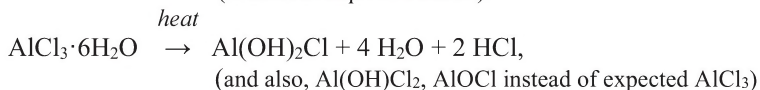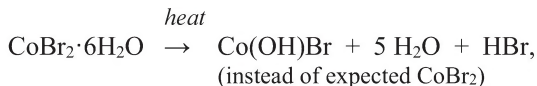
Therefore, it is not possible to prepare many anhydrous metal salts by the cheap, and seemingly obvious, heating of their hydrated derivatives. However, there are several methods of chemical removal of crystallization water from hydrated salts. All these methods use reactions of water in solid salt with an appropriate dehydrating agent. For instance, halogen anhydrides such as phosgene (COCl$_2$), thionyl chloride or bromide (SOCl$_2$ or SOBr$_2$ respectively), phosphorous pentachloride (PCl$_5$) or acetic anhydride ((CH$_3$CO)$_2$O) are widely used as water-scavenging substances. The biggest advantage of these reagents is that they all form either gaseous products, or volatile compounds, or other easily removable products. Sometimes these reactions are highly exothermic and release substantial heat. Nevertheless, there is no danger of hydrolysis, since there is an excess of the respective acid present. Chemical reactions describing the action of dehydrating reagents are presented below:

$$\text{CuCl}_2 \cdot 2\text{H}_2\text{O} \; + \; \text{SOCl}_2 \rightarrow \; \text{CuCl}_2 + \text{H}_2\text{SO}_3 + 2 \; \text{HCl}$$

$$\text{CoBr}_2 \cdot 6\text{H}_2\text{O} \; + \; 3 \; \text{SOBr}_2 \rightarrow \text{CoBr}_2 + 3 \; \text{H}_2\text{SO}_3 + 6 \; \text{HBr}$$

$$\text{AlCl}_3 \cdot 6\text{H}_2\text{O} + 3 \; \text{COCl}_2 \rightarrow \text{AlCl}_3 + 3 \; \text{H}_2\text{CO}_3 + 6 \; \text{HCl}$$

$$\text{Fe(NO}_3)_3 \cdot 9\text{H}_2\text{O} \; + \; 9 \; \text{PCl}_5 \rightarrow \; \text{Fe(NO}_3)_3 + 9 \; \text{POCl}_3 + 18 \; \text{HCl}$$
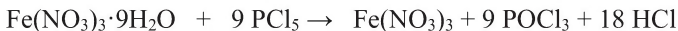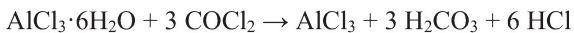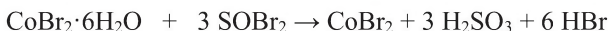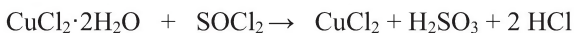
Volatile acids such as H$_2$SO$_3$ and H$_2$CO$_3$ certainly decompose to gaseous acid oxides SO$_2$, CO$_2$ and water at elevated temperatures, but that happens after acids leave the reaction mixture. Volatile phosphorous oxochloride (POCl$_3$) can be easily removed as well. This provides an exclusively nice and clean way to prepare anhydrous salts of many metals with quantitative or almost quantitative yield.

There are three nice and colorful laboratory experiments that teach students proper techniques when dealing with dehydration reactions of inorganic crystallohydrates. Two reactions describe the use of the thionylchloride, SOCl$_2$ (for Ni^{2+} and Co^{2+} salts), while the last one describes the use of acetic anhydride (for Sn^{2+} salt).

2.12. Experiment 4A: "Preparation of Anhydrous Nickel(II) Dichloride, NiCl$_2$ (*or similarly: Cobalt(I) Dichloride, CoCl$_2$*)"

Both salts – NiCl$_2$ and CoCl$_2$ – can be obtained in the same way using the same reactions. The first salt changes color upon dehydration, from emerald green to orange-brown, while the cobaltous salt changes color from pink to blue. For the purpose of rational laboratory manual pages, we only provide details of the preparation of *anhydrous nickel dichloride*. However, for the convenience of interested readers, the respective equation for the reaction of cobalt chloride dehydration is given as well.

Goals of this laboratory experiment and expected accomplishments:
1) Conduct preparation of anhydrous NiCl$_2$, according to given procedure.
2) Learn the basic procedures of using an oil vacuum pump equipped with cold trap filled with liquid N$_2$ (or dry ice); Dewar flask setup.
3) Calculate yield of a dry compound and pack it in an ampoule for storage.
4) Prepare a detailed lab report including observations, schemes, and pictures of the lab experiment emphasizing work with vacuum pump and cryogenics.

Equation for the preparation:

NiCl$_2$·6H$_2$O + 6 SOCl$_2$ = NiCl$_2$ + 12 HCl↑ + 6 SO$_2$↑
237.7 g   713.9 g   129.6 g   437.6 g   384.4 g
green   *yellow*

CoCl$_2$·6H$_2$O + 6 SOCl$_2$ = CoCl$_2$ +   12 HCl↑ + 6 SO$_2$↑
237.9 g   713.9 g   128.9 g   437.6 g   384.4 g
pink   *blue*
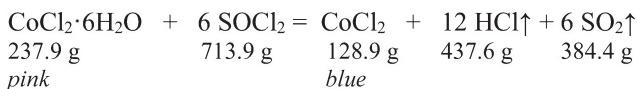
Chemicals: Nickel dichloride, hexahydrate (or Cobalt dichloride
                    hexahydrate*)
                    Thionyl chloride, SOCl$_2$

Equipment: Round bottom flask, ~ 250mL capacity
                    Condenser for reflux #19/22 with water hoses;
                    Graduated (volumetric) cylinder;
                    Glass spatulas and compactors;

Ampoule blank with stretched neck for sealing;
Vacuum system assembly that includes cold trap;
Dewar flask with liquid N_2, vacuum stopcocks, adaptors, grease, etc.;
Desiccator charged with drying agents;
Propane or blow torch with oxygen tank for ampoules closure.

Procedure: *(will be carried out in groups, with two students per group)*:

Step 1.
Place weighed 4.768g of *very fine powder* of $NiCl_2 \cdot 6H_2O$ in a round-bottom 100mL capacity flask, with an inner (female) type joint #19/22. This powdery compound should be obtained using a small size mortar and pestle and thorough grinding, within ~10 minutes. The quality of powdery nickel dichloride hexahydrate will determine the amount of time used for the preparation of an anhydrous salt, and, therefore, will define the length of the lab session.

Step 2.
Assemble simple reflux apparatus under the hood. Properly connect the Liebig reflux condenser to water in/out PVC tube lines, and attach a U-shaped drying tube filled with anhydrous $CaCl_2$ (moisture trap) at the top of the condenser. The out-bound water line should be immersed into the hood drain outlet (Figure 111).

Step 3.
Carefully open the bottle of thionyl chloride $SOCl_2$ and add 14.3g of this liquid into the flask, using a graduated cylinder. A green solid salt will immediately begin bubbling and gases will be released.

Step 4.
Place the above condenser into the flask with $NiCl_2 \cdot 6H_2O$ (or $CoCl_2 \cdot 6H_2O$) and $SOCl_2$. Place a blue plastic clip over the joint on the flask in order to make a tight connection between the two pieces of glassware. Place the flask in a water bath and secure it on a lab stand with a clamp (Figure 111).
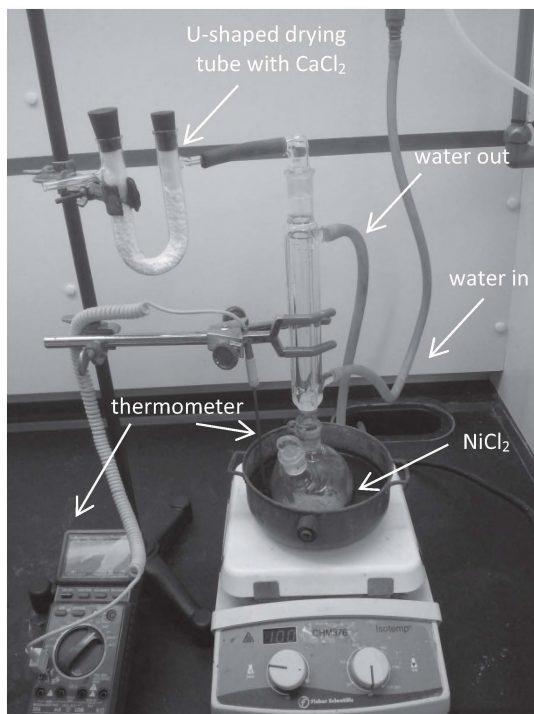
Figure 111. Complete assembly of hardware for the reflux of the hydrated salt with thionyl chloride.

Step 5.
Begin reflux of the flask content, and continue this procedure for one hour. During the reaction, the color will change from green to yellow (for Ni salt), and from pink to blue (for Co salt). If the salt does not change color from green to yellow, and there is no liquid left in the flask, add another 2-3mL of thionyl chloride to the system and continue reflux.

Step 6.
After a total of two hours of reflux, disconnect the condenser from the flask, turn the heat off and let the residual amount of $SOCl_2$ evaporate completely using flow of available inert gas (N_2 or Ar).

Step 7.
When the flask cools off, quickly remove the anhydrous nickel dichloride (or $CoCl_2$) into the weighing vial with the ground joint and matching cap.

Place this vial in the large-mouth test tube with the vacuum stopcock for further drying using an oil pump (Figure 53, Chapter 1). Make sure that there is a cold trap submerged in the Dewar flask filled with cryogenic fluid (liquid N_2, or dry ice mixture/acetone), and all connections are proper (Figure 112**A**). Slowly open the stopcock and pump your sample for ~20 minutes at room temperature. During that time, all the trapped corrosive gases, (SO_2, HCl), that were inside the solid $NiCl_2$ (or $CoCl_2$) sample, will leave, and will be condensed in the cold trap to prevent the pump from damage.
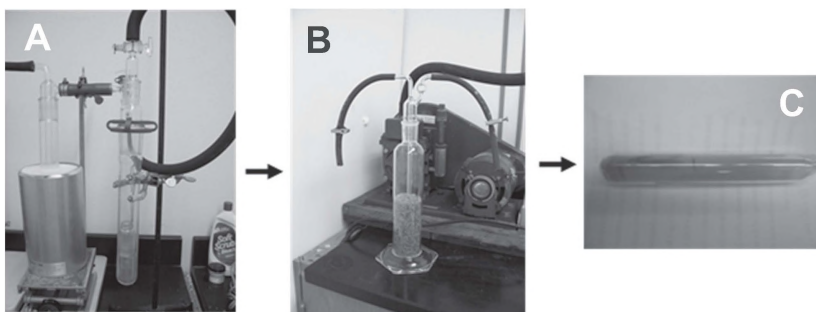
Figure 112. Drying of anhydrous nickel(II) chloride using an oil pump and cold trap filled with liquid nitrogen (**A**). Drying tower filled with silicagel used for letting dry air into the system after anhydrous salt drying (**B**). The final product is sealed in an ampoule under nitrogen (**C**). See centerfold for this image in colour.

Step 8.
Using the drying tower with a blue-colored silicagel (Figure 112**B**), allow dry air to slowly fill a large-mouth test tube with dried samples of $NiCl_2$.

Step 9.
Transfer the dried anhydrous transition metal chloride into the ampoule, clean the neck, and seal it, as shown in Figure 112**C,** for the final product.

Properties of nickelous chloride, NiCl₂: yellow-orange powder, *very hygroscopic in moist air,* and quickly turns green. F.W. = 129.6 g/M; compound sublimes at 993°C (760 mm. Hg); b.p.=1001°C (in a sealed ampoule); d = 3.521g/mL. Crystal structure of "$CdCl_2$ type", rhombohedral space group R3m; parameters: a=3.543, c=17.335Å. The compound is soluble in water, methanol and ethanol. For water amounts of anhydrous salt per 100g of solution are: 34.8g (at 0°C), 40.4g (26.3°C) and

46.7g (100°C). Anhydrous nickelous chloride, as always, has to be stored in sealed ampoules in order to preserve its quality.

Preparation of anhydrous $CoCl_2$ is fully analogous to the above. During a laboratory session, a group of students can be split into two smaller groups, making anhydrous nickel and cobalt dichlorides. In fact, exactly the same approach has been used for years in our teaching laboratory, and the vacuum station has two independent outlets for work with those two different metal chlorides (Figure 113).

Figure 113. Vacuum station with two outlets for drying of synthesized compounds from residual HCl and SO_2, which can be used simultaneously for conditioning of $NiCl_2$ and $CoCl_2$.

Some illustrations of the auxiliary preparation of $CoCl_2$ are shown in Figure 114.
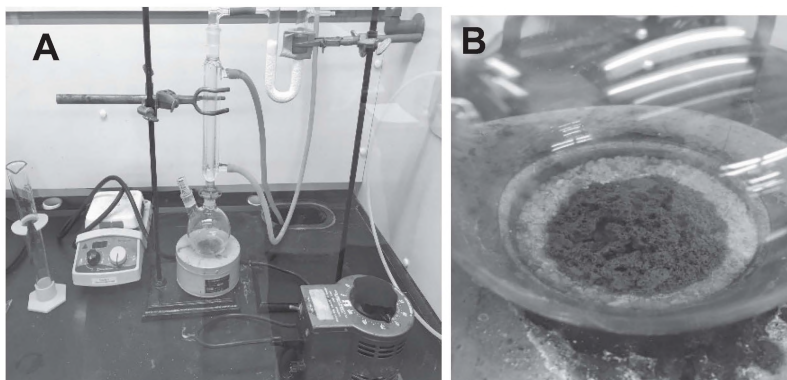
Figure 114. Assembled apparatus for the preparation of anhydrous $CoCl_2$ using a sand bath and variak for temperature regulation (**A**), and the appearance of the final product at the end of the reaction, with only traces of $SOCl_2$ left in the flask (**B**). See centerfold for this image in colour.

Properties of cobaltous dichloride, $CoCl_2$: deep blue *hygroscopic* crystalline precipitate, F.W. = 129.84 g/M; m.p.=735ºC, d = 3.566 g/mL. Crystal structure of the product is the $CdCl_2$ type. The compound absorbs moisture in open air very quickly, and rapidly changes color to pink, due to re-hydration. Thus, a vivid color change from deep blue to light pink is reversible:

$$CoCl_2 \cdot 6H_2O \;\leftrightarrows\; CoCl_2 \cdot (6\text{-}x)H_2O \;\leftrightarrows\; CoCl_2$$
$$\text{pink} \qquad\qquad \text{purple} \qquad\qquad \text{deep-blue}$$
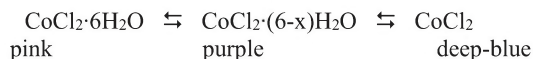
In fact, it is widely used for coloring a variety of desiccants, such as $CaSO_4$ (Drierite® and SiO_2 (see Chapter 1, Figure 20).

Yield is quantitative in both preparations. A good quality compound should have a clear yellow color, and not smell, with SO_2 and HCl. Make sure that the compound is completely dry and well-purged with N_2 in an ampoule before sealing! The number of the experiment, date, authors of the reaction, and total amount of the obtained compound, must be written on the label.

Potential hazards:

1) Thionyl chloride is a smelly liquid that produces HCl and SO_2 in moist air. These two gaseous substances are well-known irritants to

the nose and throat. Wearing gloves is required for working under the hood.
2) Hot sand baths or hot plates may cause thermal burns.
3) Liquid nitrogen can cause severe frostbite to the skin.
4) Vacuumed glassware may implode, causing lacerations.

2.13. Experiment 4B: "Preparation of anhydrous stannous dichloride, $SnCl_2$.

This is the second, alternative, laboratory experiment dedicated to teaching students the simple procedures of dehydration reaction, using an oil pump to dry a target compound. Also, this lab teaches how to handle a moderately moisture-sensitive compound.

Thus, the objective of this experiment is to learn those typical techniques for common laboratory work, using the preparation of anhydrous $SnCl_2$ as an example. This time, the dehydrating agent is acetic anhydride, which forms in the process, is volatile and removable under vacuum and during washing with organic carboxylic acid acetic acid – CH_3COOH.

Equation for the preparation:

$$SnCl_2 \cdot 2H_2O \; + \; 2\,(CH_3CO)_2O \; \rightarrow \; SnCl_2 \; + \; 4\,CH_3COOH$$
225.6 g   204.0 g   189.6 g   240.0 g
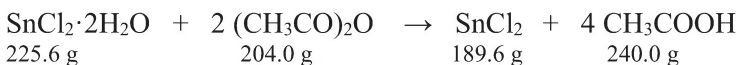
Chemicals: Stannous chloride, dihydrate;
                 Acetic anhydride;
                 Diethyl ether;
Equipment: Medium size beaker 200 - 250mL capacity;
                 Volumetric cylinder;
                 Magnetic stirrer and stirbar;
                 Spatula;
                 Ampoule blank with stretched neck for sealing;
                 Blow torch with oxygen tank;
                 An ice bath for the ampoule cooling;

Procedure: *(will be carried out in groups, with two students per group)*:

Prepare an ice bath and set it aside from your work station area. Arrange a magnetic stirrer, beaker, and stirring bar. Place a beaker of 200 – 250mL capacity, containing 10.2g of acetic anhydride and a stirbar. Wait

approximately 15 minutes. Begin slowly, and, in small portions, very carefully add 11.3g of crystalline $SnCl_2 \cdot 2H_2O$. Conduct the addition of the salt stepwise, while stirring. You may observe fast heating of the mixture after the first portions of solid stannous chloride were added into the beaker. If that is the case, you may use the ice bath mentioned earlier to cool the reaction mixture. Wait until the reaction mixture cools off, and then proceed with the addition of the new portion of $SnCl_2 \cdot 2H_2O$. Continue the reaction until all the salt is added. At this moment, you will be able to see the appearance of an anhydrous $SnCl_2$ salt as a fine white precipitate. Sometimes the reaction mixture turns to a 'sour cream-looking' paste. This is the normal appearance, and you have to manually stir the system using the glass rod.

Keep stirring the reaction mixture at room temperature for another ~60 minutes, if the system is fluid. If the reaction mixture is like paste, then use periodic, thorough, manual stirring for ~30 minutes. Filter the precipitate of the target compound, and then wash it with two portions (50mL each) of diethyl ether on the filter, without applying a vacuum, to ensure the removal of acetic acid and unreacted acetic acid anhydride. Compress salt under the vacuum on the filter to an air-dried condition using the glass compactor. Place the filter with $SnCl_2$ into a desiccator charged with solid KOH. The latter is for trapping vapors of residual acetic acid and acetic anhydride, if they are still absorbed, on the surface of the crystalline precipitate. The yield is quantitative. A good quality compound with acetic acid should not smell.

Stannous chloride, $SnCl_2$: white crystalline precipitate with a 'fatty shine', F.W. = 189.6g/M; m.p.=247°C, b.p.=623°C; d = 3.95g/mL. Crystal structure of 'PbCl₂ type' parameters: a=7.793, b=9.207, c=4.430Å. The compound is quite stable in open air. However, during prolonged exposure to moisture and oxygen, stannous chloride undergoes hydrolysis and oxidation to respective tin(IV) chloride/oxochloride.

Anhydrous stannous chloride should be stored in a sealed glass ampoule. The number of the experiment, date, authors of the reaction, and total amount of the obtained compound, with its yield, must be written on the label. The label should be attached to the sealed ampoule with the target compound. The compound in the sealed ampoule will be inspected and then accepted for storage.

Potential hazards:

1) Acetic anhydride is a corrosive and smelly substance. It is required that all work is carried out under the hood, while gloves are worn.
2) Diethyl ether is a highly flammable solvent, and work with it must be conducted only in the absence of any source of open fire.

CHAPTER 3

SYNTHESIS AND CHARACTERIZATION OF A NEUTRAL COMPLEX: CO(III) TRIS-CHELATE

3.1. Coordination Compounds and Methods of Their Synthesis and Isolation

3.1.1. Theoretical Background: Introduction into Complex Compounds

By the end of the 18th century, new and highly unusual compounds with unexpected stoichiometry between metal ions and other elements (N, S, halogens), were obtained in a reproducible manner. Moreover, the number of these compounds was rapidly growing, but there was no explanation of the nature and origin of chemical bonding between metal ions and other groups that were found to be part of these compounds. Although many of these compounds were known by humans, and used as pigments – Prussian Blue $KFe[Fe(CN)_6]$, Alizarin Red, aureolin $K_3[Co(NO_2)_6]$ hexahydrate, no understanding of their composition and structure existed. First, definitions and explanations of unusual and unexpected structures of these new compounds were offered by Alfred Werner (1866-1919), a genius chemist from Switzerland [1]. He named these new chemical compounds *coordination compounds,* or *metallo-complexes*. Typically, they contain a metal atom (or metal ion) that is located in the center of a compound. That *central atom* can be surrounded with either anions or neutral molecules. Both are called *ligands*.

There are three principal types of coordination compounds: anionic, neutral and cationic. Their classification is based on the difference between the net charge bearing by the complex particle formed. Properties of metal complexes in solutions (such as dissociation, electrical conductivity, ions mobility, etc.) provide necessary information regarding these types of complexes, and allow their classification. Examples of these types of compounds are shown below in Figure 115.

There is a very large variety of ligands used to form coordination compounds, ranging from simple halogenides (F^-, Cl^-, Br^-, I^-) [2], pseudohalogenides (CN^-, N_3^-, NCO^-, CNO^-, NCS^-, $NCSe^-$, $NCTe^-$) [3], ammonia, and monoamines, to large structures of organic amines, phosphines, macrocylic N, O-N, S-N ligands [4], Schiff-bases [5], crown ethers [6], and tetraaza-porphyrins/phtalocyanins [7], texaphyrins and sapphryrins [8], etc.

Cationic complex:
particle $Zn(NH_3)_4$ has a positive charge

Neutral complex:
particle $Pt(NH_3)_2Cl_2$ has no electric charge

Anionic complex:
particle AlF_6 has a negative charge
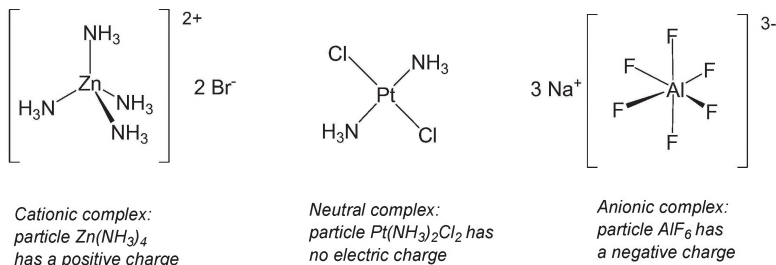
Figure 115.   Classification of coordination compounds based on a complex particle charge.

Complexes are formed due to a definite interaction between an electron pair (or electron density in general) of the ligand and vacant orbitals of the metal center. Most of the time, these interactions have electrostatic character, although covalent bonds between the central atom and ligands are quite common as well. The number of donor atoms, or groups, in the central atom's closest surroundings, is known as the *coordination number* (later as CN). These coordination numbers may vary from 1 to 10, depending on the size and origin of the central atom, and also on the ligands bound to that metal. The most typical coordination numbers for transition metal ions are 4 and 6. The number is reflected in the complexes' tetrahedral or octahedral geometries, though, which are quite often distorted.

The ligand occupies space close to the central atom, and the number of bonds it forms with it is called *denticity*. For instance, Figure 115 contains all monodentate ligands – each takes only one place next to the central atom. There are also bidentate, tridentate, tetradentate, pentadentate, and hexadentate ligands, with some common examples shown in Figure 116.

When a bidentate ligand coordinates with a metal ion, there is a formation of a metallocyclic structure, which has a special name – *chelate* [from Greek χηελασ – a claw], because of its resemblance to a crab

holding its prey (Figure 35). The most commonly occurring chelates in coordination chemistry are shown in Figure 117. The three-membered chelating biding is called *side-on* coordination, and was found mostly among complexes of large, heavy metals such as U^{6+}, Tl^+ [**9**,**10**].

dipy, 2   *terpy, 3*   *spider-amine, 4*

cyclam, 4   *5*   *EDTA, 6*
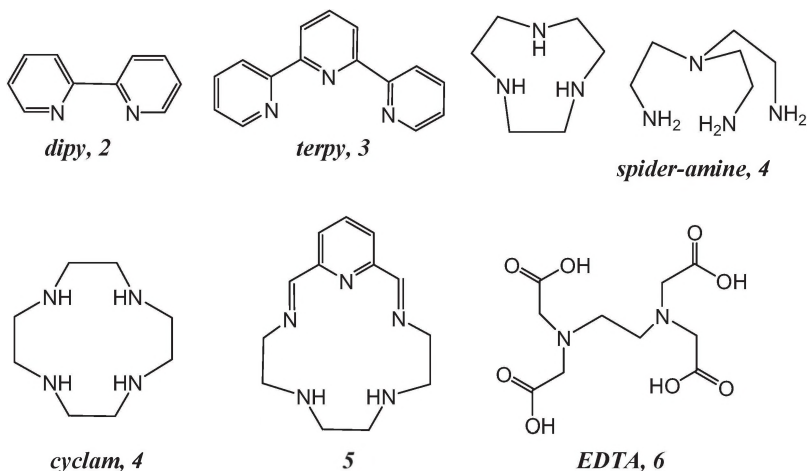
Figure 116. Structures of some frequently used organic ligands and their common abbreviations; the number next to each indicates the ligand's dentate ability.

The immediate central atom, surrounded by ligands, is referred to as the *inner sphere*, while counter ions and solvent molecules are called *outer-sphere* species. The inner sphere is specified during writing in square brackets, while outer sphere ions or molecules of the complex are just written outside. There are coordination compounds with identical sets of donor atoms in the central metal environment. Examples are cases of $[Zn(NH_3)_4]Br_2$ and $Na_3[AlF_6]$ in Figure 33, with $[ZnN_4]$ and $[AlF_6]$ coordination spheres respectively. There are also far larger groups of complexes that contain different donor atoms in the inner sphere. Ligands that do not have identical donor atoms are called *mixed donor atoms* ligands, and examples of those are EDTA (Figure 116), and side-on coordinated species, in Figure 117.
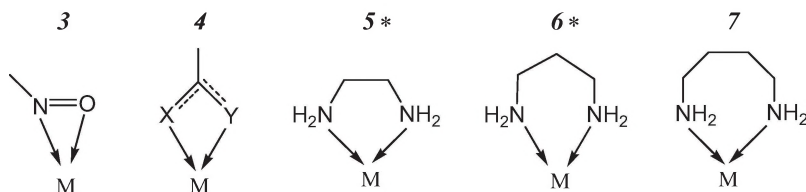
Figure 117. Schematic depiction of structures of metallo-chelates formed by the bidentate ligands; the numbers above indicate the ring size, with asterisks pointing to the most common and the most stable formations. The X and Y atoms are most often O and S in carboxylates, thiocarboxylates or mixed O,S compounds.

Coordination compounds became the second largest group of chemical compounds known to mankind, after organic substances. Thousands and thousands of metal complexes have been synthesized and studied. Needless to say, many compounds were found to be of great practical value, importance, and significance [11]. There are many metal ions that form stable coordination compounds. Typical examples are Ag(I), Au(I), Tl(I), complexes of bivalent Cu, Ni, Zn, Hg, Pb, Pt, Cd, Mn and Co, compounds of trivalent Fe, Al, Ga, Cr, Au, and lanthanides. Historically, chromium(III) and cobalt(III) played an important role in the foundation of modern coordination chemistry [12]. These central ions displayed significant *kinetic inertness towards substitution reactions*, and that fact allowed the successful preparation and isolation of a large variety of their stable coordination compounds. Kinetically inert metal ions form coordination compounds with fixed geometry, and that makes them very suitable objects for educational and training purposes. Thus, similar to organic compounds, coordination compounds exhibit several types of isomerism. There are two big groups of isomers; constitutional, and configurational, isomers. Figure 118 shows the relationship between different kinds of isomerism in coordination chemistry. Among geometrical isomers you can recognize familiar cis- and trans- isomers that were displayed in earlier general- and inorganic chemistry courses. However, when the complex compound that has the coordination number six, and is formed with an asymmetric bidentate ligand with identical or different donor atoms, another type of geometrical isomerism is observed. This is meridional/facial isomerism, or respective complexes normally referred to in the literature as *mer-/fac* isomers for [MA₃B₃] composition of the inner sphere.
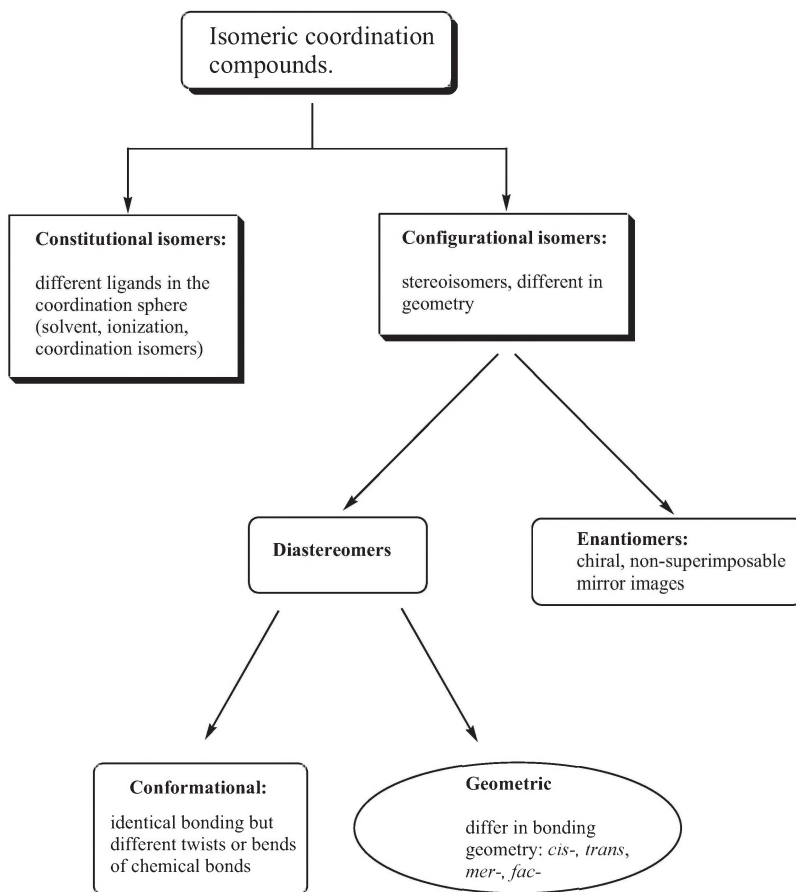
Figure 118. Schematic description of concept of isomerism of coordination compounds.

Geometrical cis-/trans- and *mer-/fac-* isomerism is exclusively a property of coordination compounds with mixed donor atoms set. Figure 119 exhibits both symmetries of the complexes formed, and typical examples of ligands for which this phenomenon was found. Symmetry is an important quality, because it defines different properties, such as color, solubility, biological activity (cis- and trans- diammino-dichloro-platinum(II) complexes!), and spectroscopic signatures of individual isomers.
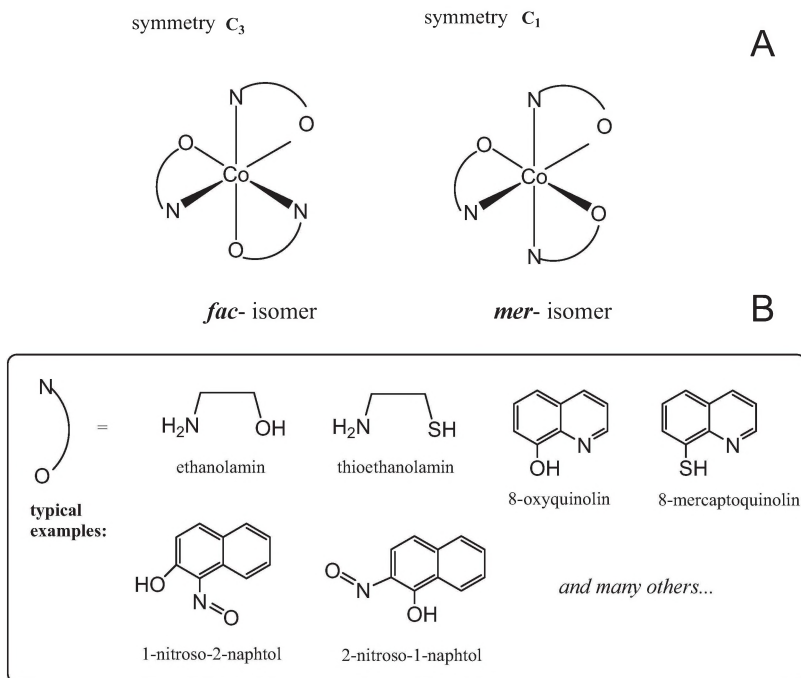
Figure 119. An explanation of the *mer-/ fac-* isomerism for bidentate ligands (**A**), and chemical structure of typical ligands that form such complexes (**B**).

In this laboratory manual, we present and describe only conventional, Werner-type coordination compounds. Those that contain direct metal-carbon bond (except metal cyanides and fulminates!) are called ***organometallic compounds***. The latter represent a very large class of complexes with covalent M-C bonding, and chemistry applications of these compounds have experienced enormous growth and intense development since '50th of the last century. The discovery of ferrocene, iron(II) bis-cyclopentadienyl, $Fe(C_5H_5)_2$ – the first 'sandwich' compound - initiated such growth. However, description of chemistry, bonding, and synthetic methods used in investigations of these compounds is out of the scope of this laboratory manual, which is entirely dedicated to *inorganic syntheses,* and the subsequent characterization of the obtained compounds.

3.1.2. Theoretical Background: Methods of Synthesis
of Coordination Compounds and Their Purification

Complex formation reactions in solutions are often accompanied by the formation of precipitate, which is filtered, washed from starting materials, and dried in a desiccator or under vacuum [see sections in Chapter 1 above, for details]. However, in numerous cases, there is no precipitation, but the system's property changes; color is gained/lost, electrical conductivity and refractive index differs in the mixture from those in starting compounds, NMR chemical shifts move, or new signal(s) appear in the EPR spectrum, etc.

There are five principal methods of preparation of the Werner-type complexes described in this book: 1) **combination reactions** – *direct synthesis* from metal and ligands, either in solution or in solid phase, or in the gas phase; 2) **ligand displacement** reactions in solutions; 3) **redox reactions** in solutions or melt; 4) **hydrothermal-type reactions** carried out in an autoclave; and 5) **thermal decomposition** reactions.

A brief description of each of the five methods above, and some typical examples of such reactions, are presented below.

1)   **Direct synthesis** is a new method of obtaining complex compounds using the reaction in an inert solvent between the metal and ligand, either in the presence of air, or anaerobically [**13**]. These reactions take longer, but often lead to products which are inaccessible by other methods of synthesis. Typical examples can be found in numerous publications by V. Kokozay, V.Pavlenko, O. Vasilieva [**14-17**] and D. Garnovskii, and B. Harisov [**18**], for numerous reactions between metals or their oxides with amines, aminoalcohols, and heterocycles. For example, a large variety of homo- and hetero-metallic complexes were obtained using these reactions:

$Cu^0 + MX_2 + 2HL + 0.5O_2 + nSolv = CuMX_2L_2 \cdot nSolv + H_2O$
      where M = Ni, Co, Zn, Cd, Pb;   X = Cl, Br, I, SCN, OAc;   Solv = DMF
      (N'N'-dimethylformamide), DMSO (dimethylsulfoxide), CH_3OH, CH_3CN.
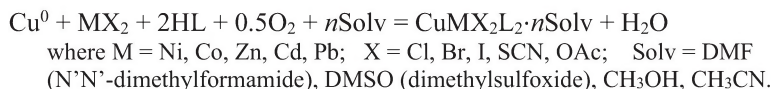
For the case of aprotic ligands, the 'Ammonium salt route' method can be used:

$Cu^0 + M^0 + 4NH_4X + nL + mSolv + O_2 = CuMX_4(L)_n \cdot mSolv + 4NH_3 + 2H_2O$
$Cu^0 + MO + 4NH_4X + nL + mSolv + 0.5O_2 = CuMX_4(L)_n \cdot mSolv + 4NH_3 + 2H_2O$
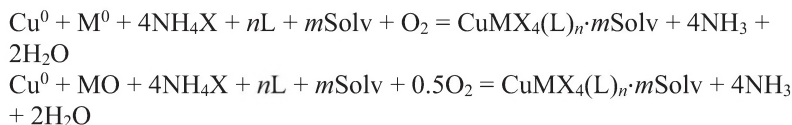
where M^0 = metals - Co, Ni, Zn, Cd; MO = oxides - ZnO, CdO.

2) Numerous complexes are obtained in aqueous solutions by **the ligand substitution reactions**. In fact, this is the most widely-used method of preparation of coordination compounds in solutions when solvated metal cations directly react with incoming ligand molecules:

dissolution   *+ NH₃*

$CuCl_2 + H_2O \rightarrow [Cu(H_2O)_6]Cl_2 \rightarrow [Cu(NH_3)_4(H_2O)_2]Cl_2 + 4H_2O$
                    pale green   royal blue

$[Fe(H_2O)_6]^{2+} + 3\ dipy = [Fe(dipy)_3]^{2+} + 6\ H_2O$
pale blue-green   bright red

$[Ni(CH_3OH)_6]^{2+} + 2\ DMG = [Ni(DMG)_2]\downarrow + 6\ CH_3OH$
    green   red-pink
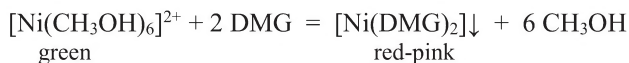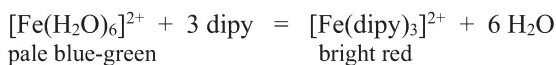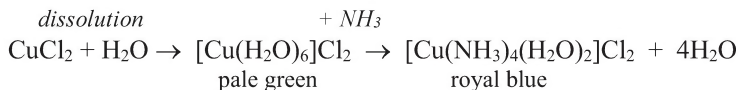
DMG: 1,2-dimethylglyoxime

3) **Redox reactions** proved to be very efficient and high-yield methods for the preparation of Cr(III) complexes from Cr(VI), Mn(III) from Mn(VII) species. During *reduction* reactions, a portion of the organic ligand is used as a reducing agent (sacrificial reagent). Also, there are numerous preparations of Co(III) and Fe(III) complexes from their divalent precursors during *oxidation* reactions [**19**].

$KMnO_4 + acac \rightarrow Mn(acac)_3 + K_2CO_3 + H_2O$
purple   green
                      acac: acetyl-acetone

$Na_2Cr_2O_7 + H_2C_2O_4 \rightarrow Na_3[Cr(C_2O_4)_3] + CO_2\uparrow + H_2O$
orange   blue-grey

$2\ [Co(NH_3)_6]^{2+} + O_2 + 2\ H_2O = 2\ [Co(NH_3)_6]^{3+} + 4\ OH^-$
      red   orange
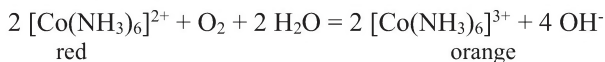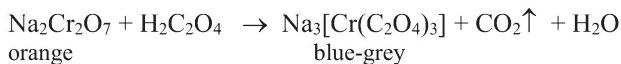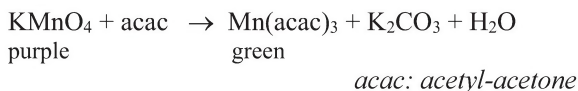
4) In the last two decades, methods of synthesis of complexes using an autoclave, in which an inert atmosphere and relatively high temperatures (below 200ºC) can be achieved, as well as high pressure up to 1 MPa (Figure 120), gained popularity. This is the so-called **hydrothermal preparation**, especially if water is part of the mixture. In many cases, liquids other than H_2O (high boiling point organic

solvents and oils, for instance) can be successfully used. Powdery compound(s) thoroughly mixed with ligand(s) and neutral solvent/oil is loaded inside a Teflon capsule. The autoclave is tightly closed and heated between 100 and 200°C for hours or days, then cooled off, carefully opened, and its contents examined. This method uses forcible conditions of high temperature and pressure to shift equilibrium towards the formation of the most thermodynamically stable product, which in many cases represents a coordination compound that is difficult (or impossible) to obtain at ambient conditions.

5) The **thermal decomposition** method typically uses already obtained coordination compounds that contain easily replaceable or volatile ligands in the *inner sphere*. Upon slow and gentle heating, those ligands are removed by other, typical *outer sphere* ligands:

$$[FePy_4Cl_2] \xrightarrow{+t} [FePy_2Cl_2] + 2\,Py\uparrow$$

$$[Cr(en)_3]Br_3 \xrightarrow{+t} [Cr(en)_2Br_2]Br + en\uparrow$$

$$[Co(NH_3)_6]Cl_3 \xrightarrow{+t} [Co(NH_3)_3Cl_3] + 3\,NH_3\uparrow$$

No.	Name
1	Sleeve Body
2	Bottom Disc
3	Polymer Chamber
4	Rupture Disc
5	Top Ring/Disc
6	Sleeve Cover
7	Locking Screw
8	Locking Rod
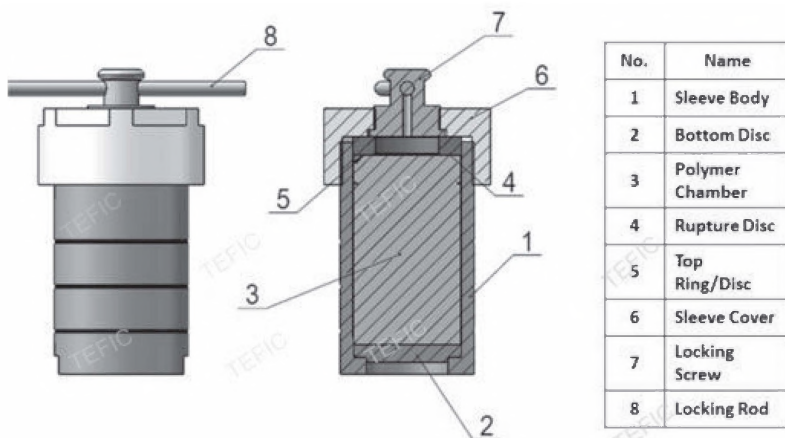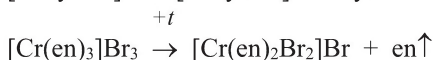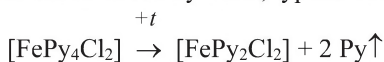
Figure 120. An autoclave; actual shape and cross-section.

Purification of synthesized coordination compounds is typically accomplished via the most common method; recrystallization from an appropriate solvent.

Solid compound is placed into the vessel (beaker, flask), with a small amount of a suitable solvent at room temperature, and the system is heated up to 60-80°C until the solid dissolves. If necessary, activated charcoal is added to a hot solution, in small amounts, to absorb colored impurities, and then this mixture is hot filtered through Celite®, then placed for crystallization, either at room temperature, or in an ice bath. This method is based on the fact that the main complex will saturate the solution at some T point, and then the excess will precipitate pure when the temperature is low. The impurity is not saturating the solution and will not precipitate, staying in a liquid phase. 99% of the time, the impurity and complex do not form co-crystals. Thus, purification of the coordination compound is achieved. This method works well when the integrity of a complex is not changed upon dissolution, e.g. no re-solvation or substitution reactions by the solvent molecules are observed, or possible. The use of well-dissolving solvents such as dimethylsulfoxide (DMSO), dimethylformamide (DMF), pyridine (Py), hexamethylphosphor-triamide (HMPA) and similar solvents is not recommended; they tend to replace ligands coordinated to the central atom and get included in the inner sphere. The method of *recrystallization is equally good for all complexes*; cationic, neutral and anionic.

Another common purification method for stability in solutions *neutral* complexes is straight-phase chromatography. Both column (more often) and preparative thin layer, later TLC, chromatographies are used. Neither of the charged complexes – anionic and cationic – are suitable for chromatography, because of the strong interactions with polar surfaces of silica (SiO_2) or alumina (Al_2O_3), containing either acidic or basic OH-groups on the stationary phase surface. That prevents complexes from moving in a solvent flow.

An extraction from aqueous to immiscible non-aqueous solvents is also used to isolate and purify the complex. Again, most of the time this method is the most suitable for *neutral* complexes when there are no problematic issues of carrying counter ions to balance complex particle charge.

Finally, high-vacuum sublimation is used for the purification of coordination compounds. The limitation in this case is the volatility/vapor pressure of solids. Ionic charged complexes (cationic or anionic) are not prone for sublimation at all; they tend to lose integrity upon heating required for efficient sublimation. On the contrary, neutral complexes, or

those with high degree of covalent bonding, are suitable for such a method.

In this laboratory manual we have selected the preparation and detailed characterization of two intensely colored coordination compounds:

- Neutral, diamagnetic complex of Co(III) well soluble in organic solvents. The ligand was chosen to be a classic organic analytical reagent that was widely used in the past for the colorimetric determination of numerous metals – nitrosonaphtol [20] (Figure 119), as it was named by its discoverers Ilinski and Knorre [21]. Two structural isomers of this ligand are known: 1-nitroso-2-naphtol, and 2-nitroso-1-naphtol. Both form water-insoluble complexes of CoL_3 composition that exist as a mixture of *mer-* and *fac-* isomers.
- Anionic, paramagnetic complex of Cr(III) soluble in water. The ligand was chosen to be oxalic acid dianion – oxalate, $C_2O_4^{2-}$ - that forms *tris*-oxalato-chromate(III) complex anion $[Cr(C_2O_4)_3]^{3-}$ this alkali metals used as counter ions. In this preparation the $K_3[Cr(C_2O_4)_3]$ was made.

During synthesis, identification, and isolation, of both compounds, a variety of different methods and techniques was applied, which makes these preparations complementary.

Thus, for the *neutral, diamagnetic CoL_3 isomeric complexes,* thin-layer chromatography (TLC) and chromatographic separation of isomers, which involve different types of glassware and labware, were used. During characterization of these complexes, the following methods were used:

1. Solid state IR-spectroscopy;
2. Comparative X-ray crystallographic studies of the initial ligands and complexes formed;
3. Solutions UV-visible spectroscopy;
4. ^1H and ^{13}C NMR including 2D methods of COSY and HSQC;
5. Cyclic voltammetry (CV);
6. Cryoscopic measurements.

For the anionic, paramagnetic $K_3[Cr(C_2O_4)_3] \cdot 3H_2O$ complex, we performed detailed characterization, both in solid state, and in solutions.

Solid state studies:
1. IR-spectroscopy,
2. X-ray analysis of mono-crystals of the complex;
3. Thermal analysis – recording of the TG/DSC traces and isolation of two polymorphs;
4. X-ray powder diffraction studies of both polymorphic modifications,
5. Solid state electronic diffuse-reflectance spectroscopy (SDR).

Solutions studies:
1. UV-visible spectroscopy and comparison of results with SDR data;
2. Electrical conductivity measurements;
3. Cryoscopic measurements
4. Determination of magnetic moment of the complex using the NMR Evans method.

The following reference materials will be presented in the order outlined above, but the first step always represents high-yield synthesis of both types of complexes. Let this journey begin.

Cited Literature

1. http://www.chemistryexplained.com/Va-Z/Werner-Alfred.html and https://www.britannica.com/biography/Alfred-Werner
2. Pies, W., Weiss, A. *Key Elements F, Cl, Br, J (VIIth Main Group). Halides and Complex Halides.* Springer Verlag, 1973; ISBN 978-3-540-06166-3.
3. Holub, A.M.; Köhler, H.; Skopenko, V.V. *Chemistry of Pseudohalides.* Elsevier, 1986, 479 pp.
4. a) Thom, V.J.; Shaikjee, M.S.; Hancock, R.D. *Inorg. Chem.*, 1986, 25 (*17*), pp 2992–3000;
   b) Farina, Paolo (2014) *Synthesis of coordination complexes using mixed donor chalcogenoether macrocycles to investigate hard/soft metal to ligand interactions.* University of Southampton, Chemistry, Doctoral Thesis, 284pp, at: https://eprints.soton.ac.uk/id/eprint/362960;
   c) *Encyclopedia of Inorganic Chemistry*, 10 Volume Set, 2nd Ed. Bruce King (Editor), 2005, 6696 pp; ISBN: 978-0-470-86078-6.
5. a) Abu-Diefab, A.; Mohameda, I.M.A. *Beni-Suef University J. Bas. App. Sci.*, 2015, *4* (2), 119-133, at https://doi.org/10.1016/j.bjbas.2015.05.004;
   b) Kumar, S.; Dhar, D.N.; Saxena, P.N. *J. Scien. & Ind. Res.*, 2009, 68 (3), 181-187;
   c) Mohamed, G.G.; Omar, M.M.; Hindy, A.M. *Turk. J. Chem.* 2006, *30*, 361-382.

6. Davis, F.; Higson, S. *Macrocycles: Construction, Chemistry and Nanotechnology Applications*. 2011, John Wiley & Sons, Ltd. 575 pp. ISBN: 9780470714621.
7. Kadish, K.M.; Smith, K.; Guilard, R. *Handbook of Porphyrin Science*, 10 volume set; 2010, 2000pp; ISBN 978-981-4280-16-7.
8. a) Sessler, J.L.; Miller, R.A. *Biochem.Pharm.* 2000, *59*, 733–739; b) Hannah, S.; Lynch, V.; Guldi, D.M.; Gerasimchuk, N.; MacDonald, C.B.; Magda, D.; Sessler, J.L. *J. Am. Chem. Soc.*, 2002, 124 (28), 8416–8427; c) Richter, D.T.; Lash T.D. *J. Org. Chem*. 2004, *69*(25), 8842-50.
9. Graziano, R.; Casselato, U.; Vigato, P.A. *J. Chem. Soc. Dalton Trans.*, 1983, 697.
10. Marcano, D.; Gerasimchuk, N.; Nemykin, V.N.; Silchenko, S. *Cryst. Growth Des.*, 2012, *12*, 2877-2889.
11. In *Comprehensive Coordination Chemistry II. From biology to nano-technology*. Volume 9; Elsevier, Amsterdam, 2003, 876 pages, ISBN 0-08-0443311.
12. https://chem.libretexts.org/Core/Inorganic_Chemistry/Coordination_Chemistry/Properties_of_Coordination_Compounds/Coordination_Compounds
13. Kharisov, B.I. (Ed.) *Direct Synthesis of Metal Complexes*. Elsevier, 2018.
14. Kokozay, V.; Shevchenko, D,V. *Materials Science-Poland*, 2005, *23* (1), 287-313.
15. Kokozay, V.N.; Vassilyeva, O.Yu. *Trans. Met. Chem.* 2002, *27* (7), 693–699.
16. Makhankova, V.G. *Global J. Inorg. Chem.* 2011, *2* (4), 265-285.
17. Nesterov,D.; Nesterova, O.; Kokozay, V.N.; Pombeiro, A.J.L. *Eur. J. Inorg. Chem*. 2014, 4496–4517
18. Garnovskii, A.D.; Kharisov, B.I. *Direct Synthesis of Coordination and Organometallic Compounds.* Elsevier, 1999.
19. Harrowfield, J.M.; Lawrence, G.A.; Sargeson, A. *J. Chem. Educ.*, 1985, *62*(9), 805.
20. Irving, H. M. N. H. *Pure & Appl. Chem.* 1978, *50*, 1129-1146.
21. Ilinski, M.; Knorre, G. V. *Ber. deutsch. Ges.* 1885, *18*, S.2728-2734.

3.2. Experiment 5A: Synthesis of *tris*(1-nitroso-2-naphtholato) cobalt(III)

The ligand is:
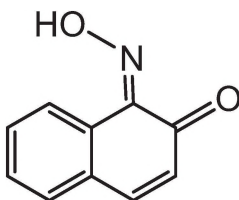
The main *goal* of this laboratory experiment is a synthesis of the coordination compound from inorganic salt and an organic ligand. The procedure described below represents the typical preparation of complex compounds, and can be found in numerous original publications in this area of chemistry.

The objectives of this laboratory experiment are: *preparation of aqueous (for metal salt) and non-aqueous (for organic ligand) solutions*, their *mixing* under stirring, *isolation* of solid precipitated complex through *filtration*, and *washing and drying* of the product of reaction.

Procedure: (*will be carried out in groups, with two students per group)*:

Generally, the vast majority of syntheses of coordination compounds is accomplished at room temperature using a small excess of the ligand. This preparation is no exception. *Note that we use cobalt(II) salt as a source of the metal ions!* The Co^{2+} oxidizes to the more stable state, as in this particular compound, +3 oxidation. Quantities of materials for the reaction are shown below.
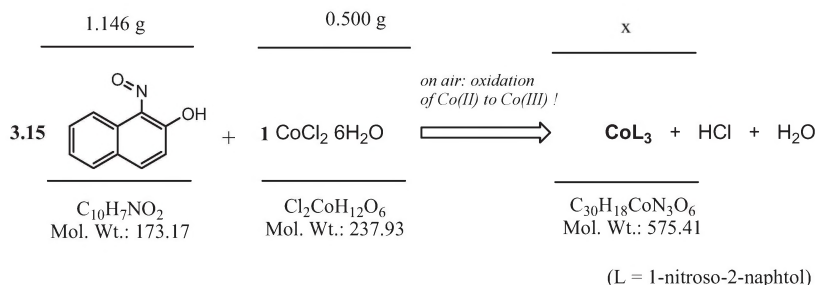
$$3.15 \quad \text{(1-nitroso-2-naphtol structure)} \quad + \quad 1 \; CoCl_2 \; 6H_2O \quad \Longrightarrow \quad CoL_3 \; + \; HCl \; + \; H_2O$$

1.146 g   0.500 g   x

on air: oxidation of Co(II) to Co(III) !

$C_{10}H_7NO_2$
Mol. Wt.: 173.17

$Cl_2CoH_{12}O_6$
Mol. Wt.: 237.93

$C_{30}H_{18}CoN_3O_6$
Mol. Wt.: 575.41

(L = 1-nitroso-2-naphtol)

Step 1.
Weigh 0.500g of $CoCl_2 \cdot 6H_2O$ for the preparation of 0.1M aqueous solution of this salt. That requires 21mL of DI water. Place salt into a medium size Erlenmeyer flask (conical flask, ~150-200mL capacity), add 21mL of water, and observe the quick dissolving of cobaltous chloride.

Step 2.
Weigh 1.146g of 1-nitroso-2-naphtol (abbreviated as *1NO-2OH* later on) and place compound also into a medium size conical flask (~150-200mL capacity). Add 10mL of glacial acetic acid to the flask and dissolve 1-nitroso-2-naphtol. [Some heating on the water bath may be required]. The solution has a dark-green/brown color at this point. Then add 6mL of DI water, dropwise, using a pipette. Mix the solution well.

Step 3.
Place the flask with ligand solution in acetic acid on the magnetic stirrer and put the stir bar into the flask. Start stirring, and begin a slow, dropwise, addition of the metal salt to the ligand solution. The color of the reaction mixture will quickly change to dark burgundy (blood) red, and particles of the fine precipitate of the same color will appear on the flask wall. The addition of metal salt should take ~5-8 minutes. Then the flask should be closed with a rubber septum and the reaction mixture left without stirring for ~30 min.

Step 4.
Filtration of the reaction mixture should be accomplished using a medium size Büchner flask (which is often known as a side-arm flask), a fritted glass filter (either *F* or *M* porosity; see Chapter 1 for details), and the aspirator, as depicted in Figure 39. Use almost no vacuum at the beginning, and then slowly increase water flow in the aspirator; this prevents the filter from fast clogging, since our solid appears as a red-

brown thick paste. Filter precipitate from the water/acetic acid mixture.
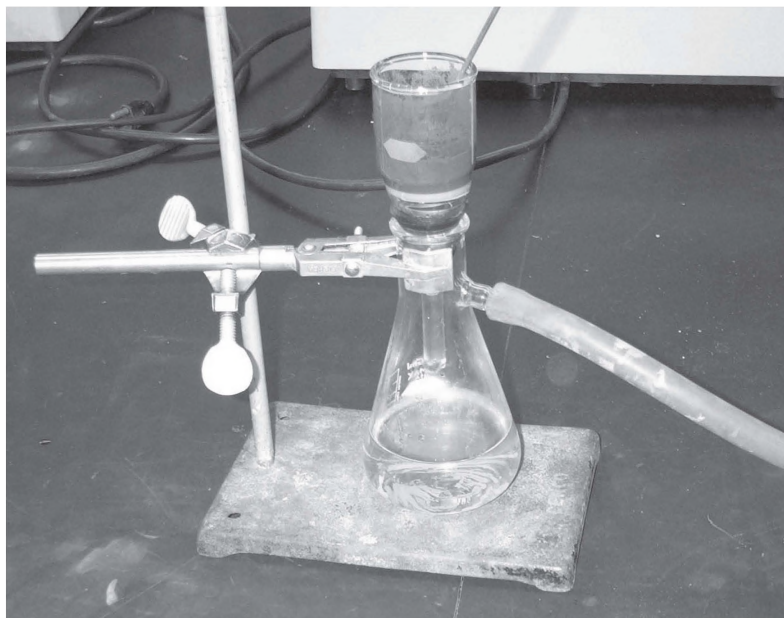
Figure 121. Filtration of the *tris*(1-nitroso-2-naphtholato)cobalt(III) using Büchner flask and fritted glass filter of **M**-type porosity.

Step 5.

Washing the complex precipitate is an important step during which residual amounts of free ligand and acetic acid should be separated from the target compound. Washing the precipitate must be done four times. Each time it should be accomplished on the filter. Thus, the first time you wash **without vacuum** applied, but with thorough stirring and re-suspension of the precipitate with a glass spatula or rod. The first washing requires ~25mL of DI water, and after filtration, the mother liquor is set aside. The second wash also consists of 25mL of water, and a filtrate (the liquid part) is discarded as well. The third washing is done with a mixture of 30mL of CH₃OH and 20mL of DI water. Finally, the precipitate is subjected to diethyl ether, to remove the residual amount of water and methanol. After filtering a fourth time, the paste-looking precipitate is placed into a vacuum desiccator that is charged with KOH pellets, to absorb traces of acetic acid and a significant amount of water.

During the next lab session, the obtained compound will be studied using different spectroscopic techniques, such as IR, UV-visible and NMR. Therefore, before making any solutions for spectroscopic measurements or pellets for recording IR spectra, you should obtain the weight of dried compound and calculate the yield of the desired target complex: *tris*(1-nitroso-2-naphtholato)cobalt(III). This is, of course, the mixture of two geometrical isomers: *mer-* and *fac-*.

Properties of the ligand, 1NO-2OH:
The pure compound has the formula $C_{10}H_7NO_2$ (F.W. = 173.17 g/M) and represents a yellow powder. The 1-nitroso-2-naphthol is soluble in acetic acid, moderately soluble in alcohols and acetone, and well soluble in DMSO, DMF and pyridine. Single crystals of this compound, suitable for X-ray analysis, were grown from $CHCl_3$ using a very slow evaporation of the solvent from a closed test tube at +4°C in the refrigerator, which took several months. Crystal data for this compound are summarized in *Appendix 3* (Table A3-1), while selected bond lengths and valence angles are shown in Figure 122. In a solid state, the initial ligand clearly exists as the **oxime** rather than the **nitroso**-compound, as is evident from the bonds' lengths C1-N1, N1-O2, typical for ketones C2-O1, and especially C3-C4 (Figure 122). This fact clearly puts the traditional nitroso- name of this compound at odds with its actual oxime structure. There is a very strong intramolecular H-bonding in the structure. Individual molecules of the compound are packed into the crystal via slipped π–π stacking interactions (*Appendix 3*, Figure A3-1).

C1 - N1 = 1.308 Å   N(1)-C(1)-C(2)   = 124.12°
N1 - O2 = 1.361 Å   C(1)-N(1)-O(2)   = 117.50°
C2 - O1 = 1.250 Å   N(1)-O(2)-H(O2) = 105.3°
C1 - C2 = 1.480 Å   O(1)-C(2)-C(1)   = 120.11°
C2 - C3 = 1.442 Å   O(1)-C(2)-C(3)   = 121.60°
C3 - C4 = 1.342 Å   N(1)-C(1)-C(10) = 116.41°
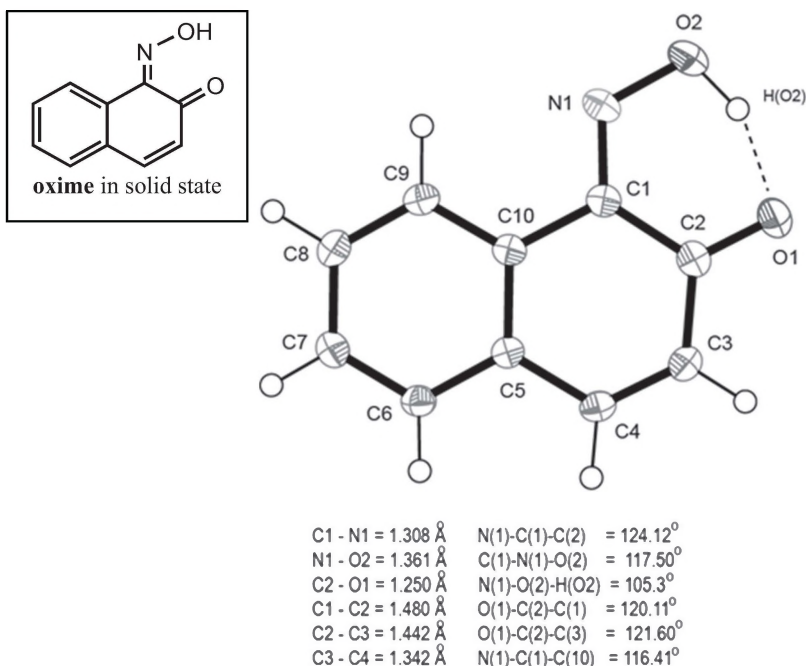
Figure 122. Molecular structure and numbering scheme for the 1-nitroso-2-naphtol. *Atomic thermal ellipsoids, here and further on in the book, are drawn at 50% thermal ellipsoids' probability level.*

Properties of the isomeric mixture of Co(1NO-2OH)₃:

The complex of the $CoC_{30}H_{18}N_3O_6$ composition (F.W. = 575.41g/M) represents a very fine carrot-red powder, both in its solid state and solutions. The mixture of isomers is soluble in acetone, ethanol, CH_2Cl_2 and $CHCl_3$, but isomers have a slightly distinct solubility with the mer-isomer being more soluble. However, in donor solvents such as DMF, DMSO and pyridine, the solubility is identical. Also, it is interesting to note that the *mer*-isomer in those solvents quickly isomerizes into the most symmetric and more polar *fac*-isomer, within minutes,.

Single crystals of the *fac*-isomer of Co(1NO-2OH)₃ suitable for X-ray analysis were obtained after the prolonged crystallization of saturated solutions of this complex in acetone-d₆, DMSO-d₆ and DMF solutions in the NMR tubes left after recording the ¹H, ¹³C{¹H} NMR spectra. Crystal data for this complex are summarized in Table A3-1 in *Appendix 3*, while selected bond lengths and valence angles are shown in

Figure 123. Contrary to the structure of the initial ligand, which is an oxime, the anion in the Co(III) complex is clearly in the nitroso-form, as is evident from the bond lengths in the C-N-O fragments (Figure 123). The bond length in C-O moieties in all three ligands is typical of aromatic phenols rather than ketones.

Metal - ligand distances, Å

Co - N1 = 1.883
Co - O4 = 1.910
Co - N3 = 1.881
Co - O6 = 1.914
Co - N2 = 1.979
Co - O5 = 1.920

Distances in ligands, Å

O1 - N1 = 1.258
N1 - C13 = 1.353
C17 - O4 = 1.281

O3 - N3 = 1.255
N3 - C11 = 1.346
C20 - O6 = 1.283

O2 - N2 = 1.252
N2 - C6 = 1.352
C15 - O5 = 1.274
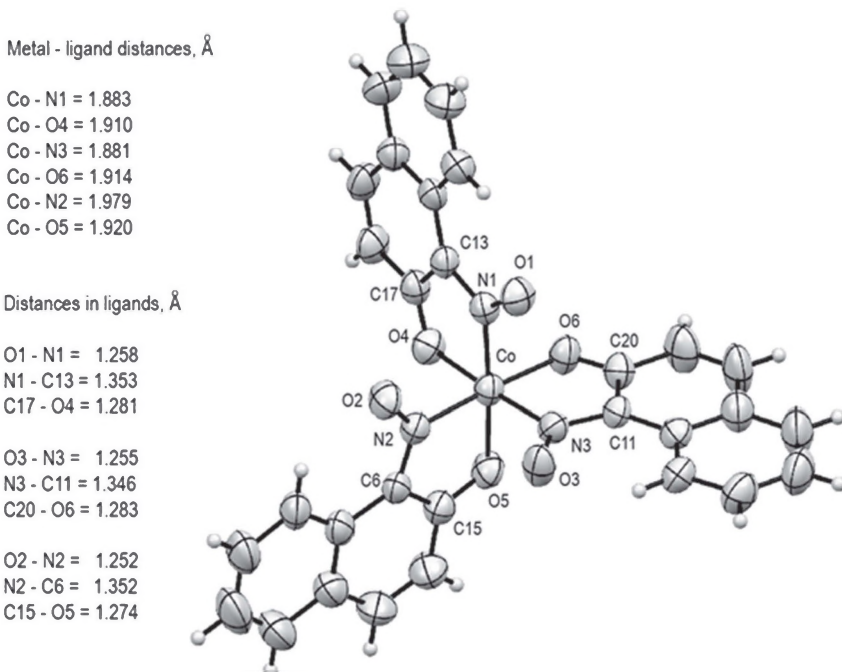
Figure 123. Molecular structure and numbering scheme in *fac*-[CoL$_3$] (L = 1-nitroso-2-naphtol).

The number of the experiment, date, authors of the reaction, and total amount of the obtained compound with its yield, must be written on the label. The label should be attached to the sealed ampoule or screw-cap vial with the target compound.

During the next lab session, the obtained compound will be studied using different spectroscopic techniques, such as IR, UV-visible and NMR, as well as cyclic volammetry (CV) and cryoscopic measurements. Therefore, before making any solutions for spectroscopic measurements or pellets for recording IR spectra, you should obtain the weight of the dried compound, to be able to calculate the yield of the target *tris*(1-nitroso-2-naphtholato)Co(III).

Goals of this laboratory experiment and expected accomplishments:

1) To perform synthesis of Co(III) complex according to provided procedure;
2) To filter and dry your sample; yield of the product will be calculated after its complete dryness;
3) To pack the complex in a screw-cap vial, because we will use compound in studies that will follow over the next three lab sessions;
4) To prepare a detailed lab report with all observations, discussion of results, and conclusions; your lab report will be due at the next laboratory session.

Potential hazards:

1) Acetic acid is a corrosive and smelly substance. Working under the hood, wearing gloves, is required.
2) Alcohols and diethyl ether are highly flammable solvents, and work with them must be conducted only in the absence of any source of open fire.
3) Vacuum – may cause an implosion of the glassware.

Cited Literature

1) Tyukhtenko, S.I.; Pilipenko, A.T.; Gerasimchuk, N.N.; Makarenko, T.I. "Synthesis, separation and NMR-investigation of the Cobalt(III) 1-nitroso-2-naphtolates." *Doklady Akad. Nauk UkSSR*, 1988, part B, N°8, 57-60.

3.3. Experiment 5B: Synthesis of *tris*(2-nitroso-1-naphtholato) cobalt(III)

The ligand is:
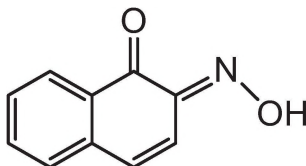
The synthesis of this compound is essentially the same as for the tris(1-nitroso-2-naphtolate) of cobalt(III) described in the preceding lab experiment 5A; both complexes are constitutional isomers.

Procedure: *(will be carried out in groups, with two students per group).*
Quantities of the materials for the reaction are shown below.
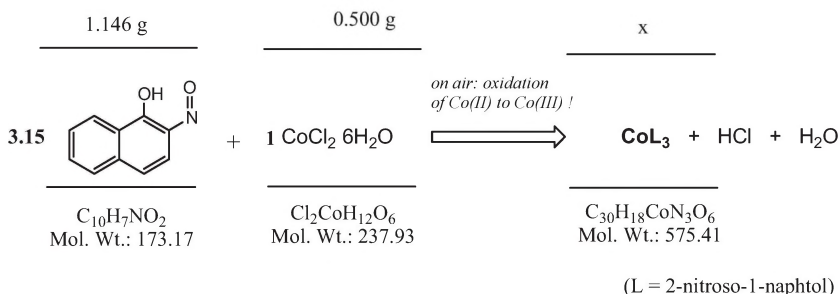
(L = 2-nitroso-1-naphtol)

Step 1.
Weigh 0.500g of $CoCl_2 \cdot 6H_2O$ for the preparation of 0.1M aqueous solution of this salt. That requires 21mL of DI water. Place the salt into a medium size Erlenmeyer flask (conical flask, ~150-200mL capacity), add 21mL of water and observe the quick dissolving of cobaltous chloride.

Step 2.
Weigh 1.146g of 2-nitroso-1-naphtol, and place the compound also into a medium size conical flask (~150-200mL capacity). Add 10mL of glacial acetic acid to the flask, and dissolve 1-nitroso-2-naphtol. Some heating on the water bath may be required to complete dissolution of the ligand. The

solution has a dark-green/brown color at this point. Then add 6mL of DI water dropwise, using a pipette. Mix the solution well.

Step 3.
Place the flask with the ligand solution in acetic acid on the magnetic stirrer, put a stir bar into the flask, and begin a slow, dropwise addition of the metal salt to the ligand under intensive stirring. The color of the reaction mixture will quickly change to practically black, and particles of fine precipitate of the same color will appear on the flask wall. The addition of metal salt should take ~5-8 minutes, and then the flask should be closed with a rubber septum and the reaction mixture left without stirring for ~20 minutes.

Step 4.
The filtration of the reaction mixture should be accomplished by using a medium size Bunsen flask (which is often known as a side-arm flask), a fritted glass filter (either *F* or *M* porosity; see Chapter 1 for details), and the aspirator. Use almost no vacuum at the beginning, and then slowly increase the water flow in the aspirator; this prevents the filter from fast clogging, since our solid appears as a thick purple paste. Filter the precipitate from the water acetic acid mixture.

Step 5.
Washing the complex precipitate is an important step during which residual amounts of the uncomplexed ligand and acetic acid should be separated from the target compound. Washing the precipitate must be done four times. Each time it should be accomplished on a filter first without the vacuum applied, but with thorough stirring and re-suspension of the precipitate with a spatula. Thus, the first washing requires 25mL of DI water, and after filtration the mother liquor is set aside. The second wash also consists of 25mL of water, and the liquid part is discarded as well. The third washing is done with a mixture of 30mL of CH_3OH and 20mL of DI water. Finally, the precipitate is subjected to ether to remove residual amounts of water and methanol. After filtering a fourth time, the paste-looking precipitate is placed into a vacuum desiccator that is charged with KOH pellets to absorb traces of acetic acid and water (Figure 124).
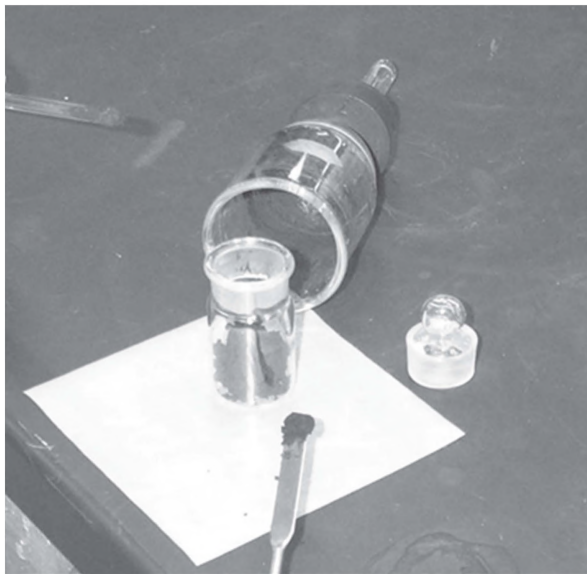
Figure 124. Filtered and washed dark red-purple precipitate of the *tris*(2-nitroso-1-naphtholato) cobalt(III) is transferred into a vial for drying in a vacuum desiccator.

During the next lab session, the obtained compound will be studied using different spectroscopic techniques, such as IR, UV-visible and NMR, as well as cyclic volammetry (CV) and cryoscopic measurements. Therefore, before making any solutions for spectroscopic measurements, or pellets for recording IR spectra, you should obtain the weight of the dried compound to be able to calculate the yield of the target *tris*(2-nitroso-1-naphtholato)Co(III).

Properties of H(2NO-1OH)
The pure compound has the formula $C_{10}H_7NO_2$ (F.W. = 173.17 g/M), and represents brown crystals. Single crystals of this ligand which are suitable for X-ray analysis were obtained after prolonged evaporation of 1.4-dioxane from its saturated solution in this solvent. Crystal data for this compound are summarized in Table A3-2 in *Appendix 3*, while selected bond lengths and valence angles are shown in Figure 125. The presented solid state structure clearly indicates the oxime character of this compound similar to its isomer – 1-nitroso-2-naphthole – discussed in Lab 5A above. Thus, the bond length C2-O2 is typical of ketones rather than phenols, and the C9-C10 bond has a double bond character, as compared to single

bonds C10-C1 and C1-C2 (Figure 125). Finally, in the oxime fragment, the C1-N1 bond is considerably shorter than N1-O2. Ironically, based on the solid-state structure data, the title ligand represents an *oxime*, and not the *nitroso* compound. The ligand forms an elegant packing, in which columns of molecules are formed by $\pi-\pi$ stacking interactions and intermolecular H-bonds, held together by van-der-Waals forces (*Appendix 3*, Figure A3-2).

C1 - N1 = 1.304 Å	N(1)-C(1)-C(2) = 113.4°
N1 - O1 = 1.370 Å	C(1)-N(1)-O(1) = 112.8°
C2 - O2 = 1.227 Å	N(1)-O(2)-H(O) = 109.6°
C1 - C2 = 1.481 Å	O(2)-C(2)-C(1) = 121.1°
C1 - C10 = 1.454 Å	O(2)-C(2)-C(3) = 121.9°
C9 - C10 = 1.339 Å	N(1)-C(1)-C(10) = 126.0°
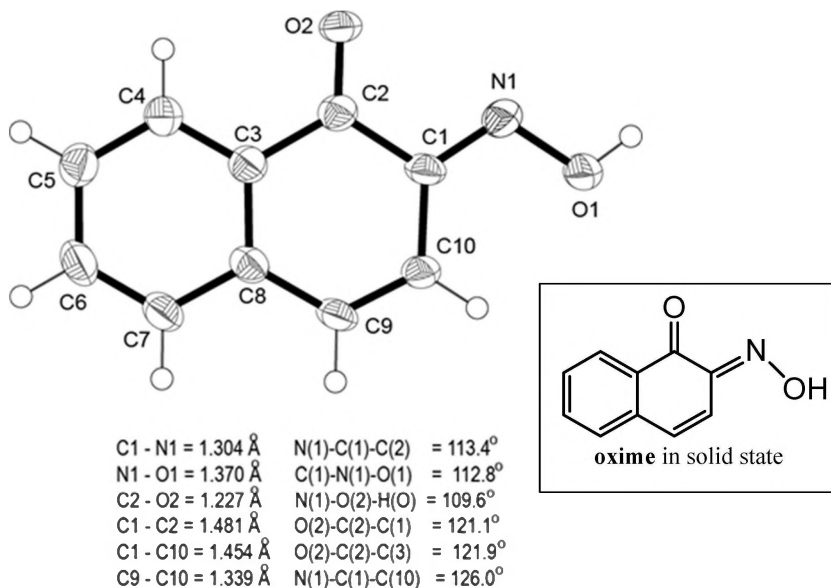
Figure 125. Molecular structure and numbering scheme for the 2-nitroso-1-naphthol. Atomic thermal ellipsoids are drawn at 50% thermal ellipsoids probability level.

Properties of isomeric mixture of Co(2NO-1OH)$_3$

The complex of the CoC$_{30}$H$_{18}$N$_3$O$_6$ composition (F.W. = 575.41g/M) represents a very fine, deep wine-red powder, both in its solid state and solutions. Contrary to the analogous mer/fac isomeric mixture Co(1NO-2OH)$_3$, Co(2NO-1OH)$_3$ isomers are much more easily soluble in common organic solvents. They are not interconverted in solutions in donor solvents, such as DMSO, DNF or pyridine. Single crystals of the *mer*-isomer of Co(2NO-1OH)$_3$·CD$_2$Cl$_2$ suitable for X-ray analysis were obtained after the prolonged crystallization of saturated solutions of this complex in the NMR tube after recording of its NMR spectra.

Metal - ligands distances, Å:

Co(1) - N(1)   1.885
Co(1) - N(2)   1.917
Co(1) - N(3)   1.920
Co(1) - O(2)   1.894
Co(1) - O(4)   1.904
Co(1) - O(6)   1.926

Distances in ligands, Å:
C(1) - O(2)   1.281
C(11) - O(4) 1.284
C(21) - O(6) 1.288

N(1) - O(1)   1.251;   N(1) - C(2)   1.354
N(2) - O(3)   1.242;   N(2) - C(12) 1.362
N(3) - O(5)   1.250;   N(3) - C(22) 1.355
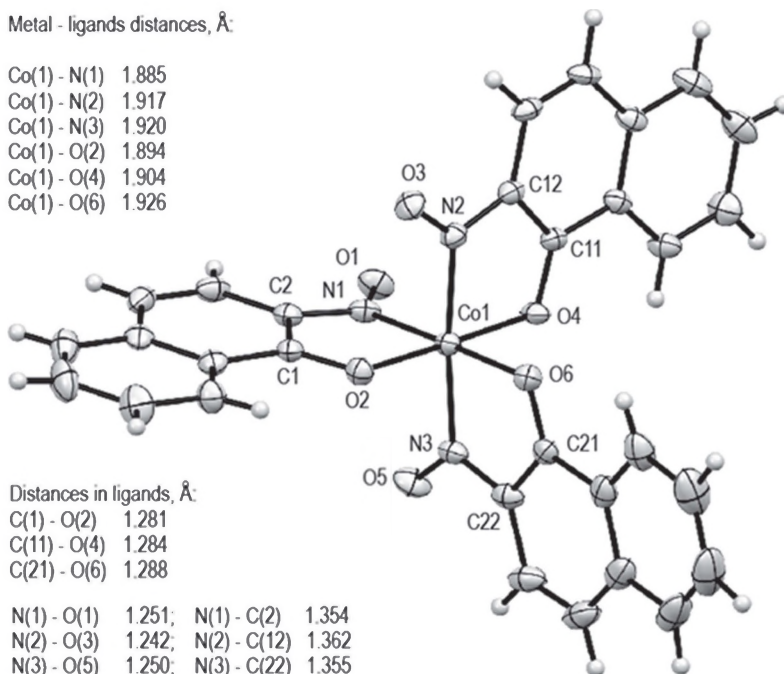
Figure 126. Molecular structure and numbering scheme for *mer*-[Co(2NO-1OH)$_3$]. The solvent of inclusion - molecule of CD$_2$Cl$_2$ – was omitted for clarity.

Crystal data for this complex are summarized in Table A3-2 in *Appendix 3*, while selected bond lengths and valence angles are shown in Figure 126. Contrary to the structure of the initial ligand, which is an *oxime*, the anion in the Co(III) complex clearly is in the *nitroso*-form as is evident from the bond lengths in the C-N-O fragments (Figure 126). The bond length in C-O moieties in all three ligands is typical of aromatic phenols rather than ketones.

Important theoretical background for the interpretation of structural data presented herein can found in the subchapter **3.1.5.**, just below the description of this preparative experiment.

The number of the experiment, date, authors of the reaction, and the total amount of the obtained compound and its yield, must be written on the label. The label should be attached to the screw-cap vial with the synthesized compound, which will be placed for storage.

Goals of this laboratory experiment and expected accomplishments:
1) To perform synthesis of Co(III) complex according to the procedure provided;
2) To filter and dry your sample; yield of the product will be calculated after its complete dryness;
3) To pack the complex in a screw-cap vial; we will use this compound in studies that will follow on the next three lab sessions;
4) To prepare a detailed lab report with all observations, discussion of results, and conclusions.

Potential hazards:
1) Acetic acid is a corrosive and smelly substance. Working under the hood, wearing gloves, is required.
2) Alcohols and diethyl ether are highly flammable solvents, and work with them must be conducted only in the absence of any source of open fire.
3) Vacuum – may cause an implosion of the glassware.

Cited Literature

1. Gurrieri, S.; Siracusa, G. "Coordination compounds of 1-nitroso-2-naphtol and 2-nitroso-1-naphtol". *Inorg. Chim. Acta.*, 1971, *4*, 650-654.
2. Charlambous J.; Soobramanien, G.; Betts, A.; Bailey, J. "Complexes of cobalt(III) with 2-nitroso-1-naphtol and 1-nitroso-2-naphtol". *Inorg. Chim. Acta*, 1982, *60*, 151-155.

3.3.1. Theoretical Background: Foundations of Chemical Crystallography

This is a structural method that allows a very accurate determination of the three-dimensional structure of any solid crystalline substance or compound [1]. Crystals are different from other solids such as plastics, glass, wood, etc., because they possess *internal repetitive, three-dimensional order that infinitely extends along x, y and z directions*. This method uses the diffraction of the X-rays on a *single crystal* of the studied specimen. The diffraction is an optical phenomenon that is based on interactions of waves with objects that are comparable or smaller in size than the applied wavelength. The latter for the X-rays are in the range of 0.43 to 1.54Å, which is useful for structural chemistry because of the typical bond length in chemical compounds being of the same magnitude. The X-rays are generated in a special device, called the X-ray tube, when accelerated electrons interact with metal anode, emitting characteristics for that metal radiation of a specific wavelength. The transition between energy levels when X-ray photons are generated is defined by Henry Moseley's Law:

$1 / \lambda = c (Z - \sigma)^2$, where c and σ are constants, and Z is the atomic number of the metal used for the anode. Therefore, the main intense line of such radiation is named after the metal used in the tube: λ(Ag)= 0.55940 Å, λ(Mo) = 0.71073 Å, λ(Ga) = 0.1340 Å, λ(Cu) =1.54056 Å. All these wavelengths are in use in structural chemistry, with Mo and Cu radiation being the most common. An example of the tube is seen in Figure 128A.

There are seven crystal systems known (Figure 127), with each of them able to fill the volume in three-dimensional space. These systems possess different degrees of symmetry. Symmetry of any object can be described by the set of symmetry elements, such as planes (mirror and gliding), rotational axis (proper or improper rotation, screw-type), and center of inversion, if it is present. When a symmetry element is used to move the physical point or object accordingly (e.g., rotate, reflect, invert), then a symmetry operation is performed. The more symmetry elements a particular object possesses, the more symmetric it is. A cube, for instance, is a, by far, more symmetric object than the parallelepiped (orthorhombic system, or 'matchbox') (Figure 127).
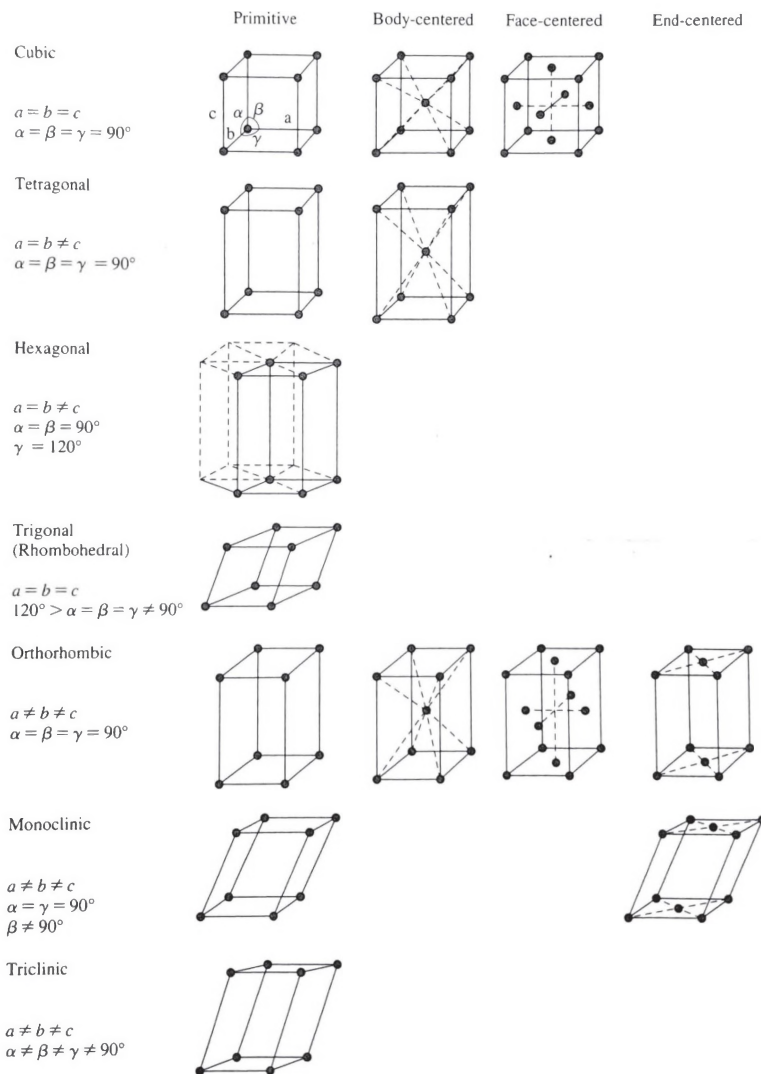
Figure 127.   The 7 crystal systems with their metrics (*left,* written column) accompanied with 14 Bravais lattice types in seven crystal systems (images on the *right*).

The unit cell is the smallest 'building block' in the crystal which allows filling of the space in three dimensions (further, 3D). Unit cells can be primitive (**P**-type), body-centered (**I**-type), face-centered (**F**-type), and partially face-centered, with only two opposite sides centered (**C**-type) (Figure 127, (right part)). Unit cells have metric dimensions: *a*, *b* and *c,* defining distances along *x*, *y* and *z* directions. Also, there are three angles: *α*, *β,* and *γ*. Both dimensions and angles sets may have only internal relations, as shown in Figure 127, (left part). Within these seven crystal systems there are fourteen ways to position physical objects in unit cells; Bravais lattice types [**2**]. It is correct to say that the black dots in those depicted unit cells may represent atoms, ions, or molecules.

   Analysis of available numerous crystal forms (from abundant collections of minerals and chemical compounds) allowed J. Hessel, in 1830, to derive only 32 crystal symmetries [**3**]. Thus, only that number of external symmetries – shape of crystal shapes – can be found. These symmetries are *crystallographic point groups*. They represent a set of symmetry operations that, being applied to the crystal, will create exactly the same image (superimposed) as prior to the operation. Each point group is also known as a *crystal class*. The addition of a translation operation on a unit cell integer, or its fraction, such as ¼, ½, leads to 230 ways of placing a physical object in 3D space. Now, in the crystal there are *gliding planes* and *screw axes* [**4**]. Those 230 possibilities, for filling 3D space in an ordered and repetitive fashion, were mathematically derived by E. Fedorov [**5**], and are called *space groups*. More specific details of crystals and mathematical/physical crystallography can be found in other sources [**6**].

   When X-rays hit the crystal, *they diffract on electrons of atoms* that occupy crystal lattice, and generate the diffraction pattern. This pattern is very complex, but represents the main objective for the X-ray analysis, which is performed on a single crystal using a special apparatus called a *diffractometer* (Figure 128). It consists of a goniometer – a mechanical device that allows motion of a single crystal around three axes, source of the X-rays (nowadays ceramic Mo or Cu tubes), and their collimation and trapping, and a system of detection of diffracted photons. Those numerous in-phase photons, which originate from diffraction on atomic planes (Figure 130), form reflections (Figure 133). Modern detectors have a very good ability to capture an array of reflections of variable intensity using the CCD cameras (charge coupled devices) which have truly revolutionized the field of X-ray analysis.
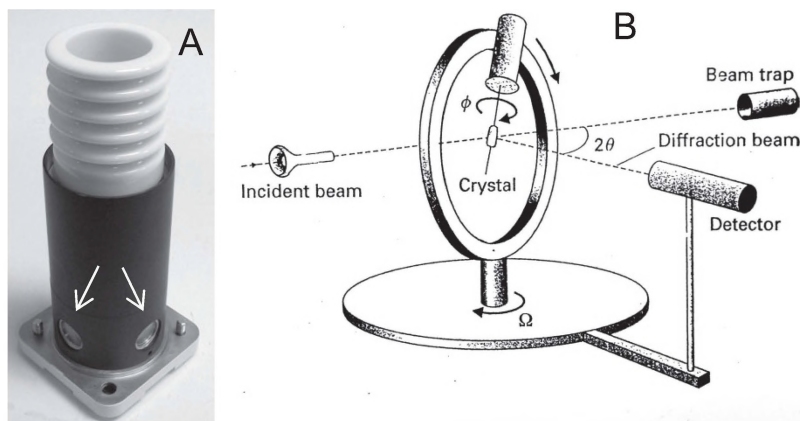
Figure 128. **A** – ceramic X-ray tube with beryllium windows shown by arrows; **B** – principal components of a single crystal diffractometer with the nomenclature and explanation of three angles: θ, ϕ and ω.

It is important to note that, in order to have a good quality structure, one needs to collect as many of those reflections as possible, to adequately represent the electronic structure of the crystal (and, respectively, the moiety that forms the crystal!). Therefore, motion of the crystal/detector pair in three directions is necessary (Figure 128**B**). Thus, in modern diffractometers, a series of runs is necessary to collect reflections sufficient for structure solution and refinement.
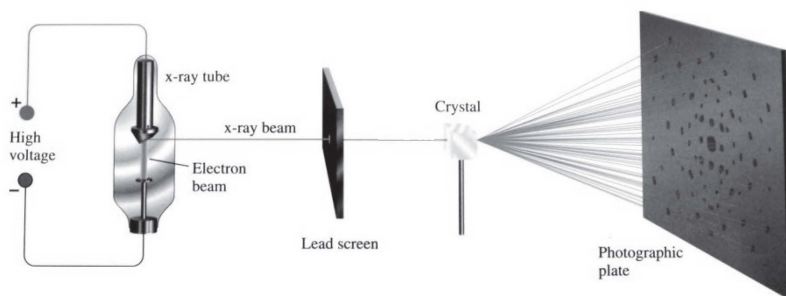
Figure 129. Schematic representation of the X-ray beam diffraction experiment on a single crystal.

$$n \, \lambda = 2 \, d \, \sin\Theta$$
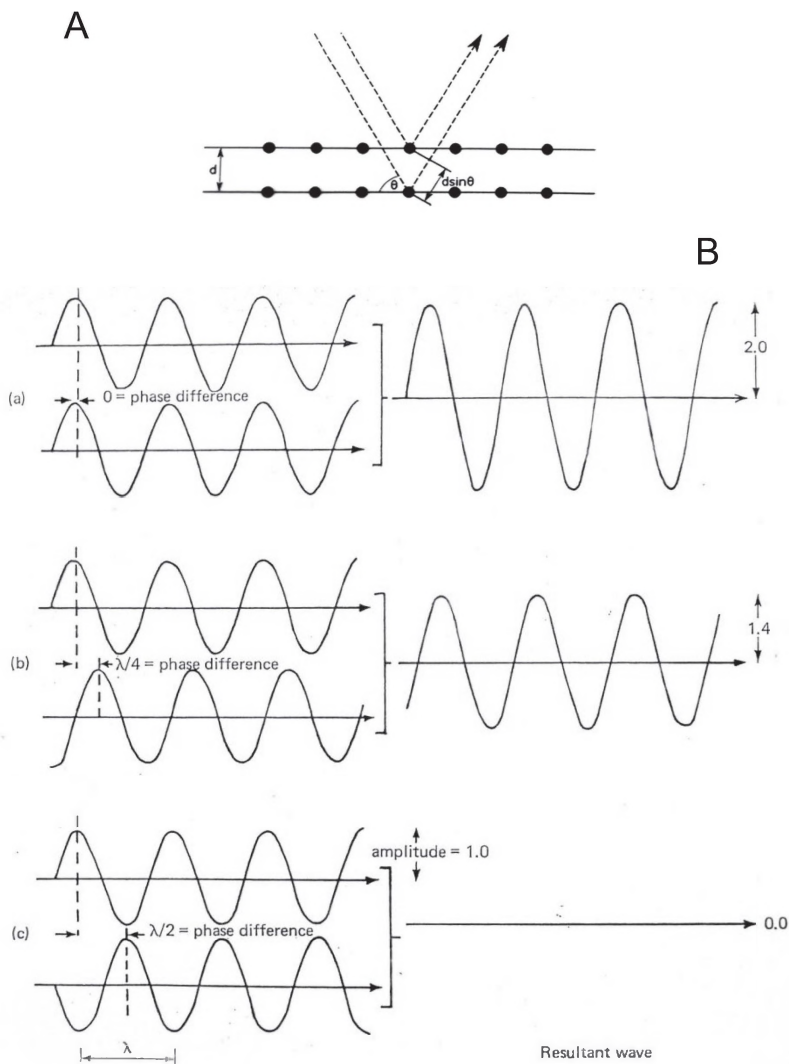
Figure 130. Conditions for diffraction on a set of atomic planes explained by Wulff–Bragg conditions (**A**) [7], and principles of interactions between waves depending on their phase shift (**B**).

More specifically for Mo-radiation, in order to collect the full-sphere of reflections (in reality ~95% coverage) in omega-angle scanning mode, it is necessary to perform four runs, with 364 static pictures taken at 0.5 degree steps, in rotation of the crystal (motion of the goniometer). That is 1,456 pictures (named frames) in one data set. The time of the exposure ('picture taking') can be set from 10 to 120 seconds, depending on the crystal's diffracting power – intensity of reflections.

Overall, the principal idea of the X-ray diffraction experiment showing the diffraction pattern is depicted in Figure 129. The photographic plate here can be referred to the face of the CCD camera (Figure 132,*I*), while the lead screen is a fine collimator that provides good focus on the crystal X-ray beam of 0.1 – 0.5mm diameter.

In order to collect a good quality dataset, some careful microscope work is required to select the best crystal for the diffraction experiment. The crystal should be single, clean and transparent, and contain no visible defects such as cracks, layers, trapped air bubbles, dust, etc. (Figure 131**D**). Crystals are placed in special clear oil for selection and handling. Crystallographic laboratories have microscopes equipped with a polarizer to make the process of selecting the right crystal specimen more efficient, since the detection of internal imperfections, including twinning, is much better.

A suitable crystal is picked from the oil with the help of a thin plastic loop (Figure 131**A**), which is mounted on a metal pin and placed on the goniometer head prior to the data collection. In the last two decades, cryostats became an essential accessory to X-ray single crystal diffractometers. Typically, these devices can be programmed to keep the temperature of an examined crystal between 290 and 100K for a long time, with accuracy ±0.2°, by gently blowing dry nitrogen from the nozzle just above the crystal (Figure 132). The utility of low-temperature X-ray diffraction experiments is three-fold: 1) lowering the atomic motion in the crystal that leads to smaller thermal displacement parameters; 2) the level of noise is significantly lower; 3) a unique possibility to study temperature-dependent structural changes during phase transitions in the crystal. Today, most of the crystallographic characterizations are conducted at low temperatures below 200K most of the time, addressing the first two issues outlined above.
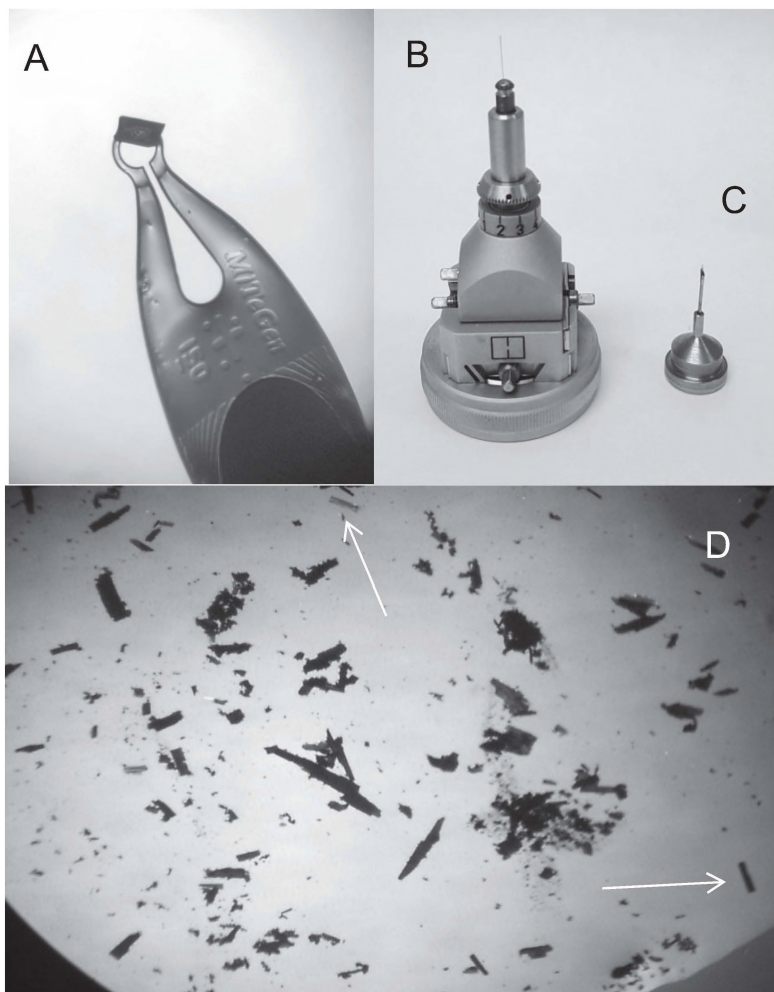
Figure 131. The goniometer head with a glass fiber, on top of which a single crystal is mounted, as shown by arrows (**A**), metal pin on a magnetic base for attachment to the goniometer head (**B**), and microscope photograph of a thin plastic loop of 150μm opening for holding a single crystal (**C**). Microscope photograph of actual sample of *mer*-Co(2NO-1NO)$_3$ samples in an immersion oil, with well-shaped crystals selected for studies indicated by arrows (**D**).
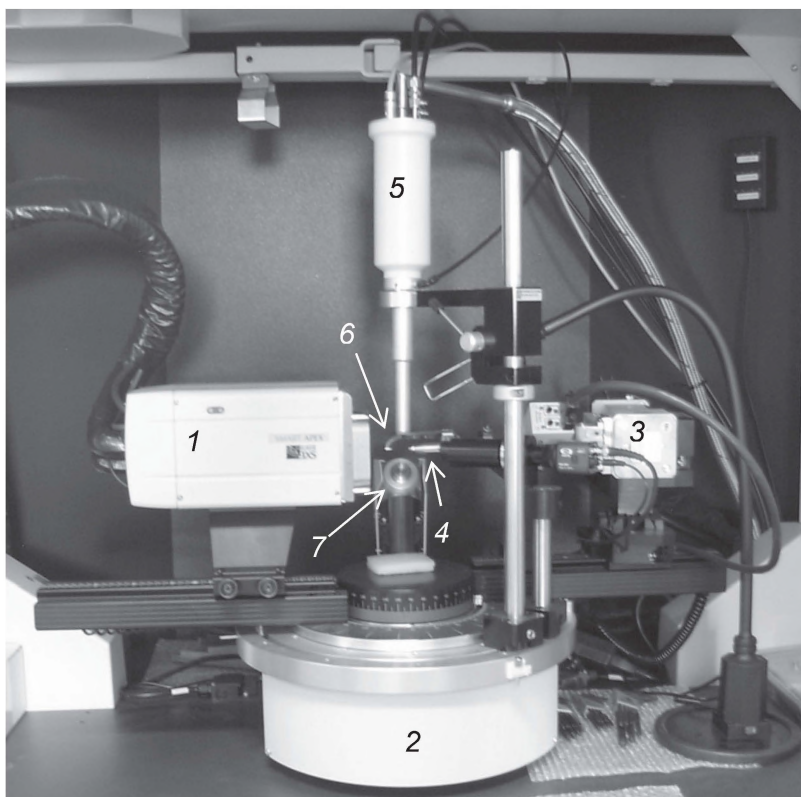
Figure 132. Typical setup of a single crystal diffractometer with major components: *1*-charge coupled device (CCD detector); *2* – goniometer; *3*- X-ray tube (in our case Mo-Kα radiation source: λ = 0.71073 Å); *4* – collimator; *5* - cryostat that provides a laminar flow of dry N_2 in 280 – 100K range; *6* - beam stop in front of the detector face.

However, there are numerous cases when introduction of the crystal into a cold cryostream leads to its thermal cracking, which makes the crystal unusable. Some crystal specimens even when started carefully, still crack when cooled down from room temperature, due to a strong internal anisotropy and very uneven packing of that contraction.

The method of X-ray crystallography is math-intensive, and requires some initial knowledge of geometry, trigonometry, and algebra, but most importantly, a positive attitude. We will outline the most important concepts necessary for understanding the basics of the X-ray

structure determination [8,9]. First of all, there are several large software packages these days that allow crystal structures' determination, and these are mostly produced by the X-ray single crystal diffractometer manufacturers, such as Bruker AXS®, and Rigaku®. There are, nevertheless, good, and free-of-charge, programs available for interested users [10-13]. Proper use of this software allows structure solution and refinement.

Now, a data set with numerous reflections is collected, as the result of the X-ray diffraction experiment. Intensities of reflections are measured against a pre-determined background. Based on symmetry of dozens of the most representative reflections, the crystal system is determined, these reflections are indexed, and metrics of the unit cell with Bravais lattice type are tentatively assigned. Figure 136 demonstrates the actual appearance of computer screen photos of a randomly chosen frame, and visualization of several reflections, to show the reader what they are, and how intense they are, compared to the background. Integration of all reflections above the trash hold allows obtaining of overall diffraction intensity, which is absolutely essential for the assignment of atoms and successful structure solution and refinement. This is because the intensity of each reflection is proportional to the number of electrons in the spot where diffraction occurred.

Secondly, we have to introduce concepts of Miller indices [14] which allow provision of the exact position for each observed reflection in 3D space. These indices are the reciprocal values of the intercepts of imaginary planes that dissect the unit cell with the crystallographic dimensions a, b and c, leading to the initiation of h, k and l indices, as explained in Figure 133 [15]. These planes, of course, are passing through atoms occupying unit cell. Waves diffract off planes of atoms (electrons), which are described by those Miller indices h,k,l (Figure 134). Well, that shortest interplanar distance d was already defined in Wulff-Bragg's Law (Figure 130 **A**). Using notation of simple geometrical considerations shown in that figure allows us to establish important relations between the angle θ for the X-rays, interplanar distances d, distance between two waves hitting planes in the crystal and diffracting from them ℓ, and the wavelength of the X-ray radiation λ (Figure 135). Thus, $\ell / d = \sin \theta$, or $\ell = d \sin \theta$. Since $n\lambda = \ell + \ell$ then $n\lambda = 2 \ell = 2d \sin\theta$. When $\ell + \ell = n\lambda$ then the two waves are in phase. Therefore $d^* = \ell /d = 2\sin\theta / n\lambda$. The former new variable d^* is a reciprocal of interplanar distances and is important for the introduction of the reciprocal space concept necessary for operation with Miller indices.
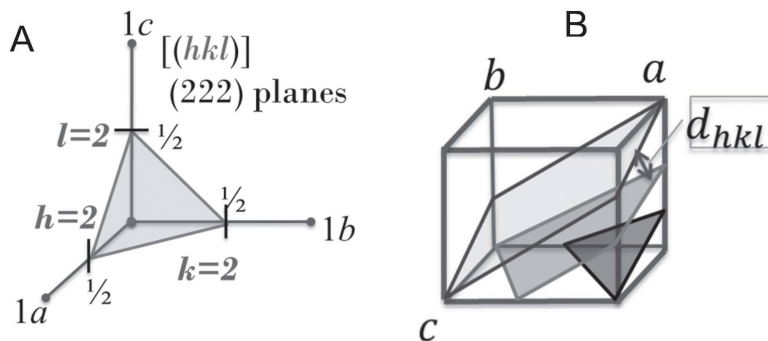
Figure 133. The graphical definition of Miller indices (**A**), and set of $d_{(hkl)}$ planes passing through the unit cell with a,b,c dimensions (**B**). Planes, certainly, contain atoms which are not shown for clarity [**14**].
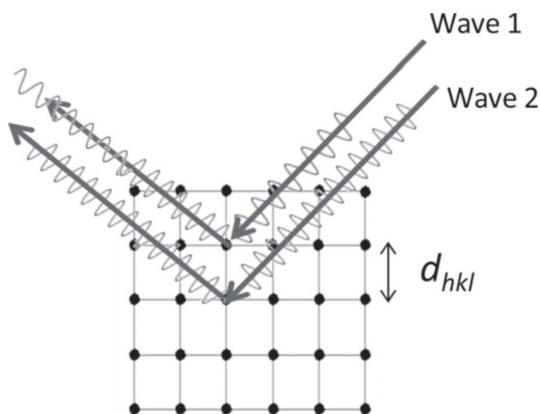
Figure 134. Schematic representation of two waves diffracting off electrons of atoms which occupy planes in the crystal. To make this description general, no unit cell is shown, but the shortest interplanar distance d is visible.
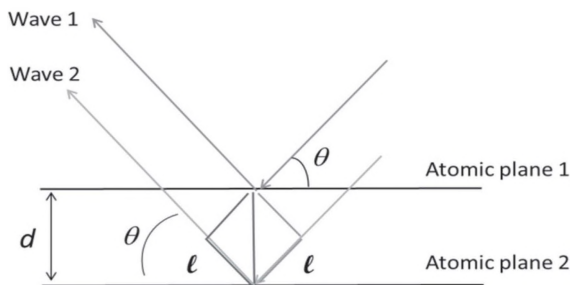
Figure 135. Explanatory drawing of the geometrical setup that describes relations between four variables in the Wullf-Bragg equation, and leads to definition of $1/d$ = $d*$.

Now there are several important equations that connect all of the above terms and variables, and lead, finally, to the electron density in the crystal that allows crystal structure solution.

Miller indices can be expressed in terms of the reciprocal space constants $a*$ (as $1/a$), $b*$ (as $1/b$), $c*$ (as $1/c$), with analogously obtained values for reciprocal angles $\alpha*$, $\beta*$ and $\gamma*$:

$$(2 \sin \theta / \lambda)^2 = (1/d_{hkl})^2 = d_{hkl}^{*2} = a^{*2} h^2 + b^{*2} k^2 + c^{*2} l^2 +$$

$$2b^* c^* kl \cos \alpha^* + 2a^* c^* hl \cos \beta^* + 2a^* b^* hk \cos \gamma^*$$

Total electron density obtained after integration of all observed reflections is:

$$\rho(xyz) = \frac{1}{V} \sum_{h}^{\infty} \sum_{k=-\infty}^{\infty} \sum_{l}^{\infty} |F_{hkl}|_{observed} \cos 2\pi \left(hx + ky + lz - \alpha'_{hkl} \right)$$

Where V is the unit cell volume, $x\ y\ z$ are coordinates of atoms, and $\sqrt{kI_{hkl}} = |F_{hkl}|_{observed}$, while α_{hkl} is a phase angle between diffracting X-rays:

$$\alpha_{hkl} = \tan^{-1} \left(\frac{\sum_i f_i \sin 2\pi (hx_i + ky_i + lz_i)}{\sum_i f_i \cos 2\pi (hx_i + ky_i + lz_i)} \right)$$

Final statements that connect all the above concepts together: $1/d = d*$ proportional to *hkl* indices where the atoms are, and I *hkl* = reflections showing what the atoms are, and $I \sim$ number of scattering electrons.
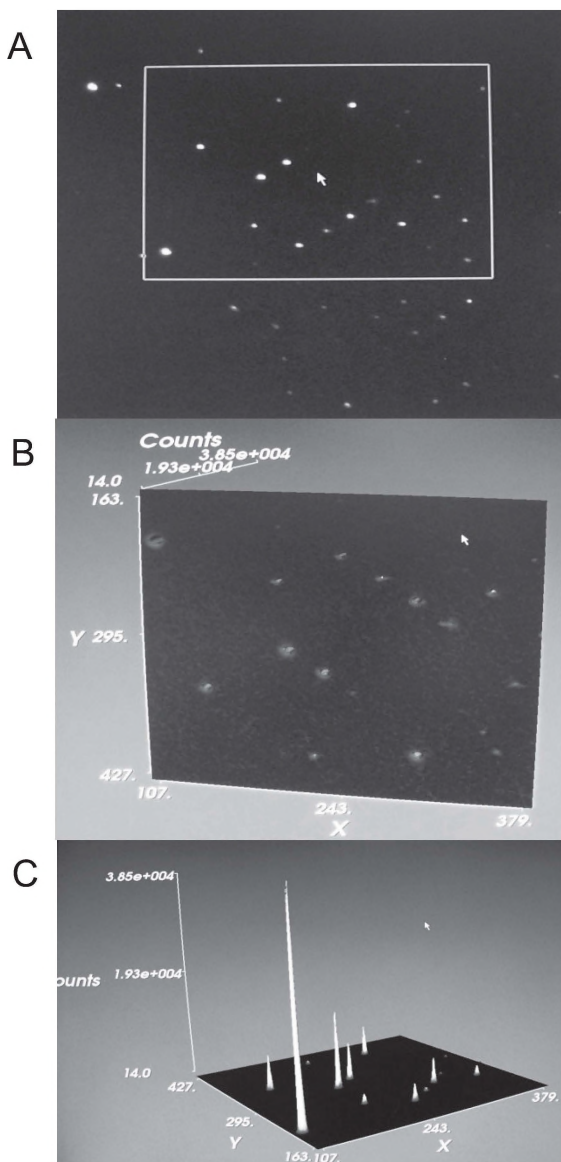
Figure 136. The computer screen-shot picture of a random frame from data collection, with all observed reflections, with some selected in a box (**A**), followed by their two-dimensional (**B**), and three-dimensional visualization (**C**).

        After data integration, a scaling process is necessary to account for internal absorbance of X-rays when they are traveling inside the crystal. The selection of the space group follows, after which two key files are generated for the structure solution; INS and HKL files that have the same filename.

        Structure solution can be done using several methods, as depicted in Figure 137, but always leads to the electron density map with assigned atoms or clusters of connected electron density. That amount of electron density roughly fits to the experimental value obtained from the diffraction experiment. A chemist-crystallographer builds a model with suggested atomic connectivity, and checks it against experimental value. This is the refinement process. If the model is correct, then the refinement successfully converges. Very good examples of crystal structure solution and refinement can be found in the literature [**9,18**], or within tutorials on the personal websites of some well-known experts [**16,17**]. Figure 137 shows three different methods of the structure solution: 1) direct method with no atoms assignment, but good overall connectivity between areas of connected electron density, which well describes the molecule; 2) tentative assignment of atoms based on the amount of electron density in places identified as potential atoms, with crude distribution of electron density in clusters which could be assigned as atoms from intrinsic phasing method; and then 3) an automated approach with both atomic assignment and their thermal motion parameters. Hydrogen atoms in the latter case (Figure 137**C**) are assigned geometrically, based on hybridization of hosting carbon atoms.

        When the crystal structure is solved and refined, it provides accurate values for the chemical bonds lengths, valence, and torsion angles. These are commonly tabulated in specially generated reports, and then further used in the writing of papers, research reports, books, etc. Students and interested readers should pay attention to the numerical values that are present in the first table of such reports; the crystal data table. Examples of such tables are presented in *Appendix 3* and *Appendix 4* of this book. The most important parameters that define the quality of determined crystal structure are briefly discussed below, using the crystal structure of 1-nitroso-2-naphtol (Figure 122 and Appendix 3) [**19**].
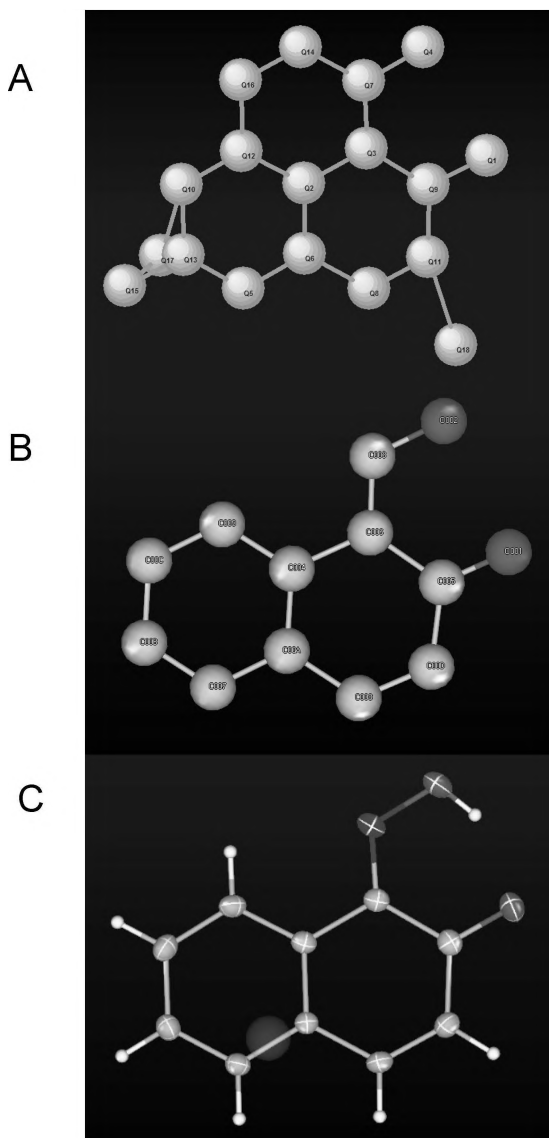
Figure 137. A series of computer screen shots showing crude structure solution using direct methods (**A**), intrinsic phasing method (**B**), and automated solution method (**C**). The case of the above structures of 1-nitroso-2-naphthol is shown here as an example.

The Θ *angle range* for data collection should be within accepted values. For Mo-Kα radiation, it is minimum 25°. In the structure presented here, this range is from 2.60 to 29.11°.

Completeness to given Θ = 29.11° is 99.5%; very good value. Normally this should be no less than 90% for high quality structure (pending good quality crystal and collected data).

Numbers of reflections: *total* = 9,742, while the number of *unique* reflections used for the structure solution and refinement was 2,044.

Intensity of those unique reflections: R(int) = 0.0444. The value R(int) should not be greater than 0.1.

Statistics of *data/restraints/parameters* = 2,244/0/145. That reads as: number of unique reflections used for the structure solutions (2,044, as shown above), and no restraints on the geometry of the molecule were applied (0). Now, the number of parameters is the number of non-hydrogen atoms (13) multiplied by 9 (3 – for atomic coordinates, + 9 for the half of 3×3 matrix that describes atomic thermal parameters U_{11}, U_{12}, U_{13}, U_{22}, U_{23}, U_{33}), plus the number of H-atoms that were experimentally found on the electron density map and refined (7), multiplied by 4 (3 – for atomic coordinated + 1 for the U_{iso} (isotropic thermal displacement parameter). Thus, 13 × 9 = 117, and then 7 × 4 = 28, totaling 145 parameters. A high-quality structure must have a reflections-to-parameters ratio $\geq$ 10 times.

The *goodness-of-fit* (or *GOF*) on F^2 shows how well your model corresponds to experimental value of F^2. This parameter in our case is 1.054, with an acceptable range of values between 0.85 and 1.25. The GOF is dependent on the reflections' weighing scheme applied in the refinement cycles, and can be adjusted, to a certain extent. Finally, correlation coefficients between actual electron structure and calculated one, are expressed as final R indices; for the most intense reflections it is labeled as R1, while for all collected and integrated independent reflections (which, of course, include weak ones, and quite possibly some spikes of the noise!), it is: R1= 0.0452 for 1,347 reflections with F^o > $4\sigma(F^o)$ and R1(all data) = 0.0783 for all 2,044 independent reflections.

Lastly, the remaining and un-assigned electron density is the *largest difference between the electron peak (- charge) and the hole (+ charge)*, and is expressed in $Å^{-3}$. These values, in the case of our crystal structure of 1-nitroso-2-naphtol, are 0.327/-0.211, which is in the completely acceptable range for organic compounds with light atoms -0.5 and +0.5 values. The light atoms are considered to be: H, C, N, O and F.

Normally, the final destination of successfully-solved and refined crystal structures is its depository in the *Cambridge Crystallographic Data Center* (abbreviated as CCDC), followed by publication in a scientific journal or a book. Thus, a chemist and/or crystallographer sends a final *crystallographic information file* (abbreviated as CIF) to the above data center, and receives the registration number, with the data file being converted into a publicly-available format known as a *reference code* (abbreviated as REFCODE). In this form, a crystal structure can be requested from the CCDC by anyone, for viewing and further analysis.

We hope that this section of the book has provided students and interested readers with some initial information about this non-spectroscopic, but very important, structural method of single crystal X-ray analysis, which is widely used in modern inorganic chemistry. Further useful information and reading, including a very nice series of web-based tutorials, can be found in the references below.

Another X-ray diffraction method – powder diffraction – is briefly presented in Chapter 4 of this book. It is mostly used, and greatly valued for, phase analysis; that is, assessment of purity, or presence of starting compounds, or intermediates in the final products of inorganic reactions.

Cited Literature

1. a) https://www.iucr.org/people/nobel-prize; b) Giacovazzo, C.; Monaco, H.L.; Artioli, G.; Viterbo, D.; Milanesio, M.; Gilli, G.; Gilli, P.; Zanotti, G.; Ferraris, G.; Catti, M. *Fundamentals of Crystallography*. 2011, Oxford University Press, 872 pp., ISBN: 9789573653.
2. Bravais, A. *J. Ecole Polytech*. 1850, 19, 1–128.
3. Lalena, J. N. *Crystallography Reviews*, 2006, *12* (2), 125–180.
4. a) Hoffman, F. https://www.youtube.com/watch?v=WuZVV2jtkKo
    b) Hoffman, F. https://www.youtube.com/watch?v=5XwZj0m8zEQ
5. a) Fedorov, E. S. (1891), "Symmetry of Regular Systems of Figures", Zap. Mineral. Obch., 28 (2): 1–146; b) Fedorov, E. S. (1971), Symmetry of crystals, ACA Monograph, 7, American Crystallographic Association.
6. Glusker, J.P.; Lewis, M.; Rossi, M. *Crystal Structure Analysis for Chemists and Biologists (Methods in Stereochemical Analysis)* 1994; in Series: Methods in Stereochemical Analysis (Book 16), 872 pp., Wiley-VCH; ISBN-10: 0471185434.
7. Laue's discovery of X–ray diffraction in 1912 drew attention of Wulff Georg (Wulff, Yuri Victorovich) to X–ray structural research on crystals. Concurrently with W. H. and W. L. Bragg (1913), he independently developed the diffraction relationship $n\lambda = 2d \sin \theta$ (the Bragg–Wulff equation), the basis for the structural analysis of crystals. G. Wulff founded the first X–ray

laboratory in Russia and carried out first diffraction research on crystal structures.

8. http://www.physics.byu.edu/faculty/campbell/animations/x-ray_diffraction.html

9. Clegg, W. *X-Ray Crystallography*. Oxford Chemistry Primers, 2015, 136 pp., ISBN: 9780198700975.

10. http://www.xtl.ox.ac.uk/crystals.1.html

11. http://www.unf.edu/~michael.lufaso/crystallo_software.html

12. http://jana.fzu.cz/

13. a) http://www.lbarbour.com/xseed/;WinGX:;
    b) http://www.ccp14.ac.uk/ccp/web-mirrors/x-seed/

14. Miller W.H. A *Treatise on Crystallography*. 1839, Cambridge, Pitt Press.

15. Courtesy of Dr. Joe Reibenspies, 2016, Texas A&M University, College Station, TX, USA.

16. Dr. J. Reibenspies at TAMU in http://xray.tamu.edu/people.php, and references/links therein.

17. Prof. G. Scheldrick in Göttingen, in: a) https://scholar.google.de/citations?user=7sHztskAAAAJ&hl=en,
    b) http://shelx.uni-ac.gwdg.de/~gsheldr/

18. Fackler, J.P. Jr.; Falvello, L.R. *Techniques in Inorganic Chemistry*. 2010; CRC Press, 219 pp., ISBN 9781439815151.

19. Tyukhtenko, S.I.; Hilton, M.; Gerasimchuk, N. *Curr. Inorg. Chem.*, 2015, *5*(2), 120-136.

3.3.2. Theoretical Background: Cryoscopic Determination of Molecular Weights of Chemical Compounds in Solutions

Determination of molecular weights of synthesized chemical compounds can be done using several methods; mass-spectrometric measurements, and investigations of colligative properties of solutions of compounds. The former method requires rather expensive equipment and well-trained personnel to perform proper and accurate recording of mass-spectra of compounds from solutions. This method is very precise, since it routinely detects masses with 0.0001a.m.u. accuracy. There are, however, a couple of problems with using this technique: 1) dissolution of a compound in appropriate solvent where no decomposition or solvent induced degradation will occur (in inorganic chemistry the latter is the main obstacle); 2) sufficient volatility and ionization ability of the target compound (in many cases the use of several ionization methods (+ or – fast atom bombardment (FAB) coupled with the use of the matrix, electro-spray, or chemical ionization) is necessary to obtain a reliable and reproducible data.

There are also traditional laboratory methods that bring *colligative properties* of solutions into the spotlight; measurements of the boiling point progression, and measurements of the freezing point depression. The term *colligative* means physical properties that are *dependent on the number of particles in solution.* Thus, pure solvent boils at lower, and freezes at higher temperatures than a solution. The method of studying the effect of the solute concentration on the increase of the boiling point is called *ebullioscopy*, while the method that detects freezing point depression is called *cryoscopy*. Both these terms are Greek names for the processes of boiling or freezing respectively. The first method requires high-accuracy measuring both temperature and pressure equipment, and the reflux apparatus. The second method is much more common in chemical laboratories and allows the relatively fast and accurate determination of molecular weights of solutes. The method of *cryoscopy* is especially well suited for the determination of molecular weights of organic compounds, as well as other non-electrolytes, such as coordination compounds. The physical phenomenon behind cryoscopy is rather simple: when solution starts freezing there is a heart of crystallization which evolves because a solid is a well-ordered state of matter, and excess of energy releases upon close packing of molecules into the crystalline solid. Therefore, temperature will rise and plateau until all solution freezes. A time profile of slow freezing of solutions has several regions, as illustrated in Figure 138. After collecting data for temperature reading during the

experiment, and building a similar plot, the freezing temperature is determined on the graph using shown extrapolation, as explained in Figure 138. Of course, there is a need to measure freezing point for pure solvent first, and then repeat the measurement after adding and dissolving a compound of interest.
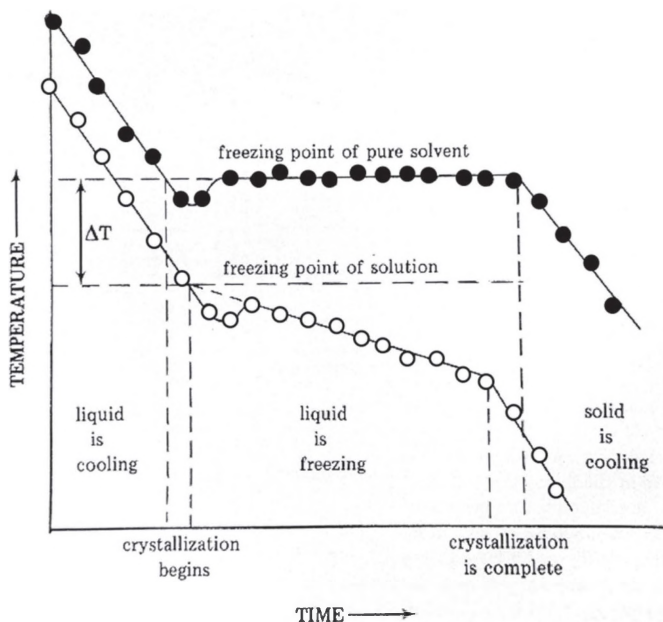
Figure 138. Typical time profile of freezing of a solvent (upper trace) and solution (lower trace), with indication and explanation of regions during the process. Determination of ΔT value for calculation of molecular weights is shown.

Thus, cryoscopic measurements represent periodic recording temperature data for solvent, and then solution. Slopes of the descending portions of traces in Figure 137, as well the lengths of plateaus, are dependent on the rate of cooling the system and the amount of solvent/solution used. The main idea is to determine experimentally the molality of solution using ΔT_F = temperature depression value, and then compare it with what you placed into the measuring vessel. That is, the number of moles of solute in the solvent. Thus, we will have the molecular weight calculated, F.W. (calc) (what we assume based on our actual masses of components), and molecular weight F.W. (found). The main idea is to determine experimentally the molality of solution using ΔT_F = temperature

depression value and then compare it with what you placed into the measuring vessel. That is, the number of moles of solute in the solvent. Thus, we will have the molecular weight calculated, $MW_{(calc)}$ (what we assume based on our actual masses of components), and molecular weight MW (found). Both values should not be different by more than 10%, to indicate a correct match between the predicted and experimental molecular weights. Now it is evident that the method of cryoscopic measurement allows investigation of processes of dimerization and other associated polymerizations or aggregation processes in solutions.

Our tris-Co(III) nitrosonaptholate, precipitated from aqueous solutions, is well soluble in organic solvents, and represents classic non-electrolytes. Therefore, it is an ideal example of a compound for learning the technique to determine its molecular weight. The basic equation for this technique is shown below:

$$\Delta T_F = K_F \cdot b \cdot i \qquad \text{where:}$$

- K_F, is the cryoscopic constant, which is dependent on the properties of the solvent, not the solute.
- b is the molality (moles of solute per kilogram of solvent).
- i is the van 't Hoff factor (number of ion particles per individual molecule of solute, e.g. i = 2 for NaCl, and 3 for $BaCl_2$). For molecular solutions – non-electrolytes – the i value is 1.
- ΔT_F, the freezing-point depression, is defined as $T_{F\,(pure\,solvent)} - T_{F(solution)}$. This value is measured experimentally.

From the equation above, it is clear that in order to have a large, more accurately measurable, temperature one has to use a solvent with a large cryoscopic constant. Table 6, below, is a compilation of literature values for cryoscopic constants (K_F) of a variety of solvents, including water. Also, it is easy to see that these solvents possess a substantial polarity (or none), or an ability to form hydrogen bonding with solute, or are able to form $\pi-\pi$ stacking during the solvation process. Also, presented therein, solvents are selected on their convenience and practicality, based on temperatures which are easily achievable in the lab and do not require specialized and expensive laboratory equipment.

Table 6. Parameters of practically useful solvents for cryoscopic measurement.

Commonly used solvent	$T_{fr.}$, ^oC	K_F, (K·kg)/mol
Water, H_2O	0.00	1.86
Diethanolamine, $NH(C_2H_5OH)_2$	28.0	3.16
Acetic acid, CH_3COOH	16.6	3.63
Dimethylsulfoxide, $(CH_3)_2SO$	18.5	3.85
Benzene, C_6H_6	5.5	5.07
Acetophenone, $CH_3C(O)C_6H_5$	19-20	5.16
Phenol, C_6H_6O	40.5	6.84
Nitrobenzene, $C_6H_5NO_2$	5.7	6.87
p-Dichlorobenzene, $C_6H_4Cl_2$	53.5	7.57
Benzophenone, $(C_6H_5)_2CO$	48.5	8.58
Succinonitrile, $(CH_2)_2(CN)_2$	57.0	19.3
Cyclohexane, C_6H_{12}	6.55	20.8
Cyclohexanol, $C_6H_{11}OH$	25.93	42.2

3.3.3. Theoretical Background: Cyclic Voltammetry (CV) of Coordination Compounds in Solutions

The method of cyclic voltammetry is a very powerful tool in studying the redox behavior of numerous compounds, including metal complexes with a central atom susceptible for the reduction/oxidation processes in solutions. Those are typical transition metals, except Zn, Cd as well as Sc, Y, lanthanides. The most useful method is for transition metals that exhibit multiple oxidation states: Fe^{2+}/Fe^{3+}, $Mn^{2+}/Mn^{3+}/Mn^{4+}$, $Cr^{2+}/Cr^{3+}/Cr^{6+}$, Co^{2+}/Co^{3+}, Cu^+/Cu^{2+}, etc. This technique is based on changing the applied potential at the working electrode (compared to the reference electrode), in both forward and reverse directions. This varying potential causes the reduction and oxidation reactions to occur in the system at the working electrode surface. The electrochemical cell current between the auxiliary electrode and reference electrode is simultaneously measured as well (Figure 139**A**). The resulting current/voltage plot typically represents a closed figure with a maximum and minimum (called peaks) that correspond to the reduction and oxidation potentials of the system (Figure 139**B**). These peaks will be observed at potentials that initiate a chemical reaction in the solution (reduction or oxidation), because they involve a flow of electrons. Peaks are labeled as potentials cathodic, E_{pc} (+), and anodic, E_{pa} (-) (Figure 139**B**).
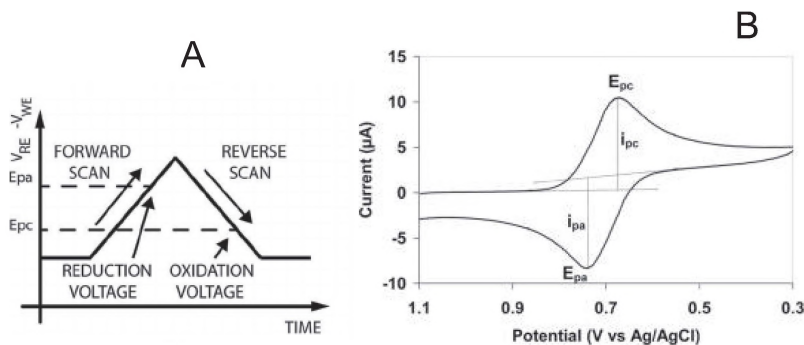
Figure 139. Triangular shape of the electric potential sweep during cyclic voltammetry experiments (**A**), and actual shape of the CV curve for a reversible redox process (**B**).

Organic solvents exhibit very low electrical conductivity, and that necessitates the addition of an electrolyte that is inert to the compounds dissolved (e.g. has zero chemical reactivity) and has inaccessible values of potentials to be observed in an electrochemical cell. That means that the solvent will be reduced/oxidized earlier than components (cations or anions) of the electrolyte. Thus, supporting electrolytes contain alkylammonium cations, normally tetrabutylammonium $N(C_4H_9)_4^+$ and inert anions with zero nucleophilicity: BF_4^-, ClO_4^-, PF_6^-. Typically, ~0.1M solutions of those are made in an organic solvent of choice for recording the CV traces, and solid supporting electrolyte is added into the cell during purging with an inert gas (N_2 or Ar), which also provides an efficient mixing. The gas flow is absolutely necessary, to remove dissolved oxygen from the air from the solution, which would obscure accurate measurements.

An electrochemical cell is made of glass, and represents a small vial of 4-6mL capacity that houses three electrodes: working electrode (glassy carbon), reference electrode (Ag/AgCl/0.1 M LiCl in dry acetone), and auxiliary electrode (Pt-wire) (Figure 140). Three electrodes are needed because the measurement of the potential and the current has to be performed in different cycles which interfere with each other [**1**].
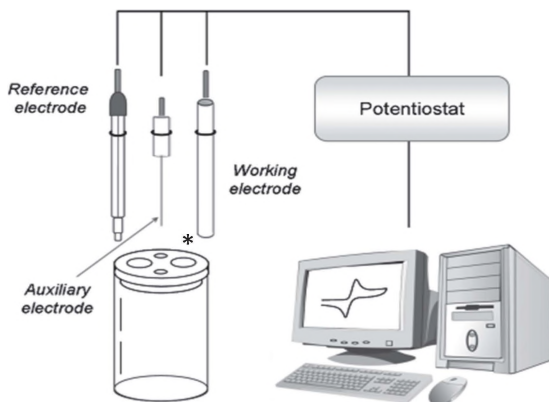
Figure 140. Experimental setup for CV measurements: shown three electrodes in the electrochemical cell with place for an inert gas purging prior to recording (marked with an asterisk).

Electrodes are connected to a potentiostat that allows for the control of the potential and the measurement of a current. This potentiostat is conjugated to a computer system, for control and recording of CV traces. The cathodic E_{pc} and anodic E_{pa} peak potentials are measured as maximum and minimum of peaks (Figure 139**B**), and the formal reduction potential is obtained by $E_0 = (E_{pa}+E_{pc})/2$. The half peak potential $E_{1/2}$ can be described by the Nernst Equation. Values of E_0 are used to evaluate the electronic status of the central atom in complexes, and compare with known compounds. At this stage, the role of bound to the metal center ligands became apparent: electron withdrawing or donating effects change the potential dramatically. The potential sweep rate (scan rate) is important [**2**], and typically it is set to be 50 mV/s.

3.4. Experiment 5C: Part 1

Cryoscopic Measurements of Molecular Weights of Synthesized Cobalt(III) *tris*(nitroso-naphtholates)

Chemicals: Dry samples of Co(III) nitrosonaphtolates:
Co(1NO-2OH)$_3$ and Co(2NO-1OH)$_3$, as the unseparated mixture of mer- and fac- geometrical isomers;
Pure DMSO as solvent

Equipment: Glassware device for cryoscopic measurements;
High accuracy thermometer (either Hg-filled Beckman thermometer, or digital thermometer) with reliable ±0.01° measurements;
Computer for data collection, processing and graphing.

Procedure (will be carried out in groups, with two students per group):

Step 1.
Weigh ~0.150g of the Co(III) complex on analytical balances, and dissolve it in ~5g of pure DMSO, which should be weighed in a vial or beaker. The amount has to be measured precisely to 3-4 digits after the decimal point. Record the weights and calculated molality of your solution.

Step 2.
Place ~ 5g of pure DMSO into the measuring glassware and immerse a high-precision thermometer. First, we need to measure the freezing temperature of water in our experiment.

Step 3.
Prepare an ice bath and measure its temperature with a low accuracy liquid thermometer (or simple digital thermometer).

Step 4.
Place glassware vessel with pure DMSO and high-precision thermometer into the cooling bath. Start stirring the solution and slow cooling the system. Stirring/mixing the solution is absolutely essential for getting reliable and accurate results! An overcooled system gives an erroneous freezing point.

Step 5.
Monitor slow temperature drop, maintaining an intense stirring. When pure solvent begins freezing it will appear as a cloudy slush, and its temperature will suddenly slightly rise. It will stay without changing until the whole volume freezes shut. Record the temperature during its sudden rise. This is your solvent's $T_{F \text{ (pure solvent)}}$.

Step 6.
Disassemble the system, empty the solvent (DMSO) from the measuring vessel, wash it with acetone, and dry it.

Step 7.
Transfer a solution of Co(III) complex from **Step 1** into a dry and clean glassware vessel, where the main experiment will be conducted. Adjust the stirring/mixing device to proper working conditions. Immerse the high precision thermometer in the mixture.

Repeat Steps 3–5 and measure $T_{F \text{ (solution)}}$. Obtain $\varDelta T_F$, and perform calculations of the molecular weight of your solute – Co(III) complex – using K_F value for the solvent (DMSO, 3.85) from Table 6 above. Determine the absolute and relative errors of your measurements by using these expressions:

$$\text{Absolute error, \%} = \text{F.W. (calc)} - \text{F.W. (found), and}$$

$$\text{Relative Error, \%} = \frac{\text{F.W. (calc)} - \text{F.W. (found)}}{\text{F.W. (calc)}} \times 100\,\%$$

Present data of your measurements in the lab report and comment on the accuracy of your molecular weight determination.

Part 2

Recording of CV traces for synthesized cobalt(III) *tris*(nitroso-naphtholates)

In this part of the laboratory exercise we will perform electrochemical characterization of the earlier bulk Co(III)-tris-(nitrosonaphtolates) obtained in labs **5A** and **5B**, as the mixture of geometrical *mer*- and *fac*-isomers. Values of measured potentials will be compared with the

literature data about Co^{2+}/Co^{3+} pairs in other coordination compounds with similar donor atoms set.

Chemicals: Both synthesized in previous lab sessions **5A** and **5B**
                      tris-Co(III)-nitrosonaphtolates;
                      Dry acetonitrile;
                      Tetrabutylammonium perchlorate (TBAP) as supporting electrolyte;
                      Ferrocene (as electrode potential reference).
Equipment: Potentiostat suitable for performing for CV measurements;
                      Electrodes: working – glassy carbon, reference – Ag/AgCl, and auxiliary – Pt-wire;
                      Polishing pad for clearing the electrode surface;
                      Thermometer.

Procedure: *(will be carried out in groups, with two students per group).*

Step 1.
Take ~5mg of the Co(III) complex and dissolve in 2mL of pure dry acetonitrile, CH_3CN, and place solution into the electrochemical cell. Start a slow flow of an inert gas (N_2 or argon), to purge the system of dissolved oxygen from the air. Failure to do so will lead to an extra broad signal at ~0.72V that will significantly distort recorded CV trace.

Step 2.
Insert all three electrodes into the cell, and connect them to the potentiostat. Add a small amount (tip of the spatula) of a supporting electrolyte.

Step 3.
Make the following settings on the potentiostat:
   a)   Sweep rate set to 50mV/sec;
   b)   The potential sweep range set from +1.00 to -0.70V;
   c)   Select the direction of reduction sweep first.

Step 4.
Stop an inert gas flow through the cell (bubbling) and record the CV trace. Save the data file in a computer in a format suitable for further processing (ASCII, DAT or CSV for Origin, Excell).

Step 5.
Repeat the same procedure as in Step 4, only this time, set the oxidation direction first.

Step 6.
Disassemble the electrochemical cell, clean it, wash with acetone, and dry. Polish the glassy carbon electrode using the pad (contains alumina on a felt) to remove potentially absorbed Co(III) complex.

Step 7.
Repeat Step 1, this time dissolving ~2mg of ferrocene in acetonitrile, purge the cell, add supporting electrolyte.

Step 8.
Repeat Step 3, but change the direction of sweep to the oxidation's first mode.

Step 9.
Measure the CV trace for the ferrocene/fericenuim couple. Save the data file. Calculate the redox potential. This will be the reference potential for reporting the data.

Expected results:
The *tris*-Co(1NO-2OH)$_3$ complex demonstrates one distinctive and apparently reversible wave (Figure 141) in the CV process, in a studied range of potentials between +1.00 and -0.70V. The half-way potential was calculated to be -0.413V, which corresponds to Co^{3+} ⇆ Co^{2+} redox pair. The method of calculating the redox potential is simple; the half-way potential represents a half-sum of the anodic peak and the cathodic peak (Figures 141, 142). Calculated this way, redox potentials for studied tris-Co-nitrosonaphtolates, measured as the mixture of geometrical isomers, are presented in Table 7.

Table 7. Redox potentials for $Co^{3+} \leftrightarrows Co^{2+}$ redox pairs in the obtained nitroso-naphtolates measured at +22°C in CH_3CN solutions. The supporting electrolyte was tetrabutylammonium perchlorate, scan rate 50 mV/s.

Complex	sweep direction	E(an),V	E(cat),V	DE, V	E ½, V
$Co(1NO-2OH)_3$	oxidation first	-0.455	-0.372		-0.413
	reduction first	-0.455	-0.371		-0.413
$Co(2NO-1OH)_3$	oxidation first	-0.291	-0.195		-0.243
	reduction first	-0.289	-0.194		-0.242
ferrocene/ ferricinium	oxidation first	+0.402	+0.584		+0.493

Measured redox potentials for both isomeric mixtures of Co(III) nitrosonaphtholates are almost doubly different in values. This evidences that in the second Co-complex, the reduction of metal center to +2 oxidation state is much easier. In turn, this observation indicates a much greater back-donation effect of the nitroso-group to Co(III) atom in $Co(2NO-1OH)_3$, as compared to its isomeric $Co(1NO-2OH)_3$.

In order to complete your laboratory work, you need to check your data against values of redox potentials for other cobalt(II)/(III) pairs, available from the literature; for example, with those presented in the set of references [3-7]. Compared, analyzed, and interpreted data of this part of the exercise must be presented in your lab report.
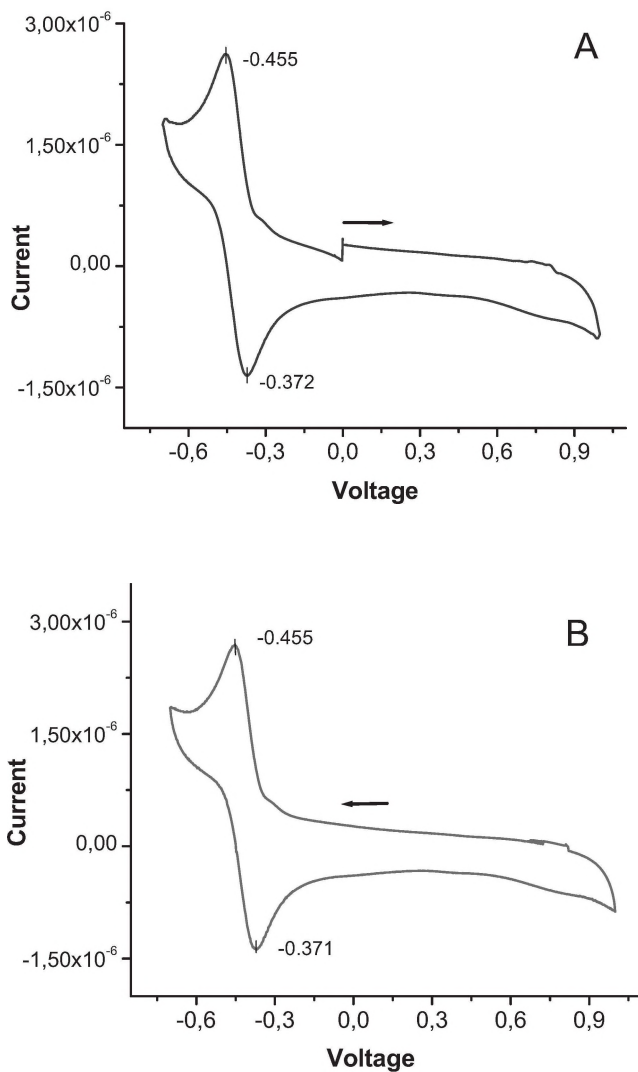
Figure 141. Cyclic voltammograms (CV) of solution of tris-Co(1NO-2OH)$_3$ in CH$_3$CN at +23°C: **A** – oxidation first, **B** – reduction first.
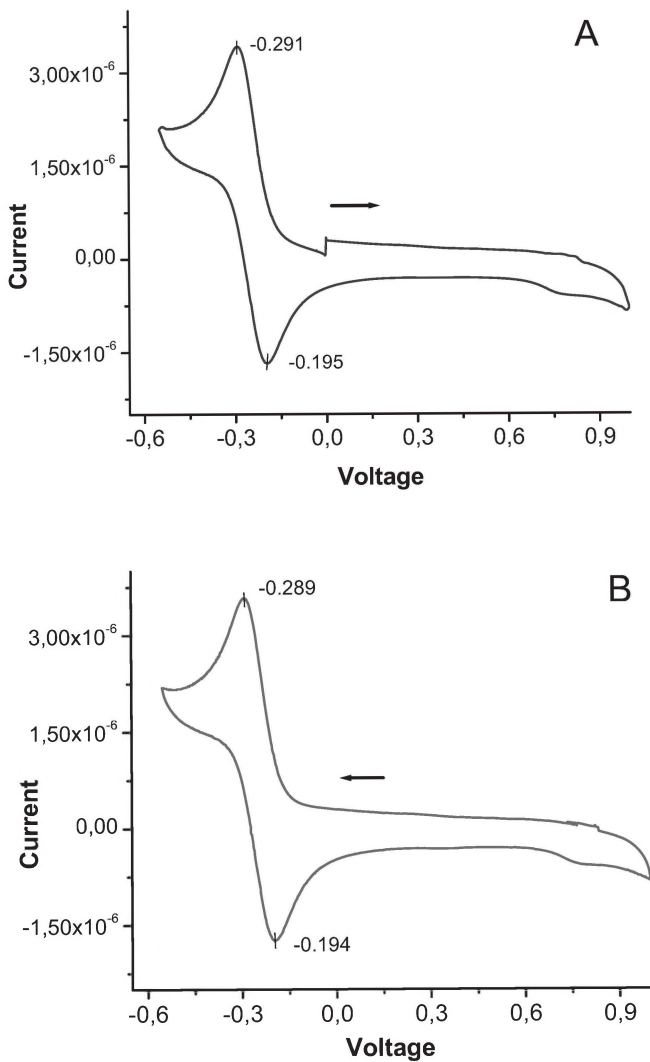
Figure 142. Cyclic voltammograms (CV) of solution of tris-Co(2NO-1OH)₃ in CH₃CN at +23ºC: **A** – oxidation first, **B** – reduction first.

Potential hazards:
   1) Organic solvent is used in this part of a laboratory work. Wearing gloves is required.
   2) Electrochemical equipment must be properly insulated and handled with care.

Cited Literature

1. Bard, A.; Faulkner, L.R. *Electrochemical Methods: Fundamentals and Applications* (2 ed.). 2000, Wiley, 864 pp. ISBN: 978-0-471-04372-0.
2. https://www.ceb.cam.ac.uk/research/groups/rg-eme/teaching-notes/linear-sweep-and-cyclic-voltametry-the-principles
3. Lange
4. Buglyo, P.; Kozsup, M.; Nagy, I.; Nagy S.; Csaba-Benyei, C.; Kovats, E.; Farkas, E. *Inorg. Chim. Acta.*, 2018, *472* (3), 234-242.
5. Ogina, H.; Ogino, K. *Inorg. Chem.*, 1983, *22* (15), 2208-2211.
6. Pandey, S.; Das, P.P.; Singh, A.K.; Mukherjee, R. *Dalton Trans.*, 2011, *40* (40), 10758-10768.
7. Araujo, M.C.; Doherty, M.D.; Konezny, S.J.; Luca, O.R.; et al. *Dalton Trans.* 2012, *41*, 3562-3573.

3.5. Purification and Separation of Geometrical Isomers of Complexes

Experiment 6A: Separation of geometrical isomers of Co(III) *tris*(1-nitroso-2-naphtholate) using column chromatography

As the result of previous experiment 5A shows, we have obtained several grams of the *tris*-CoL₃ complexes (L=1-nitroso-2-naphtol). This complex represents a mixture of two geometrical isomers; *mer*- and *fac*-. Therefore, in order to study individual Co(III) complexes, we need to perform a separation of those isomers. The best way to achieve separation is by using chromatographic methods. Since the metal complexes that have already been studied are highly colored, we will be able to use this as a visual guide for the separation and purification of the *mer*- and *fac*-isomers.

This particular complex is particularly suitable for straight phase flash-column chromatography using silicagel. The <u>aim</u> of this experiment is to learn the techniques of chromatographic separation of geometrical isomers of Co(III) nitrosonaphtholates.

The *objectives* of this laboratory exercise include: a) learning how to carry out analytical and preparative thin-layer chromatography in organic solvents; b) isolation of pure individual geometrical isomers through their extraction from the *stationary phase* (*sorbent*) by an organic solvent; c) learning the proper technique of the 'wet-method' column packing, and loading with the compounds' mixture; d) performing column separation of the isomers via a collection of a number of fractions; and e) isolation of individual isomers using a rotary evaporator.

Chemicals: solvents such as dichloromethane CH_2Cl_2, toluene,
                      chloroform $CHCl_3$, anhydrous drying agents Na_2SO_4 or
                      $MgSO_4$.

Equipment and Materials:
          Glass wool;
          Washed rough sand;
          Glass column for chromatography with Teflon stopcock;
          Silica gel for column chromatography 60-230 mesh grade;
          5-8 Erlenmeyer flasks for fractions collection;
          Round bottom flask for evaporation of fractions;
          Rotational evaporator equipped with an 'anti-bump' trap;

Soxhlet extractor assembly (includes apparatus, condenser and thimble).

Procedure: *(will be carried out in groups, with two students per group)*

Part A: Analytical Thin-Layer Chromatography of tris-Co(1NO-2OH)₃

Perform analytical TLC using silica on flexible Al-plates, according to the instructions below (Figure 143). You will need a glass development chamber with a cover cap (watch glass is perfect for this purpose!), a thick paper vapors saturation pad, capillaries, and a small test tube in which you will need to dissolve the Co(III) complex. First, place 5-10ml of the mobile phase – CH_2Cl_2 in this case – into the development chamber, and then place the pre-cut vapor saturation pad inside, close the chamber, and gently shake several times, to assure that the pad is wet with the mobile phase and the chamber is well saturated with the solvent vapors. It may take several minutes. During that waiting time, you can dissolve 1-3mg of the initial ligand in acetone final product – Co(III) complex – in small test tubes. Then perform spotting of the TLC plate with capillaries containing those solutions (Figure 40, Chapter 1). Capillaries are single-use items and should be discarded after spotting the plate. Dry those spots using an air gun (Figure 34, Chapter 1). Using the forceps, gently immerse the TLC plate into the development chamber, close the lid, and perform chromatography. Soon after contact with the mobile phase, a red-orange spot of the complex will move upwards and then split into two distinctive bands. At this point, the pure starting compound – ligand 1NO-2OH – will not move very fast, because of its high polarity and greater adhesion to the silicagel surface. Remove the plate when the solvent front reaches the top of the plate, and dry the plate. Determine the R_f values* for all spots.

~ 1 inch

~ 3-3.5 inches

using scissors cut
corners of the plate
as shown; try to keep
the angle ~ 45°
and dimension ~ 3/16"

step 1

mark slightly, with almost
invisible line the start line
with a soft pencil

~ 3/8"

TLC plate: aluminum foil
with a layer of absorbent;
typically SiO_2 (Al_2O_3 - rare)

step 2

using thin capillaries post **two
spots** on TLC plate as shown;
make one spot ~ 5-10 times
smaller concentrationthan the
other one

finish line

idividual isomers

step 3

develop plate in closed
chamber filled with
eluotropic mixture
(or mobile phase)

let spots completely
dry in open air

mobile phase: pure CH_2Cl_2 for
$Co(1NO-2OH)_3$ mixture of isomers

Figure 143.   Step-by-step instructions on how to prepare the TLC plate and
perform an analytical chromatogram for the assessment of purity of the obtained
$Co(1NO-2OH)_3$ complex.

Part B: Column Chromatography of Co(1NO-2OH)₃
Use proper column preparation (wet method) displayed in Figure 144.

place column vertically
in a labstand

pour sand into
the column for
~ 1/2" high level

use a little piece of
glasswool to plug
column's exit to a
stopcock

add sand again
on a top of the
silica in the
column to form
another ~3/8 inch
layer

add silic slowly,
with small
portionsinto the
column; then after
1/2 of the column
is filled, drain the
solvent to ~ 1 inch
level left

pour CH$_2$Cl$_2$ into
the column for
~ 1/2 hight
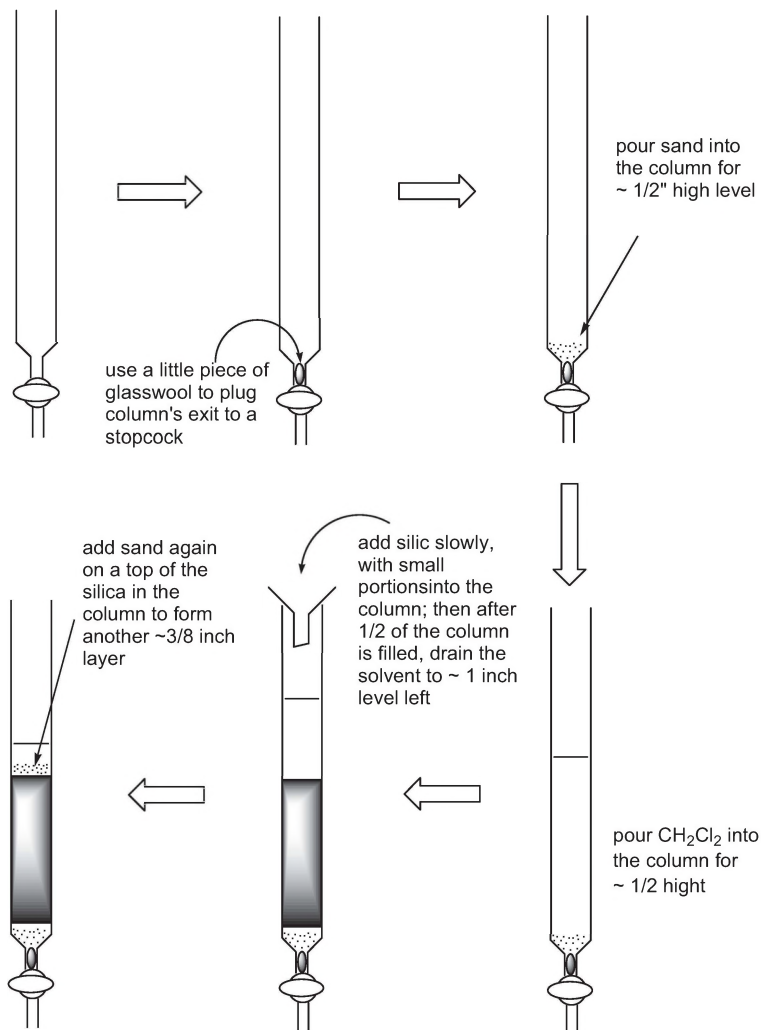
Figure 144. Step-by-step instructions for the column preparation for flash-chromatography (the instructor will show specific details during the lab session).

Careful loading of the column with concentrated solution of the Co(1NO-2OH)$_3$ complex, and slow elution of the mobile phase, allows separation of geometrical isomers, as explained below, and shown in figures 145 and 146.
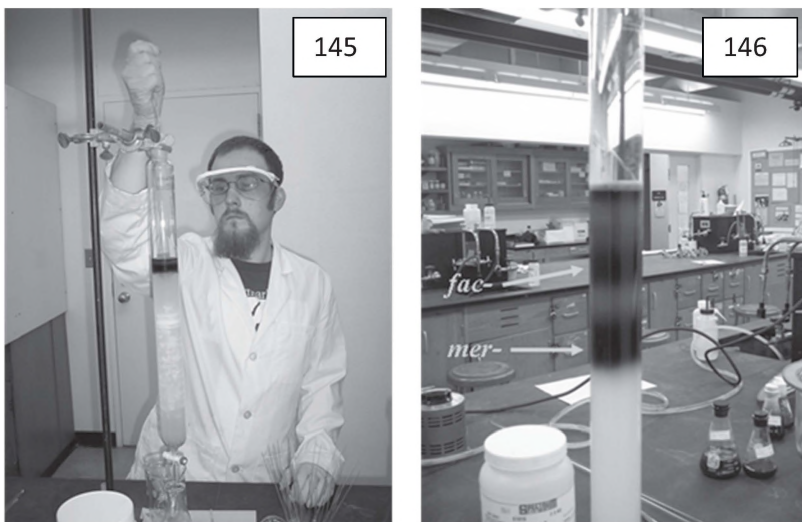
Figure 145. Proper loading of the 'wet' packed column: gloves, a pipette, and careful addition of Co(III) solution on the wet top of the column for separation. See centerfold for this image in colour.

Figure 146. Running column with geometrical isomers: state of the separation after ~2 hours (Co(1NO-2OH)$_3$ column shown).

Compound Dissolution: Dissolve the mixture of isomers (~500mg) of Co(1NO-2OH)$_3$ in dichloromethane (CH$_2$Cl$_2$) for the column separation. Filter the obtained solutions from undissolved solids using a cotton plug filtration. *Any undissolved solid will hinder proper separation of the isomers.*

Loading the Column: With the stopcock remaining closed, use a pipette to load the filtered solution dropwise onto the top of the column (Figure 145).

Eluting the Column: Separate two geometrical isomers using straight phase column chromatography (Figures 145, 146). The eluent is pure

CH₂Cl₂. The whole procedure may take *many hours* to complete. In some cases (when the amount of the isomeric mixture is more than 300mg) it can even take two days. Therefore, it requires special dedication and care. Sometimes students watch the running column in shifts, adding solvent to the column over many hours.

Combining and Drying Fractions

Now there is a need to combine the collected fractions of separated geometrical isomers into one or two flasks (depending on volume of solutions) (Figure 147), and add ~25-30g of the drying agent anhydrous Na₂SO₄ or MgSO₄. These flasks have to be left for ~24 hours, for the solution to dry. Typically, in the next lab session the solvent (CH₂Cl₂) is removed under vacuum using a rotary evaporator (Figure 148; details of the apparatus construction and function can be seen in Chapter 1, Figure 69). The obtained separated powdery complexes should be further dried in a vacuum desiccator. They will be used for recording the NMR, IR- and UV-visible spectra in the next laboratory sessions.
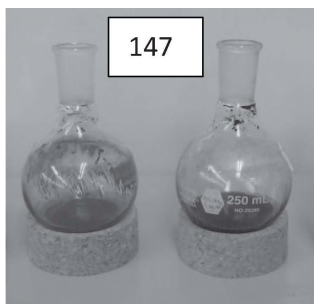
Figure 147. Flasks with column-separated pure isomers of (Co(1NO-2OH)₃: *mer* is in the left flask, *fac* is in the right flask. See centerfold for this image in colour.

Figure 148. The rotovap assembly shown at the last stage of concentration of separated isomers solutions.

---

* - the retention factor (R_f value) is measured as the ratio between the distance a spot travels on the TLC plate to the total length of the mobile phase travel. Hence, the R_f value always has a value smaller than 1.

The number of the experiment, date, authors of the reaction, and total amount of the obtained pure isomer with its yield, must be written on the labels. The labels should be attached to the screw-cap vials with separated geometrical isomers of *tris*-Co(III)-nitrosonaphtholates.

Potential hazards:
   1) Dichloromethane is halogenated solvent. It is toxic to mammals (can cause liver damage), and work with it must be carried out under the ventilation hood, using common sense and care.

   2) Silica gel is a very fine powder that can easily become airborne. Generally, it is considered to be a non-toxic substance, but may cause some irritation to your nose, mouth, or skin if exposed to it.

3.6. Experiment 6B: Separation of geometrical isomers of Co(III) *tris*(2-nitroso-1-naphtholate) using preparative thin-layer chromatography

As the results of previous experiment 5B show, we have obtained several grams of the *tris*-CoL$_3$ complex (L=2-nitroso-1-naphtol). This complex represents a mixture of two geometrical isomers: *mer*- and *fac*-. Therefore, in order to study individual Co(III) complexes, we need to perform a separation of those isomers. The best way to achieve separation is using chromatographic methods. Since these metal complexes have already been obtained, it is known that they are highly colored, and we will be able to use this as a visual guide for the separation and purification of the *mer*- and *fac*-isomers.

This particular complex can be well separated using preparative TLC chromatography. The <u>aim</u> of this experiment is to learn the techniques of chromatographic separation of geometrical isomers of the Co(III) nitrosonaphtholates.

*Step 1: Analytical Thin-Layer Chromatography of tris-***Co(2NO-1OH)**$_3$.

Follow the same procedure as the one shown for the Co(1NO-2OH)$_3$, above in Figure 143. Perform analytical TLC using silica on flexible Al-plates, according to the instructions below. Thus, dissolve several milligrams of the complex in CH$_2$Cl$_2$ and make two spots of different concentration on the TLC plate, using a glass capillary. The mobile phase for the separation is toluene: CH$_2$Cl$_2$ = 1:4. An example of a developed chromatogram is shown below, in Figure 149.

Measure and calculate R_f values for both compounds. Don't forget to check your mother liquors from last week for the presence of uncomplexed, free ligand.
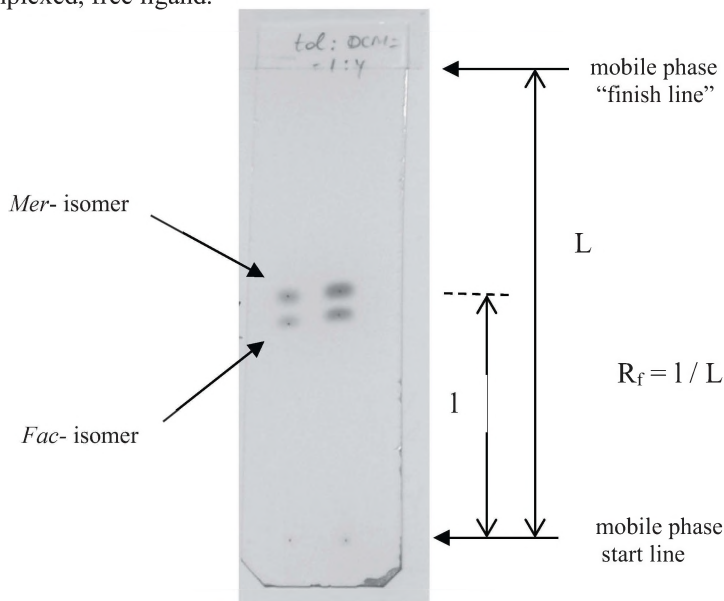
Figure 149.   Developed analytical TLC for the *tris*-Co(2NO-1OH)₃. Shown necessary measurements for the R_f determination for the *mer*-isomer.

Step 2: Preparative chromatography of tris-Co(2NO-1OH)₃

Perform preparative TLC using silica on glass plates, according to the instructions shown in Figures 150 and 151. Use toluene: CH_2Cl_2 = 1:4 mixture as mobile phase.
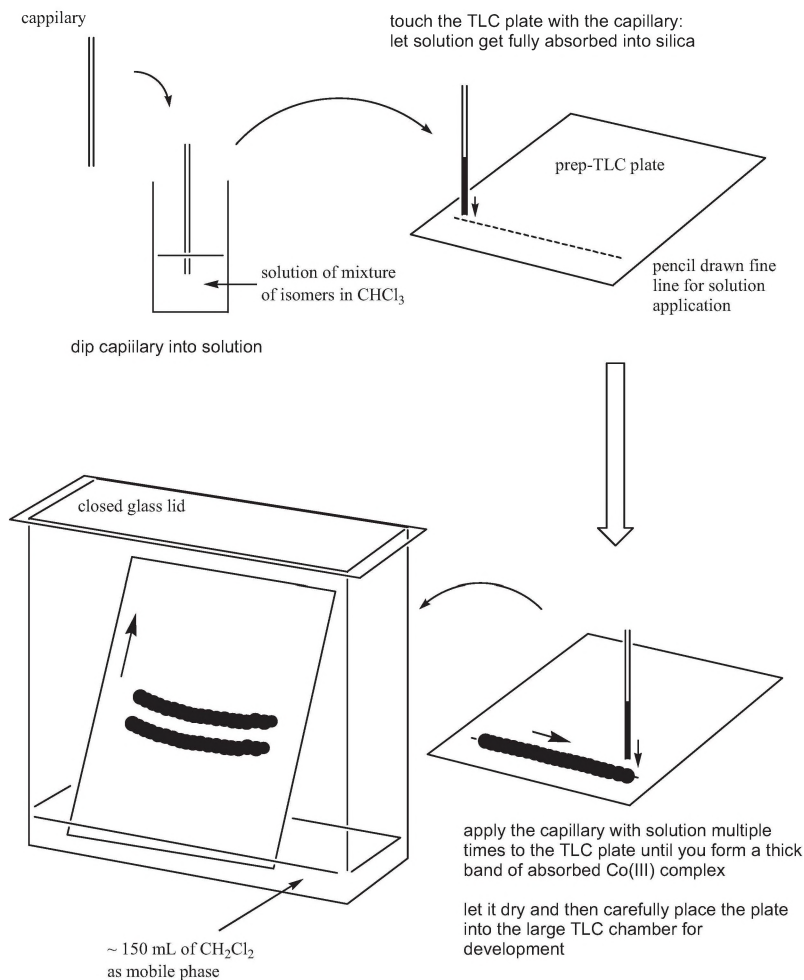
Figure 150. Step-by-step instructions on loading the prep-TLC plate with the mixture of isomers, drying, and development in a large chamber filled with the mobile phase (toluene:CH_2Cl_2 = 1:4).

After separation is achieved (Figure 151), dry the plate under the hood and scrape bands of individual isomers, followed by the removal of complexes using the Soxhlet extractor (Figure 152).
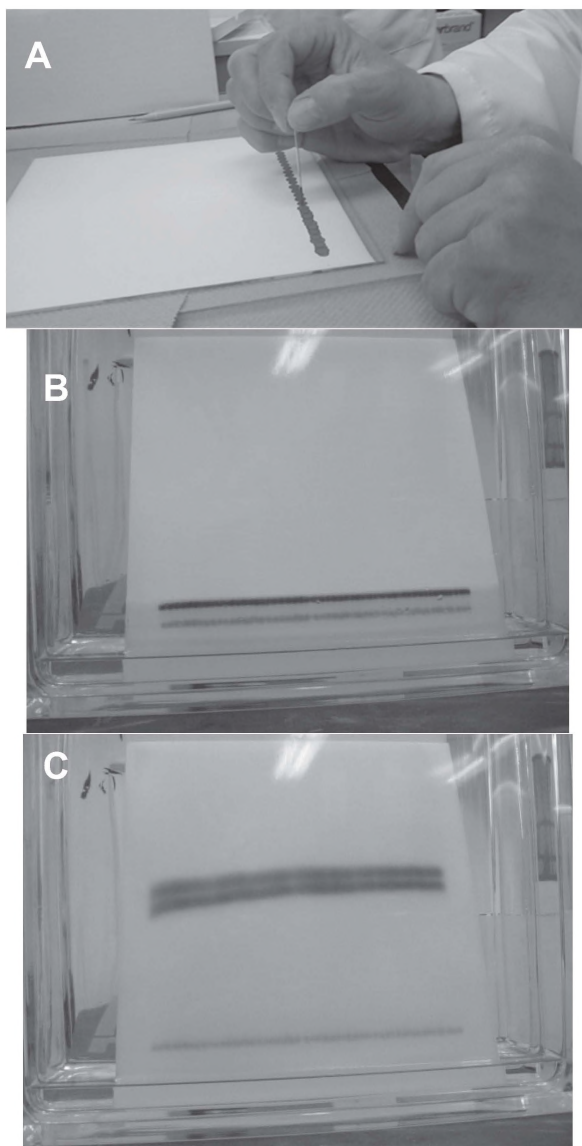
Figure 151. Prep TLC for the mixture of isomers of Co(2NO-1OH)₃. **A**: loading the plate with capillary; **B**: beginning of development; and **C**: separation of *mer*- and *fac*- isomers.
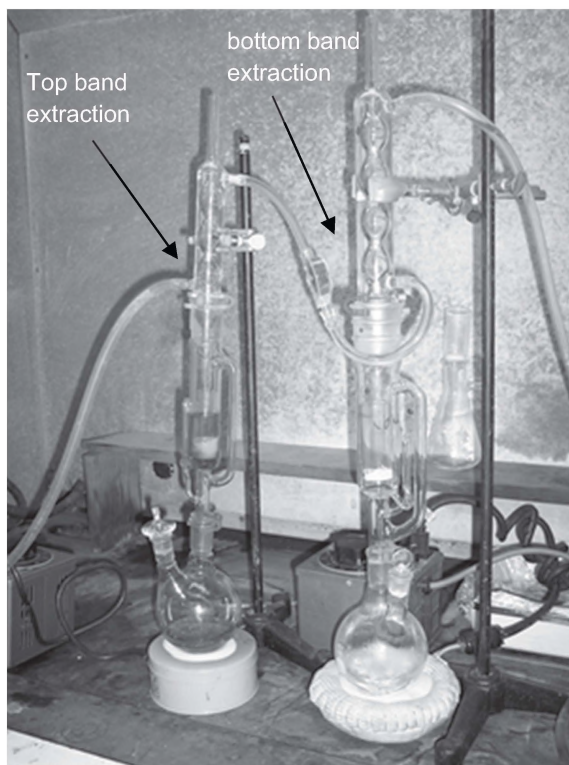
Figure 152. Isolation of individual geometrical isomers from the stationary phase (silicagel) using the Soxhlet extractors and CH_2Cl_2 as a solvent.

Objectives of this laboratory experiment and expected accomplishments:

1) Perform prep-TLC separation [for $Co(2NO-1OH)_3$] of geometrical isomers of both complexes, according to procedures provided;

2) Measure the TLC R_f values for both isomers for both Co(III) complexes;

3) Prepare a detailed lab report with all observations, discussion of results, and conclusions; your lab report will be due at the next laboratory session.

Potential hazards:

1) Toluene and dichloromethane solvents are toxic to mammals (they can cause brain and liver damage) and work with them must be carried out under the ventilation hood, using common sense and care.

2) Silica gel is a very fine powder that can easily lift off the TLC plate. Generally, it is considered to be a non-toxic substance, but may cause some irritation to your nose, mouth or skin if exposed to it.

3.7 Experiment 7: Thermal Re-isomerization of Individual Isomers and Spectroscopic Studies of the Obtained Cobalt(III) Nitrosonaphtholate Complexes

The previous experiment, **#5**, has led to the preparation of cobalt(III) neutral complexes based on the famous analytical reagents, nitrosonaphthols. One complex was synthesized, but it contains two geometrical isomers. During the last two laboratory sessions, **6A** and **6B,** we were able to separate *mer-* and *fac-* isomers of the complex, using column chromatography and preparative TLC. Both isomers are now available for further investigations.

The main *objectives* of this laboratory session are: a) to perform a 2D TLC experiment (observe the 'magic square' as the result of the isomers interconversion); and b) spectroscopic characterizations of individual isomers.

The background information for Experiments **5A** and **5B** contains theoretical information regarding two possible geometrical isomers for octahedral complexes with three non-symmetric bidentate ligands. These isomers are *mer-* and *fac-*, with respect to the mutual disposition of 3 nitrogen and 3 oxygen donor atoms in the coordination polyhedron of Co(III) [1]. This type of isomerism is very common among complexes of kinetically inert metal ions: Cr^{3+}, Rh^{3+}, Al^{3+}, Ir^{3+}, Ru^{3+}, where the ligands exchange or substitution reactions are very slow [2]. Figure 153 shows chart structures of both isomers and indicates their point groups' symmetries. The latter affects the net dipole momentum of the whole complex, which is an important parameter that defines the polarity of the compound. For instance, the polarity affects the retention of the isomers on a stationary phase during chromatographic separations. The most interesting phenomenon, however, is the fact that, in the case of Co^{3+} complexes, it is possible to observe the re-isomerization reaction; interconversion of the *mer-* isomer into *fac-*, and vice versa. Mechanistically, this is done by the

'unplugging' of one ligand and 're-plugging' it back in after rotation, as shown by the dotted lines in Figure 153.
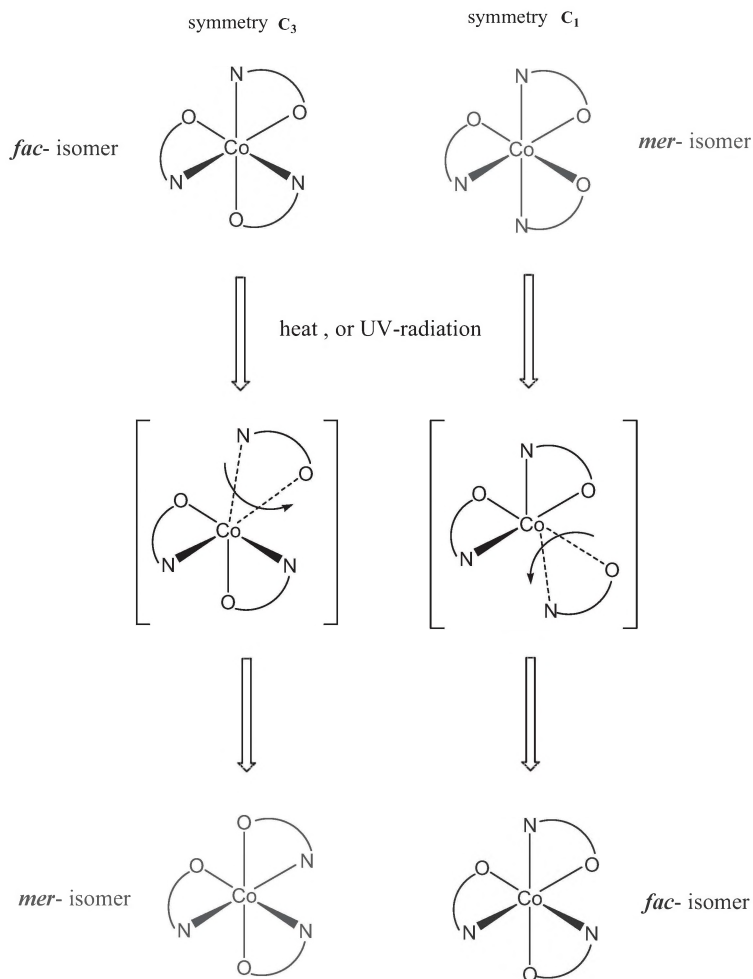
Figure 153. Point group symmetries of individual isomers in CoN_3O_3 environment and the re-isomerization path. See centerfold for this image in colour.

In this laboratory experiment we will be using methods of TLC to study the re-isomerization reaction of the $Co(1NO-2OH)_3$ and $Co(2NO-1OH)_3$ *mer-* and *fac*-geometrical isomers which were separated in previous

labs. Individual isomers are completely stable at ambient conditions, but slowly demonstrate 'scrambling' (formation of the other isomer) upon the supply of energy; either an intense UV-radiation, or by heating the sample. The first method is fast, but unfortunately leads to the photo-bleaching of samples. The second method takes a longer time, and requires many hours of heating samples under vacuum to prevent thermal oxidation of complexes. We will use that approach, leaving the TLC plates in the vacuum oven at ~140°C for several days.

Details of the 20×20cm Al-backed silicagel TLC plate loading with isomers, and then stepwise development in two directions, are explained in Figure 154.
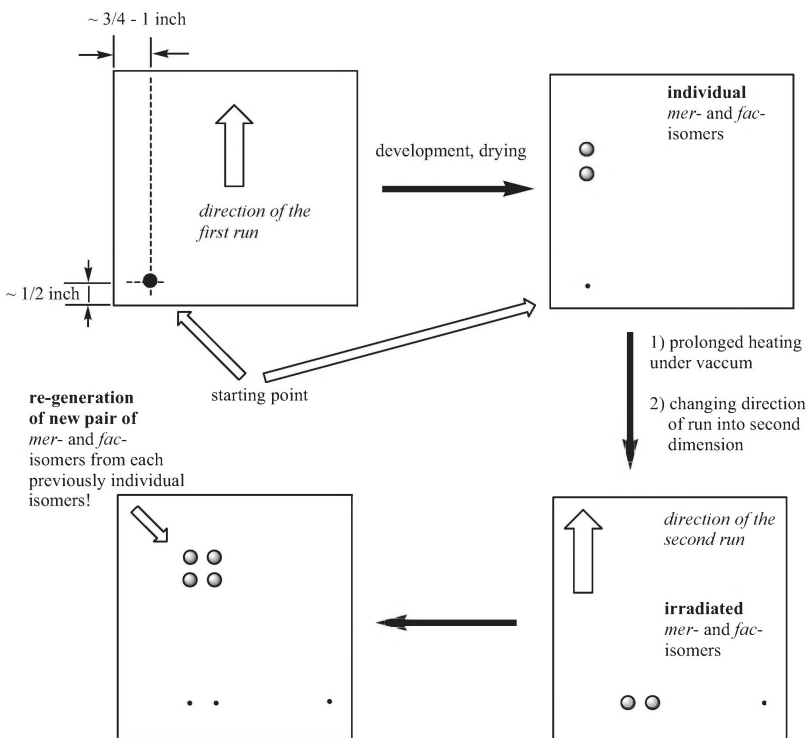
Figure 154.   Method of 2D-chromatography used during re-isomerization reactions' studies.

Chemicals: Solvents such as dichloromethane CH_2Cl_2, acetone and toluene will be used.

Equipment and Materials:

> Large glass prep-TLC development chamber with the glass lid;
> Thick paper inserts for the vapors saturation in the chamber;
> Two (for each Co^{3+} complex) 20×20 cm silicagel coated Al-backed;
> Vacuum oven (Figure 155);
> TLC plates;
> TLC glass capillaries;
> Test tube for making solutions of individual isomers.

One properly developed plate will be sufficient for the whole group of students in this class. Thus, two plates have to be prepared. This is done by:

1) adding the mixture of isomers to the left lower corner of the TLC plate, and drying spots with an air gun;
2) developing the plate for the first time, in one direction, where both *mer-* and *fac-*isomers will be separated;
3) removing the plate from the chamber and drying it with the air gun;
4) placing the plate into the vacuum oven (Figure 155), setting the temperature to 120-150ºC, pumping the oven to the highest available vacuum, and leaving it for at least 24 hours;
5) turning the heat off and letting the oven's temperature drop down to ambient conditions;
6) allowing dry air to come into the oven via a drying tower filled with blue-colored silicagel (Chapter 1, Figures 21B and 35A), to normal atmospheric pressure;
7) removing the cooled prep TLC plate from the oven;
8) rotating the plate counter-clockwise 90º and immersing it into the chamber again for development in the second direction;
9) after development, removing it from the chamber, air drying it under the hood, and observing clear manifestation of the 'magic square; [**3**]; re-isomerization takes place for pure isomers of both complexes – Co(2NO-1OH)$_3$ (Figure 156), and Co(1NO-2OH)$_3$ (Figure 157).

Record all your observations, take necessary photographs for the report, and make sketches to describe the processes of re-isomerization and 2D TLC.
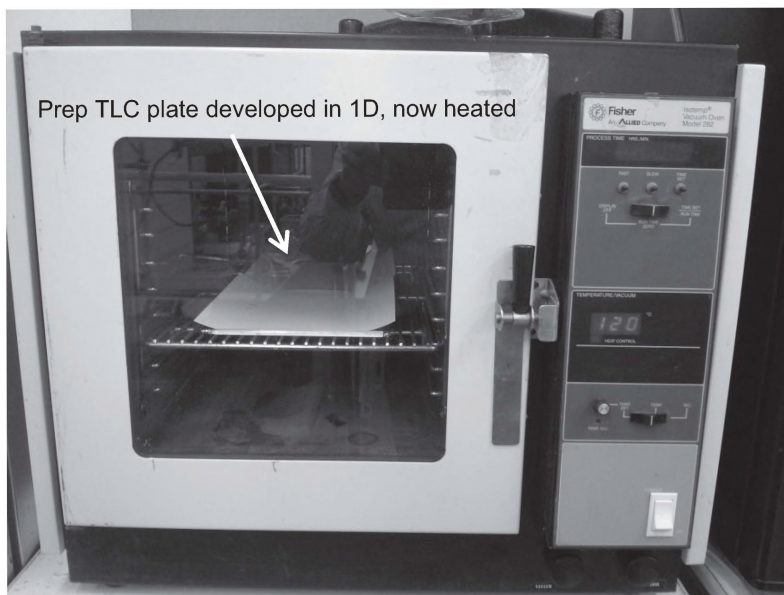
Figure 155. Vacuum oven with the TLC plate with separated isomers.

Potential hazards:
Organic solvents: dichloromethane and toluene are toxic. Work with them under the hood, and wear gloves.

Cited References

1. Miessler, G.L., Tarr, D.A. *Inorganic Chemistry*. 4th Ed, Prentice Hall, 2011.
2. Jordan, R.B. *Reaction Mechanisms of Inorganic and Organometallic Systems*. 2nd Ed, Oxford University Press, 1998.
3. Tyukhtenko, S.I.; Kofanov, V.I.; Vrubel, T.L. *J. Liq. Chrom.*, 1988, 11 (*5*), 3103-3133.
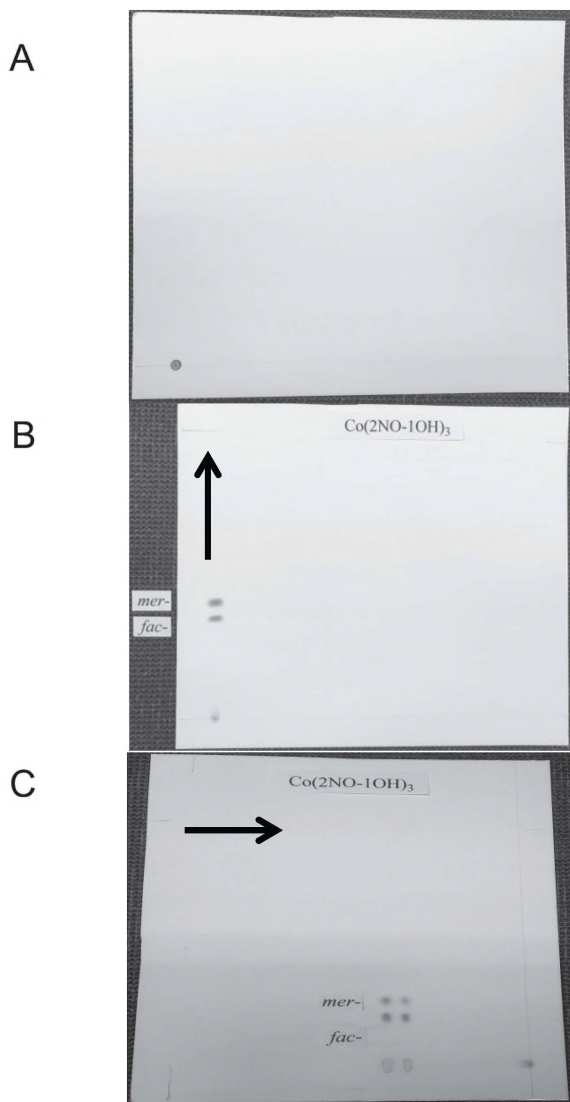
Figure 156. Detailed description of the thermal re-isomerization of Co(2NO-1OH)$_3$ explaining the appearance of the 'magic square' on the TLC plate. **A** - an initial spot with the mixture of isomers; **B** - separation of geometrical isomers in the *first* dimension shown by an arrow; **C** - re-appearance of complementary isomers in the *second* dimension, after thermal treatment in vacuum. See centerfold for this image in colour.
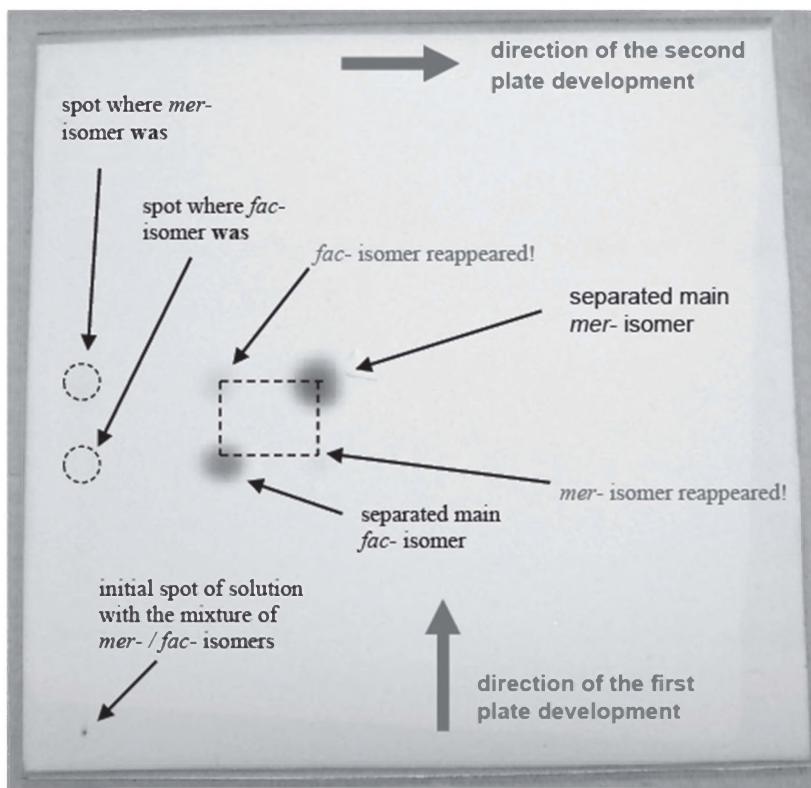
Figure 157. Thermal re-isomerization of pure, separated *mer-* and *fac*-isomers of Co(1NO-2OH)₃ leading to the appearance of the 'magic square' on the TLC plate. See centerfold for this image in colour.

3.8. Conventional Spectroscopic Characterization of Isomeric Co(III) *tris*-nitrosonaphtholates

3.8.1. Theoretical Background: Spectroscopic methods in coordination chemistry

Synthetic inorganic and coordination chemistry leads to the preparation of numerous compounds, followed by subsequent characterization which outlines areas of their potential use and practical application. These characterization techniques are summarized in Figure 158. Spectroscopic methods are the most commonly used in these investigations.

Physical methods of investigation of chemical compounds

other methods:

1) X-ray and neutron diffraction

2) magnetochemistry

3) refractometry

4) calorimetry

5) thermal analysis: TG/TGA

6) electrochemical methods (potentiometry, conductivity, CV, DPV, *etc.*)

spectroscopic:

1) vibrational (IR, Raman)

2) electronic (UV-visible, fluorescence, circular dichroism (CD) and MCD)

3) electron paramagnetic resonance (EPR)

4) nuclear magnetic resonance (NMR)

5) nuclear gamma resonance (NGR, or Mössbauer spectroscopy)

6) nuclear quadrupolar resonance (NQR)

Figure 158. Classification of modern physical methods used for identification and characterization of chemical compounds.

Spectroscopy: a set of fundamental things to consider:

1) There are typically two or more levels of energy in the system with a transition arising between them. The lower energy level is called the *ground state*, while the other, normally upper level, is called an *excited state* (Figure 159).

2) These two energy levels are *almost* equally populated, and the absorption of energy leads to the liquidation of that population difference.

3) The resonance condition is at $\Delta E = h\nu$ when an absorption of energy takes place.

4) *Spectrum* represents a plot between the energy and intensity of such transition.

5) Spectrum consists of one, or several, signals (such as bands and lines) which are graphed in transmittance, reflectance, or absorbance profile.

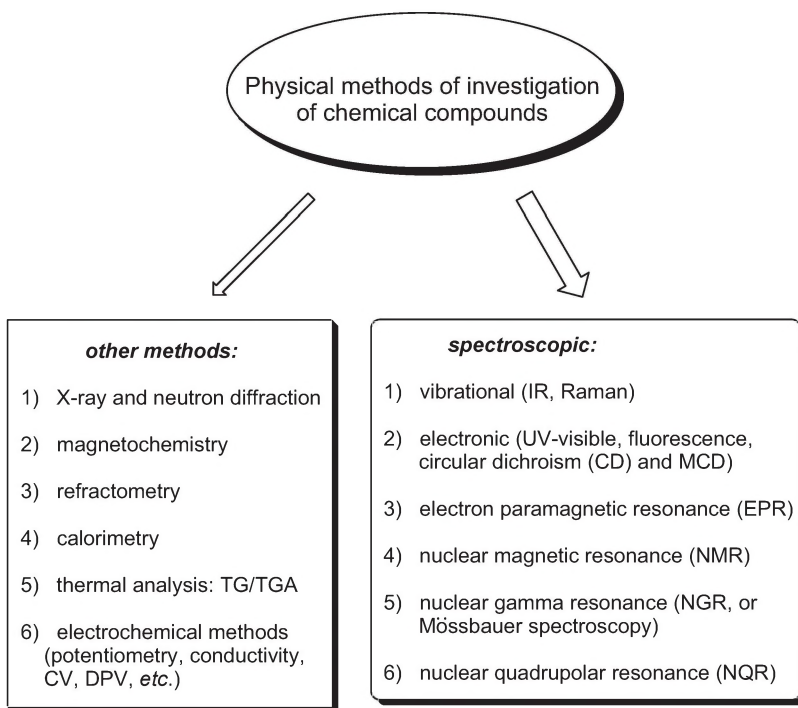6) Every excited state has its own relaxation time. A reduction of energy from the excited state to the ground state is relaxation. It may happen by: a) non-radiative path, via dipole-dipole interactions between oscillating dipoles, or molecular/atomic collisions; or b) radiative path with the emission of quantum of energy (Figure 159).

7) A spectral line/signal has a certain width which is associated with the lifetime of the excited state, according to the Heisenberg equation: $\tau\Delta E \leq h/2\pi$. The broader the line, the shorter the relaxation time, and vice versa; the longer the relaxation time, the narrower the signal.

8) The selection rule defines allowed transitions observed in spectra; $\Delta\nu = \pm 1$.

Some important fundamental physical parameters of different spectroscopic methods which will be presented in this book, are shown in Table 8. This will give the reader a good view of the energies involved and excited state relaxation times which are essential for the observation of signals and their interpretation. There are higher energy *photonic methods* (vibrational, electronic spectroscopy), and much lower energy *radio spectroscopic methods* (EPR, NMR), which use radio waves.

Table 8. Comparative characteristics of the most common spectroscopic methods.

Spectroscopic Technique	Typical energy (J / mol)	Wavelength (m)	Time scale (s^{-1})
UV-visible	$(1-6)\cdot10^5$	$(2-9)\cdot10^{-7} \sim 10^{-14}$	
Infrared, Raman	$(2-60)\cdot10^3$	$(2-50)\cdot10^{-6}$	$\sim10^{-13}$
EPR	$4-15$	$(9-30)\cdot10^{-3}$	$10^{-4} - 10^{-8}$
NMR	$(2-20)\cdot10^{-2}$	$0.6-5$	$10^{-1} - 10^{-6}$
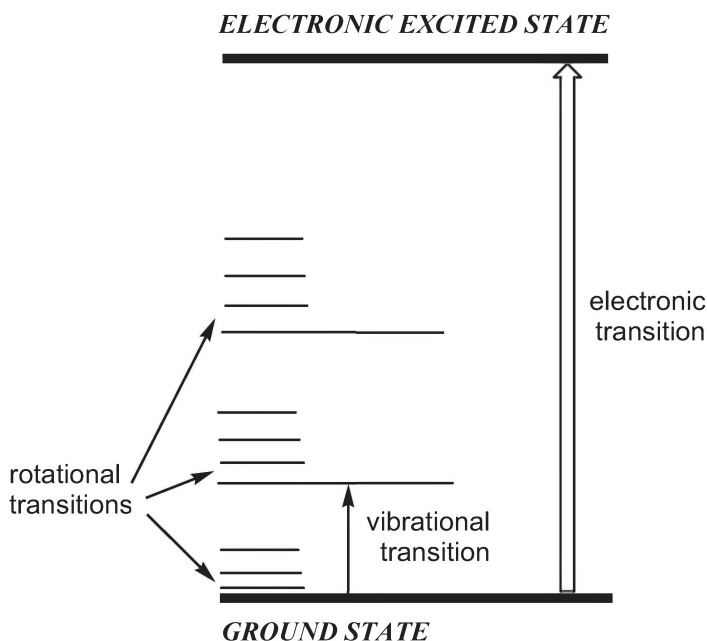
Figure 159. Schematic representation of transitions between the ground and excited state which are typically observed in spectroscopy; shown vibrational and rotational energy levels.

In all spectroscopic methods, despite their big differences, there are common features present in all instruments (called spectrometers) which record respective spectra; IR, Raman, UV-visible, NMR or EPR (Figure 160). Spectra are normally presented as *absorbance* or *transmittance* traces (Figure 161). The first way is typical for the UV-visible,

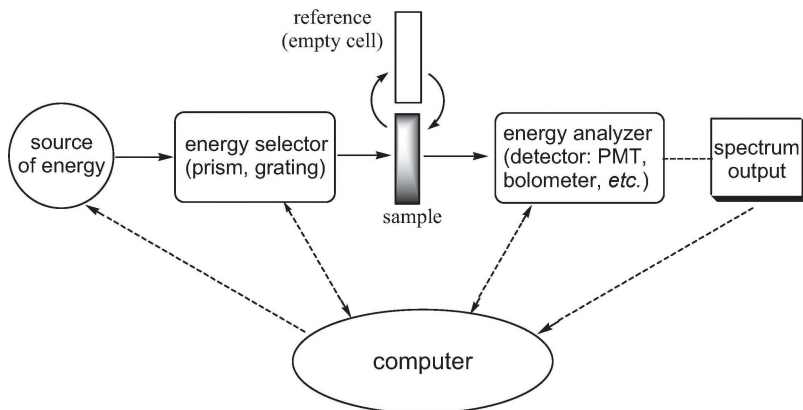fluorescence, Raman, and NMR spectra, while the second way is used in the IR-spectra.

Figure 160. Block diagram of a typical one-beam spectrometer. The reference (or background) is recorded prior to the sample measurements with its following subtraction.
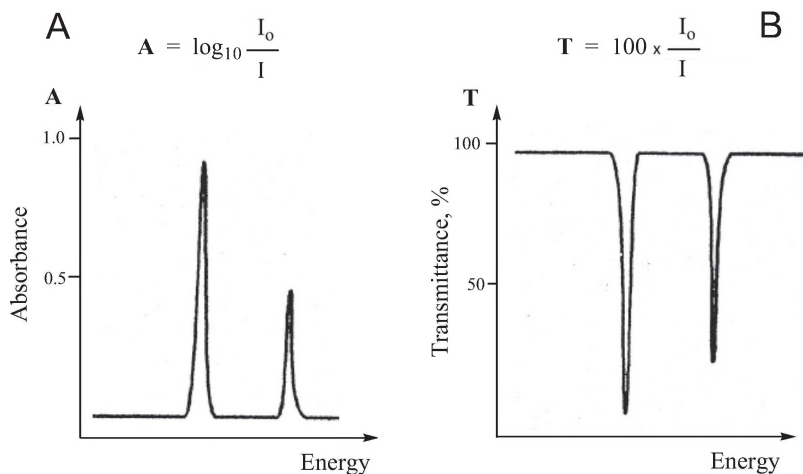

Figure 161. Two types of recording of spectrum: absorbance (**A**), and transmittance (**B**) modes.

In this laboratory manual we have selected the most important and common spectroscopic methods that are currently employed in inorganic and coordination chemistry: multinuclear NMR spectroscopy; vibrational (IR) spectroscopy; and electronic (UV-visible) spectroscopy. Below, you may find brief introductory background information regarding the basic principles of each of these techniques. For much deeper understanding of these methods, some references for further reading and comprehension, which we believe are necessary, are provided at the end of each subchapter.

3.8.2. Theoretical Background: Introduction to Vibrational Spectroscopy

Vibrational spectroscopy represents the most used technique in inorganic chemistry. It consists of infrared spectroscopy (IR), and spectroscopy of the inelastic light scattering (Raman spectroscopy). Both methods are quite different in essence, but are nicely complementary to each other [2]. In this book, only IR-spectroscopy will be used for characterization of the obtained compounds. This method uses the principle of the absorbance of energy (delivered by photons in the infrared region of the electromagnetic spectrum) by chemical sample, in all three physical states: gaseous, liquid and solid. The chemical sample possesses molecules, atoms, or ions, which naturally experience thermal oscillations. A good approximation of vibrations that describe such motion independently from the origin of chemical bond in a particular compound i.e. ionic, covalent, donor/acceptor, would be the use of the *spring model,* as shown in Figure 162. Two (or more) atoms are oscillating around some equilibrium positions, but during the resonance condition upon interaction with photon, there is a change in amplitude of vibration. In turn, a frequency of such vibration is expressed by the formula:

$$\nu = \frac{1}{2\pi} \sqrt{\frac{k}{\left(\frac{m_1 \times m_2}{m_1 + m_2}\right)}} \quad \text{where} \quad \left(\frac{m_1 \times m_2}{m_1 + m_2}\right) = \mu \quad \Longrightarrow \quad \nu = \frac{1}{2\pi} \sqrt{\frac{k}{\mu}}$$

This frequency is highly dependent on the mass of involved atoms and the 'hardness of the spring' which is the force constant k, characterizing an electron density between atoms. The μ value stands for the reduced mass. The force constant k is expressed in Newton over meter (N/m), where $1N = 1(kg \cdot m)/s^2$. In chemistry, values of k are normally in

the range of $\sim 10^{-5}$N/cm, and often for simplicity, expressed as mdyn/Å. Useful conversion of units of the frequency (wavenumber) and energy in the IR spectroscopy is as follows: $1 cm^{-1}$ = 11.96J/mol = $2.99 \cdot 10^{4}$Hz. Modern units of energy (*x*-scale) used in vibrational spectroscopy are wavenumbers – cm^{-1}, albeit, in some older texts and publications, microns (10^{-6}m) were used for the same purpose. The signal in the IR-spectroscopy is recorded as sample's transmittance. The vertical axis – transmittance of the sample – is expressed in percent (%), that could also be seen in some sources as a fractional value between 1 and 0.

$$E_p = 1/2 \; k \; (\; d_1 + d_2 \;)^2$$
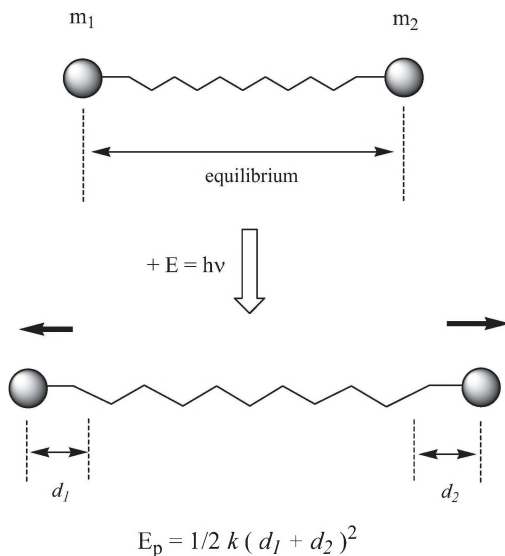
Figure 162. Schematic representation of the process of oscillation between two atoms (in chemical bond, for instance) and its relation to potential energy of the system and frequency of resonance photon.

The most useful for inorganic chemistry are oscillations (vibrations) between atoms in the sample. In compounds with molecular structures these vibrations can be: 1) along chemical bonds, leading to the change in their length (stretching), notated as Greek symbol ν; 2) between chemical bonds (deformational), leading to the change in bonding angle, and commonly notated as δ. Deformational vibrations also include a series of other vibrations such as: ρ – rocking, ω – wagging, $\delta(sz)$ – scissoring and $\delta(t)$ – twisting. The first group of stretching vibrations consists of higher in energy *asymmetric*, $^{as}\nu$, and *symmetric*, $^{s}\nu$. Some solid ionic

binary, tertiary, and quaternary compounds, which form crystal lattices, typically do not have that variety of vibrational modes, and the method described here is less informative. It is important to note that *only vibrations that lead to the dipole moment change are active in IR-spectroscopy*.

There are three overlapping regions suitable for investigation with the help of the IR-spectroscopy:

I) Near infrared (NIR) – from 10,000 to 3,333cm^{-1}, where combination vibrations can be detected as well as solvation and solvents' effects in a liquid phase;

II) Mid infrared – from 4,000 to 670cm^{-1}; this is the region most frequently used by chemists. Inside that range, there is a '*fingerprints region*', between 1800 and 800cm^{-1}, which is very sensitive to the nature of the compound, and is used for identification of many hundreds of thousands of compounds.

III) Far-infrared – from 800 to 200cm^{-1}, where low-energy deformational, as well as stretching metal-ligand, vibrations are normally observed.

Certainly, there are corresponding optical materials needed for recording spectra in these three regions. The IR-spectra in solutions are recorded in special cuvettes with salt (LiF, NaCl, KBr, AgCl, BaF$_2$, CaF$_2$, etc.), or ceramic oxides (KRS-5), chalcogenides (ZnS) windows with either constant, or adjustable path-length [1,2]. Clearly, windows material should not be soluble in those solutions! Cuvettes for recording the IR-spectra in a gas phase have a large, but constant, path-length of 5cm to 10cm, to increase the sensitivity. Further details of experimental setup, materials, optics, and standards for calibration, are out of the scope of this laboratory manual, but can be retrieved from readily available literature [3].

There are two, principally different, methods for recording the IR-spectra of samples in a solid state: a) in an inert salt matrix, and b) neat compound. The first one is a traditional method of making pellets of KBr or CsI with mechanically admixed sample of interest at 1-5 weight % concentration. Thus, after weighing ~200mg of halogenide salts and mixing it with 3-5mg of the sample, using grinding with the mortar and pestle (Figure 166 below), the mixture is placed in a special die-anvil kit and is pressed with a hydraulic press to 7 – 9 tons' pressure value. At this pressure the mixture liquefies, which helps to homogenize the sample in the salt matrix and eliminates the sample's texture; anisotropy. The resulting *homogeneous* pellet (or disk) is placed in the holder and the IR-

spectrum is recorded with the help of the FT-IR spectrophotometer. Common parameters are that resolution is set to 4cm^{-1}, with 32 to 128 repetitions, depending on the sample's concentration and the nature of compound. The chamber where the samples are placed for recording is continuously purged with dry air (very inexpensive) or dry nitrogen. A background spectrum is necessary to record measurements of the sample in advance. Then, the recorded spectrum of the sample needs to be corrected, because the background spectrum always contains traces of moisture and CO_2 from the air. The KBr has a window of transparence for the IR-radiation from 10,000 to 400 cm^{-1}, while CsI from 10,000 to 150cm^{-1}. The overall quality of a spectrum recorded using the 'inert salt matrix' method is very high, albeit that spending 25-35 minutes per sample is required.

Recently, other methods of recording the IR-spectra were introduced in laboratory practice: multiple internal reflectance (MIR), and attenuated total reflectance (ATR) methods (Figure 163). Neither of these methods use an inert salt KBr, or CsI matrices, but instead use a few crystals/crumbs of the neat compound of interest. Neat liquids, or solutions literally require just one drop for recording the IR-spectrum. The method is quick, and is an excellent choice for in-line control in chemical manufacturing and quality control procedures. The ATR method has also gained considerable popularity in academic and research institutions, due to rather dramatic time savings. However, fast data gathering is often not commensurate with its quality; in many cases spectra suffer poor resolution.

During the last 50 years, a very large number of the IR-spectra of different classes of chemical compounds were recorded, tabulated, and analyzed. Many commercial vendors of IR-spectrometers also provide access to databases that contain systematized and categorized information about hundreds of thousands of compounds. This offers the option of computerized matching of spectra of unknown or analyzed substances against those pre-recorded and stored in databases. Access to this option for such analysis could be prohibitively expensive for many users.

When numerous IR-spectra were recorded and analyzed, it turned out that all functional groups in organic compounds show bands in relatively narrow regions. Thus, a concept of *groups' frequencies* was intensively developed. Therefore, the option of human-based comparative analysis of recorded spectra became an alternative route for interpretation of the IR-spectra of chemical compounds, and provided a reasonably good assignment of the observed spectral bands. More detailed description and presentation of these tables is beyond the scope of this laboratory manual.

However, we can recommend an extensive set of tables created to help with bands' assignment: the most comprehensive up-to-date reference materials were compiled by Lambert, Shurvell, Lightner and Cooks [4].
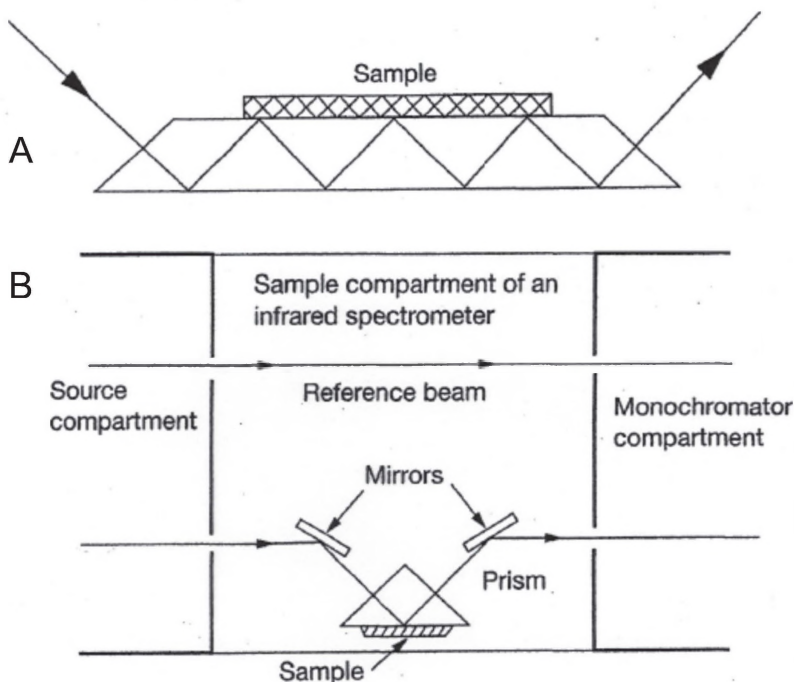
Figure 163. Schematic diagrams of principles of the MIR spectrometry (**A**), and ATR method (**B**).

During the interpretation of vibrational spectra of inorganic and coordination compounds, chemists look for two features:

1) Change in bands' position in the compound of interest compared with spectra of the initial compound. That is, for example, a comparison of the spectrum of the ligand with that for the complex.
2) Change in bands integrity – which is splitting and their intensity.

A very good description of principles with the vast number of cases of chemical samples directly related to inorganic, and more so to coordination chemistry, can be found in classic work by Nakamoto [5].

Prepared in this laboratory manual are two coordination compounds of kinetically inert Co(III) and Cr(III) which contain organic ligands that exhibit rich vibrational spectra. Therefore, the IR-spectroscopy method is of great utility for both samples, and assignment of bands in spectra represents a very good practical training for students and interested chemistry professionals.

Cited Literature

1. A. Gordon, R. Ford. *Chemist's Companion: A Handbook of Practical Data, Techniques and References*. Wiley Interscience Publication; New-York – London – Toronto – Sydney, 1972.
2. H. Lux. *Anorganisch-chemische Experimentierkunst*. 2nd Ed. by J. A. Barth (Verlag), Leipzig, 679 pp., 358 figs. 1959.
3. a) https://wp.optics.arizona.edu/optomech/wp-content/uploads/sites/53/2016/10/Saayman-521-Tutorial.pdf; b) https://www.edmundoptics.com/resources/application-notes/optics/the-correct-material-for-infrared-applications/
4. Lambert, J. B.; Shurvell, H. F.; Lightner, D. A.; Cooks, R.G. *Organic Structural Spectroscopy*. 319 pp., Pearson, 2011. ISBN-13: 978-0321592569.
5. a) Nakamoto, K. *Infrared and Raman Spectra of Inorganic and Coordination Compounds: Part A: Theory and Applications in Inorganic Chemistry*. 421 pp., John Wiley & Sons, Inc. 2009, ISBN: 9780471743392; b) Nakamoto, K. *Infrared and Raman Spectra of Inorganic and Coordination Compounds, Part B: Applications in Coordination, Organometallic, and Bioinorganic Chemistry*. 400 pp., John Wiley & Sons; ISBN 0470405872.

3.8.3. Theoretical Background: Basics of Electronic Spectroscopy

Electrons in an atom, molecule, or ions, can gain extra energy upon interaction with photons. When energy is absorbed in the ground state, at specific resonance conditions for each electron of $\Delta E = h\nu$, the electron moves into excited state. Most of the time this would be the first excited state having quite a short lifetime (Table 8). Upon relaxation, the electron returns to the original energy level. The most common types of electronic transitions are summarized in Figure 164. Thus, the highest in energy are $\sigma \rightarrow \sigma^*$ transitions, which occur at very high energies in the so-called 'vacuum UV-region', beyond 190nm, followed by $\pi \rightarrow \sigma^*$ and $\pi \rightarrow \pi^*$ transitions in the range of 200 – 350nm [1]. All those have high intensity. The latter is expressed as molar absorptivity coefficient ε, which is calculated from the formula $\mathbf{A = \varepsilon \cdot M \cdot l}$ (M = molarity of solution; l = light path-length, typically 1 for 1cm cuvette, or 0.1 for 1mm cuvette).

The visible range of the electromagnetic spectrum between 350 and 800nm contains two types of relatively low intensity transitions important for inorganic chemistry: $n \rightarrow \pi^*$ and $d \rightarrow d$ for metal ions of 3d – 5d series that contain unpaired electrons [2]. The former transitions typically occur in numerous organic ligands that provide donor atoms with lone pairs for binding metal ions. Those are commonly nitrogen atoms in Schiff-bases, heterocyclic amines, oximes, N-oxides, etc. Their intensities are normally found in the ε value of 10 – 100 range [1, 3-5].

As far as d→d transitions are concerned, energies of electrons involved in such transitions can be ranked as shown in Figure 164.

These d→d transitions can further be spin allowed/forbidden and the same allowed/forbidden for Laporte rules, which leads to a significant variety in the intensity of bands in electronic spectra (Table 9). Therefore, results of UV-visible spectroscopy are reported and presented in the literature, for example, as the band with λ=680 nm (170), where the value in parentheses represents the molar extinction coefficient ε.

Knowing the number and the range of d→d transitions and their intensities (ε) allows assignment of bands in electronic spectra of transition metal complexes. More thorough and detailed information about UV-visible spectra of transition metal complexes, especially those for 3d-metals series, can be found in classic books by R. Drago [2] and B. Lever [6]. More broadly, specifics of recording of spectra, cuvettes materials, detectors, standards for calibration, and other experimental details, can be found in a classic book by Calver and Pitts [7], and via common lab suppliers [8].
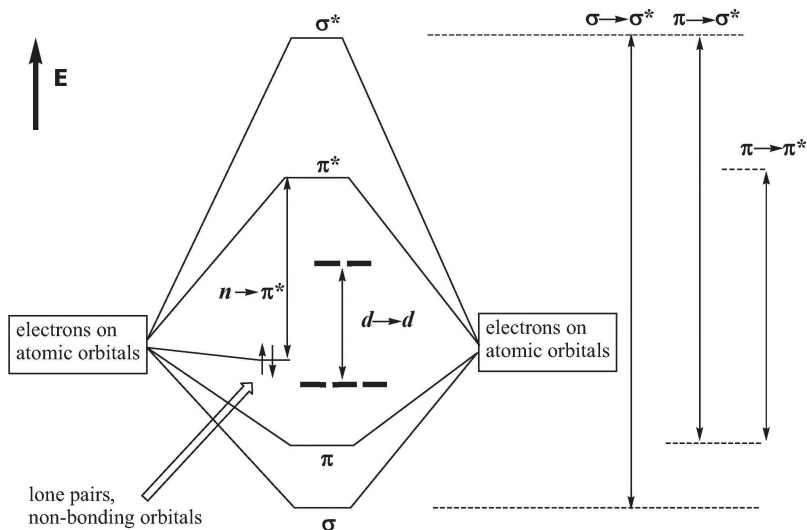
Figure 164. Schematic representation of main types of electronic transitions in chemical compounds (including complexes and organometallic compounds) showing their relative energies.

It is important to note that the presence of d-d transitions is often masked by far more intense CT (charge transfer bands), which can be of 'metal-to-ligand-charge-transfer' (MLCT) and its opposite back-bonding transitions LMCT, as well as MMLCT by origin [9]. Therefore, special care must be taken in the determination of the molar extinction coefficient ε for the band(s) in electronic spectrum, prior to its/their tentative assignment.
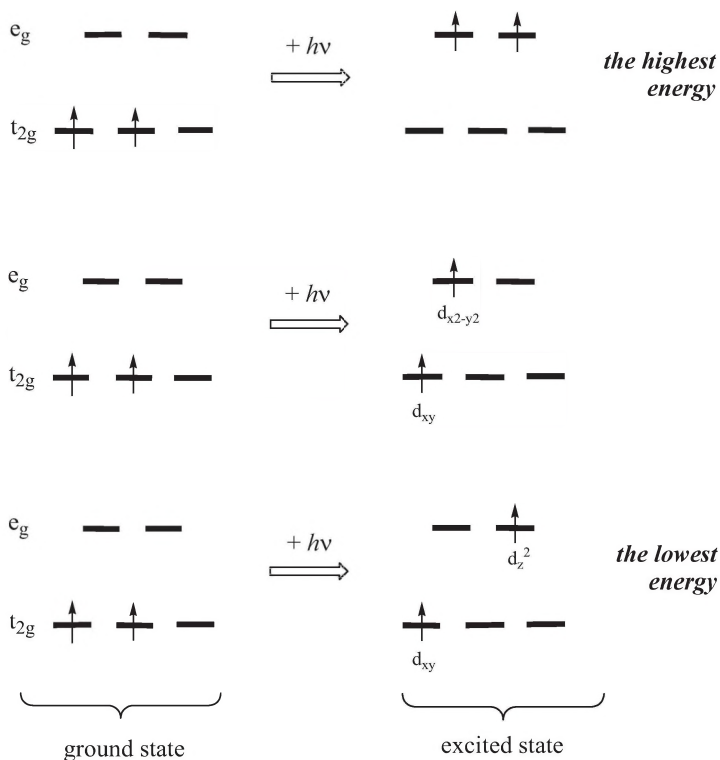
Figure 165. Possible *d-d* electronic transitions between two levels of energy: shown is an example for d^2 system.

Two intensely-colored coordination compounds of Co(III) and Cr(III) were selected for preparation and studies in this laboratory manual. These are described in Chapters 2–4, and we will examine their electronic spectra. Students will learn how to measure molar extinction coefficients for observed bands quantitatively, and make assignments for observed transitions. It is necessary to note that all measurements should be carried out for solutions with such concentration of complexes that the maximum absorbance in regions of interest (200 – 350 for the UV-part, and 350 – 800 or more for the visible part) will not exceed A=1.5. It should be remembered that the absorbance scale is a ten-based logarithm, and the amount of light coming to the detector through the sample is ~150 times less at A=1.5 than at A=0.05.

Table 9. Electronic transitions typically observed in UV-visible spectra of inorganic species.

Transition	value of ε	Chemical example
Spin allowed and Laporte allowed (CT = charge transfer)	$\sim 10^4$	$[CrO_4]^{2-}$, $[MnO_4]^-$
Spin allowed and Laporte forbidden (no center of symmetry)	$2 - 6 \cdot 10^2$	$[CoCl_4]^{2-}$, $[NiI_4]^{2-}$
Spin allowed and Laporte forbidden (present center of symmetry)	$\sim 10^1$	$[Co(H_2O)_6]^{2+}$ $[Fe(H_2O)_6]^{2+}$ $[Cr(H_2O)_6]^{3+}$
Spin forbidden and Laporte forbidden	~ 1	$[Mn(H_2O)_6]^{2+}$ $[Fe(H_2O)_6]^{3+}$

Moreover, a proper choice of solvent for measurements is absolutely essential, since it can obscure important regions of interest for a chemist. Thus, the best solvents for electronic spectroscopy would be those that do not contain chromophores – compounds with double and triple bonds. These tend to absorb photons in the UV-region of the spectrum. Therefore, solvents such as ROH (R = H in water, CH_3, C_2H_5, C_3H_7), ethers (tetrahydrofurane THF, $(C_2H_5)_2O$, $(C_3H_7)_2O$), saturated hydrocarbons (including cyclohexane), and chlorinated hydrocarbons (CCl_4, $CHCl_3$ and CH_2Cl_2) are the most suitable for recording spectra in the range of 200-1100nm. At the same time, most common solvents, such as acetone $(CH_3)_2CO$, acetonitrile CH_3CN, DMF $HC(O)N(CH_3)_2$ and DMSO $(CH_3)_2SO$ are blocking the UV-region of the spectrum completely, and must be avoided. The same is true for liquid olefins, aromatic hydrocarbons and heterocyclic compounds, despite their good ability to dissolve numerous inorganic and coordination compounds.

Cited Literature

1. Lambert, J. B.; Shurvell, H. F.; Lightner, D. A.; Cooks, R.G. *Organic Structural Spectroscopy*. 319 pp., Pearson, 2011. ISBN-13: 978-0321592569.
2. Drago, R. *Physical Methods for Chemists*. 2nd Ed., Scientific

Publishers, ISBN-13: 978-0030751769, 1977.

3.   Feuer, H. (Ed.) *The chemistry of the nitro and nitroso groups, Volumes 1-2*, Interscience Publishers, 1970, 447 pages.

4.   Jolly, W. *The synthesis and characterization of inorganic compounds*. 590 p. Englewood Cliffs, N.J. : Prentice-Hall, 1970.

5.   a) Gerasimchuk,N.; Esaulenko, A.N.; Dalley, K.N.; Moore, C. *Dalton Trans*., 2010, *39*, 749–764; b) Robertson,D.; Cannon, J.F.; Gerasimchuk, N. *Inorg. Chem*. 2005, *44* (23), 8326-8342.

6.   Solomon, E.I.; Lever, A.B.P. *Inorganic Electronic Structure and Spectroscopy, Applications and Case Studies*. Wiley, 1999, Science, 672pp.

7.   Calvert, J.G.; Pitts, J.N. Jr. *Photochemistry*. John Wiley and Sons, Inc., New York, 1966.

8.   a) http://www.internationalcrystal.net/icl101.htm;
     b) http://www.perkinelmer.com/category/cuvettes;
     c) http://www.starnacells.com/d_ref/stds.html

9.   K. Li, G. So Mi Tong, Q. Wan, G. Cheng, W.-Y. Tong, W.-H. Ang, W.-L. Kwong and C.-M. Che, *Chem. Sci*., 2016, *7*, 1653.

3.9. Experiment 8: Recording of the IR- and UV-visible Spectra of the Starting Isomeric Nitrosonaphthols and their Co(III) Complexes

In previous laboratory exercises **5** and **6,** we have obtained isomeric *tris*-Co(III) nitrosonaphtholates, and performed separation of their geometrical isomers. Also, in experiment **7,** we investigated thermal re-isomerization of *mer*- and *fac*- isomers upon their heating under vacuum at 120-150ºC. We observed a much greater thermal stability of the $Co(1NO-2OH)_3$ complexes, as compared to their isomeric $Co(2NO-1OH)_3$.

Now it is time to continue their characterization using methods other than the NMR spectroscopic. Next in importance and significance are methods of IR-spectroscopy and electronic spectroscopy.

Chemicals: Solid KBr (the IR-spectroscopy grade!) and dichloromethane, CH_2Cl_2, will be used.

Equipment and Materials:
        FT-IR spectrophotometer;
        A die and anvil set, for pressing salt pellets;
        Hydraulic (or any other pressing device) press for making disks (pellets) in KBr;
        Any UV-visible spectrophotometer working in the 200 – 850nm region;
        A set of quartz cuvettes for recording spectra in solutions.

Learning objectives of this laboratory experiment and expected accomplishments:
        How to use available FT IR and UV-visible spectrophotometers;
        How to make good quality KBr pellets with compounds of interest;
        Analysis and interpretation of recorded spectra.

Part A. IR-spectroscopy

During this work we will be using a standard set of hardware which is normally used for recording vibrational spectra of solid compounds in salt matrices. These are typically KBr and CsI, with the latter allowing the recording of spectra in the far-IR region down to 150cm^{-1} [1]. The usual set consists of items such as: polished agate mortar/pestle; a hardened steel 13mm die/anvil combo (two polished plates between which a sample is

placed, and plunger); spatula; and the IR-grade KBr; all shown in Figure 166.
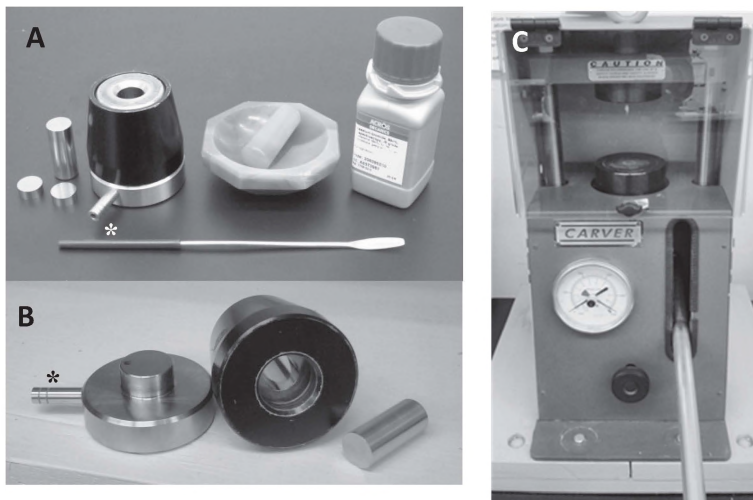
Figure 166. Necessary hardware for pressing KBr disks (pellets) (**A)**, opened anvil set with the plunger (**B**), and nine tons hydraulic press (**C**). * Vacuum port.

Step 1.
Using an agate mortar and pestle, 100mg of IR grade potassium bromide, and ~2-5mg of the initial ligand (the first one used in the lab **5A**: 1-nitroso-2-naphthol), make a mixture for the IR pellet.
Step 2.
Press the pellet in a dry KBr matrix using the press and anvil/die set, according to the instructions provided. The pressing pressure, however, should not exceed 6 tons, on grounds of hardware longevity. A good pellet should be transparent (clear).

In order to avoid trapping air in the sample matrix (a mixture of grounded KBr + sample), use one of two methods:
-   Provide a suction (make a vacuum) using a portable membrane pump placed next to the hydraulic press and connected to the anvil/die set via hose [barbed hose outlets are indicated by asterisks on Figure 166].
-   Press slowly and release pressure 2-3 times before reaching ~6 tons value.

Disassemble the die/anvil set, promptly remove the pellet, and place it into the instrument's pellet holder (for standard 13mm pellets), and insert the holder into the instrument compartment.

Step 3.
Record the solid-state IR spectra of the starting ligand and Co(III) complexes, separated in the previous laboratory exercise. Use 32 repetitions (scans) in the range $400 - 4000 cm^{-1}$ at $4 cm^{-1}$ resolution, subtracting the background with the same number of repetitions (scans).

Step 4.
Print your data as a three-page printout. The first page is for a general (panoramic) view of the whole spectrum, while page two will be only for the 'fingerprint' region $400 - 1800 cm^{-1}$, and page three will be for the region of $2000 - 4000 cm^{-1}$. Page two should contain peak values to be analyzed and interpreted.

Step 5.
Make combination plots of the ligand and one of the complexes, to see: a) bands' positions shifts from the ligand to the complex; and b) appearance of new bands. An example of overlaid spectra of the ligand and one separated isomer is shown in Figure 167.

Pay close attention to both indicators of the effect of complex formation on the IR-signature of compounds. Intensities of bands are not of a great importance in this case, since they are directly proportional to the dipole moment change during vibrations, and that may be significantly different from a compound to compound. The best way of seeing changes in bands' position is drawing a perpendicular from the top spectrum to the lower one. Write down your observations of new bands, and those that are shifted upon complex formation.

Step 6.
Perform bands' assignment using the 'functional groups frequencies' approach [**4**], literature data for these compounds [**2,3**], and handbook tables [**1**]. Match your bands with those in the literature. Write and discuss it your lab report.
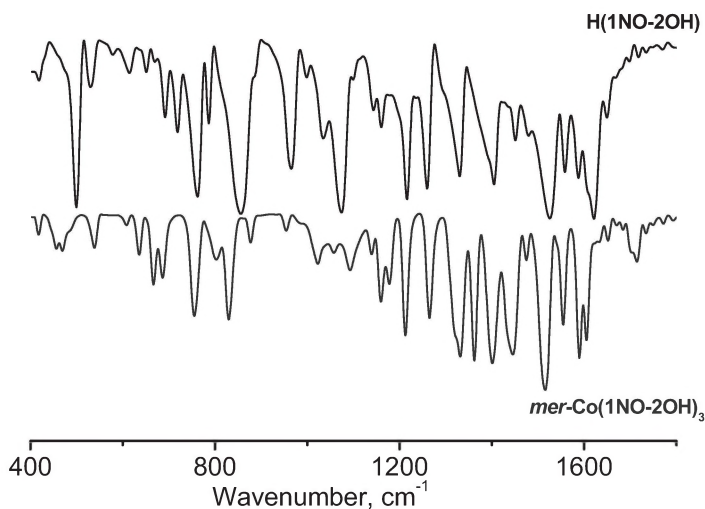
Figure 167. Overlaid IR spectra of the 'fingerprint region' of the initial ligand (top) and its Co(III) complex, *mer*-isomer (bottom).

Repeat Steps 1 – 6 for separated *mer*- and *fac*- isomers of the Co(1NO-2OH)$_3$, which are available after separation in multi-milligram quantities.
      Repeat Steps 1 – 4 for the *second ligand* used for the lab preparation **5B**, and then for the solid complexes of Co(2NO-1OH)$_3$ separated by the preparatory thin layer chromatography.

Make combination plots of the IR-spectra of both separated Co(III) complexes. An example of overlaid spectra of the *mer*- and *fac*-isomers is shown in Figure 168.
      Pay close attention to the appearance of a great similarity in the spectra of isomers, but also to the appearance of new bands. The best way of seeing changes in bands' position is drawing a perpendicular from the top spectrum to the lower one. Write down your observations of new bands and those that are shifted upon complex formation.
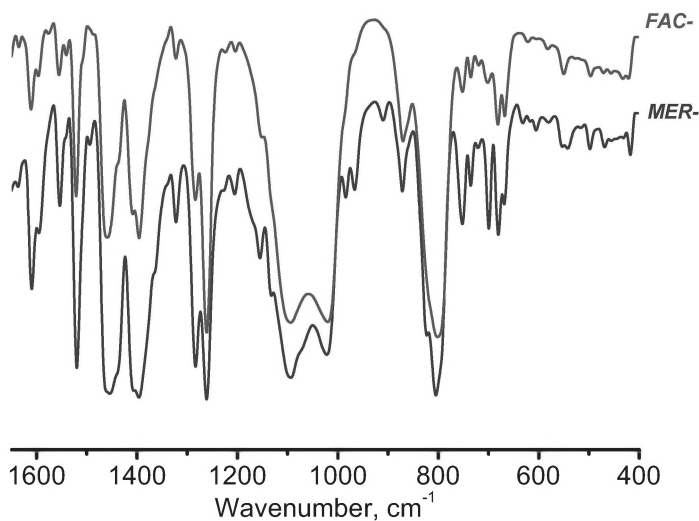
Figure 168. Overlaid spectra of two separated isomers of the $Co(2NO-1OH)_3$ complex in the 'fingerprint region'.

Deceivingly, it appears that spectra are identical, but they are not. There are several new bands, and especially different spectra in the low frequency $650 – 400 cm^{-1}$ range, where metal-ligands vibrations are. Thus, the coordination environment $[CoO_3N_3]$ in both isomers has different symmetry; C_1 for *mer*-isomer and C_3 for *fac*-isomer (Figure 37, Chapter 3). Therefore, according to the group theory, a low symmetry compound should have more bands in the region of metal-ligand vibrations, and they are clearly observed (Figure 169). Perform assignment of bands in this region of spectrum, based on literature data available to you from sources listed above.
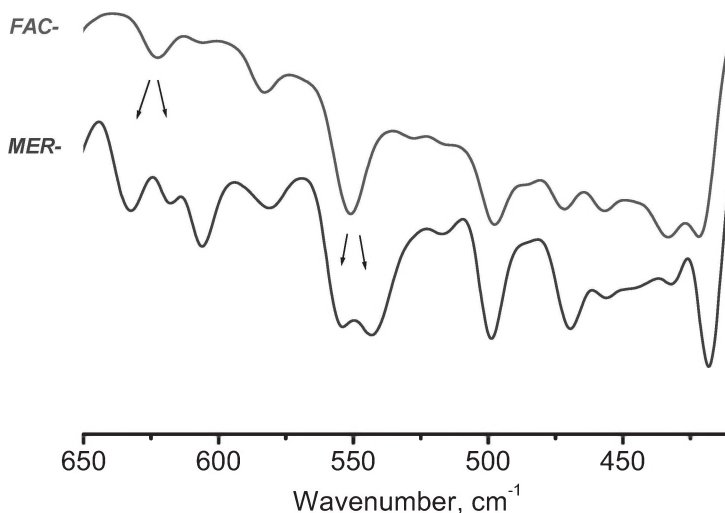
Figure 169. Overlaid spectra of two separated isomers of the $Co(2NO-1OH)_3$ complex in low frequency region of the metal-ligand vibrations.

Repeat Step 6 as above, for the isomeric Co(III) complex. Write down all your observations and discuss it your lab report.

Part B. UV-visible spectroscopy

Turn on an available UV-visible spectrophotometer and let it warm up for 10 minutes.

Step 1.
Place ~3mg of individual isomers of Co(III) 1-nitroso-2-naphtholate complex into the small test tube in the test tube rack. Add ~5mL of chloroform and dissolve the sample completely.

Step 2.
Using the pipette, transfer your solution from the tube into a 100mL volumetric flask. Accurately rinse the test tube and dilute the solution in the flask to the mark with pure solvent ($CHCl_3$). Calculate the

concentration of the obtained solution. Repeat the same procedure for the second isomer, so you will have two solutions of known concentration.
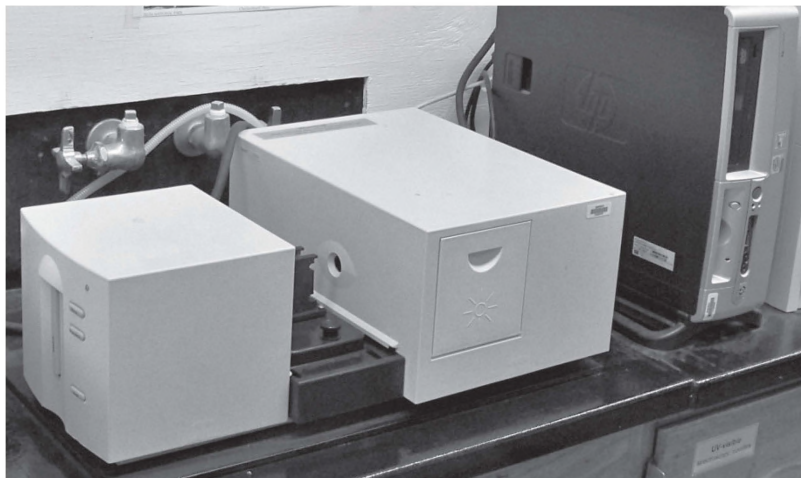
Figure 170. Robust laboratory UV-visible spectrophotometer conjugated with PC and printer [shown here is the 'working pony' – HP 8453 Diode Array instrument; any other instruments will do the same work].

Step 3.
Fill a 1cm quartz cuvette with pure solvent and record the blank UV-visible spectrum. Then empty the cuvette, wash it with your complex solution and fill it with the solution made in the previous step. It usually takes about 3.5 – 4.0mL of CHCl$_3$ solution. It might be necessary to use a cuvette with a smaller path length for the more colorful isomer (Figure 171), and a 0.1cm cell has been used in the past.

Step 4.
Record the UV-visible spectrum of the complex in the range of 200-1100nm. Print your data and table of peaks' wavelength with absorbances corresponding to them.

Figure 171. A small set of quartz cuvettes necessary for electronic spectroscopy of the majority of chemical compounds obtained in synthetic laboratories; 1mm and 10mm path-lengths cells with Teflon stoppers.

Step 5.
Calculate the extinction coefficient for the absorbance of the compound in the visible region using the formula:

$$\varepsilon = A / l \cdot M$$

Here: **A** = absorbance at the maximum of the wavelength; **l** = path length of the cuvette (1cm in our case); **M** = molarity of the prepared solution.

Each peak in the spectrum must be presented with its molar extinction coefficient such as shown below: λ = 240nm (28,300), or ε^{240} = 28,300. Plot UV-visible spectra of individual isomers on the same page, and comment on the differences which explain apparent color differences for both complexes in solid state. An example is shown in Figure 172. Provide absorption bands assignment based on available data in literature [1-4].

Repeat Steps 1–5 for *mer*- and *fac*- isomers of the second complex Co(2NO-1OH)$_3$ separated by preparative TLC.

Print your data and the table of peaks' wavelength with absorbances corresponding to them. Observe the difference in spectra of both isomers. Make overlaid plot UV-visible spectra of individual isomers and comment on their differences. Notice small differences in color for both complexes in solutions. Shoulders in spectra are also cited as '~510nm (sh)'. Typical spectra are shown in Figure 173. Provide bands' assignment to the best of your ability, using literature data in [1-4].
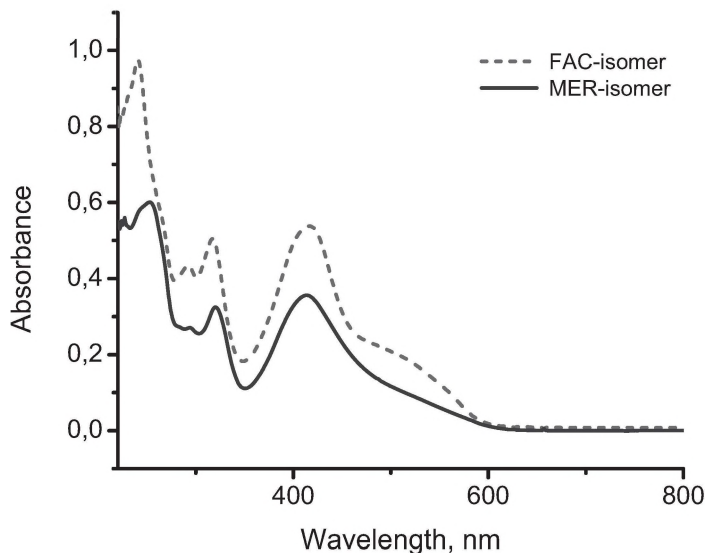
Figure 172. Overlaid spectra of solutions of separated isomers of Co(1NO-2OH)$_3$ in CHCl$_3$ in 1mm quartz cuvette.

Labeling and reporting:

Your lab report should contain your observations and sketches, recorded spectra with peaks, assignments, and conclusions. These will be: matching bands in IR to those reported in the literature; determination of λ_{max} and ε for the absorbance of the complex for all peaks; and assignment of the NMR signals in all experiments.

The number of the experiment, date, authors of the reaction, and total amount of the obtained compound with their yields, must be written on the label. The label should be attached to the screw-cup vial with the target isomeric compound, after all the above measurements have been completed.
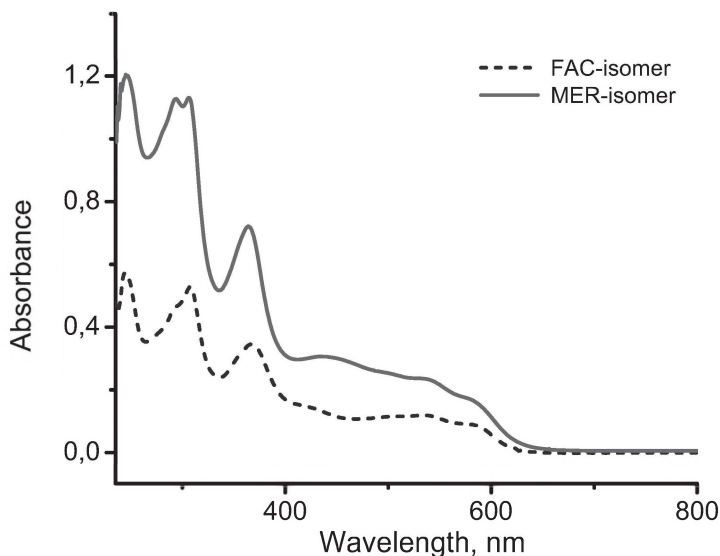
Figure 173. Overlaid spectra of solutions of separated isomers of $Co(2NO-1OH)_3$ in CH_2Cl_2 in 1cm quartz cuvette.

Potential hazards:
Chloroform, dichloromethane and other organic solvents are toxic if a substantial amount of their vapors is inhaled. Work with them under the hood, and wearing gloves is required.

Cited Literature

1. Gordon, A.; Ford, R. *Chemist's Companion: A Handbook of Practical Data, Techniques and References*. Wiley Interscience Publication; New-York – London – Toronto – Sydney, 1972.
2. Gurrieri, S.; Siracusa, G. Coordination Compounds of 1-nitroso-2-naphtol and 2-nitroso-1-naphtol. *Inorg. Chim. Acta*, **1971**, *5*(4), 650-654.
3. Charambous, J.; Maple, P.; Nassef, A.; Taylor, F.B. Complexes of Nickel(II) with 1-nitroso-2-naphtol and 2-nitroso-1-naphtol. *Inorg. Chem. Acta*, **1978**, *26*, 107-111.
4. Lambert, J. B.; Shurvell, H. F.; Lightner, D. A.; Cooks, R.G. *Organic Structural Spectroscopy*. 319 pp., Pearson, 2011. ISBN-13: 978-0321592569.

3.10. NMR Spectroscopic Studies of Isomeric Nitroso-naphthols and Their Diamagnetic Co(III) Complexes

3.10.1. Theoretical Background: Introduction to the NMR Spectroscopy. Parameters of Common One-dimensional (1D) Spectrum

Nuclear Magnetic Resonance (NMR) Spectroscopy is an analytical spectroscopic method for the determination of content, structure, and dynamics of broad range substances. From the NMR spectrum we can derive chemical shifts, relative intensities of peaks, magnetic spin coupling through bonds (scalar), and through space (NOE: Nuclear Overhauser Effect).

For a more sufficient explanation of the NMR phenomenon, it is better to consider the quantum mechanical behavior of a nucleus in a permanent magnetic field. Nuclei, as spinning charges (due to protons), generate their own magnetic field. Not all nuclei, however, possess magnetic moment. There are ^{12}C, ^{16}O, ^{40}Ca, ^{56}Fe and similar others with zero magnetic moment and spin quantum number I = 0. They are NMR inactive. Also, there are two big families of magnetically active nuclei; those that have I = ½, called *dipole nuclei* and those having spin quantum number I > ½, named quadrupolar nuclei. Representative dipole nuclei important for synthetic chemistry are ^{1}H, ^{13}C, ^{15}N, ^{19}F, ^{29}Si, ^{31}P, ^{57}Fe, ^{119}Sn, and ^{195}Pt, whilst quadrupolar nuclei are ^{2}H (deuterium), ^{10}B, ^{11}B, ^{14}N, ^{27}Al, and ^{59}Co. Some important properties of the most useful dipole nuclei are summarized in Table 10. Clearly, the natural abundance and receptivity of nuclei are essential for practical purposes.

The magnetic field generated by a nucleus with spin +½ is opposite in direction from the field generated by a nucleus with spin -½. In the absence of an external magnetic field, there are two quantum states for the nuclei with spin ±½ such as ^{1}H and ^{13}C, for example (Figure 174). These states have the same energy, and consequently equal population, because both 'up' (+½, or ↑) and 'down' (-½, or ↓) orientations of magnetic dipoles are equally possible. An external magnetic field causes the alignment of nuclear magnetic moments, parallel and antiparallel to the applied field, with a slight excess of magnetic moments aligned parallel. Now, the 'up' state (↑) has a lower energy (ground state), as it is aligned with the external field, whereas the 'down' state (↓) has a higher energy (excited state) and the opposite orientation to the applied field.

Table 10. The NMR properties of some important dipole nuclei.

Nucleus	% Natural Abundance	NMR frequency at $B_0 = 4.7$ T	Receptivity relative to ^{1}H	Chemical shifts range, ppm
Commonly used:				
^{1}H	99.99	200.0	1.0	-30 to +20
^{13}C	1.11	50.2	0.016	-100 to +300
^{19}F	100.0	188.2	0.83	-200 to +200
^{31}P	100.0	81.0	0.066	-100 to +250
Less common:				
^{15}N	0.37	20.26	$3.8 \cdot 10^{-6}$	-350 to +800
^{29}Si	4.7	39.8	0.0078	-350 to +40
^{119}Sn	6.58	74.5	0.052	-1000 to +8000
^{195}Pt	33.8	43.0	0.099	-200 to +15000

The NMR spectroscopy method is based on the absorption of radio-frequency photons by nuclei in the ground state, when the external magnetic field is present. This energy absorption triggers transition of spin from its ground state to the excited state, and can be detected by the NMR spectrometer. Radio-frequency radiation is absorbed only when the energy of photons corresponds to the difference in energy between two states (ΔE). The frequency of absorbed electromagnetic radiation is proportional to ΔE which, in turn, is proportional to the applied magnetic field strength B_0. It is essential that the lifetime of the nuclear excited state (milliseconds to seconds range) is significantly longer than the lifetime of the electronic excited state. By the factor of a million, at least! A long lifetime of NMR excited states generates very narrow resonance lines, and thus provides high resolution spectral information. In addition, it allows investigation of internal molecular dynamics over a very broad range of timescales. However, the relatively low energy of NMR transitions creates very small population difference between levels. As a result, NMR spectroscopy is recognized as a relatively insensitive analytical method. Often, it requires to accumulate a lot of spectra and average them together to increase the signal-to-noise ratio (*S/N*).
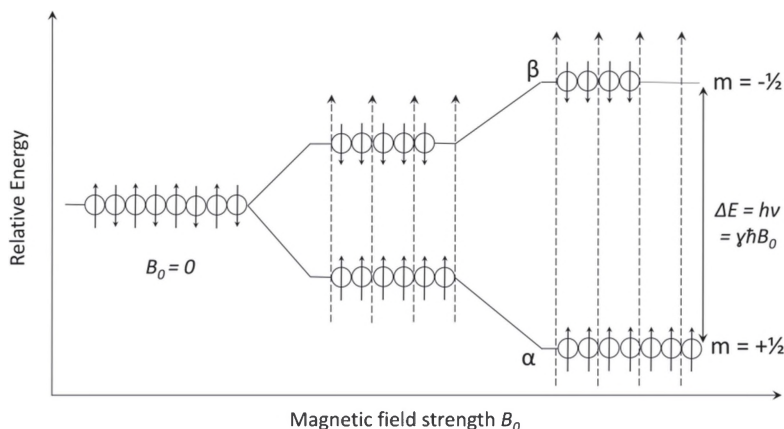
Figure 174. Visualization of two quantum states for a nucleus with spin quantum number ½. Energy difference between two states increases with the increasing strength of applied magnetic field.

The frequency of absorbed electromagnetic radiation not only depends on the type of nucleus, but is also very sensitive, and varies slightly depending on the local electronic environment. As a consequence, different proton and carbon atoms in a molecule will have characteristic peak absorption frequency in NMR spectra. That is why NMR spectroscopy is a powerful tool for structure elucidation and probing the conformational dynamics.

An external permanent magnetic field affects the motion of electrons in a molecule, and thereby induces a magnetic field within the molecule. The direction of induced field is opposite to that of the applied field. In turn, this generated own small magnetic field modifies the external magnetic field within the nucleus. Thus, the induced field shields the nuclei from the applied field. Therefore, a stronger external field is needed to match the energy of radio-frequency radiation with the energy difference between ground and excited states. Chemical shift represents a measure of the degree to which a certain nucleus in molecule is shielded from the applied field, on the order of one part in a million (ppm). All resonances for different nuclei do not occur at the same position in the NMR spectra. For example, protons residing in different molecular environments will be shielded, to greater or lesser degrees, and consequently will have different chemical shifts in the proton NMR spectrum. The extent of shielding is a function of several structural features of molecules. This allows identification of different atoms in the

molecule, based on their characteristic chemical shifts, molecular symmetry and electronegative or electropositive effects of substituents. Because the extent of shielding is proportional to the external magnetic field, B_0, the independent units for chemical shifts (δ values, ppm) are used. Proton and carbon chemical shifts in organic compounds experience the influence of proximal electronegative atoms (O, N, S, F, Cl, etc.) in the covalent bonding networks, and directly from the space proximity of different unsaturated groups, such as aromatic, C=C, C=O, and C=N. Therefore, chemical shift values provide unique information about the structure of molecules.

Signal splitting observed in the NMR spectra is due to the phenomenon called spin-spin coupling, or J coupling. Spin-spin couplings, in addition to the chemical shifts, also provide an important piece of information about the structure of molecules. This describes the magnetic interactions between nonequivalent neighbor nuclei, which are very close (two or three chemical bonds) in the bonding network of molecules.

To better explain this concept, we will look at the ^{1}H NMR spectrum of one of the organic ligands that was used for the preparation of coordination compound with cobalt (III) ions, described above in this chapter. For simplicity, we choose 1-nitroso-2-naphthol, which will be cited as **HL** further on in Figure 175. The ^{1}H NMR spectrum of this compound was recorded in benzene-d_6 (C_6D_6), because in this solvent there is an excellent, unobstructed view of all six protons in the molecule without overlapping signals. The H3 magnetic nucleus of **HL** will align with the external field B_0 ('up' orientation, $\uparrow$), or will align against the field B_0 ('down' orientation, $\downarrow$). Both, H3 and H4 protons are spin-coupled to each other in the molecule through three chemical bonds. The H3 proton, therefore, would disturb the external magnetic field around the H4 proton, either by slightly increasing it or slightly decreasing it, depending on the H3 direction of orientation. It means that in half of the molecules, H4 resonance will be shielded (slight upfield shift) by the H3, and in the other half, H4 peak will be deshielded (slight downfield shift). That is why the H4 peak appears in the NMR spectrum as two sub-peaks, called a doublet. The magnitude of separation between sub-peaks is called a coupling constant (J), and has units of hertz (Hz).

The same analysis is applicable for the nuclei H3, which also appears in the spectrum as a doublet, due to spin-spin coupling with the proton H4. That is because the relationship between coupled nuclei is mutual. The appearance of additional neighboring protons in the molecule usually causes more complicated splitting, and the number of sub-peaks will be equal to the number of neighboring protons, causing the splitting

plus one. Using this **n+1** rule (**n** – is the number of neighbors), one can predict how many peaks to expect from spin-spin coupling. Depending on the number of distinct nuclei involved in a J coupling network, resonance lines may split into doublets, triplets, or quartets, and higher order multiplets may appear. J coupling is field-independent, and always reported in Hz. It is essential that the strength of J coupling between two nuclei depends on several factors, including types of nuclei, distance (number of bonds between nuclei), and orientation. The origin of chemical bonds (σ-, π, etc.), bond length, and angles between these bonds, influence spin-spin coupling in a complex manner. In organic molecules, [1]H-[1]H J coupling is usually in the range of 0-20 Hz.

Direct through-space interactions between pairs of nuclei can also be observed in the NMR spectra. This effect is called the Nuclear Overhauser Effect (NOE), and is recognized as one of the most important effects in NMR spectroscopy. The NOE is a change in the NMR peak intensity of one nucleus, when another magnetic nucleus, close by, experiences saturation due to the radio-frequency irradiation. The NOE depends only on the distance between two nuclei, and the magnitude is proportional to the $1/r^6$, where r is the distance separating two nuclei in space. Usually NOE effects can be observed if two nuclei are residing within the distance less than 5Å from each other. The distances derived from the measured NOEs are used for the three-dimensional structure determination of small molecules, polymers and proteins.

As an example, the 1D ^{1}H NMR spectrum of 1-nitroso-2-naphthol is demonstrated in Figure 175. It is a simple graph of peak intensities versus frequency (chemical shifts of these peaks). The information contained in this spectrum includes number of signals, signal intensities (as measured by the area under each separate peak), and splitting pattern (multiplicity of individual peaks). We have seven magnetically nonequivalent protons in total (six of them are aromatic protons), and consequently we observe seven well-separated resonances with different multiplicity (Figure 175a). All peaks appear independently from their multiplicity as an integrated area of 1.0 proton. Aromatic peaks have splitting patterns according to the **n+1** rule stated above. The J values (separation of split peaks) and chemical shifts can be easily extracted from this spectrum.
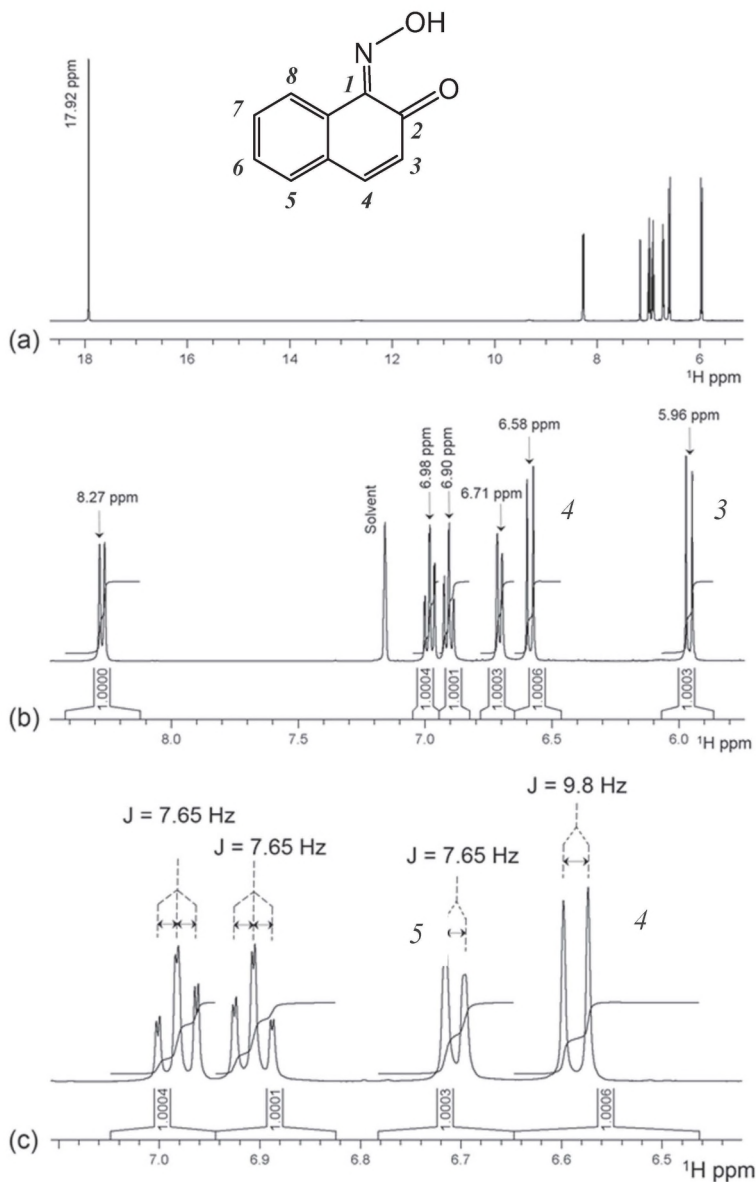
Figure 175. (**a**) The 1D ¹H NMR spectrum of 1-nitroso-2-naphthol (**HL**) in deuterobenzene C₆D₆. (**b**) The aromatic region of spectrum with integrated peaks. (**c**) Expanded aromatic fragment demonstrating spin-spin splitting patterns.

In this part of Chapter 3, we will assign signals in the proton, and carbon NMR spectra of a known ligand and known synthesized complex with diamagnetic metal ion such as low-spin Co(III). The assignment procedure is aimed to pair all resonances in the ^{1}H and ^{13}C NMR spectra with the hydrogen and carbon atoms in the chemical structures of molecules. This scrupulous work, described in a 'step-by-step walk through the molecule' manner, will provide an efficient way to learn and practice the interpretation of spectra. Hence, this tedious procedure represents a very good example of how to perform structure elucidation for other small molecules, which students and interested readers can encounter in their chemistry practice.

3.10.2. Theoretical Background: Introduction into *Homonuclear* 2D NMR Spectroscopy

Nuclear magnetic resonance spectra are certainly the most informative spectra for molecular structure elucidation. That is because these spectra have a very high information content about the relative positions of nuclei, the spatial localization and chemical bond multiplicity, conformational and configurational changes, and interactions with other molecules. The NMR data interpretation is the identification of various correlations between NMR-derived spectral parameters and molecular structure. Knowledge of these correlations would result in correct structure elucidation of analyzed molecules. Analysis and interpretation of NMR spectra is a key technique for structure elucidation, and requires considerable attentional capacity, as well as extensive practice. This chapter provides one-dimensional (1D) and two-dimensional (2D) NMR spectra of selected compounds for students to learn the interpretation, and to interpret NMR data.

In the 2D NMR spectrum (example shown in Figure 176) we have two frequency axes, and intensities presenting the third axis. The 2D spectrum represents a stack of several 1D NMR spectra. Each of the 1D spectrum in the packet is different from the previous one by a small change in evolution time. Fourier transformation in two-time domains generates a map of spin-spin correlations. Depending on the way the experiment is done, one can obtain correlations either via chemical bonds, or through the space. More detailed explanation of the principles of a variety of 2D NMR methods, as well as interpretation of spectral information obtained in such a way, will be covered in several sections below.

The 2D NMR experiments allow us to find the correlations between two atoms in a different type of molecules, based on the

interactions through chemical bonds and through space. Correlations appear due to spin-spin coupling between nuclei, and no correlations are expected in the absence of coupling. These correlations can be used firstly for unambiguous assignments of NMR resonances, and secondly, to define structural properties of chemical compounds.
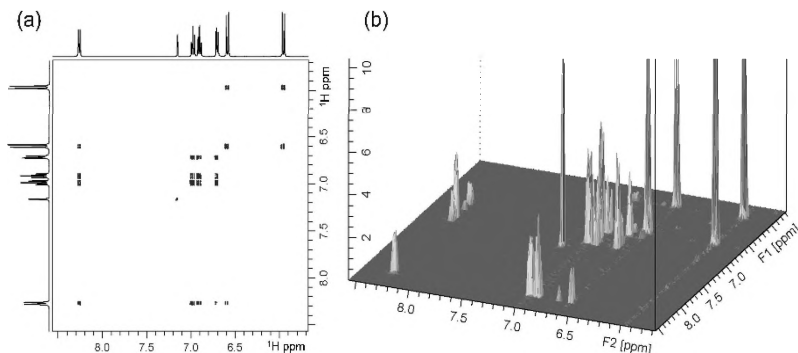

Figure 176. (**a**) The 2D ^{1}H-^{1}H COSY NMR spectrum of 1-nitroso-2-naphthol in C_6D_6 (contour plot). (**b**) Actual view of the 2D COSY spectrum with the third axis representing peak intensities.

2D NMR spectra consist of a series of 1D NMR spectra consequently acquired at different timing (t_1 and t_2). The process of spectra acquiring is repeated until there is enough data to be processed by 2D Fourier transform algorithm. After a 2D Fourier transformation in both dimensions (t_1 and t_2), the spectrum is represented as a topographic map which contains spin-spin correlations between atoms. 2D NMR experiments can be divided into two groups, homonuclear (correlations between two nuclei of the same type, e.g., ^{1}H to ^{1}H) and heteronuclear (correlations between two different types of nucleus, e.g., ^{1}H to ^{13}C). Each group allows identification of correlations either through the chemical bonds or through space.

2D ^{1}H-^{1}H **CO**rrelation **S**pectroscop**Y** (or, abbreviated, as 2D ^{1}H-^{1}H **COSY**) is the simplest 2D NMR experiment for explanation, understanding, and interpretation. This experiment generates a 2D map which correlates nuclei through chemical bonds only (usually up to four bonds). Specifically, COSY is useful for assigning resonances in 1D NMR spectra, because it simply shows us the proton spins that are coupled to each other, and consequently allows identification of spin system patterns present in the analyzed sample. Comparison of the spin system patterns

found, with the structural formula of the compound, often provides
possibility for near-complete resonance assignment in spectra. In addition,
the peaks (multiplets) overlapped in the 1D spectrum could be observed in
2D COSY spectrum as separated peaks, because the overlapping of
diagonal peaks do not necessarily line up the crosspeaks (peaks appearing
due to the correlations).

      2D ^{1}H-^{1}H **N**uclear **O**verhauser **E**ffect **S**pectroscop**Y** (or further
abbreviated as 2D ^{1}H-^{1}H **NOESY**) correlates the protons that are close to
each other in space, even if they are not bonded. The intensities of
detected crosspeaks are inversely proportional to the sixth power of the
through-space distance between two correlated protons. Therefore, the
NOESY spectrum is a graphical representation of nuclei spatial
proximities. NOESY can also detect chemical and conformational
exchange, and thus provides a relatively simple way to obtain information
about the dynamic behavior of molecules. In this case, the technique has a
name 2D ^{1}H-^{1}H **EX**change **S**pectroscop**Y** (or later abbreviated as 2D ^{1}H-
^{1}H **EXSY**). It is exactly the same experiment as 2D NOESY, but users
employ it for different purposes. Using EXSY experiments, the dynamic
information can be obtained without prior knowledge of molecular
structure and resonance peak assignment. NOESY spectra look very
similar to COSY spectra, but the crosspeaks arise from the protons that are
proximal in the space (<5Å). The NOESY techniques can help to solve the
stereochemical (conformational and configurational) puzzles such as
distinguishing cis/trans, E/Z or exo/endo isomers and others.

      2D ^{1}H-^{1}H **J-RE**solved **S**pectroscopy (later cited as 2D ^{1}H-^{1}H
JRES) allows the dispersal of the overlapping resonances by separating
chemical shifts and J-couplings into two independent orthogonal axes of a
2D contour plot. This technique is very useful for the extraction of
chemical shifts and J-couplings, from the regular 1D ^{1}H NMR spectra with
intensive overlapping of multiplets. In 2D JRES spectra, we have a
horizontal axis with chemical shifts only, and a vertical axis with
corresponding J couplings, which can be read now, directly from this axis
of a 2D spectrum. It is important to note that the projection along the
chemical shift axis represents a 1D decoupled proton spectrum, thereby
significantly simplifying analysis of spectra.

      Detailed step-by-step analysis and interpretation of ^{1}H and ^{13}C
NMR spectra of both ligands and their metal complexes *has never been
done in such detail* as presented in this book. Stable diamagnetic
complexes of isomeric organic chelating reagents, synthesized in earlier
laboratory sessions **5A** and **5B,** represent excellent examples, not only for
two different chromatographic separation techniques (**6A** and **6B**), but also

for characterization using the NMR method. These seemingly simple organic nitrosonaphthols ligands and their Co(III) complexes show unexpected complications in their NMR spectra recorded in commonly used NMR solvents ($CDCl_3$, CD_2Cl_2, and acetone-d_6) due to overlapping of signals. Therefore, we provide detailed explanation and interpretation of applied NMR techniques that led to a complete assignment of signals in 1D and 2D spectra.

        We hope that readers, once they have followed and comprehended the NMR methods described below, will value and successfully use them in the future for other samples of organic compounds/ligands and their metal diamagnetic complexes. An example of the approach to rigorous interpretation of multiple NMR spectra using the 'walk through' method is provided for education and training purposes.

3.10.3. Theoretical Background: 2D *Heteronuclear* NMR Spectroscopy – General Considerations

^{1}H-^{13}C HSQC (Heteronuclear Single Quantum Coherence) and ^{1}H-^{13}C HMQC (Heteronuclear Multiple Quantum Coherence) are NMR techniques designed for the identification of directly connected nuclei; proton and carbon. Both experiments allow us to pair C-H resonances and provide exactly the same information. However, there are two principal differences between these experiments: (1) HSQC has much more pulses and delays than HMQC, and the period between the excitation pulse and the acquisition is longer in the case of HSQC, making pulse calibration procedure more critical; (2) The HMQC spectrum shows ^{1}H-^{1}H couplings along the indirect ^{13}C dimension, whereas these couplings are absent in the HSQC spectra. ^{1}H-^{1}H interactions along the ^{13}C dimension can be used for the estimation of a major ^{1}H-^{1}H coupling constant, however the presence of several couplings may cause a complex peak profile, making correct estimation of ^{1}H-^{1}H J couplings more challenging. For the routing spectroscopy applications, these details are often of little consequence. In practice, the HMQC experiments look to be more robust in terms of miscalibrations and experimental imperfections, in comparison with HSQC. Nevertheless, HSQC has become the primary technique nowadays, as it has more favorable spectral characteristics for high-resolution studies, and is more flexible toward the sequence modification. We will describe and use HMQC in parallel with the HSQC, as it lays the foundation for the closely related long-range Heteronuclear Multiple Bond Correlation (HMBC) experiment. In both HMQC and HSQC spectra, a ^{13}C spectrum is displayed on one axis and a ^{1}H spectrum is displayed on the other axis.

Only protons directly bonded to ^{13}C will produce crosspeaks. Crosspeaks show which proton is attached to which carbon.

The HMBC (Heteronuclear Multiple Bond Correlation) technique is a modified version of HMQC, aimed at the determination of long-range ^{1}H-^{13}C connectivity. The HMBC spectra looks very similar to the HMQC spectra, with the difference that they show 2-bond, 3-bond and even 4-bond coupling (H-C-C, H-C-C-C and even H-C-C-C-C). Here we can see which carbon is next to the carbon directly attached to the hydrogen. Thus, the quaternary carbons will be detected also.

3.10.4. Theoretical Background: NMR Analysis of the *mer*- and *fac*- isomers of Coordination Compounds

Synthesized in laboratory experiments **5A** and **5B**, diamagnetic tris-chelate complexes of Co(III) have distorted octahedral geometry. The donor atoms environment of the central atom in these complexes is CoN_3O_3, and allows the existence of two geometrical isomers: meridional (later *mer*-), and facial (later *fac*-), as presented in this chapter earlier. Thus, in the *mer*-isomer, 2 out of 3 ligands reside on the same side or face of the octahedron, and one can find 3 ligands in a row on an octahedron (called '***meridional***'). Just as a reminder, in the *fac*- isomer all 3 ligands reside on the same face of the octahedron (called '***facial***'). Consequently, the *mer*-isomer has a lack of symmetry (just identity E, or symmetry operation C_1), while the *fac*- isomer is characterized by the presence of three-fold rotational symmetry (axis C_3). The bond angle between 3 ligands is 90°-90°-180° for the *mer*- isomer, and 90°-90°-90° for the *fac*- isomer (see Figure 153 in this chapter for clarification).

Since the *fac*- isomer has three equivalent ligands because of their symmetry relation through the rotational three-fold axis C_3, the presence of only one set of signals in spectra is expected. Thus, corresponding to magnetically nonequivalent protons and carbons of a single ligand, we expect to observe six signals in the ^{1}H and ten signals in the proton decoupled $^{13}C\{^{1}H\}$ NMR spectra. In spectra of the *mer*- isomer, three sets of signals may be expected, because of the total lack of symmetry and subsequent absence of the NMR-equivalency between three ligands. Thus, *mer*- and *fac*- stereoisomers can be easily distinguished by their individual ^{1}H and or $^{13}C\{^{1}H\}$ NMR spectra.

Synthetic products of complexation reactions typically represent statistically generated 3:1 mixtures of the *mer*- and the *fac*- isomers. Hence, in the mixture there will be four different ligand environments of equal population. This normal statistical 3:1 *mer*- to *fac*- ratio is observed

in the case of the absence of steric constraints upon the coordination of ligands to the central atom. The presence of a significant steric constraint favors the *mer-* isomer considerably, and its presence may be dominant.

The mixtures of isomers can be separated using the TLC or column chromatography, but rarely recrystallization. In previous laboratory sessions above, we have performed successful separation of individual geometrical isomers. That makes assignment and interpretation of the NMR spectra of individual isomers achievable and explainable. In turn, this provides very good practice for students and readers interested in structure elucidation.

3.11. Experiment 9: Recording of multinuclear 1D NMR spectra (^{1}H, ^{13}C{^{1}H}), and 2D spectra of samples of isomeric nitrosonaphthols and their Co(III) complexes

The university departments (or R&D divisions in private companies) may have their NMR facilities equipped with different types of NMR spectrometers and magnets with different magnetic field strengths. All the NMR spectra presented and analyzed in this book were recorded using the standard pulse sequences supplied with the Bruker AVANCE 400 MHz NMR spectrometer. The data were processed and visualized using Bruker TopSpin 3.5 pl 7 software. However, the same content of spectral information could be obtained using different types of NMR spectrometers with proton resonance frequency of 100 MHz and higher.

Common modern instruments with carrying frequencies for protons ranging from 300 to 800 MHz offer the possibility of recording ^{1}H, ^{13}C, ^{15}N, ^{19}F and ^{31}P NMR spectra, using optimized preset parameters stored on the instrument computer in separate folders dedicated to each of those dipole nuclei. Students may also find an option for recording a variety of the outlined above 1D and 2D spectra, using default parameters in the spectrometer's computer main menu. These normally allow the user to obtain good quality data for subsequent interpretation.

NMR sample preparation. With the aim of accessing the maximum information content at the expense of minimal NMR experimental time for spectrometers with relatively low resonance frequency, we recommend that you use 5-20mg of compounds for recording a good quality ^{1}H spectrum.
The accuracy of the sample preparation procedure can prevent the appearance of artifacts in the recorded spectra. Regular 5mm NMR tubes can be used, and they should be clean and dry to prevent various

contaminations. The samples should be dissolved only in *deuterated solvents*. Usually proton NMR spectra are recorded for compounds dissolved in deuterated solvents. There are two major reasons for that. First of all, deuterated solvents allow the continuous stabilization of magnetic field strength during the accumulation of NMR data. Secondly, the amount of solvent in the NMR tube always significantly exceeds the amount of dissolved substance, therefore a regular (proton-containing) solvent would simply dominate the ^{1}H NMR spectrum. The optimal volume of solvent is no less than 0.6ml for a 5mm NMR tube.

Common practice is to dissolve the sample of interest in a separate 2-3ml vial, and *not* in the NMR tube, especially if the solubility of a compound is not well known. If necessary, dissolution can be aided with ultrasound waves, using the sonicator (Chapter 1, Figure 29). As mentioned above, the amount of compound is normally 5-20mg for recording a good quality of the ^{1}H NMR spectrum using 8 – 64 repetitions (scans). However, this might be not sufficient for fast collection of the ^{13}C{^{1}H} NMR spectrum, since the concentration could be low and will require prolonged accumulation. In authors' laboratories this acquisition is normally set for an overnight run. Certainly, if the amount of compound permits making high concentration of solute, it is an ideal way to proceed. However, saturated solutions become more viscous, and that leads to line broadening and the baseline distortions. Thus, a delicate balance is needed between the permitted amount of material to use, the time of accumulation of the ^{13}C{^{1}H} NMR spectrum, and its quality/interpretability.

When solute is completely dissolved, it is promptly transferred from the vial into the NMR tube and closed with the plastic cap. *Remember: the deuterated solvents for NMR, such as DMSO-d$_6$, acetone-d$_6$, methanol d$_4$, acetonitrile CD$_3$CN and D$_2$O are hygroscopic. Exposure to the air in the lab leads to the appearance of a broad signal at ~3ppm in the spectra, due to absorbed moisture.* The residual precipitations after initial sample preparation should be filtered out. Make sure that the solution in your NMR tube is homogenous and clear.

In this experiment, students will need to record:

1) A set of spectra for the pure ligand **HL** (1-nitroso-2-naphtol);
2) A set of spectra for pure geometrical isomers, separated in previous experiments.

Sample measurement. Now, a sample can be immersed in the magnetic field of an NMR spectrometer. These days, for a majority of NMR spectrometers, the routine 1D and 2D NMR experiments for small molecules are usually set up with dedicated parameter sets, which aim to provide good quality data with minimum operator experience and intervention. In addition, the existence of automated processing software provides a fast, efficient and easy way to prepare spectra for interpretation.

Note: Recording a good quality 1D proton NMR spectrum may take up to 20 minutes, while for ^{13}C NMR spectra, even a period of several hours may not be sufficient. Similar extended times are typical for all 2D experiments. Therefore, recording those overnight, prior to the day of the laboratory session, is recommended. These recordings can be carried out either by an instructor, or by a dedicated and trained staff member responsible for the NMR facility. Thus, printouts of ^{13}C and 2D spectra after long acquisitions should be distributed among students on the day of this laboratory experiment.
        After completing your experiment, you can start NMR data processing and visualization, using available software. As an alternative, the spectra can be recorded, processed and visualized for you by the facility associated staff or competent researchers.

Data presentation. Students should be instructed to present recorded spectra in a neat manner. That is: 1) a clearly drawn chemical structure of the compound (on the printout with spectra), with the numbering scheme for both H and C atoms being the same; 2) all peaks/signals assigned to corresponding atoms; 3) coupling constants (if available and applicable!).

Data storage. It is important to recognize that recording spectra quickly will take up a considerable amount of space on the computer's hard drive. Therefore, special care should be taken for data preservation and multiple safe backups made.

3.12. Analysis and Interpretation of 2D *Homonuclear* NMR Spectra of the ligand – 1-Nitroso-2-Naphthol

2D COSY spectra

The simplest way to present a 2D NMR spectrum is to make a contour plot, where the resonance peak intensities are shown by contour lines drawn at proper intervals, similar to those of topographical maps. Figure 177 represents the 2D ^{1}H-^{1}H COSY spectrum of 1-nitroso-2-naphthol. We can see that the proton 1D NMR spectrum of the compound is plotted along both the horizontal (F2) and vertical (F1) axes. Each axis is calibrated according to the chemical shift values (parts per million, ppm).

The COSY spectrum displays distinct spots (peaks) on a diagonal, running from the upper right corner down to the lower left corner of the 2D spectrum. We call these peaks diagonal because they reside on the diagonal line defined by F1 = F2. In fact, we can view the diagonal as our 1D spectrum. The diagonal divides the spectrum into two equal halves. In addition to the existing diagonal peaks there are peaks residing off the diagonal, called crosspeaks. Notably, the 2D COSY spectrum is symmetric about the diagonal; specifically, the crosspeaks are symmetric about the diagonal, e.g. two equivalent crosspeaks correspond to each spin-spin coupling. The diagonal peaks serve as reference points, whereas off-diagonal or crosspeaks provide important structural information.

The peaks on the diagonal display a multiplet fine structure, and reflect the 1D spectrum of compound. In turn, the COSY crosspeaks also display a multiplet fine structure, which is caused by the scalar couplings. The fine structure resolution level of the crosspeaks depends on the experimental settings used during the acquisition of the data. In high resolution COSY spectra (Figure 177), the coupling constants can be determined from the fine structure of the cross and diagonal signals. The appearance of a crosspeak between two resonances indicates the presence of spin-spin coupling between corresponding nuclei.
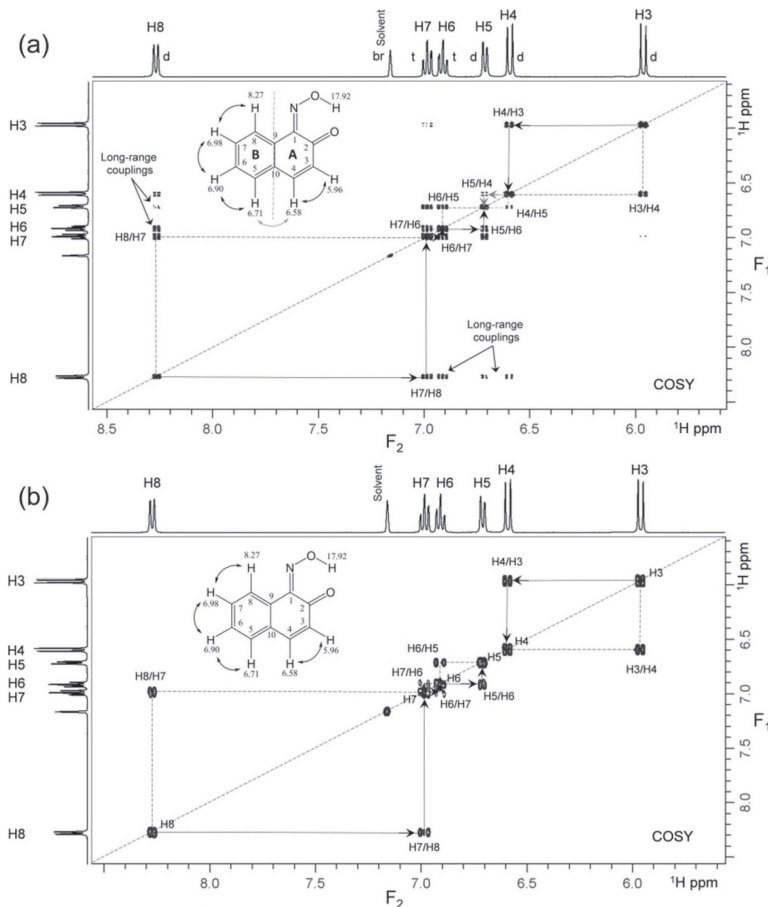
Figure 177. (**a**) The COSY spectrum of **HL** with the long-range couplings often appearing in the spectra of aromatic systems. For comparison, the COSY spectrum with filtered out crosspeaks due to the long-range couplings is presented in part (**b**). These crosspeaks were filtered out by decreasing the spectral resolution. COSY vicinal correlations are shown as black arrows on the structure of **HL**.

Usually, the aim of COSY spectra analysis is the identification of crosspeaks' coordinates, rather than the determination of coupling constants. Therefore, very often COSY spectra are optimized for low resolution, as no fine structure of crosspeaks needs to be resolved. COSY analysis can be done by 'walking through' each spin system, by moving

vertically from individual peaks on the diagonal to their corresponding crosspeaks, then again back horizontally to the diagonal. Both symmetrical cross-peaks corresponding to the coupled pair of protons can be used equally for 'walking' in the pathway diagonal-crosspeak-diagonal. This procedure can also be done in reverse order, starting from the cross-peak and drawing horizontal and vertical lines toward the intersection with the diagonal.

Repeating this procedure paves the way for complete identification of coupling partners or *spin connectivities*. To begin analysis of COSY spectra, we always have to identify a starting point (peak) for 'walking'. It must be a proton resonance that is well resolved, and its unambiguous assignment can be done based on either its chemical shift, or coupling pattern. It is useful also to draw vertical and horizontal lines from each signal on the diagonal toward crosspeaks. Once the lines have been drawn on the COSY spectrum in Figure 177, you can clearly see that each signal on the diagonal corresponds to the same peak on each coordinate axis, and each cross-peak connects coupling partners residing on the two axes.

The spectrum is rather complex in appearance. Nevertheless, we are going to identify all present coupling interactions. Using the structural formula of the ligand **HL,** and 1D NMR spectrum of **HL** in deuterobenzene (C_6D_6), we describe how you should interpret high resolution 2D NMR COSY spectrum. It can be seen that the spectrum consists of six well resolved multiplets: four doublets and two triplets, corresponding to six aromatic protons in the structure of **HL**. Multiplicity of resonances is indicated as follows: *d*, doublet; *t*, triplet; *br*, broad. An extra signal at 7.16ppm (broad singlet) is due to the residual non-deuterated fraction of benzene, because the deuteration is not '100%' (*as you'll always see in any NMR grade deuterated solvents!*). Notably, two doublets at 5.96 and 6.58ppm are much sharper than doublets at 6.71 and 8.27ppm. Dividing **HL** schematically, for two aromatic rings *A* and *B*, will help us to identify the individual spin systems, and to reveal connections between spin-coupled nuclei. The structure of ring *A* predicts the appearance of two doublet resonances with vicinal ${}^1H$-${}^1H$ couplings through three chemical bonds (${}^3J_{HH}$), whereas the structure of ring *B* predicts the existence of two similar doublets and, in addition, two triplets. The presence of two extra protons will contribute to the additional splitting (broadening) of corresponding doublets from the ring *B*. This allows us to assign two broader doublets, at 6.71 and 8.27ppm, to the ring *B*. By process of elimination, the doublets at 5.96 and 6.58ppm must be assigned

to the ring *A*. These two distinct proton resonances in the ring *A* can be recognized as an AB spin system.

The resonances from the ring *B* (two doublets and two triplets) can be classified as an AMPX spin system. Among the two doublets of the ring *B*, the downfield resonance at 8.27ppm can be definitely assigned to the H8 proton. The observed large downfield shift of this resonance is due to the spatial proximity of the lone electron pair belonging to the oxime nitrogen. At least one definitely assigned resonance can now be used as a starting point, to observe and analyze couplings between aromatic protons which are established by the appearance of crosspeaks in the 2D NMR COSY spectrum (Figure 177).

Our first task is to track the only three-bond mediated vicinal couplings between protons. Starting at the lower left corner of the spectrum with the H8 peak, we can identify all coupling partners in the ring *B*. According to the structure of **HL**, the H8 proton has only one vicinal partner H7, which appears in the spectrum as a triplet signal. We follow horizontally from the H8 diagonal peak to the right, along the solid line, and observe that the H8 peak has connectivity to several crosspeaks of various intensities.

One can easily notice that there are a lot more crosspeaks in the 2D COSY spectrum of **HL** than is expected for vicinal coupling correlations only. It is well known that the COSY technique, in some cases, can detect interactions between nuclei over ranges that extend beyond three bonds. Specifically, in aromatic systems, the presence of π electrons usually makes a greater contribution to the observation of four and five-bond correlations. Often, these additional peaks have relatively lower intensities than the principal peaks correlating vicinal interactions in the spin systems. However, sometimes the 2D COSY spectra show comparable intensities of crosspeaks corresponding to three and four-bond correlations. This feature complicates the straightforward identification of vicinal partners in the aromatic systems, as can be seen for the case of **HL**.

At this point, the unambiguous identification of crosspeaks correlating vicinal interaction between H8 and H7 protons, requires additional experiments with modified parameters or specific data processing. The way of solving the problem is to filter out the spectrum cross-peaks due to long-range interactions. In general, decreasing the spectral resolution will lead to the disappearance of crosspeaks originated from smaller J-couplings. In practice, filtration of these weaker interactions can be achieved simply by recording the spectrum with a wider spectral width, and/or by application of specific apodization (also called window or weighting) function, for instance a 90°-shifted sine-bell

(also called cosine-bell) function. This function gives greater weight to the beginning of the *free induction decay* (FID). Because the signal-to-noise ratio is larger at the beginning of the FID, the sensitivity will increase, at the expense of resolution. In both cases the spectral resolution will be compromised, and as a consequence, the only crosspeaks corresponding to the vicinal J-couplings will be present in the 2D COSY spectrum.

In Figure 177 **b,** vertical and horizontal lines ('boxes') are drawn, by moving from the diagonal peaks to the right and up, as well as up and to the right back to the diagonal peaks belonging to vicinal partners, to help you identify the principal correlations. In this spectrum, the only crosspeaks remaining are those that correlate vicinal interactions between nuclei, whereas crosspeaks corresponding to the long-range correlations are filtered out. Thus, additional experimentation with decreased spectral resolution, and/or application of a weighting function compromising the resolution, can resolve the ambiguity with vicinal correlation between the H8 and H7 protons. It is obvious now, that in our 'walking through-the-molecule' process, starting from the diagonal peak H8, we have to stop at the first crosspeak, corresponding to a triplet signal at 6.98ppm. This triplet represents a vicinal partner of the signal H8, and must be assigned to the proton H7. By process of elimination, the second triplet signal at 6.90ppm should be assigned to the proton H6.

Now, from the crosspeak between H8 and H7 signals, we continue our walk and go straight up, returning back to a diagonal at the position of peak H7. The second vicinal partner of the H7 proton is H6, which also appears in the spectrum as a triplet. Therefore, from the H7 peak, we move to the right and stop at the first crosspeak, representing the correlation between the H7 and H6 triplets.

To provide a clear view of details, and to simplify the analysis of the crowded spectral region in Figure 177**a**, the fragment of COSY spectrum is zoomed in on, and displayed in Figure 178.
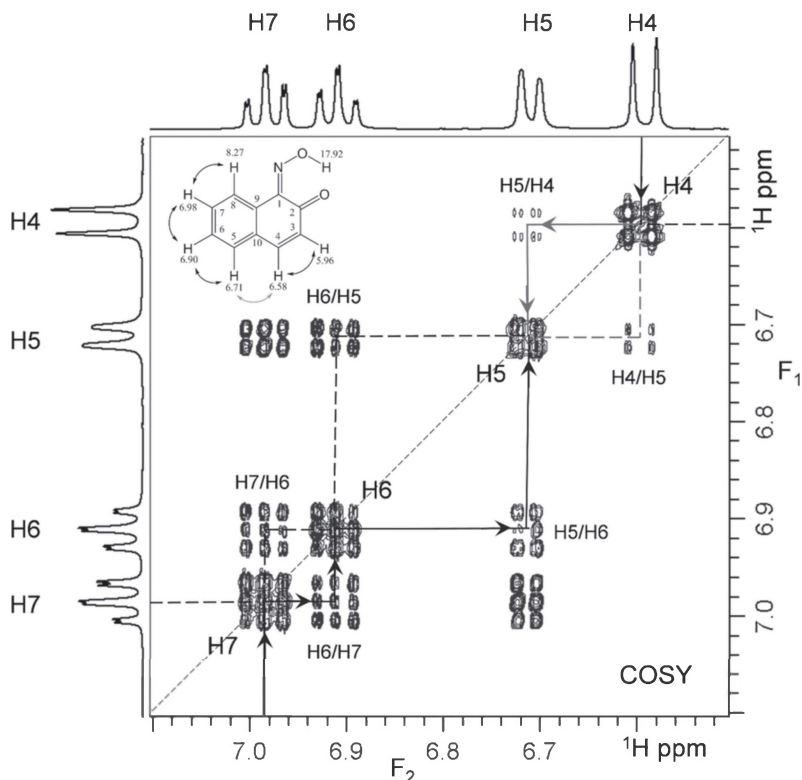
Figure 178. An expansion of the COSY spectrum fragment from Figure 177**a,** showing the fine structure of crosspeaks and details of the diagonal – crosspeak – diagonal walking procedure in the crowded spectral region of **HL**. Long-range correlation between H4 and H5 is shown as a green arrow on the structure of **HL**.

From the crosspeak correlating H6 and H7 protons we move straight up, and again return to the diagonal, but now at the position of triplet resonance (6.90ppm) belonging to the proton H6. In turn, the second vicinal partner of H6 should be a doublet resonance, according to the structure of **HL**. For reasons given, from the H6 diagonal peak we move horizontally to the right and stop at the crosspeak, correlating a triplet signal of the H6 proton with the last unassigned doublet signal in the ring B, at 6.71ppm. Then, moving straight up to a diagonal peak at 6.71ppm, which obviously belongs to the H5 proton, we are completing the assignment of resonances from the ring B.

There are only two doublet resonances (H3 and H4) connected by vicinal interactions in the spin system of ring A (Figure 177). Following this spin system from the diagonal peak at 5.96ppm, we move left to the corresponding crosspeak, and down to the diagonal peak, at 6.58ppm. This completes our walk through the spin system of ring A, as we achieve a dead end in connectivity. At this point, we cannot tell unambiguously which peak is H4 and which peak is H3. However, this puzzle can be resolved by taking advantage of the presence of long-range crosspeaks (4-bond connectivity) in our 2D COSY spectrum.

Figures 177**a,** and Figure 178, clearly show the presence of weak crosspeaks between the doublet H5 from the ring B and the doublet at 6.58ppm arising from the ring A. At the same time, there are no detectable crosspeaks between the doublet H5 and the doublet at 5.96ppm. According to the structure of **HL**, these observed crosspeaks obviously correlate H5 and H4 protons, separated by four chemical bonds, and residing in different rings. Now, from the diagonal peak H4, we can move horizontally to the left weak crosspeak, and finally straight down to the diagonal peak H5, thereby establishing connectivity between the spin systems of two rings, and providing unambiguous assignments of H3 and H4 doublets. Thus, the peak at 5.96ppm is assigned to the proton H3, whereas a peak at 6.58ppm is assigned to the proton H4.

2D NOESY spectra

The 2D ^{1}H-^{1}H NOESY spectrum of **HL**, presented in Figure 179, contains a diagonal and cross peaks, and looks very similar to a COSY spectrum (Figure 177**b**). We should always look first at the COSY spectra before attempting to analyze the NOESY spectra. The diagonal in a NOESY spectrum also consists of the 1D spectrum. The crosspeaks appear between the same pairs of aromatic protons, residing in the ortho position to each other and coupled through vicinal interactions. However, the NOESY crosspeaks indicate which protons of **HL** are physically close to which other protons in the space within the distance of < 5Å, regardless of whether there are chemical bonds between them or not. The crosspeaks between the same pairs of protons in a COSY spectrum exist only due to the J-coupling through the chemical bonds.
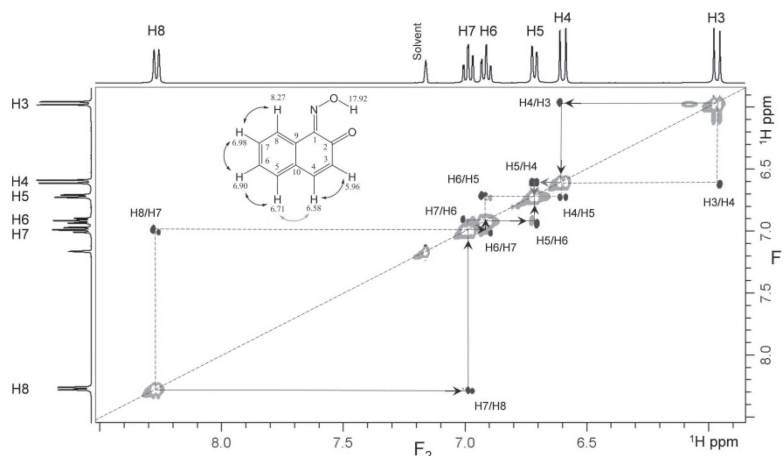
Figure 179. The 2D NOESY spectrum of **HL**. The main diagonal peaks are phased as negative (gray color). The crosspeaks due to NOE interactions appear in the opposite sign to the diagonal peaks (blue color). Positive NOE interactions between atoms in the ortho positions are shown as black arrows on the structural formula of **HL**, and other positions as green. See centerfold for this image in colour.

The Nuclear Overhauser Effect and corresponding crosspeaks can be negative or positive. In the case of a negative NOE effect, the crosspeaks will be negative with negative diagonal signals, whereas for a positive NOE effect we will get positive crosspeaks with a negative diagonal. The peaks from chemical exchange will show the same sign as diagonal peaks, and will be easily distinguishable from positive NOEs. However, they can be confused with negative NOEs. NOEs are very influenced by the molecular tumbling rate (the rate of molecular spinning), and the strength of the NMR magnet. For small molecules (F.W. < 600 a.m.u.), in the fast motion limit, the NOE is positive, it is zero for medium-sized molecules (700 < F.W. < 1200), and is negative for larger molecules (F.W. >1200). Therefore, for the **HL** molecule with F.W. = 173 a.m.u., we are expecting to observe only positive NOE effects. By convention, we have to phase and plot the diagonal peaks as negative absorptive peaks. With this processing, all crosspeaks observed in the NOESY spectrum of Figure 179 have the opposite phase to the main diagonal peaks, clearly indicating that NOEs are positive.

An interpretation of this spectrum requires the drawing of horizontal and vertical lines from each crosspeak toward the intersections with the diagonal. The lines should have ended on the two diagonal peaks

representing spatially proximal pair of protons. Similarly to the case of COSY spectra analysis, the H8 proton can be used as a starting point for the analysis of through-space interactions between aromatic protons. Moving down vertically, and right horizontally, from the most downfield crosspeak corresponding to H8, we can unambiguously assign the spatially proximal partner of the H8 proton. Obviously, the diagonal peak at 6.98ppm belongs to the H7 proton, which is in close spatial proximity to the H8 proton, according to the structural formula. In addition, there are no NOE crosspeaks between the H8 signal and the proton signal at 6.90ppm. The absence of NOE correlations with H8 proton and multiplicity (triplet) of signal at 6.90ppm allows the straightforward assignment of this peak to the proton H6. Thus, the NOESY spectrum allows the unambiguous distinction between two triplet resonances corresponding to the protons H7 and H6.

The same analysis is applicable for solving the puzzle with the assignment of two upfield resonances, H3 and H4. According to the structure of **HL**, the H3 proton is expected to show the through-space correlation with only one proton H4, which is in ortho position to H3. In turn, H4 has two adjacent protons; H3 and H5, suggesting the appearance of NOE correlations with two spatially proximal partners. Indeed, the peak at 5.96ppm demonstrates the existence of only one through-space correlation, whereas the peak at 6.58ppm demonstrates two correlations, providing a basis for unambiguous distinction between H3 and H4 proton resonances. Thus, the NOESY spectrum allows for unambiguous distinction between two triplets, H7 and H6, as well as between two doublets H3 and H4, and can be used for the verification and/or completion of resonance assignments from COSY spectra.

It should be noted, that the main and critical difference between COSY and NOESY spectra is very low intensity of NOE crosspeaks. Intrinsically, the NOE interactions are relatively weak, and therefore successful recording of COSY spectra for the sample may not be successful with a NOESY experiment.

2D JRES spectra

The 2D ^{1}H-^{1}H JRES spectrum of **HL** is presented in Figure 180**a**. It can be seen that this kind of 2D NMR experiment allows us to separate the chemical shift and spin-spin coupling through chemical bonds from all the multiplets present in the spectrum. These two important NMR parameters (δ and J) are directly projected onto two different axes, F2 and F1. The projection of the 2D spectrum of **HL** onto the chemical shift axis (F2)

represents the 1D ^{1}H NMR spectrum (Figure 180**b**), with fully filtered out spin-spin couplings (broadband-decoupled). The resonance multiplicity is projected onto the F1 axis. The clear simplification resulting from the elimination of multiplets from the chemical shift axis will be very useful for the analysis of crowded spectra and mixtures of isomers.

In the deuterobenzene C_6D_6 all the resonances of **HL** are very well resolved and separated. For this case, the chemical shifts and J-couplings can be easily extracted from both 1D (Figure 180**c**) and 2D spectra. However, the 1D spectra of nitrosonaphthols in many other organic solvents could have some overlap and crowd. More overlapping and crowding will be observed in the spectra recorded on the low-field NMR spectrometers, where the chemical shift differences can be smaller relative to corresponding J-couplings. Application of 2D ^{1}H-^{1}H JRES spectroscopy for these cases would help to extract correct values of δ and J.

In this chapter, we have learnt how to analyze and interpret 2D homonuclear COSY, NOESY, and JRES NMR spectra, with the aim of assigning the NMR resonance peaks and elucidating the structure of a simple organic compound.
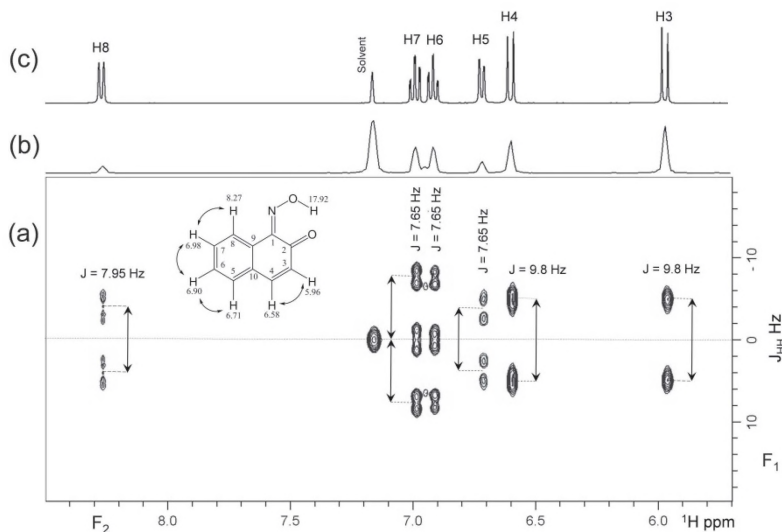

Figure 180. (**a**) The 2D ^{1}H-^{1}H JRES spectrum of **HL**. The corresponding 1D projection along the chemical shift axis is shown on top, part (**b**), and regular 1D spectrum with J-couplings is shown as part (**c**).

3.13. Analysis and Interpretation of 2D *Heteronuclear* NMR Spectra of the 1-Nitroso-2-Naphthol

2D HSQC and HMQC spectra

Initially, only *homonuclear* correlations (proton-proton) were identified between similar nuclei of **HL**. For example, homonuclear COSY spectra were used to find 3-bond correlations (H-C-C-H) between protons. Identified correlations allowed us to assign, unambiguously, only the proton resonances attached to the carbon skeleton of **HL**.

For complete chemical structure characterization, the NMR resonance assignment of all carbon atoms must be accomplished, which is not an easy task, as you may observe from Figure 181. The goal of complete assignment can be achieved with the use of the 2D *heteronuclear* correlation experiments, where magnetization transfer is between two dissimilar nuclei (proton-carbon). Now we describe this procedure, and perform analysis of spectra.

It is common practice to run conventional 1D proton and carbon NMR spectra ahead of the 2D data acquisition. These reference spectra will be used to determine the optimal parameter sets for ^{1}H and ^{13}C dimensions of the 2D experiments, and in addition, can be used as external projections in the 2D spectra. When a 2D spectrum is ready for analysis, the proton spectrum can be plotted along one axis (F2), and the carbon spectrum along the other axis (F1). It is more convenient to use these separately recorded 1D spectra as external projections, instead of the actual skyline projections of the 2D data matrix (internal projections). The internal projections have the resolution of a 2D spectrum, which is usually much lower than the resolution of a normal 1D spectrum. The assignment of all resonance peaks in the conventional 1D proton NMR spectrum of L was described earlier in this chapter. Here, we will describe how to assign the carbon NMR resonances for the **HL**. The ^{13}C NMR spectrum of the ligand, with *broadband ^{1}H decoupling* (where the effect of proton couplings with carbon ^{13}C nuclei was removed), is shown in Figure 181.

This is a typical spectrum for aromatic compounds, displaying single carbon resonances in the region of 120-180ppm. According to the structural formula, there are ten unique carbon environments in the benzene rings, and correspondingly, we see ten different, and well-separated, peaks (Figure 181). Note that four out of ten resonance peaks have reduced intensities, and likely belong to four quaternary carbons of the **HL**. One of these carbons appears downfield, at 145.05ppm, and another appears much further downfield at 182.65ppm. The ^{13}C chemical

shift of the signal at 182.65ppm obviously indicates carbon in the carbonyl group, and chemical shift at 145.05 indicates carbon in the oxime group.
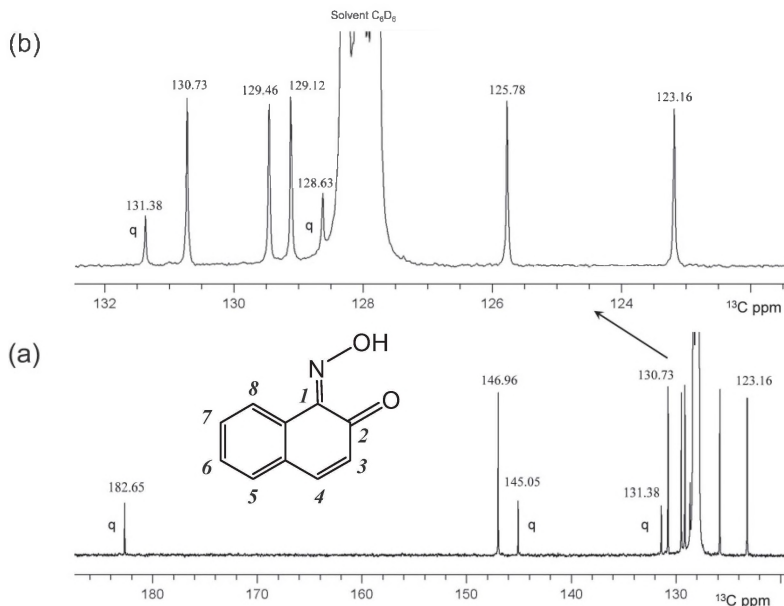

Figure 181. (**a**) The ^{13}C NMR spectrum of **HL** in C_6D_6 with broadband proton decoupling. The extension of crowded region (122-132ppm) is shown in panel (**b**).

Thus, these two quaternary carbons can be safely assigned correspondingly to the positions 2 and 1 in the structural formula of the **HL,** based on their characteristic chemical shift values. All other resonances can be unambiguously assigned only with the help of heteronuclear 2D NMR experiments. As an example, Figure 182 shows the HSQC and HMQC spectra of **HL**.
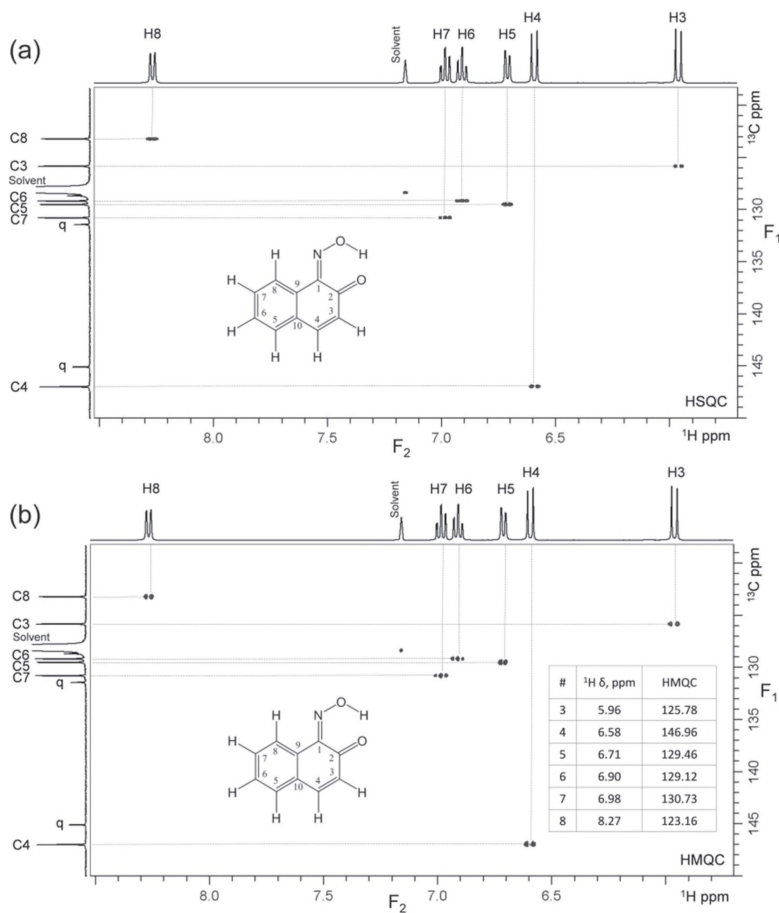
Figure 182. (a) The HSQC spectrum of **HL**. For comparison, the HMQC spectrum of **HL** recorded with similar parameters is displayed in panel (**b**). The crosspeak coordinates extracted from spectra as a proton, and carbon chemical shift values (δ,ppm), are presented in the inset table.

The analysis and interpretation of these spectra is simple. It suggests a straightforward identification of crosspeaks' coordinates in ppm units. Initially, recorded 1D regular proton and carbon spectra will serve for the positioning of crosspeaks in the 2D spectra. In the dimension F1, 2D spectra contain reference carbon signals, whereas the F2 dimension

contains reference proton signals. Figure 183 displays an expanded region of 2D HSQC spectrum from Figure 182a to provide a detailed view of proton-carbon correlations and crosspeaks' multiplicity.
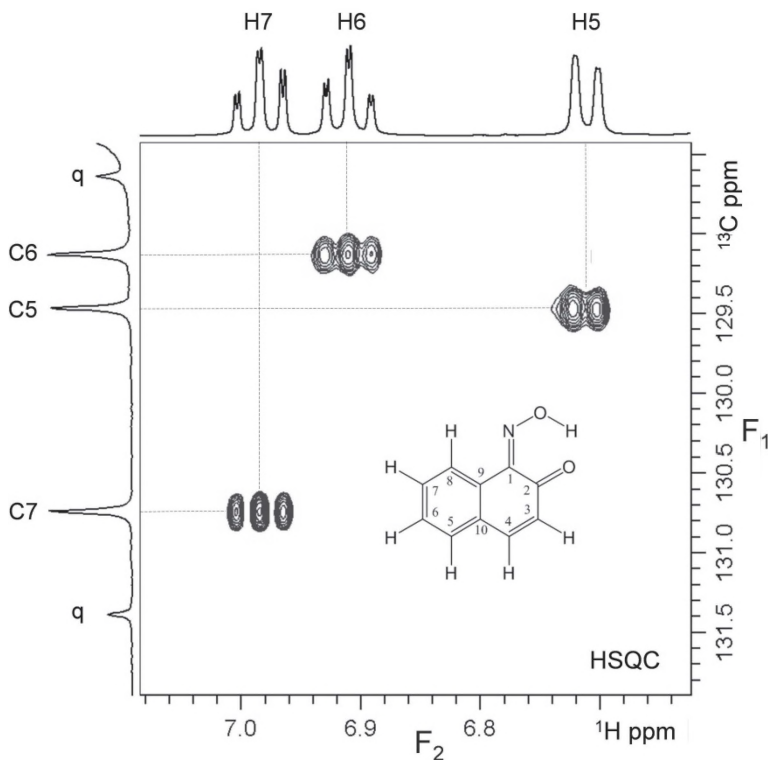
Figure 183. Extended fragment of the 2D HSQC NMR spectrum of **HL,** demonstrating in detail the multiplicity of crosspeaks, and the assignment procedure for carbon atoms resonances.

If we draw a vertical line from each proton peak in the spectrum on the top, and a horizontal line from each carbon peak in the spectrum on the left side of 2D spectra, the lines would intersect exactly at the positions of crosspeaks correlating C-H pairs. That means that the selected proton is attached to the indicated carbon, and both represent the same position in the structural formula. It can be seen from Figures 182 and 183, that only one correlation exists for each of protons in the HSQC and HMQC

spectra. For example, the vertical line drawn from the H3 position intersects with only one crosspeak, which in turn, has an intersection with a horizontal line drawn from the carbon identified as C3 directly connected to H3.

The carbon reference spectrum also contains resonance peaks corresponding to the quaternary carbons (q), which clearly do not show correlations in 2D spectra. Therefore, if no crosspeaks signify upon drawing a horizontal line from selected carbon, no proton is present over this carbon. Indeed, the four resonances with reduced intensities in a 1D carbon spectrum do not show up the crosspeaks in the HSQC and HMQC spectra, confirming our preliminary assignment of these peaks as the quaternary carbons. Thus, the only protons directly connected to carbons produced the crosspeaks, whereas the quaternary carbons do not show correlations in this type of spectra. It should be noted, that HSQC and HMQC experiments provide the simplest way for the assignment of carbon resonances. For a proper interpretation of all identified correlations, it is convenient to collect the results in a table, as is shown in Figure 182, above.

2D HMBC spectra

The HMBC spectrum of **HL** is shown in Figure 184. As you can see, this spectrum looks similar to the HSQC and HMQC spectra. Indeed, HMBC is an HMQC experiment adjusted for the detection of smaller carbon-proton couplings in the range of 4-15Hz. This allows detection of correlations (crosspeaks) between a proton and distal carbons residing two, three, and even four chemical bonds away in the molecular skeleton. Therefore, the number of correlations corresponding to each proton in the HMBC spectra is much larger. This number depends on the number of carbon atoms residing within 2-3 chemical bonds of the proton of interest.
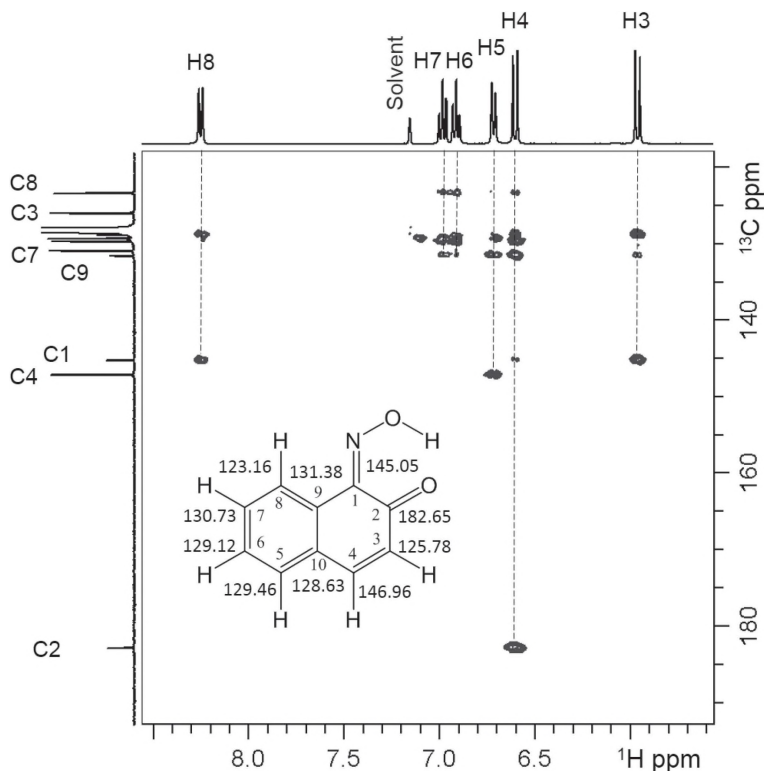
Figure 184. The HMBC spectrum of the **HL** in deuterobenzene, C_6D_6. Separately recorded 1D ^1H and ^{13}C NMR reference spectra are displayed on the top and left side of 2D spectrum respectively.

The HMBC experiment contains a special filter to minimize the contribution from one-bond correlations appearing in the HSQC/HMQC spectra. As a result, these correlations are significantly suppressed in the HMBC spectra. The long-range correlations for each proton can be easily identified by drawing vertical lines from the proton signals in the 1D reference spectrum on the top of the 2D spectrum. All detectable correlations for the selected proton can be found along this line, and collected in the table as a set of crosspeak coordinates. Similarly, lines drawn horizontally from each carbon in the 1D carbon reference spectrum intersect all crosspeaks which correlate the selected carbon with remote protons. You may notice significant variations in the relative intensities of

crosspeaks along the line drawn for each selected proton. The intensity of crosspeaks depends on the coupling constant value. The magnitude of possible long-range proton-carbon couplings is typically found between 0 and 15Hz. Therefore, it would be better to perform two experiments optimized for different coupling constants. For example, the first one may be optimized for 5Hz, while the second one for 10Hz couplings.

With the goal of minimizing the NMR time, it is reasonable to conduct one experiment with the average coupling constant value set as 8Hz. For aromatic systems, however, the two-bond couplings can have values between 40-50Hz, whereas three-bond couplings have 5-10Hz. Very often, the two-bond correlations do not show up in the spectra at all, or appear as a very weak crosspeaks.

Figure 185 is an expansion of the spectrum from Figure 184, and illustrates more clearly the identification of crosspeaks' coordinates in a crowded region of aromatic carbon signals. The line drawn from H3 proton parallel to the carbon axis intersects two strong crosspeaks and one weak crosspeak. As a rule, protons of aromatic fragments will give the strongest three-bond HMBC correlations in the spectra.

Now we need to identify all carbon signals that are three bonds away from H3. According to the structural formula of **HL**, there are only two carbons residing three bonds away from H3; these are C10 and C1. This is in agreement with the number of strong crosspeaks observed for H3 proton correlations on the map (Figure 185). Therefore, we can unambiguously assign crosspeaks with coordinates 128.63 and 145.05ppm to the quaternary carbons C10 and C1. It is pretty clear that the C1 carbon has a crosspeak at 145.05ppm, based on the characteristic chemical shift values of oxime carbon atoms connected to the more electron-withdrawing nitrogen atom. By the process of elimination, the second signal at 128.63ppm has to be assigned to the carbon C10.

There is an additional weak peak (w) at 131.38ppm, also corresponding to the quaternary carbon. Looking at the structural formula, and taking into account that two out of four quaternary carbons have been already assigned, this weak crosspeak could only be assigned to the carbon C9. Thus, we can observe four-bond coupling between H3 and C9, which is not unusual for conjugated aromatic systems. The line drawn from H4 intersects three strong crosspeaks corresponding to three-bond couplings between H4 and carbons with coordinates 129.46, 131.38 and 182.65ppm. In this case there are three carbons interacting through 3-bond distance; C5, C9, and C2.
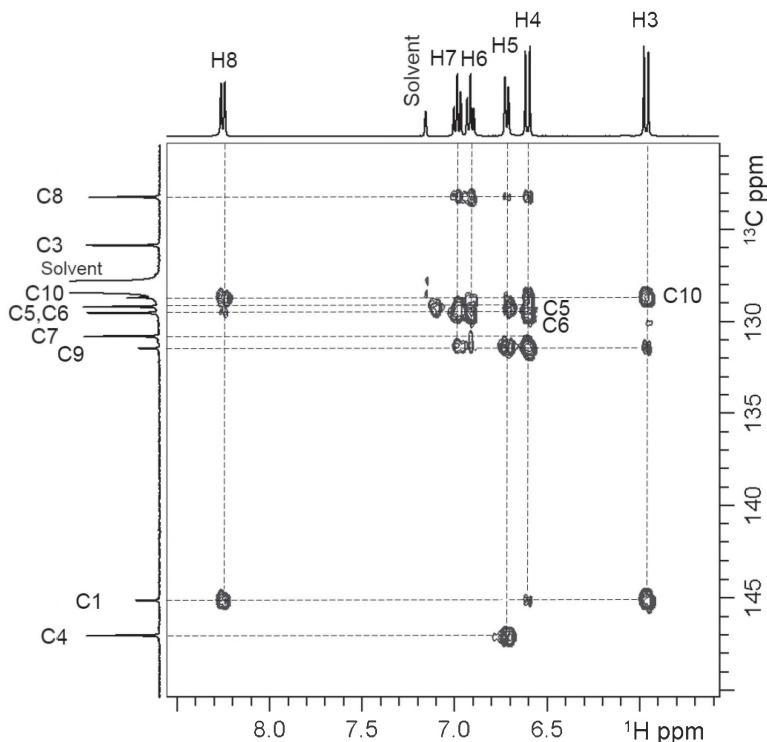
Figure 185. An extended fragment of the HMBC spectrum simplifies the extraction of crosspeaks' coordinates for **HL**.

Two out of these three signals belong to quaternary carbons with chemical shifts 131.38 and 182.65ppm. Evidently, a signal at 131.38ppm could be assigned to the carbon C9, because the signal at 182.65ppm belongs to the carbonyl carbon, based on its characteristic chemical shift value and was already assigned as discussed above. Additionally, for H4 we have one two-bond (128.63ppm) and one four-bond (145.05) correlation, with C10 and C1, correspondingly. Similarly, H5 correlated through multiple bonds with carbons: C8, C10, C6, C9, and C4. H6 correlated with carbons C8, C10, C5 and C9, H7 with carbons C8, C6, C5 and C9, and H8 with carbons C10, C5, and C1. All these results are collected in Table 9. Detailed analysis of the remaining correlations is not difficult, and can be done by the riders independently.

Now, students are assigned to verify and explain all identified correlations in the HMQC spectrum, displayed in Figure 182.

Table 9. Coordinates of crosspeaks in the 2D HMQC and HMBC spectra of the **HL**.

#	^{1}H δ, ppm	^{13}C δ, ppm	
		HMQC	HMBC
1			145.05
2			182.65
3	5.96	125.78	128.63 (C10), 131.38 (C9) w, 145.05 (C1)
4	6.58	146.96	123.16 (C8) w, 128.63 (C10), 129.46 (C5), 131.38 (C9), 145.05 (C1) w, 182.65 (C2)
5	6.71	129.46	123.16 (C8) w, 128.63 (C10) w, 129.12 (C6), 131.38 (C9), 146.96 (C4)
6	6.90	129.12	123.16 (C8), 128.63 (C10), 129.46 (C5), 131.38 (C9) w
7	6.98	130.73	123.16 (C8), 129.12 (C6), 129.46 (C5), 131.38 (C9)
8	8.27	123.16	128.63 (C10), 129.46 (C5) w, 145.05 (C1)
9			131.38
10			128.63

Finally, the existence of any unexplained correlations or crosspeaks could be due to incorrect hypotheses about the molecular structure of a compound of interest, or mistakes made during the extraction of crosspeaks from the spectrum. Thus, the HMBC NMR experiment allows the identification of long-range C-H correlations, which provide unique information about the skeleton of a molecule, and can be recognized as a powerful tool for the structure elucidation of small molecules.

Lastly, the diagram presented in Figure 186 can serve as a most compact presentation of data obtained from the HMBC experiment for **HL**.
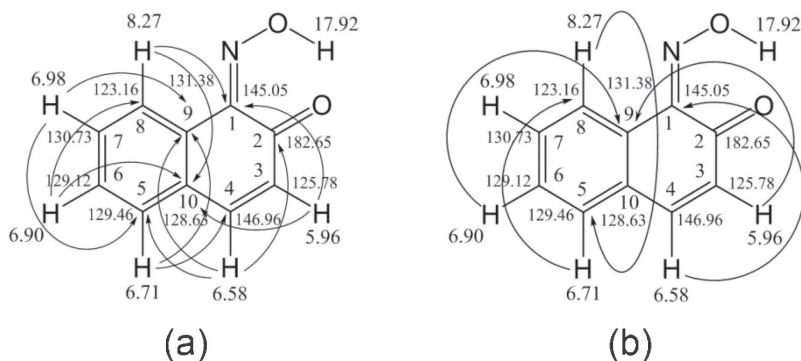
Figure 186. Strong three-bond NMR correlations of the **HL** (**a**), and much weaker four-bond correlations (**b**). Important long-range correlations from HMBC spectrum used for the assignment of carbon resonances, are shown by curved arrows.

The combination of 1D ^{1}H and ^{13}C NMR spectra with homonuclear and heteronuclear 2D NMR spectra often provides sufficient information for an unambiguous assignment of all observed resonances and completes the structure elucidation of small molecules.

3.14. The 2D NMR Spectra of *tris*-chelate complexes of Co(III) with 1-nitroso-2-naphthol: Analysis and Interpretation

3.14.1. Analysis and Interpretation of the 1D ^{1}H NMR spectra of the Co-complex mixture and individual separated isomers

Figure 187 displays the comparison between 1D ^{1}H NMR spectra of free ligand, the mixture of isomers, and the chromatographically separated *mer*- and *fac*-isomers of CoL$_3$.

First of all, one can clearly differentiate the spectra by the presence of signal sets for individual protons. For example, the most downfield, well-separated resonance signal corresponding to the proton H8 in the free ligand (Figure 187**a**) appears in the spectrum on panel **b** as four similar peaks with nearly equal abundance. On panel **c,** this resonance appears as three identical peaks, also with equal abundance. On panel **d**, H8 resonance exists as a single peak, similar to panel **a** representing the NMR spectrum of free **HL**. You can observe exactly the same behavior

for well-separated upfield resonances assigned earlier to the H3 and H4 protons. The other resonances demonstrate severe overlapping in 1D NMR spectra and cannot be used for detailed analysis. Taking into account that the *fac*-isomer due to the axis C_3 has three equivalent chelated ligands, with six magnetically nonequivalent protons, only one set of these resonances should be expected in the ^{1}H NMR spectrum.
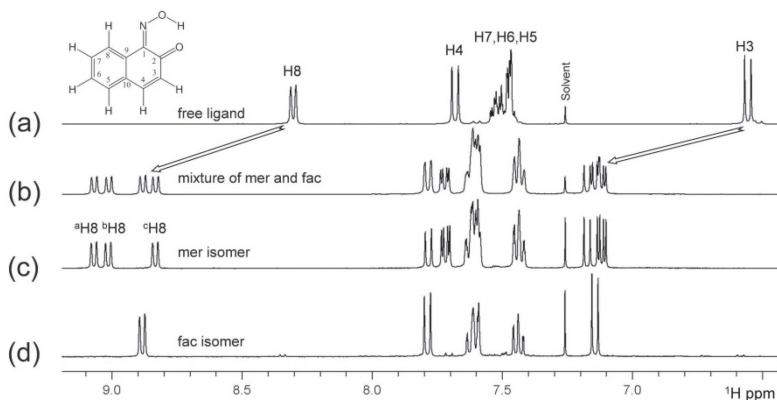

Figure 187. ^{1}H NMR spectra (aromatic region) of (**a**) free **HL**, (**b**) mixture of the *mer*- and *fac*-isomers of CoL$_3$, (**c**) the *mer*-isomer, and (**d**) the *fac*-isomer in CDCl$_3$ at 300° K.

In the case of the *mer*-isomer characterized by the lack of symmetry (only axis C_1), the NMR-equivalency between three ligands is absent, and a triplicate set of resonances should be expected. Consequently, four sets (1+3) of resonances should exist in the spectrum of the *mer*- and the *fac*-isomers mixture obtained from the synthesis. Indeed, this is the case (see Figure 187 **b**). Thus, the spectrum with the single set of resonances (panel **d**) can be safely assigned to the CoL$_3$ *fac*-isomer. The spectrum with three sets of peaks (panel **c**) belongs to the *mer*-isomer, and the spectrum with four sets of peaks (panel **b**) belongs to the nearly statistical 3:1 mixture of the *mer*- and *fac*-isomers with four different ligand environments of equal abundance. The equal abundance of four inequivalent environments in the mixture of isomers (panel **b**) is clearly demonstrated by the equal integral intensities of peaks corresponding to the proton H8.

You may also notice changes in the resonance peaks' positions in the spectra of isomers with respect to the free ligand. These chemical shift changes of ligand NMR signals are indicative of complex formation.

Analysis of *complexation-induced chemical shifts* (CIS) can provide important information about the affinity of ligands, location, and strengths of binding or complexation events, as well as the structure of complexes. As a rule, this analysis requires the unambiguous resonance assignments of both proton and carbon signals in the spectra of inorganic complexes. Obviously, 2D NMR spectroscopy will also be a proper and powerful tool for the structure elucidation of inorganic complexes. Keeping in mind that the simplest way to learn NMR spectra interpretation is to practice the assignment of peaks for a known structure, we will try to assign the resonance peaks in the 2D NMR spectra of CoL_3.

3.14.2. Analysis of *homonuclear* 2D NMR spectra: 2D COSY, NOESY and JRES spectra of the *mer*-CoL_3

Figure 188 represents the ^1H-^1H COSY spectrum of the *mer*-CoL_3 dissolved in $CDCl_3$. As in the case of the COSY spectrum analysis for the free ligand **HL** presented earlier, our first task will be to track the only three-bond mediated vicinal couplings between protons.
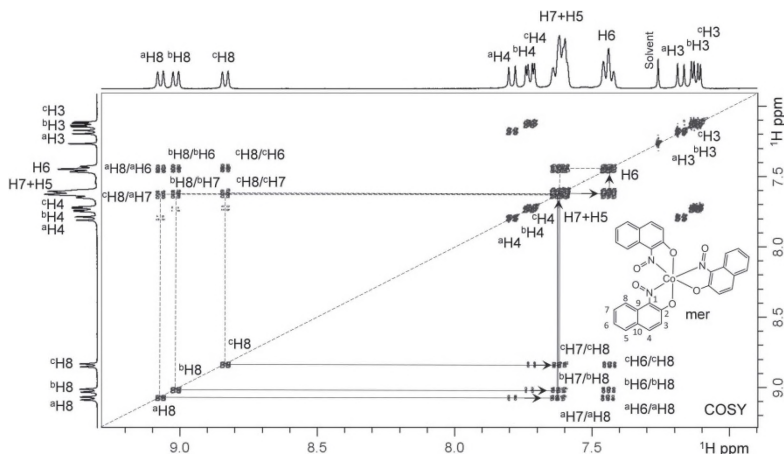
Figure 188. The 2D COSY spectrum of the mer-CoL_3 with details of diagonal – crosspeak – diagonal walking procedure for the identification of correlations between $^{a,b,c}H8$ and $^{a,b,c}H7$ protons.

As said above, for the *mer*-isomer we observe three sets of ligand proton resonances. We can label these sets of signals, as corresponding to three different geometrical positions of the same ligand within the coordination sphere of cobalt ion, as *set a*, *set b*, and *set c*. One can see that only three out of six resonances demonstrate well-resolved triplicate sets of doublets. We can use our previous assignment results for the free ligand as a starting point in the assignment procedure for complexes. Based on this, the well separated triplicate sets presumably belong to the protons H8, H4, and H3.

To confirm this assignment of peaks, a complete analysis of homonuclear 2D NMR spectra for the *mer*-CoL$_3$ is required. Important fragments of the COSY spectrum are zoomed in on, and presented in Figures 189 and 190, to provide the possibility of clear analysis in crowded regions. Starting from the most downfield resonance, which can be safely assigned to the [a]H8 proton (Figure 188), we follow horizontally to the right along the solid line, and observe the connectivity of the [a]H8 peak to several crosspeaks of various intensities.
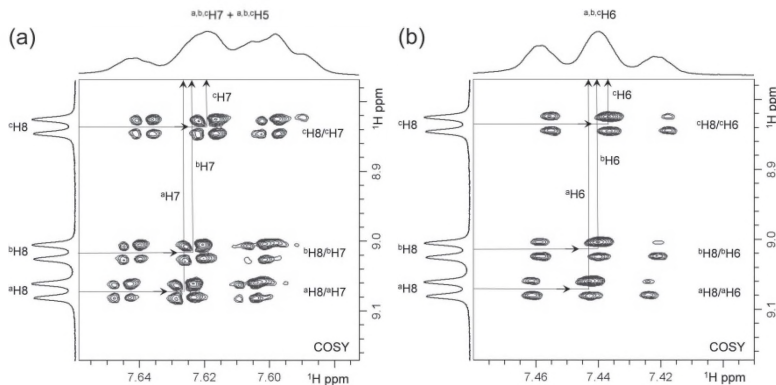
Figure 189. Expanded fragments of COSY spectrum for mer-CoL$_3$ demonstrating an accurate identification of correlations between (**a**) [a,b,c]H8 and [a,b,c]H7 and (**b**) [a,b,c]H8 and [a,b,c]H6 protons.

In this case, the correct choice of vicinal partner for the H8 proton may be done easily with the help of the NOESY spectrum (Figure 191). Similarly to the COSY spectra analysis, the [a]H8 proton will be a good starting point to begin the analysis of through-space correlations.
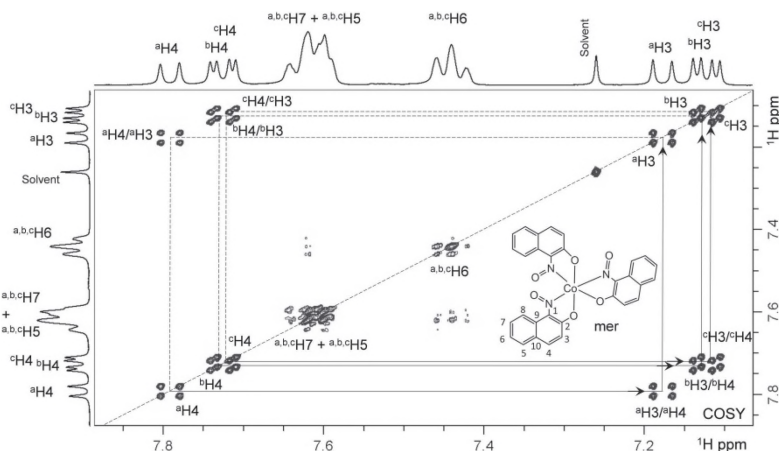
Figure 190. Expanded fragment of COSY spectrum for mer-CoL₃ demonstrating fine details of diagonal–crosspeak–diagonal walking procedure for the identification of correlations between [a,b,c]H4 and [a,b,c]H3 protons.

Upon drawing the horizontal and vertical lines from each crosspeak toward the diagonal, the lines should intersect the two diagonal peaks of the spatially proximal pair of protons. Alternatively, moving right horizontally from the specific diagonal peak toward the crosspeak, stopping at this crosspeak, and then moving up vertically back to the diagonal, will also identify spatially proximal protons. Following the latter procedure, it is easy to find a NOE crosspeak between [a]H8 and a triplet signal at 7.63ppm. Therefore, the diagonal peak at 7.63ppm could be definitely assigned to the [a]H7 proton, which is spatially proximal to the [a]H8 proton, according to the structural formula. Based on the NOESY spectrum analysis, we have to stop at the crosspeak with coordinate 7.63ppm in our COSY walking procedure starting from the proton [a]H8. Thus, the COSY crosspeak with the triplet fine structure at 7.63ppm represents a vicinal correlation between the [a]H8 and [a]H7 protons. We have only two triplet resonances in one set of peaks corresponding to one ligand position within the cobalt ion coordination sphere.

Therefore, by process of elimination, the second crosspeak with the triplet fine structure could be definitely assigned to the correlation between [a]H8 and [a]H6 protons through four chemical bonds. Now we continue our walk, and from the crosspeak between the [a]H8 and [a]H7 protons, we go straight up, returning back to the diagonal at the position of peak [a]H7. According to the structural formula of deprotonated **L**⁻, the

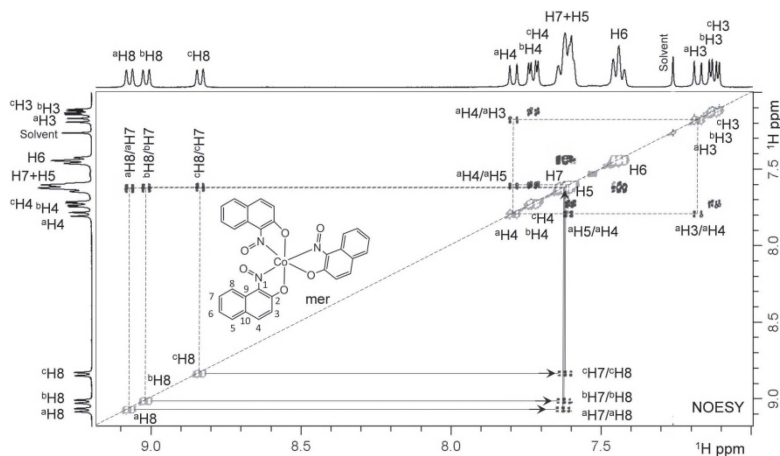second vicinal partner of the ᵃH7 proton is ᵃH6, which also appears in the NMR spectra as a triplet resonance.

Figure 191. The 2D NOESY spectrum of the mer-CoL₃ demonstrating the identification of through-space correlations between pairs of ᵃ,ᵇ,ᶜH8 - ᵃ,ᵇ,ᶜH7, ᵃH4 - ᵃH5 and ᵃH4-ᵃH3 protons. See centerfold for this image in colour.

The next step will be to move from the ᵃH7 diagonal peak to the right, and stop at the crosspeak, with the triplet fine structure at 7.44ppm obviously representing a vicinal correlation between the ᵃH7 and ᵃH6 protons, as we have already provided a definite assignment of the ᵃH6 resonance. From this crosspeak we move straight up, and again return to the diagonal, but now at the position corresponding to the proton ᵃH6. At this moment we can clearly realize that proton ᵃH5, as a second vicinal partner of the ᵃH6 proton, is heavily overlapped with the ᵃH7 signal. This will prevent the correct identification of the ᵃH5 peak position from the COSY spectrum. A similar walking procedure can also be used for the remaining b and c sets of resonances.

The detailed identification of ᵃ,ᵇ,ᶜH7 and ᵃ,ᵇ,ᶜH6 crosspeaks coordinates in the crowded spectral regions, for three different sets of resonances, is presented in Figure 189. One can clearly see that the multiplets of these resonances, which are heavily overlapped in the 1D spectrum on the top of the 2D spectrum, could be observed in COSY as well-separated peaks. This is because the overlapping of diagonal peaks does not necessarily line up all the crosspeaks. The remaining well-

separated crosspeaks with the doublet fine structure in the COSY spectrum (Figure 188) obviously belong to the three sets of resonances from protons H3 and H4.

The tentative assignment of these resonances in the COSY spectrum can be confirmed by a 2D NOESY experiment (Figure 191). The H4 proton is expected to show the through-space correlations with two adjacent protons, H3 and H5, whereas the H3 proton should show this type of correlation with only one proton. Inspection of a 2D NOESY spectrum shows that, indeed, the peak at 7.79ppm demonstrates correlations with two signals, whereas the peak residing at 7.18ppm shows only one correlation. For simplicity, the lines are drawn only for the correlations $^aH4$-$^aH3$ and $^aH4$-$^aH5$.

Thus, the NOESY spectrum allows us to distinguish unambiguously between the H3 and H4 doublet resonances. With this definite assignment of H4 and H3 protons, we can complete the identification of correlations between them for three different sets of resonances in the COSY spectrum. Expansion of a COSY spectrum fragment containing the details of diagonal-crosspeak-diagonal walking for H4 and H3 protons is presented in Figure 190. Starting from the diagonal peak at 7.79ppm ($^aH4$) we are moving right, toward the corresponding crosspeak, and then straight up back to the diagonal peak at 7.18ppm ($^aH3$).

Similarly, the crosspeaks' coordinates can be identified for the protons ($^{b,c}H4$) and ($^{b,c}H3$). However, for proton H5 resonances, we cannot observe separated peaks in a 2D COSY spectrum. A well-separated H4 proton signal in a 1D spectrum is not a vicinal partner of H5, and there are no detectable crosspeaks between these two protons, due to the potential long-range (four bond) coupling in a COSY spectrum. However, due to the spatial proximity of H5 and H4 protons, we can expect the existence of a through-space correlation between them in the NOESY spectrum. Indeed, the NOESY spectrum (Figure 192) clearly demonstrates the existence of through-space correlations between protons $^{a,b,c}H5$, which are heavily overlapped with $^{a,b,c}H7$ protons in a 1D spectrum, and well-separated $^{a,b,c}H4$ protons. The same standard diagonal-crosspeak-diagonal walking procedure in the expanded region of a NOESY spectrum is applicable for the identification of $^{a,b,c}H5$ protons' crosspeaks.
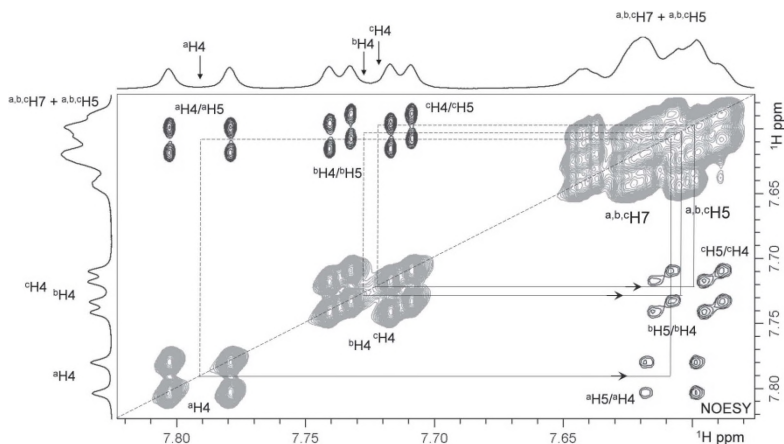
Figure 192. Expanded fragment of the 2D NOESY spectrum for the *mer*-CoL₃, demonstrating the identification of through-space correlations between ^{a,b,c}H4 and ^{a,b,c}H5 protons. See centerfold for this image in colour.

The 2D JRES spectrum of the *mer*-CoL₃ is presented in Figure 193. One can see that this type of 2D experiment achieved a complete separation of chemical shifts and J-couplings along two dimensions. The projection along the chemical shift axis represents a decoupled (absence of the proton-proton interactions) spectrum of the *mer*-CoL₃, which significantly simplifies a regular 1D NMR spectrum, and allows straightforward and quick identification of chemical shifts, coupling patterns, and J couplings. The unique potential for an accurate extraction of these parameters from the expanded fragment of 2D JRES spectrum of CoL₃ is demonstrated in Figure 193**b**. The chemical shift and J coupling values for all 18 proton resonances derived from 2D COSY and NOESY spectra can be verified, corrected, or completed, with the help of 2D JRES spectra.

Thus, the combination of 2D COSY, NOESY and JRES spectral data allowed the complete and unambiguous assignments of all proton resonances for three different geometrical positions of the same ligand in the *mer*-isomer of the CoL₃. The results obtained from the homonuclear 2D NMR spectra at 300° K are collected in Table 10.
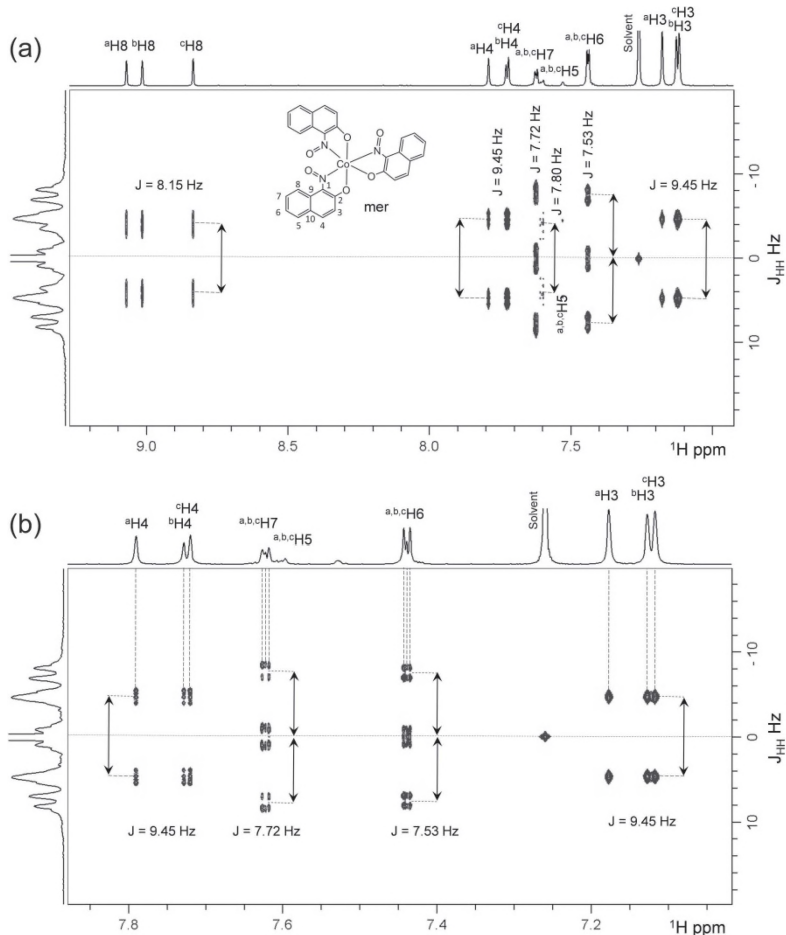
Figure 193. (**a**) The 2D ^{1}H-^{1}H JRES spectrum of the *mer*-CoL$_3$. Corresponding 1D projection along the chemical shift axis is shown on the top of the 2D spectrum; (**b**) expanded fragment of the same spectrum demonstrating an accurate determination of chemical shifts and J couplings.

Table 10. Proton chemical shift values for the *mer*-CoL₃ complex derived from the homonuclear 2D NMR spectra.

#	¹H δ, ppm		
	Ligand a	Ligand b	Ligand c
3	7.176	7.126	7.117
4	7.791	7.728	7.720
5	7.607	7.604	7.597
6	7.443	7.440	7.436
7	7.625	7.622	7.618
8	9.070	9.015	8.835

3.14.3. Practical considerations for the 1D ^{13}C NMR spectra of individual *fac*- and *mer*- isomers of CoL₃

Figure 194 shows the comparison between the 1D ^{13}C{^{1}H} NMR spectra of free ligand **HL**, and chromatographically separated individual *mer*- and *fac*-isomers of the CoL₃. The ligand has ten chemically different carbon atoms, so ten signals are observed in its ^{13}C{^{1}H} NMR spectrum. Because of the higher symmetry of the *fac*-isomer (C₃), the complex has three equivalent chelate ligands with ten magnetically nonequivalent carbons. Hence, the presence of ten resonance peaks in the ^{13}C proton decoupled NMR spectrum is expected. In fact, it was clearly shown in Figure 194**c**.

In the spectrum of the *mer*- isomer, which has no symmetry (C₁), up to 30 carbon resonances (3 sets) should be expected, due to the nonequivalency of three ligands. In fact, as is seen from Figure 194**b**, the ^{13}C{^{1}H} NMR spectrum of the *mer*-isomer consists of almost 30 resonance lines (3 sets of resonances). Each set corresponds to one of three ligands in the coordination sphere of cobalt ion.

The higher symmetry *fac*-isomer has 10 resonance lines (1 set), which evidence the equivalency of three coordinated ligands (Figure 194**c**). The coordination of ligands to cobalt ion caused substantial chemical shifts for carbon atoms resonances of the oxime and carbonyl groups residing at the positions 1 and 2 (Figure 194).

The 1D ^{13}C NMR spectra of individual *mer*- and *fac*-isomers will be used as reference spectra for 2D heteronuclear NMR experiments.
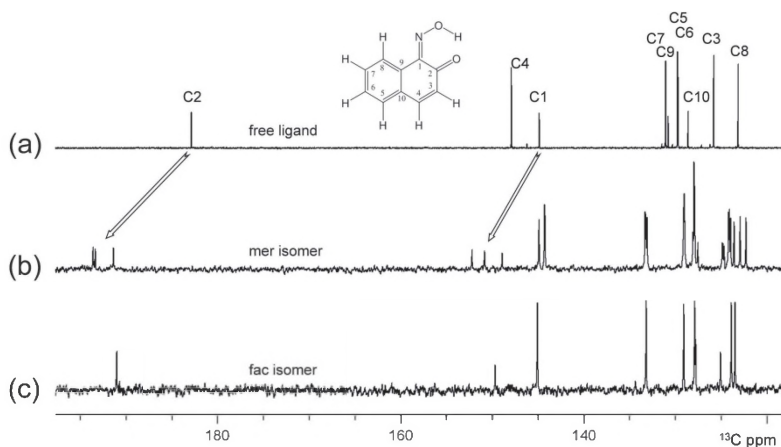
Figure 194. The $^{13}C\{^{1}H\}$ NMR spectra with broadband proton decoupling of: (**a**) free **HL**; (**b**) the *mer*-isomer of the CoL$_3$; and (**c**) the *fac*-isomer of the CoL$_3$ in CDCl$_3$ at 300° K.

3.14.4. Analysis of *heteronuclear* 2D NMR spectra: 2D HSQC, HMQC and HMBC spectra of the *mer*-CoL$_3$

As we have already learned, the chemical structure elucidation of small molecules requires complete assignment of carbon resonances in the NMR spectra, in addition to the assignment of proton resonances. This goal could be achieved with the help of 2D heteronuclear correlation experiments, such as 2D HSQC/HMQC and HMBC. In this part of this chapter we will go through the full procedure of carbon NMR resonance assignment for the *mer*-CoL$_3$, which was chosen as a good teaching and training example.

Figure 195 shows the HSQC and HMQC spectra of the *mer*-CoL$_3$. Previously recorded 1D regular proton and carbon spectra of the *mer*-CoL$_3$ will be used for the positioning of crosspeaks in 2D NMR spectra. The dimension F1 in the 2D spectra of CoL$_3$ contains reference carbon signals, whereas dimension F2 contains reference proton signals. As was demonstrated for the case of the free ligand, the carbon resonance assignment procedure suggests a straightforward identification of crosspeaks' coordinates, in ppm, from the 2D heteronuclear spectra. Drawing vertical lines from proton resonances in the 1D spectrum on the top, and horizontal lines from carbon resonances in the 1D spectrum on the left side of 2D spectra, will help to identify the positions of all crosspeaks. The lines would intersect exactly at the positions of crosspeaks' correlating
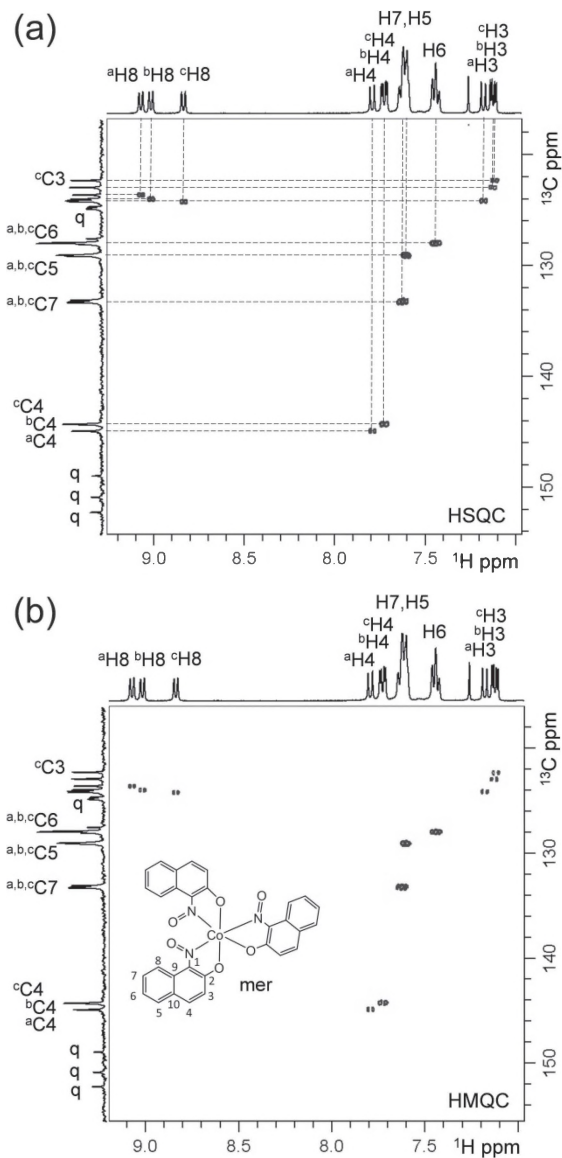
Figure 195. (**a**) The HSQC spectrum of the *mer*-CoL₃ with identified proton-carbon correlations; (**b**) The HMQC spectrum of the *mer*-CoL₃ recorded with similar parameters for comparison.

proton-carbon pairs. Because the only protons directly connected to the carbons produced the crosspeaks, the only one correlation for each of protons exists in the HSQC /HMQC spectra, and the quaternary carbons are not observed.

The extended fragment of 2D HSQC NMR spectrum for the *mer*-CoL_3 (Figure 196) demonstrates, in detail, the carbon resonances assignment procedure, and an accurate determination of crosspeaks' coordinates. All the proton-carbon correlations identified from HSQC/HMQC spectra are collected in Table 11.

Table 11. Proton-carbon one-bond correlations for the *mer*-CoL_3 complex derived from the 2D HSQC/HMQC NMR spectra.

#	^1H, ^{13}C δ, ppm					
	Ligand a		Ligand b		Ligand c	
3	7.176	124.065	7.126	122.874	7.117	122.246
4	7.791	144.854	7.728	144.255	7.720	144.216
5	7.607	129.067	7.604	128.988	7.597	128.955
6	7.443	128.029	7.440	127.921	7.436	127.840
7	7.625	133.267	7.622	133.171	7.618	133.037
8	9.070	123.553	9.015	123.923	8.835	124.152

The HMBC spectrum of the *mer*-CoL_3 is shown in Figure 197. From this spectrum we can identify the correlations (crosspeaks) between all the protons and distal carbons residing two, three, and four chemical bonds away in the skeleton of the molecule. Therefore, the number of correlations corresponding to each proton in this spectrum depends on the number of carbon atoms residing within 2-3 chemical bonds from the proton. Drawing the vertical line from each proton signal in the 1D reference spectrum on the top of the 2D HMBC spectrum allows the identification of long-range correlations for protons. Similarly, the line drawn horizontally from each carbon peak in the 1D carbon reference spectrum intersects all crosspeaks which correlate a selected carbon with remote protons.

Figure 198 shows the expanded fragment of HMBC spectrum from Figure 197 and provides greater accuracy for the identification of crosspeak coordinates in the crowded regions. The assignment of the quaternary carbons can be accomplished by the analysis of the strongest three-bond HMBC correlations. For example, the line drawn from the signal corresponding to the proton [a]H3, parallel to the carbon axis, intersects two strong crosspeaks.

The only [a]C10 and [a]C1 carbons reside three bonds away from a proton [a]H3, according to the structural formula of L^-. Therefore, we can definitely assign the crosspeaks with coordinates 127.498 and 152.172ppm to the quaternary carbons [a]C10 and [a]C1. Obviously, the crosspeak at 152.172ppm belongs to the correlation of the [a]H3 proton with [a]C1 carbon, based on the characteristic chemical shift value of oxime carbons. The crosspeak at 127.498ppm should be assigned to carbon [a]C10, by process of elimination. The same analysis is applicable for [b]H3-[b]C10, [b]H3-[b]C1, [c]H3-[c]C10 and [c]H3-[c]C1 correlations. The line drawn from the peak of [a]H4 proton intersects three strong crosspeaks, corresponding to three-bond couplings between [a]H4 and carbons with coordinates 124.830, 128.960, and 193.350ppm. In this case, there are three carbons which can interact with [a]H4, via three chemical bonds. They are [a]C5, [a]C9, and [a]C2 carbons. Two out of three are quaternary carbons, with chemical shifts 124.830 and 193.350ppm. Definitely, the peak at 124.830ppm could be assigned to the carbon [a]C9, because the peak at 193.350ppm belongs to the carbonyl carbon [a]C2, based on its characteristic chemical shift value.

Again, the same analysis is applicable for [b]H4-[b]C9, [b]H4-[b]C2, [c]H4-[c]C9 and [c]H4-[c]C2 correlations. Thus, all 12 quaternary carbons for the *mer*-CoL$_3$ complex could be unambiguously assigned with the help of the HMBC spectrum. All detectable correlations for protons of the *mer*-CoL$_3$ were identified along the lines, and collected in Table 12 as a set of crosspeak' coordinates.
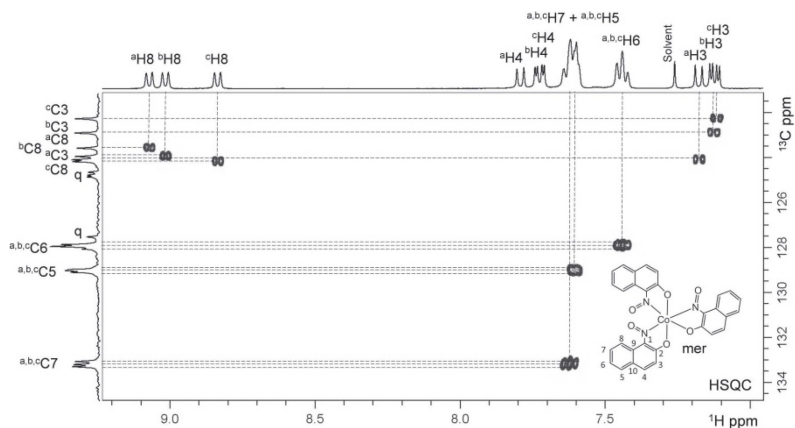
Figure 196. Expanded fragment of the 2D HSQC spectrum for the *mer*-CoL₃ demonstrating the identification of proton-carbon correlations in details.

Therefore, this tedious description of analysis and interpretation of the NMR spectra of the ligand and its diamagnetic metal complex is over. We have presented in this chapter a very decent (in our opinion) example of ligand and complexes. The combination of *homo-* and *heteronuclear* 2D NMR spectral data allows complete and unambiguous proton and carbon resonance assignments, and provides the basis for efficient structure elucidation of small inorganic complexes.

We hope that students and interested readers have followed our explanations and learned the principles of how to carry out this scrupulous, but unambiguous analysis of spectra.

In the next and last part of this chapter we present several spectra of the *fac*-isomer of the CoL₃, and students will have to practise the methods they have learned, and develop skills for the interpretation of spectra.
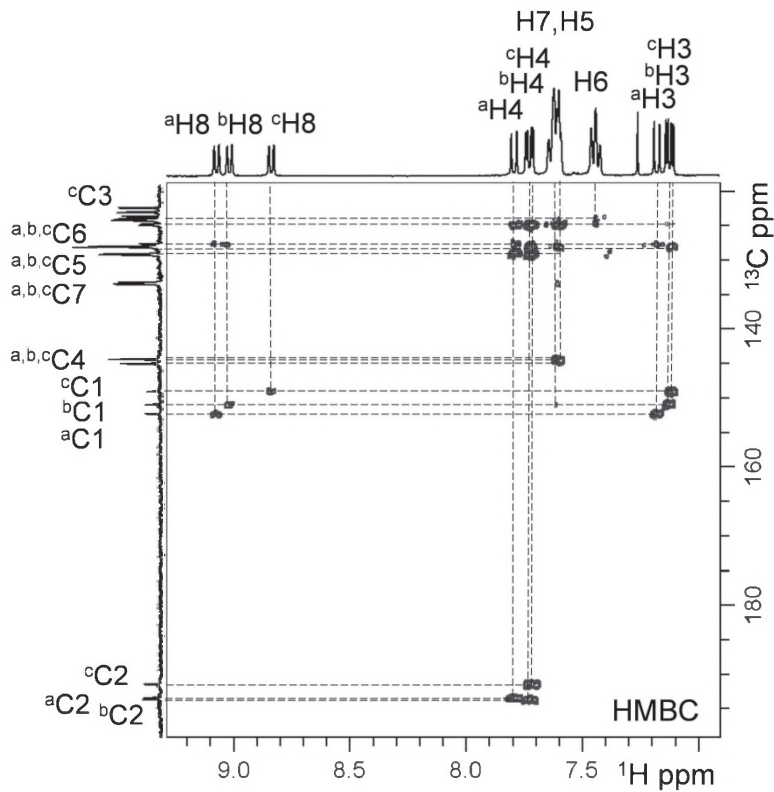
Figure 197. The 2D HMBC spectrum of the mer-CoL$_3$ in CDCl$_3$ demonstrating the identification of long-range proton-carbon correlations.
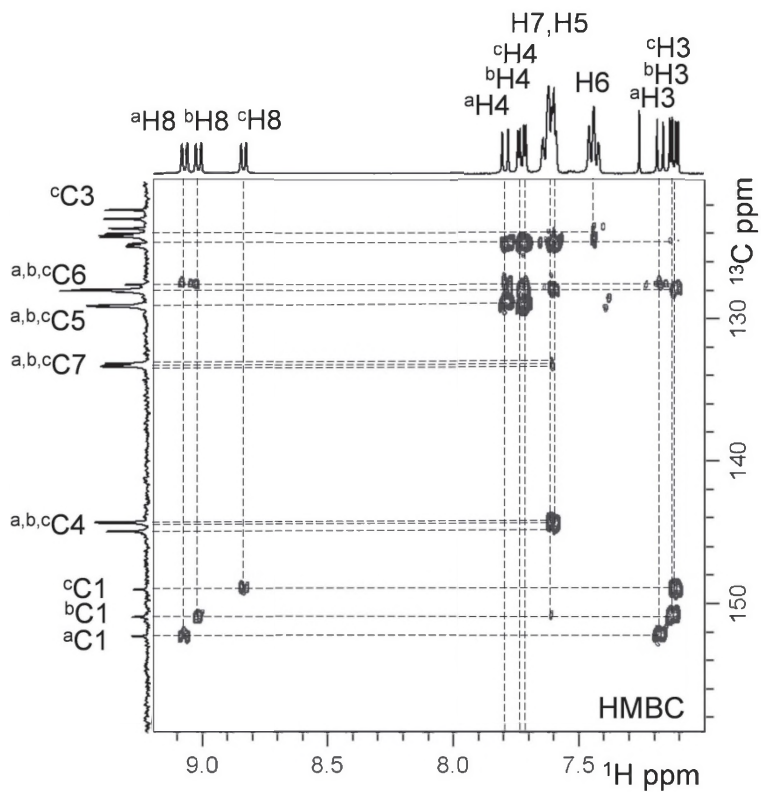
Figure 198. Expanded fragment of the 2D HMBC spectrum simplifies the extraction of long-range proton-carbon correlations for the *mer*-CoL₃.

**Table 12.** The crosspeaks' coordinates in the 2D HMQC and HMBC spectra of CoL$_3$.

#	^{1}H δ, ppm		^{13}C δ, ppm	
			HMQC	HMBC
1	a b c			152.172 150.811 148.884
2	a b c			193.346 193.591 191.358
3	a b c	7.176 7.126 7.117	124.065 122.874 122.246	127.500 (C10), 152.176 (C1) 127.845 (C10), 150.816 (C1) 128.032 C10), 148.889 (C1)
4	a b c	7.791 7.728 7.720	144.854 144.255 144.216	124.830 (C9), 193.350 (C2), 128.960 (C5), 127.500 (C10) 124.750 (C9), 193.592 (C2), 128.992 (C5), 127.845 (C10) 124.624 (C9), 191.360 (C2), 129.068 (C5), 128.032 (C10)
5	a b c	7.607 7.604 7.597	129.067 128.988 128.955	
6	a b c	7.443 7.440 7.436	128.029 127.921 127.840	123.553 (C8) 123.923 (C8) 124.152 (C8)
7	a b c	7.625 7.622 7.618	133.267 133.171 133.037	124.830 (C9), 127.500 (C10), 144.854 (C4) 124.750 (C9), 127.845 (C10), 144.255 (C4) 124.624 (C9), 128.032 (C10), 144.216 (C4)
8	a b c	9.070 9.015 8.835	123.553 123.923 124.152	127.500 (C10), 152.176 (C1) 127.845 (C10), 150.816 (C1) 128.032 (C10), 148.889 (C1)
9	a b c			124.825 124.745 124.621
10	a b c			127.498 128.032 127.842

3.14.5. Practical Exercise: Assignment of all signals in 1D and 2D NMR Spectra of the *fac*-isomer of CoL₃.
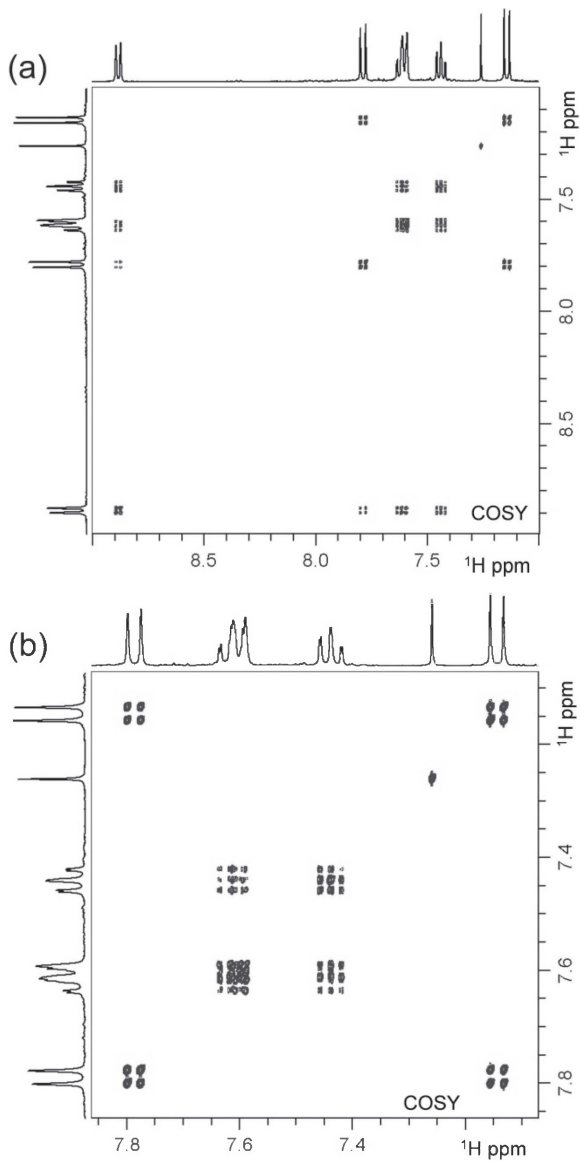
Provide complete proton and carbon resonance assignments for the *fac*-isomer of CoL₃ using NMR spectra provided here and recorded during your laboratory practice.
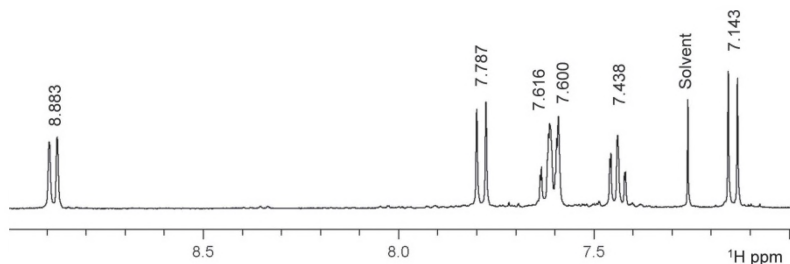
A. The ¹H NMR spectrum of the *fac*-CoL₃ in CDCl₃ at 300°K.
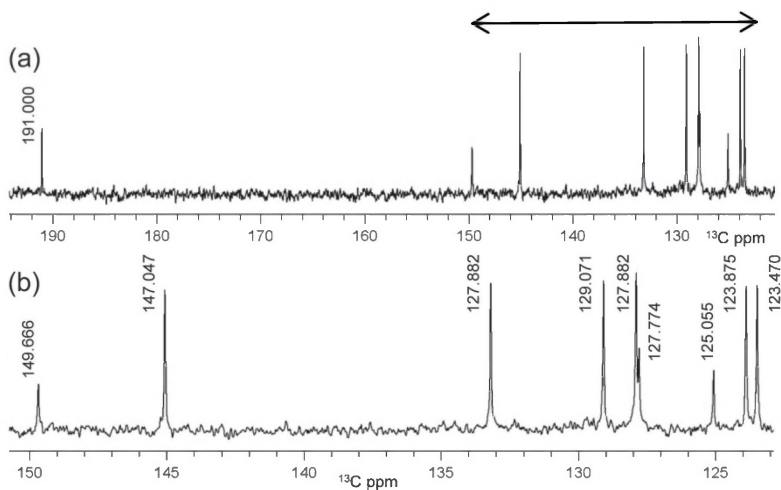
B. The ¹³C{¹H} NMR spectrum of the *fac*-CoL₃ in CDCl₃ at 300°K (**a**), and (**b**), expanded fragment of this spectrum in the region shown by arrows.

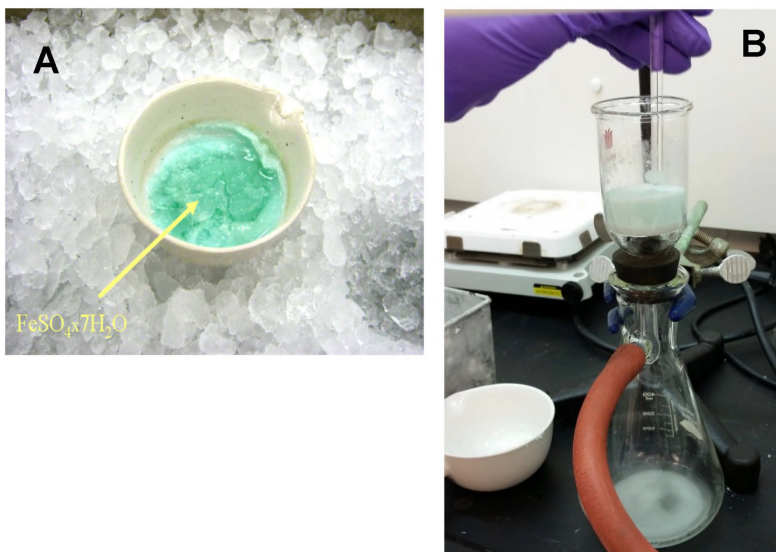**C.**   The 2D COSY spectrum of the *fac*-CoL₃ in CDCl₃ at 300°K (**a**), and (**b**), expanded fragment of this spectrum.

Figure 92. Crystallization of FeSO$_4$ heptahydrate on an ice bath (**A**) and filtration of the salt (**B**).

Figure 95. Initial solution of Cu^{2+} acetate.

Figure 96. The reaction mixture after addition of hydrazine hydrate, purged with N$_2$ and cooled to room temperature.

Figure 97. Test tubes with Cu₂O precipitate after first centrifugation.

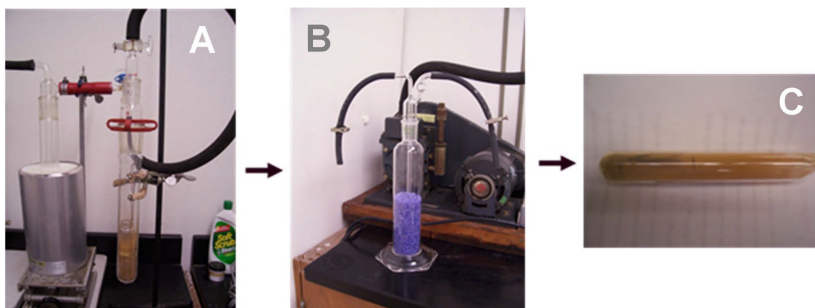**Figure 98.** Gravity filtration of the reaction mixture using dense and thick paper filter.

Figure 112. Drying of anhydrous nickel(II) chloride using an oil pump and cold trap filled with liquid nitrogen (**A**). Drying tower filled with silicagel used for letting dry air into the system after anhydrous salt drying (**B**). The final product is sealed in an ampoule under nitrogen (**C**).
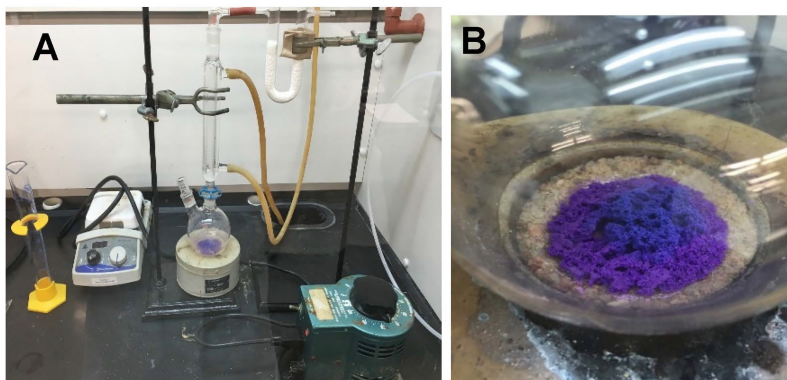
Figure 114. Assembled apparatus for the preparation of anhydrous $CoCl_2$ using a sand bath and variak for temperature regulation (**A**), and the appearance of the final product at the end of the reaction, with only traces of $SOCl_2$ left in the flask (**B**).

Figure 145. Proper loading of the 'wet' packed column: gloves, a pipette, and careful addition of Co(III) solution on the wet top of the column for separation.

Figure 147. Flasks with column-separated pure isomers of (Co(1NO-2OH))$_3$: *mer* is in the left flask, *fac* is in the right flask.
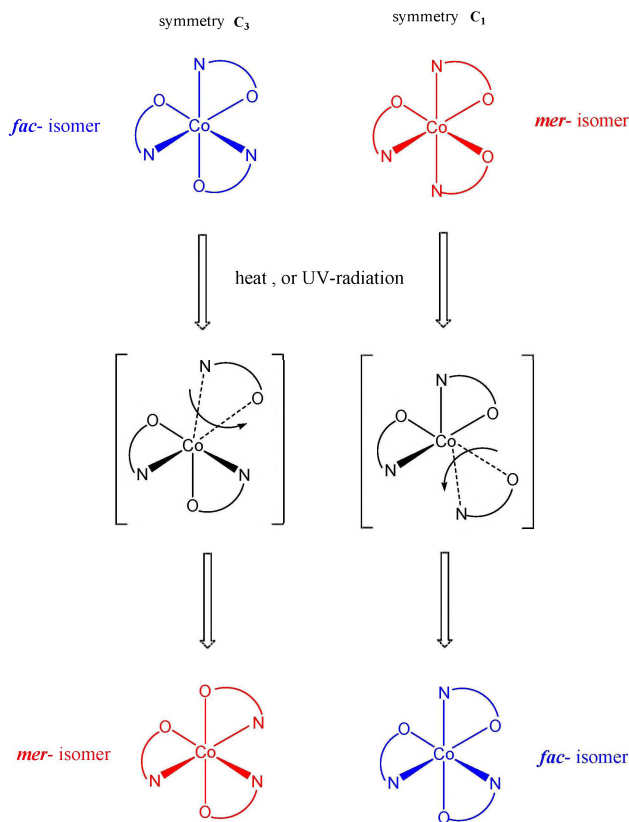

Figure 153. Point group symmetries of individual isomers in CoN$_3$O$_3$ environment and the re-isomerization path.
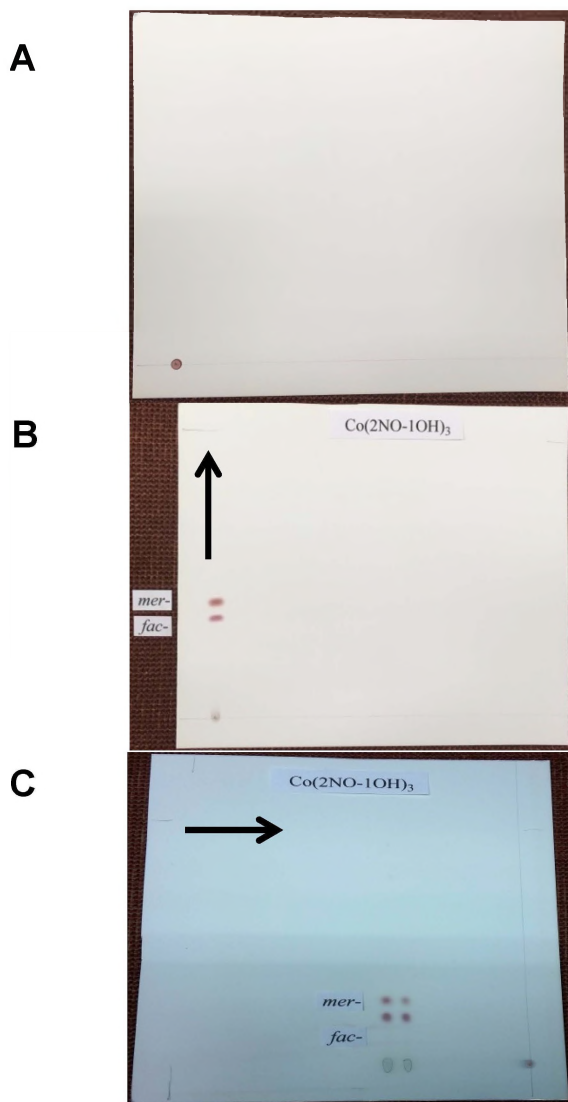
Figure 156. Detailed description of the thermal re-isomerization of Co(2NO-1OH)$_3$ explaining the appearance of the 'magic square' on the TLC plate. **A** - an initial spot with the mixture of isomers; **B** - separation of geometrical isomers in the *first* dimension shown by an arrow; **C** - re-appearance of complementary isomers in the *second* dimension, after thermal treatment in vacuum.
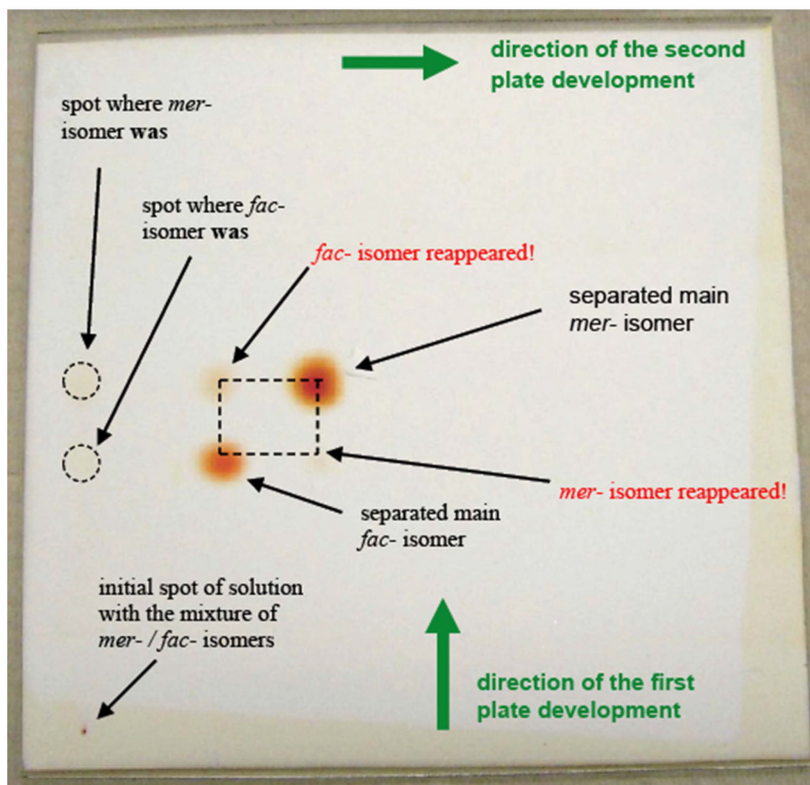
Figure 157. Thermal re-isomerization of pure, separated *mer-* and *fac*-isomers of Co(1NO-2OH)₃ leading to the appearance of the 'magic square' on the TLC plate.
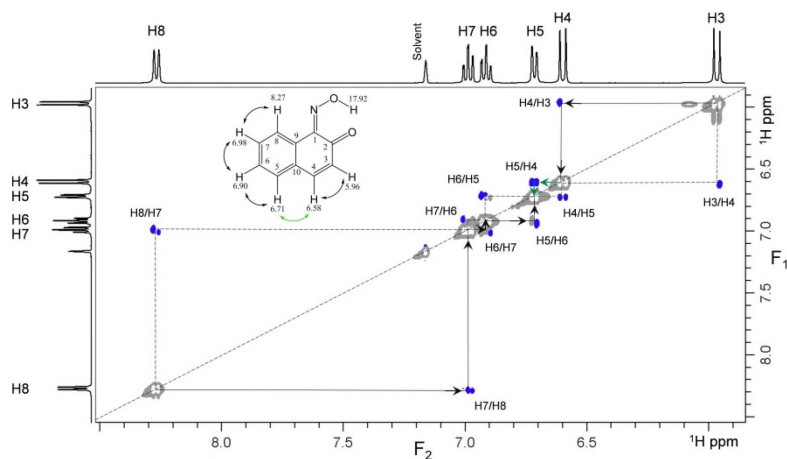
Figure 179. The 2D NOESY spectrum of **HL**. The main diagonal peaks are phased as negative (gray color). The crosspeaks due to NOE interactions appear in the opposite sign to the diagonal peaks (blue color). Positive NOE interactions between atoms in the ortho positions are shown as black arrows on the structural formula of **HL**, and other positions as green.

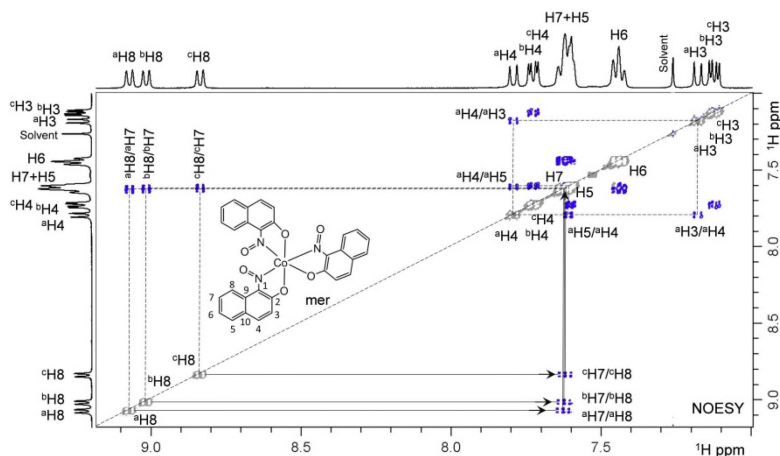**Figure 191.** The 2D NOESY spectrum of the mer-CoL$_3$ demonstrating the identification of through-space correlations between pairs of ^{a,b,c}H8 - ^{a,b,c}H7, ^{a}H4 - ^{a}H5 and ^{a}H4-^{a}H3 protons.
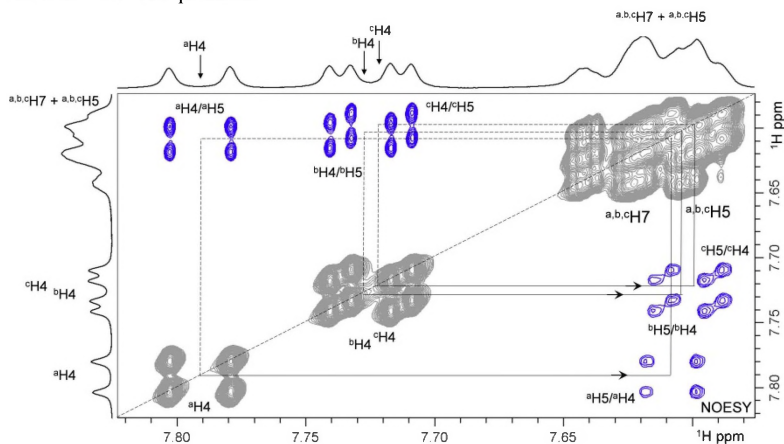
Figure 192. Expanded fragment of the 2D NOESY spectrum for the *mer*-CoL$_3$, demonstrating the identification of through-space correlations between ^{a,b,c}H4 and ^{a,b,c}H5 protons.
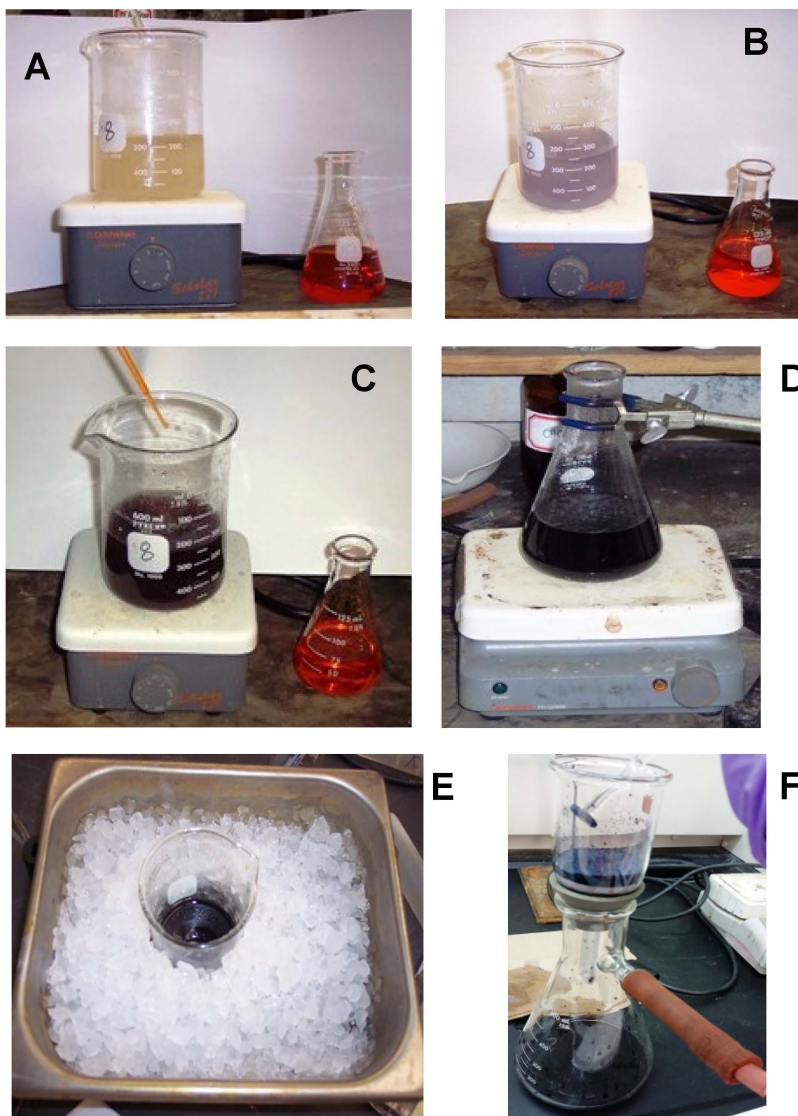
Figure 198. Synthesis of K$_3$[Cr(C$_2$O$_4$)$_3$]·3H$_2$O: **A** – preparation of solutions for the reaction; **B, C** – slow dropwise addition of the dichromate to the oxalic acid/K-oxalate mixture; **D** – evaporation of water from solution; **E** – slow crystallization of the target complex on ice; **F** - filtration.
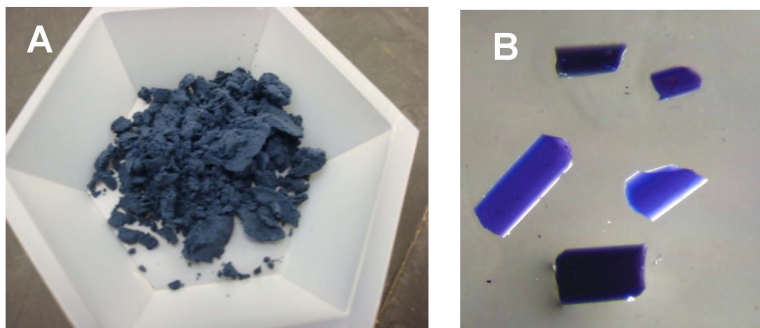
Figure 199. Suitable for studies samples of the $K_3[Cr(C_2O_4)_3] \cdot 3H_2O$: **A** – dried crystalline material for solutions and solid states state studies, **B** – single crystals of the complex used for the X-ray analysis.

Figure 200. Sample of contaminated with the dichromate complex (**A**), and recrystallized pure product (**B**).

CHAPTER 4

SYNTHESIS AND CHARACTERIZATION
OF THE ANIONIC PARAMAGNETIC COMPLEX

4.1. Preparation of Coordination Compounds Using Redox Reactions

During the last several laboratory experiments, we have synthesized coordination compounds of cobalt(III), and then later studied their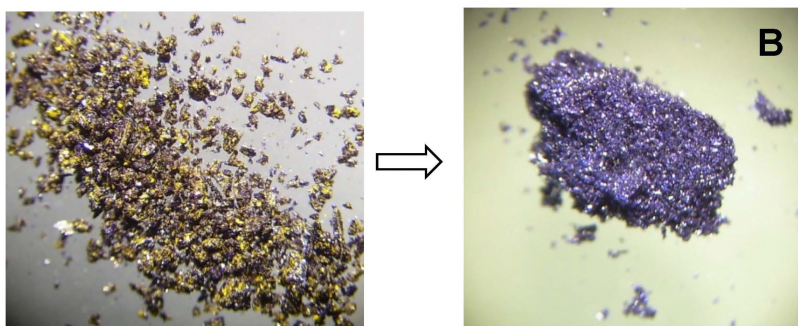 properties. There was a typical preparation for transition metals complexes. An interesting synthetic peculiarity of our previous reaction was the practically immediate oxidation of Co^{2+} into Co^{3+} in open air in the presence of powerful chelating agents such as nitrosonaphthols.

There are many different methods of synthesis of coordination compounds. This laboratory experiment explores ways to prepare a complex compound using the redox properties of a desired central atom. In other words, metals that do form highly oxidized anionic species, such as MnO_4^-, $Cr_2O_7^{2-}$, CrO_4^{2-}, MoO_4^{2-}, MnO_4^{2-}, ReO_4^- etc., can be used as sources for the generation of less positive metal cations, via the reduction reaction in the presence of a complexing agent. Typically, the presence of the ligand in excess provides the possibility for the reduction of a highly positive metal center to a suitable, less positive, oxidation state. Certainly, part of the ligand in such a case will be consumed (oxidized) in the metal reduction process. The examples are abundant.

The most conventional cases of reactions of that type are the formation of oxalate complexes of trivalent Mn, Cr, Mo and Re, with the synthesis of acetylacetonates of these metals shown in Figure 197.

Metals are reduced from their high positive oxidation states +7 and +6, commonly to +3 oxidation state. Generally speaking, this method of introduction of the lower valence metal ion into acetylacetonates is the best way of synthesis of these compounds. There are numerous known complexes of this type:

A

acac (*enol-* form)

$K_2Cr_2O_7$ +

acac
(*keto-* form)

$\Longrightarrow$

Cr(acac)₃ + products of
acac oxidation: CO_2, K^+-
salt of the oxoacid, *etc*.

B   Λ   enantiomer   Δ   enantiomer

mirror plane

M = trivalent Cr, Mo, Re, W, Mn;
R = CH_3, other alkyl, CF_3,
        aryl, substituted aryl groups
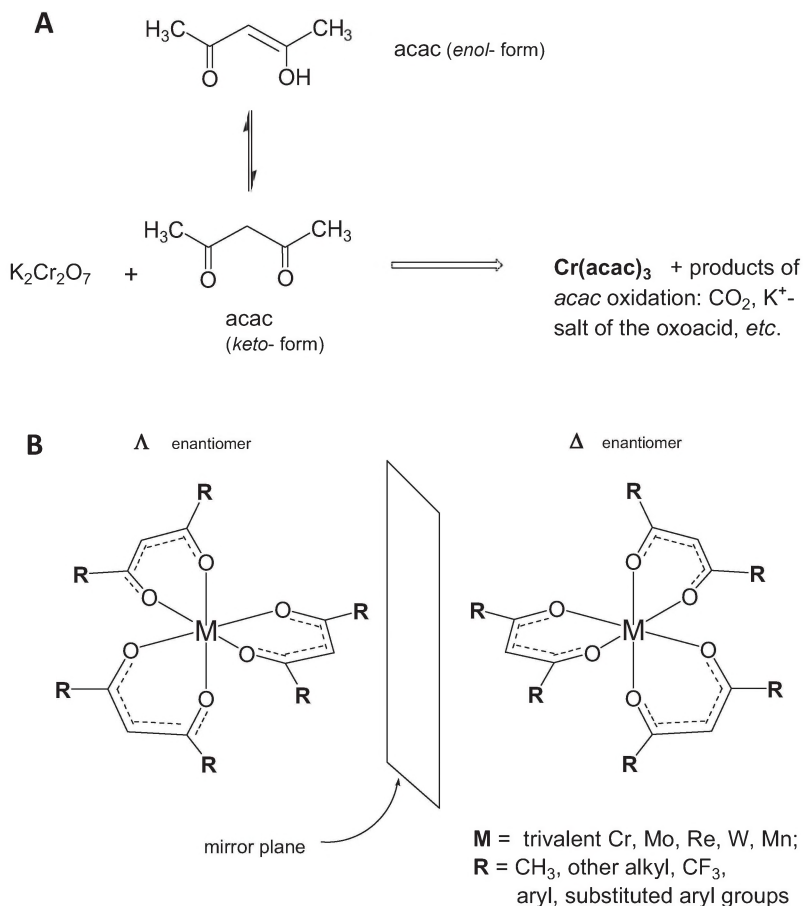
Figure 197. Redox synthesis of tris-acac derivatives using metal precursors in high oxidation states (**A**), and optical isomerism of the obtained compounds containing three chelate rings (**B**).

In this chapter we will describe the synthesis of a different complex compound; anionic, paramagnetic complex of Cr(III), which was obtained as the result of an outlined redox reaction. An investigation of this compound will be performed in a great detail, to set an example for future studies of this type of compounds for students and interested readers.

4.2. Experiment 10. Synthesis of Potassium tris-oxalato{chromium(III)}, $K_3[Cr(C_2O_4)_3] \cdot 3H_2O$

The main *goal* of this laboratory experiment is to learn the technique and procedures of the complex formation during the reduction reaction. The synthesis of Cr(III) *tris*-oxalate complex will be used as a typical example for numerous similar preparations. Objectives for this lab are: a) preparation of two solutions of the oxidizing and reducing agents; b) mixing of those solutions under heating and monitoring the reaction completion; c) isolation of the target metal complex through crystallization; and d) assessment of purity of the complex using optical microscope and qualitative UV-visible spectroscopy.

Equation for the preparation:

$$H_2C_2O_4 + K_2C_2O_4 + K_2Cr_2O_7 \rightarrow K_3[Cr(C_2O_4)_3] + CO_2 \uparrow + H_2O$$
$$\quad 90\ g \qquad 166\ g \qquad 294\ g$$
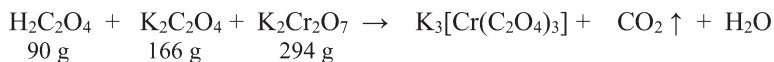
Chemicals:	Oxalic acid, dihydrate;
	Potassium oxalate, monohydrate;
	Potassium dichromate;
Equipment:	Analytical balances;
	Medium size beaker (150 - 200mL capacity);
	Sand bath or water bath for heating;
	Ice bath for cooling;
	Filterware: Bunsen flask with glass filter frit;

Procedure: *(will be carried out in groups, with two students per group; details shown in Figure 198).*

Step 1.
Weigh 13.5g of oxalic acid dihydrate and 6.0g of neutral potassium oxalate monohydrate. Place these substances in a medium size beaker, add 100mL of distilled water and then, using the stirbar, dissolve the compounds; heat the mixture if necessary (Figure 198**A**).

Step 2.
Weigh 6.0g of potassium dichromate $K_2Cr_2O_7$ and dissolve it in a minimal amount of water at room temperature. Observe the bright yellow color of

the solution formed. The solubility of $K_2Cr_2O_7$ is: 4.9g/100mL H_2O at 0°C and 102g /100mL at 100°C (Figure 198 **B**).

Step 3.

At room temperature, add dropwise, while stirring, the concentrated solution of potassium dichromate to the mixture of oxalic acid and potassium oxalate in step 1. The addition of dichromate should be slow; it should take at least 10 minutes! At this point the reaction mixture will change color from yellow to dark green (Figures 198**C**).

Step 4.

Place the beaker (or an Erlenmeyer flask if reaction was carried out in it, as shown in Figure 198**D**) on a hot plate and evaporate the water until the very first crystals start to appear on the wall of the beaker (flask). You should be very attentive at this stage and not allow the complex to crystallize! This may happen rapidly when too much water is evaporated.

Step 5.

Remove the beaker (flask) from the heating device and place it in an ice bath for crystallization (Figure 198**E**). After ~20 min, filter the chromium complex using the glass fritted filter and Büchner flask. Compress the precipitate on the filter by the glass compactor to make it air-dried. After that, remove the crystalline precipitate from the filter and place it between filter papers (or paper towels) to remove residual moisture. Leave the precipitate in the desiccator to dry before packaging for storage. Your final product should look like the one shown in Figure 199.
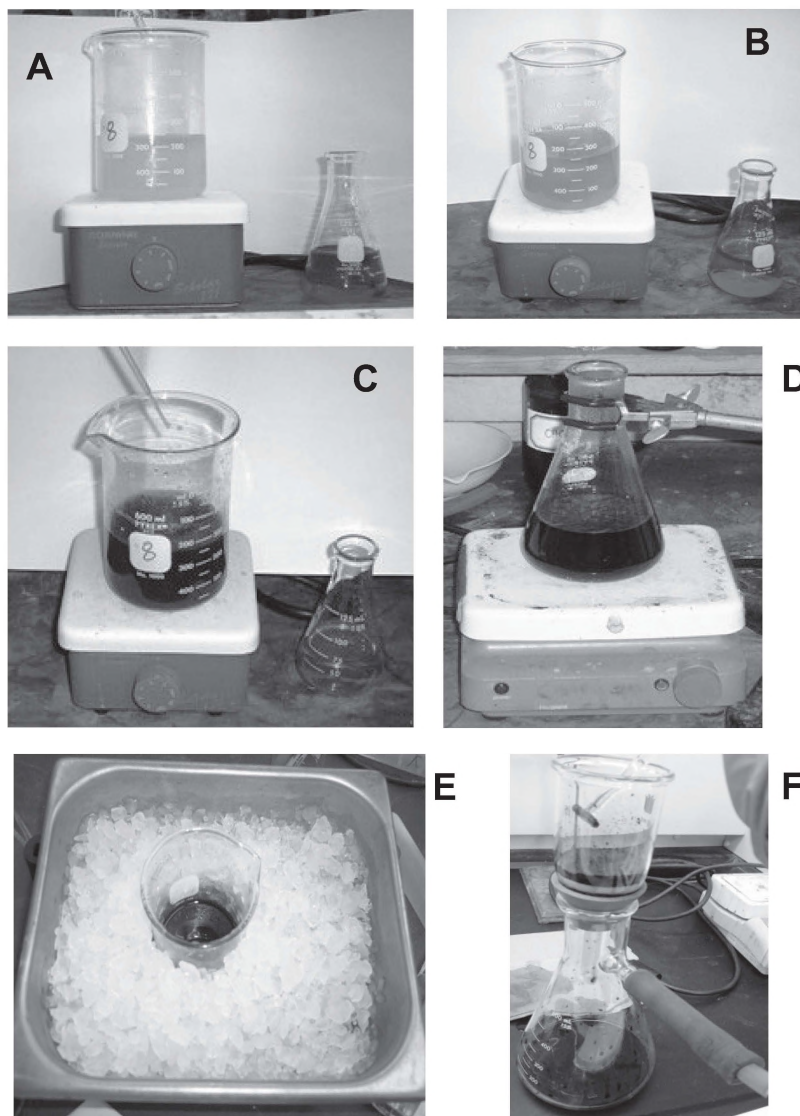
Figure 198. Synthesis of K₃[Cr(C₂O₄)₃]·3H₂O: **A** – preparation of solutions for the reaction; **B, C** – slow dropwise addition of the dichromate to the oxalic acid/K-oxalate mixture; **D** – evaporation of water from solution; **E** – slow crystallization of the target complex on ice; **F** - filtration. See centerfold for this image in colour.

Properties of potassium *tris*-(oxalato{chromium(III)}, $K_3[Cr(C_2O_4)_3]\cdot 3H_2O$: dark-green prismatic crystals with a bluish shine at the edges (Figure 199 **B**); F.W. = 485.4 g/M. The complex is well soluble in water, DMSO, DMF and pyridine [1]. The substance is stable in air and can be stored in a vial, but as always it is better to keep it in a sealed ampoule because of slow loss of crystallized water.
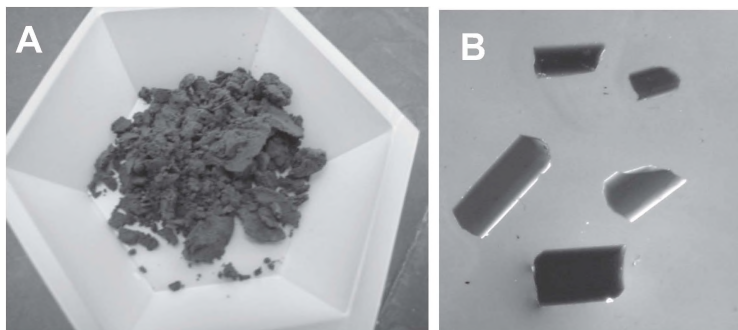

Figure 199. Suitable for studies samples of the $K_3[Cr(C_2O_4)_3]\cdot 3H_2O$: **A** – dried crystalline material for solutions and solid states state studies, **B** – single crystals of the complex used for the X-ray analysis. See centerfold for this image in colour.

Prior to storage this compound must be examined under the microscope on presence of the starting compound – yellow/orange crystals of $K_2Cr_2O_7$.
The yield for this complex should be calculated based on the initial amount of used $K_2Cr_2O_7$. The yield should be written on the label that identifies the final Cr^{3+} compound.
The number of the experiment, date, authors of the reaction, and total amount of the obtained compound with its yield must be written on the label, which should be attached to the sealed ampoule with the target compound.

NOTE:
Some students have succeeded in isolating the pure $K_3[Cr(C_2O_4)_3]\cdot 3H_2O$ complex right away, but some students have obtained a complex that is not pure (Figure 200**A**). This may be due to faster-than-needed addition of the potassium dichromate to the mixture of potassium oxalate and oxalic acid solutions. The latter group of students will need to recrystallize the compound using a minimal amount of hot water.
Typical examples of a crystalline sample contaminated with the initial orange potassium dichromate are shown in Figure 200**A** (as the

microscope photograph at 20x magnification), whereas good quality pure specimens are presented in Figures 199**A** and Figure 200**B**.
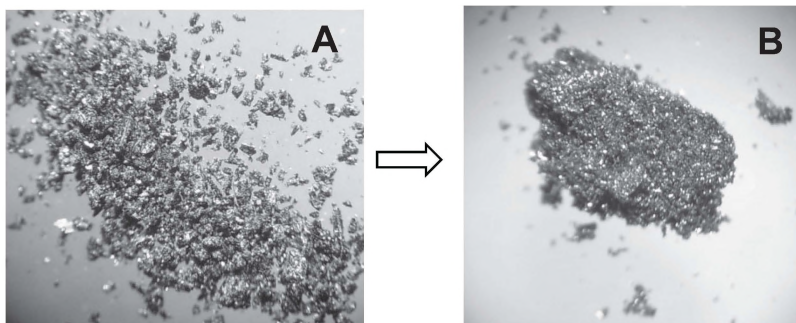

Figure 200.   Sample of contaminated with the dichromate complex (**A**), and recrystallized pure product (**B**). See centerfold for this image in colour.

    Typically, this procedure requires 10mL of water per ~5g of the impure complex which is placed at room temperature in a beaker of ~100mL capacity on a stirrer/hot plate combo (Figure 30, Chapter 1). The system should be warmed up to ~65-70°C until all solid dissolves. If not all crude product dissolves, add 1-2mL of water. When no solid is visible in the system, place the beaker on an ice bath. Complex forms at these conditions saturated aqueous solution. At the same time, impurities, which are minor components, do not form a saturated solution, and will not precipitate upon cooling.
    The pure complex, which precipitates after 10-15 minutes on an ice bath, should be filtered, dried, and subjected to further studies. After drying within several days in the desiccator at ambient pressure, the complex represents a nice crystalline dark-blue material (Figure 200**B**).

Potential hazards:
    1) Hot surfaces of the heating device and glassware;
    2) Potassium dichromate is an oxidizer and known to be toxic; gloves are required at all times during the work.
Goals of this laboratory experiment and expected accomplishments:
    1) Carry out preparation of Cr(III)complex according to provided procedure.
    2) Visual control of purity of the complex using an optical microscope (in reflectance mode). This procedure will be carried out for the first time during this laboratory course.

3) Dry your sample to the best of your ability between paper towels, weigh it, and pack it in the screw-cap vial (we will need the complex during the next two labs); the yield of the complex can be calculated using dried sample.

4) Prepare detailed lab report with all observations, discussion of results and conclusions; your lab report will be due at the next laboratory session.

4.2.1. Understanding of the Crystal Structure of Potassium *tris*-oxalato{chromium(III)}, K$_3$[Cr(C$_2$O4)$_3$]

In this chapter, we continue the presentation and discussion of the results of the X-ray analysis of synthesized by students compounds that were included in this laboratory manual. The aim is to train students to analyze the data, notice the most important structural features, and learn how to present this data. We did introduce the basics of X-ray single crystal analysis in Chapter 3, when we discussed the data for both organic chelating ligands; isomeric nitroso-naphtols and their cobalt(III) complexes.

Here we will outline procedures only of the crystal growth, crystal selection and mounting, and then make only brief crystallographic analysis of the last compound; potassium salt of the *tris*(oxalate)-chromium(III).

After the synthesis of the complex in experiment **11**, an effort has been made to grow single crystal specimens suitable for X-ray analysis, by using the recrystallization technique. Thus, ~0.5g of the complex was dissolved in 5mL of preheated to ~80°C water in the beaker, and then slowly cooled off to room temperature. Small block-type crystals appeared within several hours. Crystals were carefully dislodged from the walls, placed onto the paper filter, and air dried. Their appearance is shown in Figure 199**B** above.

Students are required to participate in microscope work to become familiar with the process of crystal selection and mounting. This work includes: a) the placement of a small quantity of crystals in an immersion oil; b) the assessment of the crystals' quality by gentle manipulation (tumbling) of crystals using a very fine glass or metal needle; c) the selection of only transparent, well-formed crystals without cracks and without 'rainbow' colors under polarized light for studies; and d) the placement of the crystal onto the tip of a fine glass fiber attached to a copper pin that will be mounted on the goniometer head (Figure 201). The last step is accomplished by using a drop of vacuum grease to hold the

crystal selected for studies on the glass fiber tip (Figure 201). After crystal centering, data were collected, using a standard scheme typically applied during crystallographic studies of inorganic/organometallic compounds with Mo-Kα radiation source (λ=0.71073 Å). That is: 1) low temperature experiment to minimize thermal motion of atoms and lowering the detector noise; 2) full-sphere of reflections data collection, which transforms into 4 runs of 364 photographs at 10 sec exposures each, for strongly diffracting crystals (as the studied complex is); 3) 0.5° step width.

Crystal data for this compound are presented in Appendix 4 at the end of the book. The CCDC registration number is 1839658, and it can be retrieved for further viewing and analysis .

The complex crystallizes in a monoclinic system in P2$_1$/c space group [1,2]. Students are required to do a literature search and determine whether this group is centrosymmetric or not. The ASU, *asymmetric unit*, of the structure consists of one isolated complex anion moiety of $[Cr(C_2O_4)_3]^{3-}$, three potassium cations to balance the charge, and solvents of crystallization/purification (Figure 202). These are two water molecules, and one molecule of methanol that was used during crystals handling (washing/drying) after the synthesis.
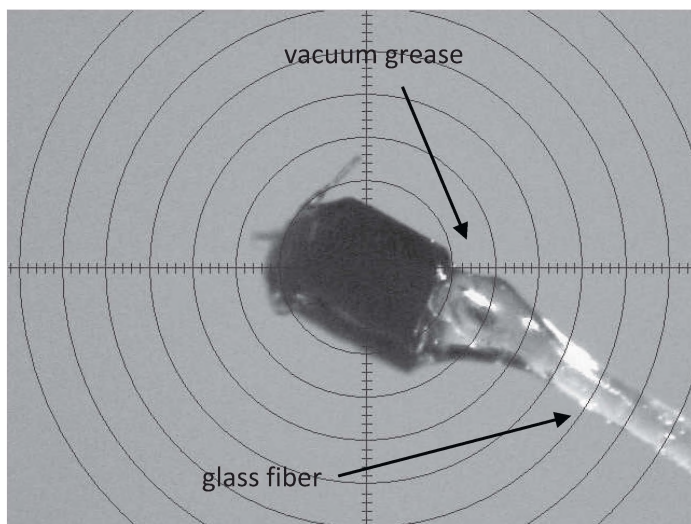

Figure 201. Videomicroscope photograph of crystalline specimen of the K$_3$[Cr(C$_2$O$_4$)$_3$]·xH$_2$O selected for studies and mounted on the tip of a glass fiber. The smallest circle seen inside the crystal has 0.1mm diameter.

Students should know by this current experiment that the ASU represents a 'building block', or 'elemental brick' using which, a structure can create a three-dimensional space, using symmetry operations present in the determined space group. Which ones are those? The first explanation of this topic was given during the analysis of crystal structures of ligands and their Co(III) complexes in Chapter 3.
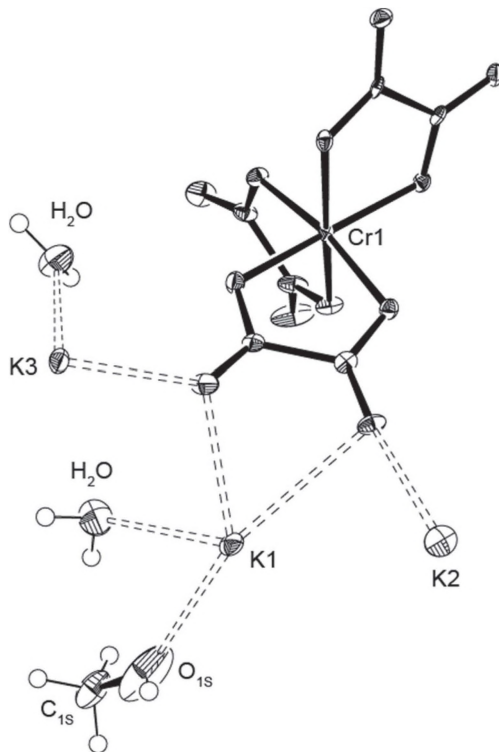
Figure 202. The asymmetric unit in the structure of $K_3[Cr(C_2O_4)_3] \cdot 2H_2O \cdot MeOH$.

Counter-cations of potassium are surrounded by solvents molecules (water, methanol), and have long, over 3Å, electrostatic contacts coordinated to Cr(III) oxalate groups, and will not be analyzed. It is important to notice, however, significantly *variable lengths* of those contacts, and *irregular sets of angles* at K^+ ions. Both evidenced the ionic character of bonding, between them and $[Cr(C_2O_4)_3]^{3-}$ anions. The atomic

numbering scheme in the structure of the anion is shown in Figure 203. Selected bond lengths and angles are summarized in Table 13, below.

Also, students need to analyze Cr – O bonds, make clear distinction between them, and then calculate the average. Then students need to determine the 'bite angles' in the structure. Finally, students need to find values for the sum of ionic radii of Cr(III) and oxygen atoms from the literature sources [3], to make an assessment of the ionic/covalent character of bonds in the anion.

Furthermore, students need to analyze the geometry of the coordination polyhedron of the metal center. Is it octahedral, or trigonal-prismatic? Conclusions should be made and included in the report describing this crystal structure.

The next step is the assessment of bonding in the ligand; oxalate anion. Students need to find resources values for C-O single and C=O double bonds from the literature and/or web, and compare them with those determined for the $C_2O_4^{2-}$ dianion in the structure of Cr(III) complex.

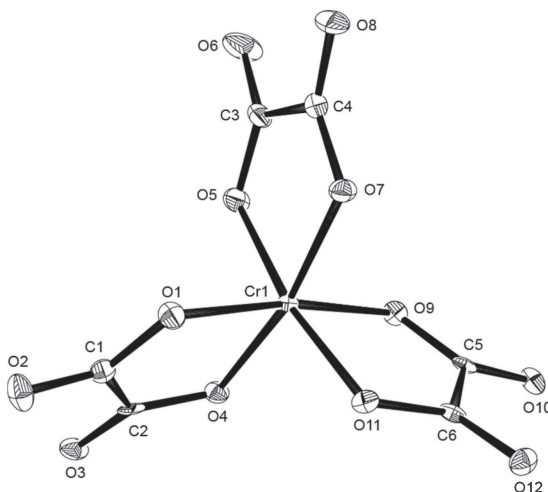**Figure 203.** The numbering scheme in the *tris*-oxalato-Cr(III) anion.

Table 13. Selected bond lengths (Å) and angles (°) in $[Cr(C_2O_4)_3]^{3-}$ anion.

Bonds in oxalate groups:			
C1-O2	1.221(5)	C1-O1	1.301(5)
C1-C2	1.561(5)	C2-O3	1.227(5)
C2-O4	1.289(5)	C3-O6	1.213(5)
C3-O5	1.288(5)	C3-C4	1.550(5)
C4-O8	1.223(5)	C4-O7	1.287(5)
C5-O10	1.216(5)	C5-O9	1.288(5)
C5-C6	1.562(5)	C6-O12	1.233(5)
C6-O11	1.284(5)		
Angles in oxalate groups:			
O2-C1-O1	125.5(4)	O2-C1-C2	120.6(3)
O1-C1-C2	114.0(3)	O3-C2-O4	125.6(4)
O3-C2-C1	120.5(3)	O4-C2-C1	113.9(3)
O6-C3-C4	120.0(4)	O5-C3-C4	113.6(3)
O6-C3-O5	126.4(4)	O9-C5-C6	113.6(3)
O8-C4-O7	126.1(4)	O8-C4-C3	120.5(3)
O7-C4-C3	113.4(3)	O10-C5-O9	126.3(3)
O10-C5-C6	120.0(3)		

Bonds in Cr(III) center:			
Cr1-O9	1.962(3)	Cr1-O1	1.963(3)
Cr1-O5	1.966(3)	Cr1-O7	1.982(3)
Cr1-O4	1.985(3)	Cr1-O11	1.989(3)
Angles at Cr(III) center:			
O9-Cr1-O5	91.31(11)	O1-Cr1-O5	95.45(12)
O9-Cr1-O7	95.22(11)	O1-Cr1-O7	91.66(11)
O5-Cr1-O7	81.80(11)	O9-Cr1-O4	91.08(11)
O1-Cr1-O4	83.04(11)	O5-Cr1-O4	89.36(11)
O7-Cr1-O4	169.24(11)	O9-Cr1-O11	82.71(11)
O1-Cr1-O11	91.35(11)	O5-Cr1-O11	170.19(11)
O7-Cr1-O11	90.97(11)	O4-Cr1-O11	98.49(12)

Finally, the presence of three chelate rings at the central atom necessitates the formation of optical isomers: Λ and Δ. Indeed, there are two enantiomers present in the structure (Figure 204). Determine which one is which, and include your observations in the lab report. A good method for determination of the absolute configuration in coordination compounds can be found in a book by G. Miessler and D. Tarr [**4**]. Is the overall structure chiral? – Give the answer and provide your arguments in the lab report as well.
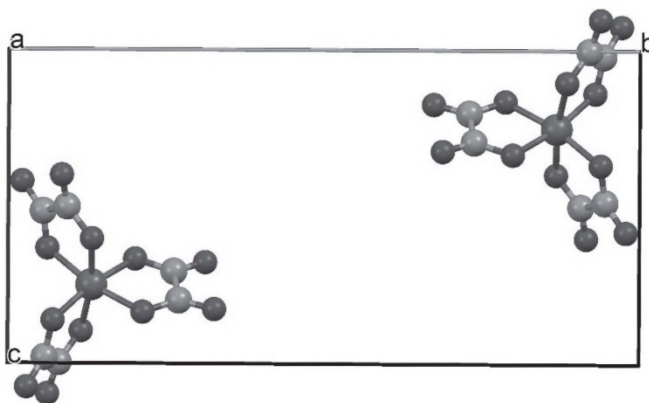
Figure 204. View along *a*-direction of the fragment of the crystal structure of the $K_3[Cr(C_2O_4)_3]\cdot xH_2O$ showing only two out of four anionic complexes in the unit cell. The K^+ ions and solvent of crystallization water/methanol molecules are not shown for clarity.

Cited Literature

1. http://chemistry.bd.psu.edu/jircitano/6symmetry.pdf
2. https://www.youtube.com/watch?v=NaRjGfq19GE
3. Shannon, R.D. *Acta Cryst*. **1976**, A32, 751-767.
4. Miessler, G.; Tarr, D. *Inorganic Chemistry*. 4th Ed. Pearson, 754 pp., 2011; ISBN 978-0-13-612866-3.
5. a) Taylor, D. *Austr. J. Chem*. **1978**, *31*(7), 1455 – 1462; b) Hu, C.; Heger, G.; Kalf, I.; Englert, U. *Zeitsch. für Kristallogr*. **2005**, *220* (11), 926–929; c) J. N. van Niekerk, F. R. L. Schoening. *Acta Cryst*. **1952**, *5*, 475-476

4.3. Characterization of the Anionic Cr(III) Complex

4.3.1. Theoretical Background: Electrical Conductivity
of Aqueous and Non-Aqueous Solutions

Electricity is the flow of charge carriers from one electrode to another. The most common carriers are electrons and ions, both positive and negative. This fact indicates that ions in solution will conduct electricity. Therefore, conductivity is the ability of a solution to pass current. Conductivity may be measured by applying either direct, or an alternating electrical current, (I) to two electrodes immersed in a solution, and measuring the resulting voltage (V) (Figure **204**). Direct current, however, may lead to electrolysis of solutions, and accurate readings of the metering device becoming unstable and/or unreproducible. It is mostly applied in qualitative measurements and in the teaching curriculum. For research and analytical purposes, the alternating current method is used. During this process, the cations migrate to the negative electrode, the anions to the positive electrode, and the solution acts as an electrical conductor [**1**].
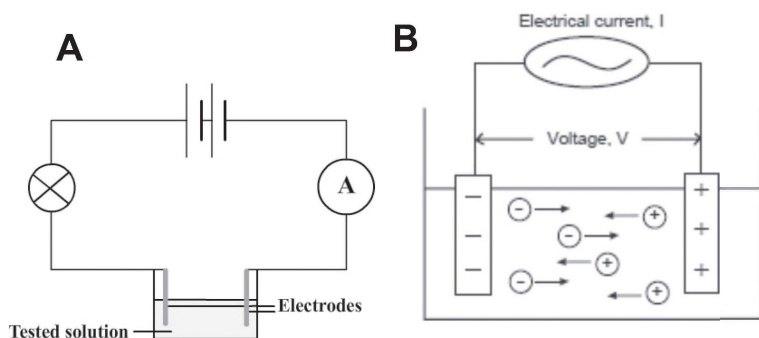
Figure 205. Principal schematics of solutions' conductivity measurements: **A** – direct current, **B** – alternating current.

Most of the time conductivity is typically measured in aqueous solutions of electrolytes. Electrolytes are formed in solutions because of the dissociation. The ions formed in a solution are responsible for carrying the electric current.

Electrolytes include acids, bases, and salts, and can be either strong or weak, based on the value of their dissociation degrees. The degree of dissociation, α, is a ratio between dissociated particles to a total number of particles. Therefore, values for dissociation degree are confined

to $0 < \alpha < 1.0$. Strong electrolytes have α ranging from ~0.6 to 1.0, while weak electrolytes have α less than 0.1 (for instance, neat acetic acid with $\alpha = 0.04$).

   Both cationic and anionic coordination compounds are very much prone to dissociation. Thus, cationic $[CuEn_3]Br_2$ (En = 1,2-diaminoethane), and anionic $Na_2[CdI_4]$ complexes, fully dissociate in aqueous solutions, and form 1:2 and 2:1 electrolytes. The method of measuring solutions' electrical conductivity plays an important role in the characterization of complexes. Solutions of strong electrolytes conduct electricity because the positive and negative ions can migrate largely independently under the influence of an electric field (Figure 205**B**).

   During measurement of electrical conductivity by the AC method, the frequency was chosen by convention to be 1000 Hz (1 kHz). This avoids electrolysis and at the same time allows some migration of ions to electrodes. The conductivity of solutions is highly dependent on the number of ions, which is a solute concentration. Electrochemists have decided to use 0.001M solutions (1mM) of compounds to assess their conductivity [**2**]. This concentration allows making a reasonable assumption that no interactions of ions with each other, or aggregation, can be contributing factors to the distortion of a true conductance.

   The conductivity reading of a sample will also change with temperature. Conductivity measurements are temperature dependent: if the temperature increases, conductivity increases. For example, the conductivity measured in a 0.01 M KCl solution at 20°C is 1.273mS/cm whereas, at 25°C, it is 1.409mS/cm. The normal temperature range is usually 20°C or 25°C, with reference values commonly given in this interval. It is mandatory always to associate the temperature together with a conductivity result, and report data, such as: $\kappa = 35mS/cm$ (20ºC). If no temperature correction is applied, then the conductivity value must be reported at measurement temperature.

   Useful data comparing water conductivity from different sources and probes constants can be seen in Figure 206.
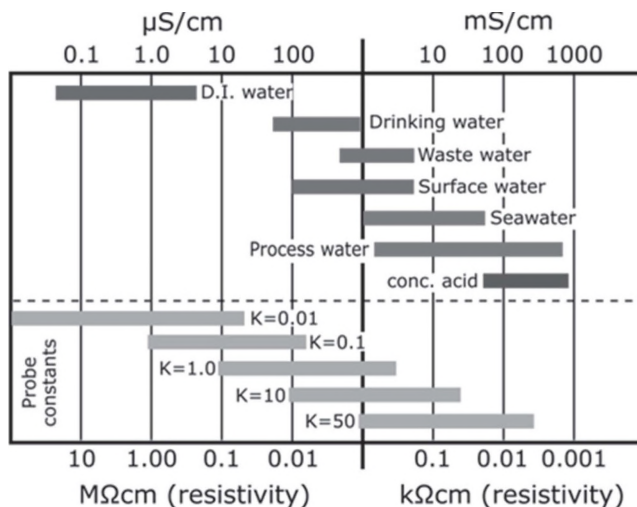
Figure 206. The diagram of the range of conductivity and resistivity of a variety of water samples.

Most conductive solutions measured are aqueous solutions, as water has the capability of stabilizing the ions formed by a process called solvation. However, there are numerous applications of an electrical conductivity method for characterization of non-aqueous solutions, such as nitromethane CH_3NO_2, nitrobenzene $C_6H_5NO_2$, acetone $OC(CH_3)_2$, acetonitrile CH_3CN, dimethylformamide $HC(O)C(NH_3)_2$, methanol and ethanol, dimethylsulfoxide $OS(CH_3)_2$. An excellent review of the properties of these solvents, and numerous examples of investigations of coordination compounds is summarized by Geary [**2**].

Definition of terms
Resistance. The resistance of the solution (R) can be calculated using Ohm's law (V = R · I). **R = V/I**, where V = voltage (volts), I = current (amperes), and R = resistance of the solution (ohms).
Conductance G is defined as the reciprocal of the electrical resistance
(R) of a solution between two electrodes. **G = 1/R (S)**, and the conductivity meter, in fact, measures the conductance, and displays the reading converted into conductivity.

Cell constant, K is the ratio of the distance (d) between the electrodes to the area (a) of the electrodes. **K = d/a**, where K = cell constant (cm^{-1}), and

a = effective area of the electrodes (cm^2), while d = distance between the electrodes (cm).

Thus, electrical conductivity $\kappa = G \cdot K$, where κ = conductivity expressed in (S/cm), and G = conductance (S), where G = 1/R, and K = cell constant (cm^{-1}).

Cited Literature

1. http://www.analytical-chemistry.uoc.gr/files/items/6/618/agwgimometria_2.pdf
2. Geary, W.J. The use of conductivity measurements in organic solvents for the characterization of coordination compounds. *Coord. Chem. Rev.*, 1971, *7*, 81-122.

4.4. Experiment 11: Characterization of Anionic Potassium *tris*-oxalato{chromium(III)}

In solutions:
- UV-visible spectra;
- measurements of electrical conductivity;
- cryoscopic data;
- magnetic moment measurements using the NMR Evans method.

This laboratory experiment is a continuation of the characterization of the dried anionic *tris*-oxalato(chromium(III)) complex that was prepared, dried, and packed into the screw-cap vial in our previous lab (Figure 199**A**). Some students have succeeded in isolating the pure $K_3[Cr(C_2O_4)_3] \cdot 3H_2O$ complex, while some students may have obtained a complex that is not pure (Figure 200**A**). Aside from the visual inspection of the obtained solid product under the microscope (Figure 200), the method of UV-visible spectroscopy becomes very useful as well. A typical example of a spectrum from the sample contaminated with the initial orange potassium dichromate is shown in Figure 207, whereas the expected electronic spectra from a good quality pure specimen are presented in Figure 209 below.

The latter group of less successful students will need to recrystallize the compound using a minimal amount of hot water, as described above in part 4.1.1 of this chapter.

*** Only good quality samples are permitted to be studied in this laboratory work.** Control of quality is easily attainable by UV-visible spectroscopy of aqueous solutions of $K_3[Cr(C_2O_4)_3]$: it should contain only 3 bands – 1 π–π^* transition in the oxalate anion, and 2 d-d transitions in Cr^{3+} cation in an octahedral crystal field.*

The synthesized and purified $K_3[Cr(C_2O_4)_3]$ anionic complex also represents a very suitable compound for educational purposes: there are several physical methods that can be used for a common, yet elegant characterization of the obtained coordination compound.
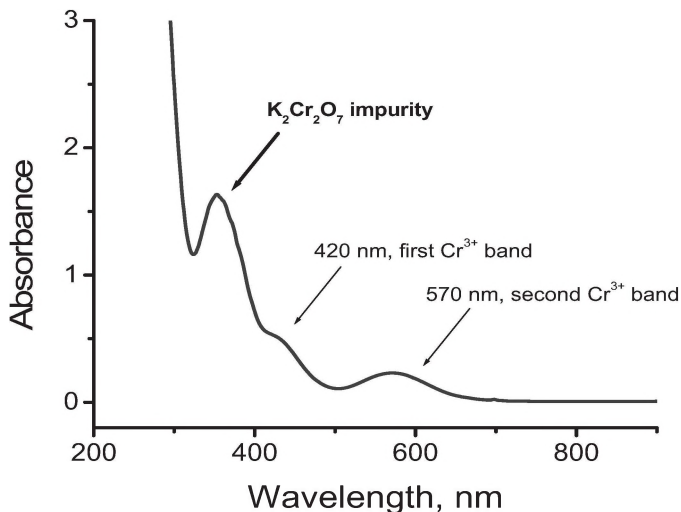
Figure 207. UV-visible spectrum of solution of an impure complex that contains the starting material.

The main *objective* of the laboratory experiment #11 is performing several important physical and spectroscopic characterizations of the obtained compounds that were outlined above.

Chemicals and equipment will be detailed in each part of this extensive laboratory exercise. The only one common for all chemical experiments is our freshly obtained $K_3[Cr(C_2O_4)_3] \cdot 3H_2O$.

Procedure: *(will be carried out in groups, with two students per group).*

Part 1

- **Recording of UV-visible Spectra in Aqueous Solution.**

The origin of color in the octahedral complexes of trivalent chromium is depicted below. Thus, the UV-visible spectrum of the complex contains three bands in the 200-900nm range: one band in the UV-region for the $\pi-\pi^*$ transition in the coordinated oxalate anion, and two more bands in the visible region due to the *d-d* transitions in the Cr^{3+} cation (Figure 208).
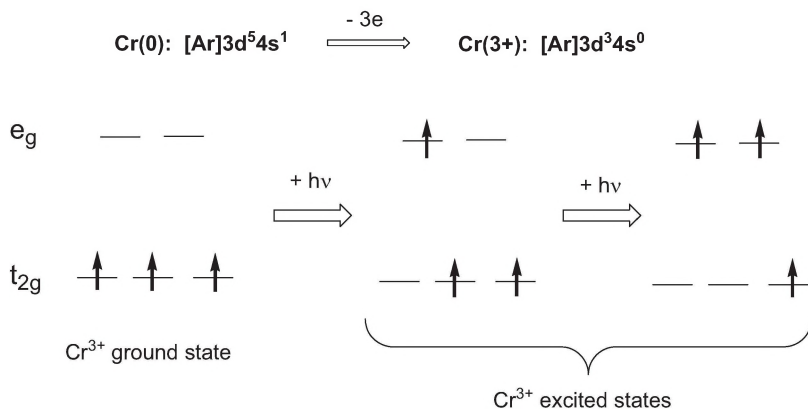
Cr(0): [Ar]3d^{5}4s^1 $\xrightarrow{\text{- 3e}}$ **Cr(3+): [Ar]3d^{3}4s^0**

Figure 208. Schematic diagram showing the origin of Cr(III) electronic spectrum.

Equipment:

> Any available UV-visible spectrophotometer operating in the range of 200 – 800nm;
> Cuvettes (quartz desirable; see Figure 171 in Chapter 3).

Step 1.

Place ~50mg of your chromium(III)-oxalato complex into the test tube. Add 10mL of water using a pipette and dissolve your sample.

Step 2.

Fill a 1cm quartz cuvette with the solution made in the previous step. It usually takes about 3.5 – 4.0mL. Fill a 1mm quartz cuvette with the same solution (will take ~0.4mL). Diluted x10 times in that way, the solution allows you to see the $\pi-\pi^*$ transition in the organic ligand.

Step 3.

Record the UV-visible spectrum of background (pure water) first, then two spectra of the complex in 1mm and 1cm cuvettes. Make a printout of your data. Your spectra should look as shown below, in Figure 209.
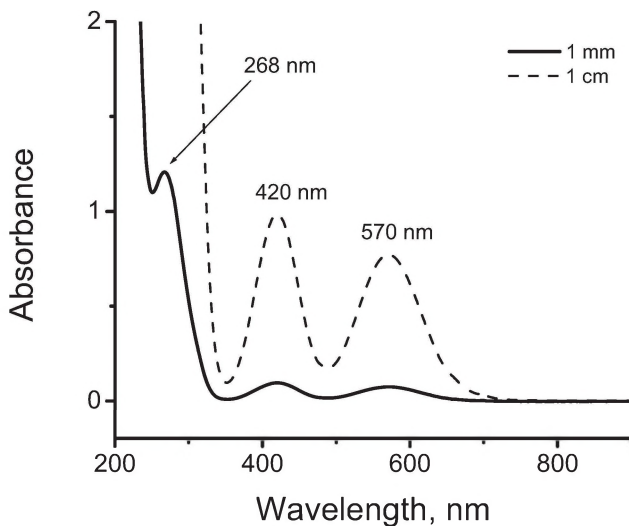
Figure 209. Electronic spectra of pure $K_3[Cr(C_2O_4)_3]\cdot 3H_2O$ in water in cuvettes with a different path length.

Step 4.
Calculate the extinction coefficient for the absorbance of the compound in the visible region using the formula:

$$\varepsilon = A \:/\: l \times M$$

Recorded spectra and calculated molar extinction coefficients for each peak should be included in your lab report.

Cleanup:

All cuvettes must be washed with water, and then with ethanol, and air-dried without placing them in the drying oven.

Part 2

• **Measurements of Electrical Conductivity of Solutions.**

The method of measurement of electric conductivity of solutions is a valuable tool for determining the constitution of the coordination compound. Thus, the solutions of neutral complexes show the absence of conductivity, while both cationic and anionic complexes exhibit a wide

range of conductivity. The value of the electric conductivity of the solution is directly proportional to the number of ions in the solution. Thus, solutions of two-ionic electrolytes conduct less than three-ionic compounds, and these, in turn, conduct less than four-ionic complexes. It was previously found that 0.001M solutions can be treated as diluted systems, and any association at such low concentration can be considered negligible [1]. We will look at the solution conductivity of several coordination compounds. Thus, the electrolytic dissociation of the compounds shown below in aqueous solutions leads to the following ionization reactions, which will generate different numbers of ions in the solutions. Thus, we will be able to observe 2-, 3-, 4-, and 5-ionic electrolytes (see Figure 210 below). In this case, it is important to compare the solutions conductivity of our potassium this-(oxalato) chromium(III) complex against the values of conductivity for known compounds. An actual conductivity probe and the meter are shown in Figure 211.

Chemicals:

   Used in this particular part of laboratory experiment are the inexpensive coordination compounds that cover the useful range of types of electrolytes: 1:1, 1:2, 1:3, and 1:4. We selected $Na[B(C_6H_5)_4]$, $K[SbF_6]$, $K_2[TiF_6]$, $K_3[Fe(CN)_6]$, and $K_4[Fe(CN)_6]$. Our chosen set has a common feature: all represent anionic complexes similar to the obtained $K_3[Cr(C_2O_4)_3]\cdot 3H_2O$.
   * Any other water-soluble complexes can be used as well. For example, KBF_4, $Na_2[SiF_6]$ (or K derivative), $[Co(NH_3)_6]Cl_3$, $Na_3[Co(NO_2)_6]$, etc.*

Equipment:

   Analytical balances;
   Electric conductivity meter with the cell;
   Six volumetric flasks of 100mL;
   Vortex to aid compounds dissolution;
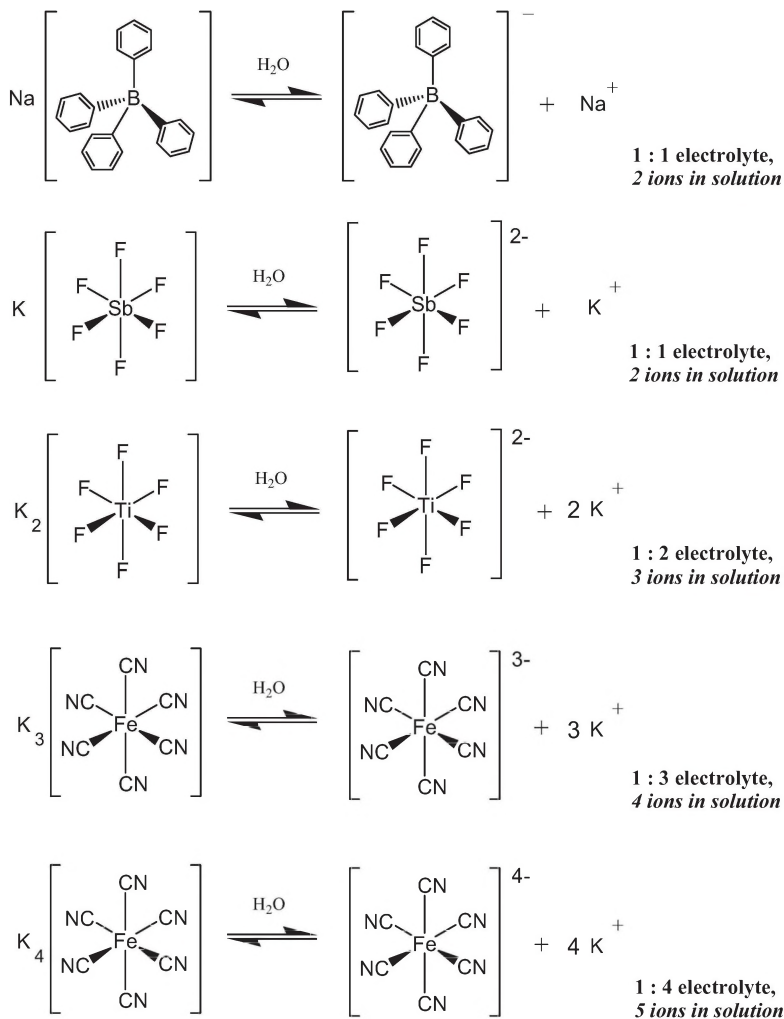   Thermometer.

Figure 210. Equations for dissociation of selected in this laboratory exercise complex compounds explaining the number of ions generated in solutions.
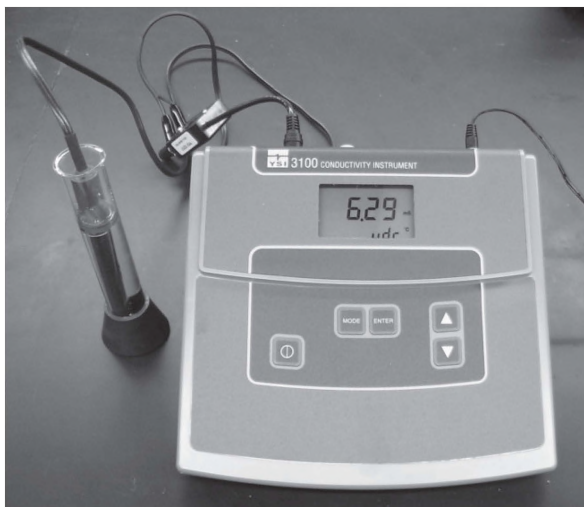
Figure 211. An experimental setup for measurements of electrical conductivity of 0.001 M solutions of standard compounds and the complex prepared in Lab #**11** $K_3[Cr(C_2O_4)_3]$.

Step 1.
Prepare 0.001M aqueous solutions of the following coordination compounds: $Na[B(C_6H_5)_4]$, $K[SbF_6]$, $K_2[TiF_6]$, $K_3[Fe(CN)_6]$, $K_4[Fe(CN)_6]$ and $K_3[Cr(C_2O_4)_3]$. Thus, the required amounts are:

0.0342 g of $Na[B(C_6H_5)_4]$	in 100mL volumetric flask,
0.0274 g of $K[SbF_6]$	in 100mL volumetric flask,
0.0240 g of $K_2[TiF_6]$	in 100mL volumetric flask
0.0329 g of $K_3[Fe(CN)_6]$	in 100mL volumetric flask,
0.0422 g of $K_4[Fe(CN)_6]$	in 100mL volumetric flask,

and, finally, our synthesized complex 0.0433 g of $K_3[Cr(C_2O_4)_3]$ in a 100mL volumetric flask.

Step 2.
Use a clean test tube for your measurements. The tube should be held in a vertical position by a clamp on the lab stand. Fill it with your solutions in such a manner that there will be no spills, which means filling to ~1/4 of the volume. Measure the electric conductivity of each solution three times. Thoroughly wash the conductivity cell with DI water each time before changing the solutions of complexes to be studied.

Step 3.
Record your data. Take an average value of conductivity for each complex and plot 'conductivity VS number of ions in solution'. Determine an electrolyte type for $K_3[Cr(C_2O_4)_3]$ using the graph, by drawing a perpendicular from the point on your graph corresponding to the chromium(III) complex to the *x*-axis with the number of ions. Your value should be close to 3±0.5. You may use Excel, ORIGIN, or any other suitable graphing program of your choice for your data processing, plotting, and analysis.

Include the plot of your measured conductivity data and the table with values into your lab report.

Cleanup:
> It is essential to properly dispose of all solutions into an inorganic waste container. All volumetric flasks must be washed and dried in drying oven.
> It is very important to keep the conductivity meter and electrode clean! So, wash it several times with distilled water and then keep it in a test tube filled with DI water.

Part 3

- **Cryoscopic Measurements of Solutions of Electrolytes.**

Similar to the principles outlined above in Chapter 3, the method of determination of molecular weight of compounds in solutions is a very useful tool for investigations of the number of particles generated in solutions of electrolytes upon dissociation. It is reflected in the value of the van't Hoff's coefficient *i*, in the equation below:

$\Delta T_F = K_F \cdot b \cdot i$ where:
- K_F is the cryoscopic constant, which is dependent on the properties of the solvent, not the solute.
- *b* is the molality (moles of solute per kilogram of solvent).
- *i* is the Van't Hoff factor (number of ion particles per individual molecule of solute, e.g. i = 2 for NaCl, and 3 for $BaCl_2$). For molecular solutions – non-electrolytes – the *i* value is 1.
- ΔT_F, the freezing-point depression, is defined as $T_{F\,(pure\ solvent)} - T_{F\,(solution)}$. This value is measured experimentally.

Equipment:

> High accuracy thermometer (either Hg-filled Beckman thermometer, or digital thermometer: reading to 0.01° accuracy is necessary).
> Glass vessel equipped with stirring device for carrying the experiment.

Step 1.
On analytical balances, weigh ~0.250g of the $K_3[Cr(C_2O_4)_3] \cdot 3H_2O$, and dissolve it in ~5g of distilled water, which should be weighed in a vial or beaker. The amount has to be measured precisely, to 3-4 digits after the decimal point. Record weights and calculated molality of your solution.

Step 2.
Place ~ 5g of pure water into the measuring glassware and immerse a high precision thermometer. We need to measure the first freezing temperature of water in our experiment.

Step 3.
Prepare ice bath from crushed ice (~0.5kg) and table salt (~2 tablespoons), and mix it well with a large spatula. Measure its temperature with a low accuracy liquid thermometer (or simple digital thermometer) to make sure that it is cooled to at least -5°C.

Step 4.
Place glassware vessel with pure water and high precision thermometer into the cooling bath. Start stirring the solution and slow cooling the system. *Please maintain stirring (mechanical or manual) at all times, to prevent the system from overcooling and obtaining erroneous freezing point data!*

Step 5.
Monitor slow temperature drop, maintaining stirring. When water begins freezing it will appear as a cloudy slush, and its temperature will suddenly slightly rise. It will stay without changing until the whole volume freezes solid. Record the temperature changes all the time. Make a table of values and build a graph: *TIME* vs *T*. Extrapolate the plateau part of the graph, as shown in Figure 138 (Chapter 3) to the *T* axis. This is your solvent's $T_{F(pure\ solvent)}$.

Step 6.
Disassemble the system, empty water from measuring vessel, clean and dry it.

Step 7.
Transfer a solution from Step 1 into a dry and clean glassware vessel where the main experiment will be conducted. Adjust stirring/mixing device to proper working conditions. Immerse high precision thermometer in the mixture.

Repeat Steps 3 – 5 and measure $T_{F\ (solution)}$. Obtain ΔT_F, and perform calculations of the van't Hoff factor i. It should have value between 2 and 3. Include obtained value in the lab report. Repeat Step 6 and move to another task – recording UV-visible spectra of $K_3[Cr(C_2O_4)_3]\cdot 3H_2O$ in solution.

Potential hazards:
                    Ice bath with subzero temperature could cause frostbite
                    to your fingers and hand.

4.4.1. Theoretical Background: magnetism of coordination compounds of transition metals

Any substance being placed in a magnetic field will interact with it, either by repulsion from it, or by attraction. Types of response on such interaction are summarized in Table 14.
         Three main types of magnetic material are presented in Figure 212. The magnetic properties of a coordination compound are associated with the unpaired electrons and orbitals in that compound. Diamagnetic compounds have no unpaired electrons, and are thus repelled slightly by the magnetic field [2]. On the other hand, paramagnetic compounds are attracted by external magnetic field, a consequence of one or more unpaired electrons behaving as tiny magnets. The measure of this magnetism, commonly associated with the change in a sample mass, is called the magnetic susceptibility, χ_g.
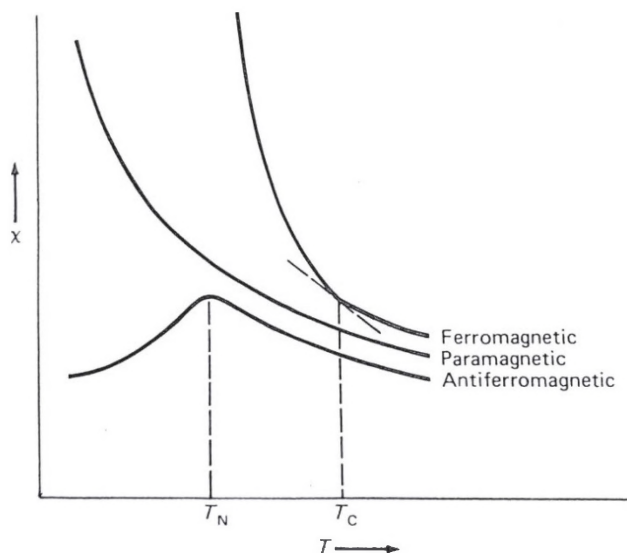
Figure 212. Three types of magnetically active substances and their distinction based on variable temperature behavior. Specific points: Neel for antiferromagnetic ordering, and Curie for ferromagnetic ordering, are notated as T_N and T_C respectively.

Table 14.   Types of magnetic behavior observed in different substances.

Type	Nature of phenomenon	Sign	Magnitude, in emu units (Field dependence)
*Ferro*magnetism	alignment of spins from dipole-dipole interactions	+	$10^{-2} - 10^{-4}$ (*dependent!*)
Anti-ferromagnetism	spin pairing from dipole-dipole interactions	+	10^{-1} to 10^{-4} (*dependent!*)
Paramagnetism	angular momentum of	+	0 to 10^{-4} (independent)
Diamagnetism	paired electrons field induced circulation	-	$\sim 10^{-6}$ (independent)

Paramagnetism and Diamagnetism of Transition Metal Ions: The magnetic properties of transition metal ions are directly related to unpaired electrons and orbital angular momentum.

Paramagnetic contributions from electron spin: Individual electrons have magnetic moments, indicated by their 'spins' (spin quantum number m_s = ½ or 'up'; m_s = -½ or 'down'), that may be aligned either with, or against, an external magnetic field.   When a species has unpaired electrons, it has a net magnetic moment and is paramagnetic. When a paramagnetic substance is placed in an external magnetic field, the unpaired electron spins may align either with the external field, reinforcing it, or against the external field. Because of energy considerations, there is a slight excess of the electrons with spins aligned with the external field.

Cooperative effects: The previous discussion assumed that each transition metal ion acted independently.   In some solids, where the magnetic centers are close to each other and can interact, enhanced magnetic effects (e.g., ferro- and ferrimagnetism) may be observed. These topics are beyond the scope of this experiment.

Diamagnetism: When all electron spins are paired, the net spin magnetic moment is zero, and the species is diamagnetic. The χ_g in these species is independent from the applied magnetic field. Diamagnetism does not simply imply a lack of magnetic properties. Instead, the paired electrons of diamagnetic substances produce a weak magnetic field *opposed* to an external magnetic field, so the internal magnetic field is weaker than the external field. All atoms of all substances provide a diamagnetic contribution to the substance's magnetism. Therefore, experimentally measured susceptibility χ_g of a paramagnetic substance must be transformed into molar susceptibility χ_M and corrected on atomic diamagnetism, based on its chemical composition. One worked out example of this procedure is presented in Experiment 12, below.

Crystal field theory: When a transition metal ion is surrounded by six ligands in an octahedral arrangement the electrostatic field splits the energies of the metal ion d orbitals. The field repels electrons in orbitals that interact directly with ligand electron pairs, and as a result, the $d_{x^2-y^2}$ and d_{z^2} orbitals are raised in energy, as shown in Figure 213**A**. As a result, five equal in energy (degenerate) d orbitals become separated by energy, and

exhibit splitting that is called *octahedral crystal field splitting* (Figure 213**B**)
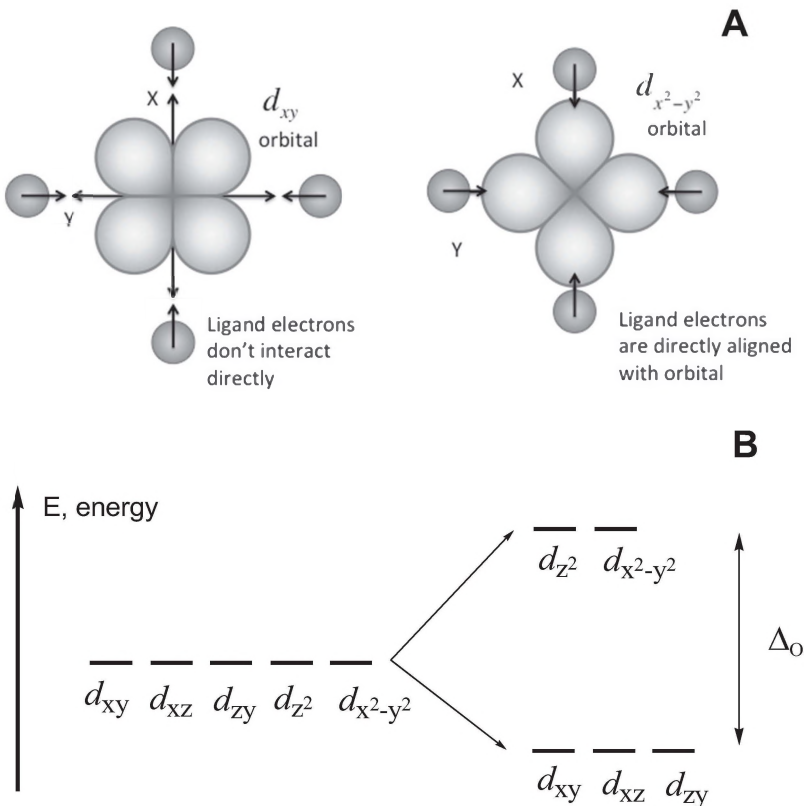

Figure 213. Incoming ligands and d electrons repulsion (**A**), and resulting crystal field splitting diagram in an octahedral field (**B**).

According to Hund's rule, electrons will be arranged to maximize the number of unpaired electrons within the number of available orbitals. When Δ_o is large, however, the lower energy *d* orbitals will be filled first. For ions with d^1, d^2, or d^3 orbital populations, the electrons will enter the t_{2g} set of orbitals, irrespective of the value of Δ_o. However, for ions with four or more d electrons, the value of Δ_o becomes critical. The fourth electron may either enter the e_g set of orbitals, or may pair up with another electron in the t_{2g} set. The outcome depends on the size of Δ_o compared to

the energy required to pair two electrons in the same orbital. When Δ_o is relatively small, the fourth electron enters the e_g set of orbitals, and there are four unpaired electrons. When Δ_o is large, the fourth electron is paired with another electron in the t_{2g} set, and there are only two unpaired electrons. The two different results are referred to as 'high spin' and 'low spin', as shown in Table 15, below.

Similar arguments may be made for ions with five or more d electrons. The number of unpaired electrons for high spin (HS) and low spin (LS) d^1 - d^{10} configurations are tabulated on the right, with the cases having different results highlighted. It should be apparent that the magnetic properties of metal ions might depend strongly on the crystal field splitting, Δ_o, for the compound in which they are found. For example, Co^{3+}, d^6, is paramagnetic with four unpaired electrons for complexes with low values of Δ_o (HS case), but diamagnetic for large values of Δ_o (LS case).

Classic magnetic measurements were carried out most of the time for *solid samples,* either at room temperature, or using variable temperatures from 300K to 6K. The most common and fast method of assessment of a compound's magnetic status is using room temperature measurements, using the Gouy method with the help of Johnson Matthew balances (see section 4.2.5, below). However, solutions may also be measured using the NMR Evans method, which is described here.

Table 15. Electronic configuration on *d*-orbitals and its spin state assignment. Entries highlighted in bold font indicate cases where the high spin (HS) and low spin (LS) results differ.

		Number of unpaired electrons			
	HS	LS		HS	LS
d^1	1	no LS	**d^6**	**4**	**2 or 0**
d^2	2	no LS	**d^7**	**3**	**1**
d^3	3	no LS	d^8	2	0
d^4	**4**	**2 or 0**	d^9	1	1
d^5	**5**	**3 or 1**	d^{10}	0	always LS

Part 4

- **Solutions Measurements Using the NMR Evans Method.**

This method is based on the paramagnetic induced shift of ^1H signals in the NMR spectrum of solvent peaks between solution and pure solvent [**3**]. Thus, unpaired electrons of the metal atom will cause signals to move, as compared to their position in a pure solvent. The chemical shift difference can be measured, and, knowing the mass of the dissolved studied sample, the value of χ_g can be measured according to the simple equation below:

$$\chi_g{}^{complex} = \frac{0.003 \times \Delta\delta}{4\pi \times \Delta m} + \chi_g{}^{solvent}$$

Here, $\Delta\delta$ is a chemical shift difference in ppm, and Δm is a mass of the sample in mg/mL, while $\chi_g{}^{solvent}$ represents the diamagnetic susceptibility of the used deuterated solvent, or the mixture of solvents. Values of χ_g for solvents of interest are: for $CD_3OD = -12.76 \times 10^{-6}$; and for $D_2O = -0.67 \times 10^{-6}$.

Chemicals:
        Deuterated solvents D_2O and CD_3OD for the Evans method.
Equipment:
        400 MHz Varian INOVA NMR spectrometer;
        1mm x 3mm concentric Wilmad tubes for the Evans method *(to save on the cost of this experiment, the author made his own insert into a standard 5mm NMR tub,e by using an appropriate diameter thin Pyrex tube and propane torch).*

The experimental setup for the Evans measurements is shown in Figure 214, below.

Step 1.
Accurately weigh 4-8 mg of powdery $K_3[Cr(C_2O_4)_3]\cdot3H_2O$ complex, using high precision balances capable of measurements to 0.01mg.

Step 2.
Carefully place the sample into a Pyrex vial of 4mL capacity, and add to it 0.7 mL of D_2O, to dissolve the complex completely. After the complex dissolves, add 0.3 mL of CD_3OD and mix it with the solution using the pipette.

Step 3.
Using the pipette, place 1.0 mL solution of the complex in the outer Evans tube **A** (Figure 214).

Step 4.
Place 0.5 mL of CD_3OD in the inner Evans tube **B** (Figure 214), and then carefully insert tube **B** into tube **A**.

Step 5.
Record the ^1H NMR spectrum of the complex using the available NMR spectrometer. Print the spectrum and measure the chemical shift difference between the paramagnetically shifted CH_3-group in the complex solution and the pure solvent.

Step 6.
Calculate the value of magnetic moment of the chromium(III) complex using the above equation for χ_g^{complex} and then apply the above formulas.

Cleanup:
Very carefully disassemble both tubes, pour the paramagnetic solution from tube **A** into the waste container, wash it with water, then acetone, and dry using N_2-gas from the tank or compressed air. *No use of drying oven is allowed, since heating the most common and inexpensive thin 5mm NMR tubes may lead to the tube bending ('swording').*
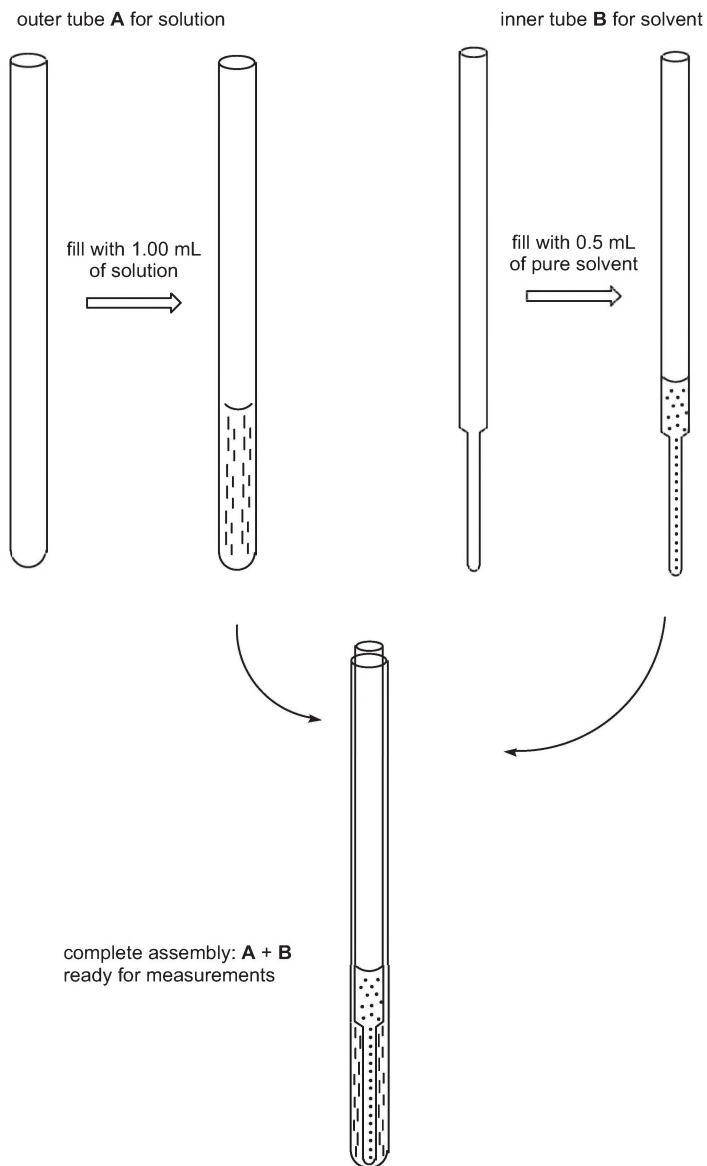
Figure 214. The experimental setup for the Evans method of determination of the magnetic moment of the complexes in the solutions.

Sample Calculation

A typical ^{1}H NMR spectrum in the Evans method should look similar to that shown below in Figure 215. The compound $K_3[Cr(C_2O_4)_3]\cdot 3H_2O$ (F.W.= 487.4 g mol^{-1}) in an amount of 6.61mg was prepared in solution, being dissolved in D_2O first (0.3mL), and then 0.7mL of CD_3OD was added to form a transparent blue-grey solution.

Chemical shifts for the diamagnetic component (inner tube, solvent) were identified as multiplet belonging to the CH(D) group of methanol which appears as a quintet with central signal at 3.370ppm (Figure 215). Respective environments in the presence of paramagnetic centers of Cr^{3+} represent a broader signal to the right of that multiplet, at 3.108ppm (Figure 215). Chemical shifts difference, $\Delta\delta$, therefore, is 0.262ppm.

Calculation of solvents (deuterated water and methanol) contribution into overall mass susceptibility χ_g of the complex is the following:

χ_g ^{solvent} = 0.7 (-0.72$\cdot$10^{-6}) + 0.3 (-0.67$\cdot$10^{-6}) = -0.71$\cdot$10^{-6},

where 0.7 and 0.3 are fractions of solvents water and methanol, and negative values in brackets represent mass susceptibilities of those pure solvents. Using the formula below, the complex mass susceptibility was obtained as:

$$\chi_g\,^{complex} = \frac{0.003 \times \Delta\delta}{4\pi \times \Delta m} + \chi_g\,^{solvent}$$

χ_g = (0.003$\cdot$0.262)/4π(6.62) + (-0.71$\cdot$10^{-6}) = 0.94$\cdot$10^{-6} - 0.71$\cdot$10^{-6}) = 0.87$\cdot$10^{-6}; this is χ_g ^{complex}
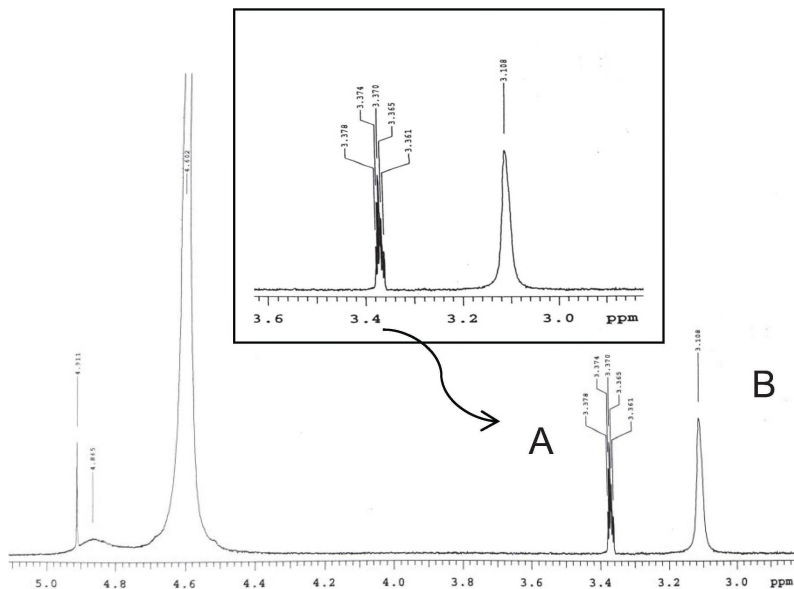
χ^{Molar} = 0.87$\cdot$10^{-6} (487.4) = 4.26$\cdot$10^{-3}

Figure 215. The experimental ^{1}H NMR spectrum of solution of Cr^{3+} complex in CD_3OD/D_2O mixture. Methyl groups of the solvent in diamagnetic (**A**) and paramagnetic environments (**B**) are shown in the inset.

The necessary diamagnetic correction χ^{DIA} was calculated using the Pascal Tables below, and amounted to: $3 \cdot (-34 \cdot 10^{-6})$ for oxalate anions, $3 \cdot (-13 \cdot 10^{-6})$ for three water molecules, $3 \cdot (-18.5 \cdot 10^{-6})$, and the same value for diamagnetic *closed-shells* of Cr-cation, giving total value of $-2.15 \cdot 10^{-4}$.

Therefore, corrected paramagnetic susceptibility of the complex is: $\chi^{para} = \chi^{Molar} - \chi^{DIA}$, or $4.26 \cdot 10^{-3} + (-2.15 \cdot 10^{-4}) = 4.47 \cdot 10^{-3}$.

The value of magnetic moment is: $\mu_{eff} = 2.83[(4.47 \cdot 10^{-3}) \cdot 298]^{1/2} = 3.27$ B.M. That value corresponds to the number of electrons, n, calculated from formula: $n = [(3.27)^2 + 1]^{1/2} = 3.52$ e, that we can round to ~ 3 unpaired electrons, which are indeed on 3d-orbitals of this central atom.

Theoretical value for spin-only magnetic moment is obtained from known formula [**4**]:

$\mu_{eff} = [n(n+2)]^{1/2}$, which for $n = 3$ gives 3.87 B.M.

Thus, determined in this particular example, the value of magnetic moment of the complex is 3.27B.M. with the absolute error of -0.6B.M., and relative error ~16%.

Finally, prepare your rather large lab report, which must contain your work and observations of all three parts of this study of the $K_3[Cr(C_2O_4)_3]$ complex *in solutions*, conductivity, cryoscopy, UV-visible spectroscopy data, and must determine the value of magnetic moment. This lab report must be similar in scope and thoroughness to the one generated from a series of laboratory experiments characterizing the *tris*-Co(III)-nitroso naphtolates, above.

This type of report is very typical of real investigations in the area of modern inorganic chemistry – coordination chemistry, where chemists:

1. Make and isolate complex compound;
2. Identify and characterize it *in solutions,* using a variety of physical methods suitable for the particular compound.

Cited Literature

1. Geary, W.J. The use of conductivity measurements in organic solvents for the characterization of coordination compounds. *Coord. Chem. Rev*., 1971, *7*, 81-122.
2. Orchard, A.F. *Magnetochemistry*. Oxford Chemistry Primers, 2003; ISBN 978-0-19-879278-9.
3. a) D.F. Evans*, J. Chem. Soc*. 1959, 2003;
    b) http://pubs.acs.org/doi/pdfplus/10.1021/ed069p62.1
    c) http://www.wilmad-labglass.com/Support/NMR-and-EPR-Technical-Reports/NMR-007-Coaxial-Inserts-in-NMR-Studies/
4. Drago, R.S. *Physical Methods for Chemists*. 2nd Ed., Surfside Scientific Publishing, Gainesville, FL. 1972.

4.4.2. Theoretical Background: foundation of the X-ray powder diffraction method for phase analysis of solids

In Chapter 3, we briefly described the basic principles of X-ray diffraction, and introduced the single crystal analysis method as the main tool for accurate determination of structure of a chemical compound. Thus, after successful structure solutions and refinement, precise values of bonds lengths and valence angles are established.

In this chapter, we introduce another method that involves the interaction of X-ray radiation with crystalline matter. The X-ray powder diffraction analytical technique is widely used in modern chemistry, geology, material science, and pharmaceutical manufacturing, for structural identification of crystalline compounds. The principles of X-ray diffraction analysis were laid out in the beginning of the 20th century by the works of Laue [1], Wullf and Bragg [2]. The X-rays are high energy electromagnetic radiation in the 0.1 to 100 Å (10^{-11} to 10^{-8}m) wavelength range. Laue showed that the X-ray wavelength was suitable for observation of a diffraction phenomenon on crystalline inorganic materials, like $CuSO_4 \cdot 5H_2O$ and ZnS, since X-rays were comparable to the interatomic distances of these compounds.

A crystalline material structure can be described as a specific three-dimensional atomic or molecular arrangement, with a repeating elementary pattern, called a *unit cell*. The unit cell determination and complete structural analysis are performed mostly for a single crystal, and were discussed above in Chapter 3, Part 1.

A repetitive order of elementary structural unit in three dimensions forms a lattice that can be viewed as a series of planes, with specific spacings d in between them. The crystal lattice, therefore, represents three-dimensional gratings for diffraction of the X-rays. Wullf's-Bragg's law (Figure 216) determines the relation between the incident X-ray wavelength λ and inter planar spacing d of the reflecting parallel planes. Diffraction and constructive interference occurs when a monochromatic beam of X-rays reflects on a number of parallel atomic planes of the crystal lattice. The constructive interference of in-phase waves results in an increase in the amplitude of the reflected signal. The difference in the travel paths of X-rays scattered thus is proportional by an integer to the incident wavelength λ. The angle between a transmitted and scattered X-ray is equal 2θ, therefore, the X-ray powder diffraction pattern is a plot of 2θ, ranging from 5° to 100° and intensity of the scattered beam.
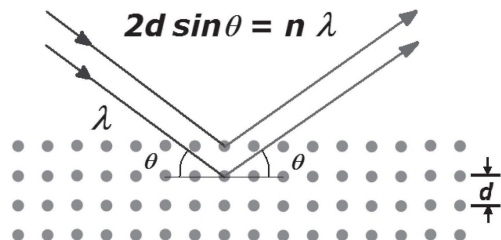
Figure 216. The Wullf's-Bragg's Law explanation: blue incoming arrows from the left represent incident monochromatic X-rays with wavelength λ, while red out-coming arrows represent scattered at crystal lattice X-rays of the unchanged wavelength, θ is a diffraction angle and d- inter planar spacing.

Since sin θ cannot exceed 1, and experimental λ can be of a certain value, Wullf's-Bragg's law derives that the minimum experimentally determined value of d- spacing is equal to ½ λ.

In order to record a powder pattern different from single-crystal, diffractometer type is needed. The basic equipment for the X-ray diffraction analysis experiment consists of the source of X-rays, a collimator, rotating (or static) sample holder, goniometer, and a detector rotating around the sample [3]. The X-rays are generated in a cathode vacuum tube with a tungsten heating element that emits electrons. These electrons are further accelerated with 30-50 kV potential, and driven to bombard anode metal plate. A number of metals are considered to be suitable anode materials, but copper and molybdenum are most commonly used. A specific set of X-rays, Kα1, Kα2 and Kβ, are generated when inner shells electrons of the metal plate are dislodged. To obtain monochromatic X-rays, the radiation beam is filtered by passing it through a highly absorbent material (specific for Kβ) : in the case of copper, source nickel filter is used. The resulting Kα= (2Kα1+Kα2)/3 is weighed by intensity wavelength. Cu Kα source emits rather intense radiation of wavelength of 1.5418 Å, which was found to be useful in many applications of the X-ray diffraction analysis [4].

The X-ray beam is focused by a special device called a collimator, prior to exposing a sample. There are several commercial designs of X-ray powder diffractometers. Some have a rotating sample, some do not. When a sample is exposed to the X-ray beam, diffraction occurs. At a certain diffraction angle the Braggs condition is met, and a constructive interference causes an increase in intensity of the scattered beam. This increase in intensity is registered by an electronic detector. The

X-ray diffractometer detector is rotating around a sample at a 2θ angle, ranging from 5° up to 100° [**5**].

*The X-ray diffraction pattern is **specific to sample structure**. Each sample scan contains a set of 2θ peaks, or d-spacings, that correspond to a specific plane of repeating pattern.* This observation makes the powder diffraction method very important for the composition (phase) analysis of numerous organic, and inorganic, compounds and minerals.

An example of the powder XRD patterns for pure oxalic acid dihydrate, $H_2C_2O_4 \cdot 2H_2O$ (which is one of the reagents used in preparation of the Cr(III) complex above), and its anhydrous form, just $H_2C_2O_4$, is shown in Figure 217. Many might think that both compounds intuitively could have close (if not the same) structures, since it is chemically the same acid! In fact, both have totally different metrics of the unit cells and crystal data, as shown in Table 16. As a result, crystal structures are different, and interplanar d- spacings are completely different as well, which is illustrated in Figure 217.

There are several factors that influence peaks' appearance in the X-ray diffraction pattern. A higher atomic number increases intensity. The smaller the crystal size, the wider the peak. The shorter the interplanar spacings d, the larger 2θ values for the peaks are observed. Another significant factor that influences peak intensities, and number of peaks in X-ray diffraction scan, is sample orientation. A single peak may be observed for a single crystal, whereas several peaks of different intensities may be found in the X-ray diffraction pattern of a polycrystalline sample of the same compound.

Table 16. Crystal data for the oxalic acid: dihydrate and anhydrous forms.

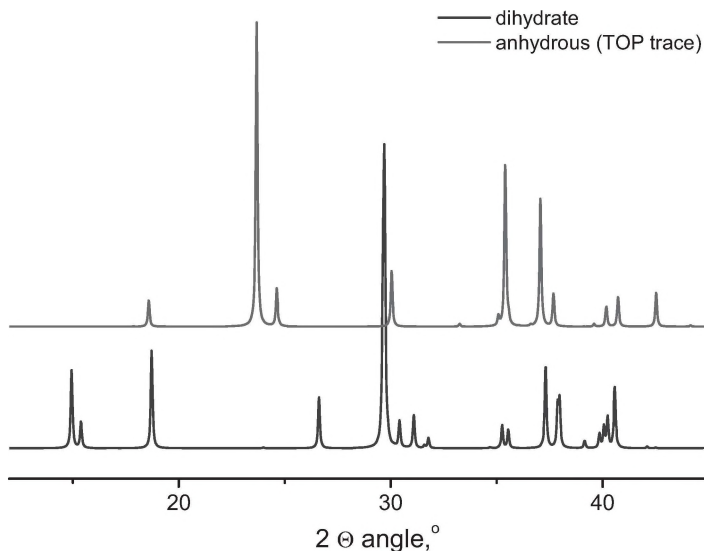| Moiety	Unit cell constants: Å,°	Refcode	Lit. Citation
$H_2C_2O_4 \cdot 2H_2O$		OXACD01	[6]
	a = 6.1024; α = 90 b = 3.4973; β = 105.77 c = 11.9586; γ = 90 monoclinic, P2$_1$/n Z=2; V = 245.61 A^3		
$H_2C_2O_4$		OXALAC11	[7]
	a = 5.3170; α = 90 b = 5.9435; β = 116.07 c = 5.3988; γ = 90 monoclinic, P2$_1$/c Z=2; V = 153.07 A^3		

Figure 217. Two overlaid powder patterns for oxalic acid showing their difference which are used for purity or phase analysis.

Some materials can crystallize in several different patterns, or polymorphs. Polymorphs can have the same composition, but different unit cell, or can be different solvates. Each polymorph has a characteristic set of peaks in X-ray diffraction scan. This 'fingerprint' property is used for qualitative and quantitative phase analysis [**9**]. Non-crystalline, or amorphous, materials consist of randomly-oriented molecular units, and do not exhibit any kind of repetitive pattern. The X-ray diffraction pattern of amorphous materials looks like a wide peak that covers the entire 2θ range.

The X-ray diffraction scans which contain indexed d-spacings and intensities, compose a fingerprint of a particular material. This property is the base of qualitative XRPD analysis. In many cases, a visual comparison of the XRPD pattern of an unknown with a standard, is sufficient for the positive identification of an unknown. Another qualitative way of phase identification is comparison of d-spacings and relative intensities (normalized as a percentage of the highest peak) of the standard and unknown sample. For most crystalline materials, $0.2°$ difference between a sample and a reference 2θ diffraction angle is generally regarded as acceptable. Unlike diffraction angles, peak relative intensities may vary due to orientation.

Naturally, using the software databases and comparisons can expedite the identification process. The International Center for Diffraction Data stores XRPD patterns and other structural information, as well as the solid phase properties of tens of thousands of compounds, and it is continuously being updated [**8**].

Phase quantification analysis is used for the determination of solid state composition of the material. All mixtures, solid solutions, and polymorphs can be quantified down to 2% content, if XRPD patterns of pure materials are available. The mixtures with known components content are prepared and analyzed. If characteristic angle peaks are present and comparable to the standard pattern, phase content is determined. Most common accuracy of the phase analysis of inorganic and complex compounds is around 5%.

Comments on sample preparation:
Fine sample grinding is essential to obtain small particles that will not exhibit preferred orientation. The optimal size of particles 1-10μm can be obtained using specialized mills, or an agate mortar-and-pestle set, and verified with an optical microscope. During the grinding process, the following processes may take place: phase transfer, contamination, decomposition, solid state reaction, etc. Therefore, it is advisable to compare the XRPD patterns of the specimen, before and after grinding, to assure its integrity [**9**].

Cited Literature

1. http://homepage.lnu.se/staff/pkumsi/1FY805/Laue.html
2. a) Schwarzenbach, D. *Crystallogr. Rev*., 2014, *20*(2), 155-156; DOI: 10.1080/0889311X.2013.876419;
   b) https://www.doitpoms.ac.uk/tlplib/xray-diffraction/bragg.php;
   c) Sir Lawrence Bragg, *The development of X-ray Analysis.* 1975, G.Bell & Sons Ltd. 270 pp.
3. John Wormald "*Diffraction methods,*" Oxford University Press 1973, 100 pp.
4. Leonid V. Azaroff, Martin J. Buerger "*The powder method in X-ray crystallography.*" 1958 McGraw-Hill book company 342 pp.
5. http://xrayweb.chem.ou.edu/notes/symmetry.html
6. Martin, A.; Pinkerton, A.A. *Acta Crystallogr. Ser B*., 1998, *54*, 471.
7. Bhattacharya, S.; Saraswatula, V.G.; Saha, B.K. *Cryst. Growth & Des*., 2013, *13*, 3651.
8. http://www.icdd.com/
9. US Pharmacopeia, 38 pp. 692-698 <941> "Characterization of crystalline and partially crystalline solids by X-Ray powder diffraction (XRPD)"

4.5. Experiment 12: Characterization of anionic potassium *tris*-oxalato{chromium(III)} in *solid state*

Part A

- Recording of IR-spectra;
- Recording diffusion reflectance spectra;
- Magnetic moment measurements using Gouy balances.

1.   Obtaining the IR-Spectrum of a Solid Complex.

Chemicals: Solid KBr (the IR-spectroscopy grade!);
                     $K_3[Cr(C_2O_4)_3] \cdot 3H_2O$ and oxalic acid dehydrate -
                     $H_2C_2O_4 \cdot 2H_2O$.

Equipment and Materials:
                     FT-IR spectrophotometer;
                     A set of the die and anvil for pressing salt pellets;
                     Hydraulic (or any other pressing device) press for making disks
                     (pellets) in KBr.

Step 1.
Using an agate mortar and pestle, ~150mg of IR grade potassium bromide and ~2-5mg of the Cr(III) complex obtained in the Experiment **10,** grind both together to make a fine powdery mixture for the IR pellet.

Step 2.
Press the pellet in a dry KBr matrix using the press and anvil/die set, according to the instructions provided. The pressing pressure, however, should not exceed 6 tons, on the grounds of hardware longevity. Good pellet should be homogeneous and transparent.
In order to avoid trapping air in the sample matrix (a mixture of grounded KBr + sample) use one of two methods:
   Provide suction (make a vacuum) using a portable membrane pump placed next to the hydraulic press and connected to the anvil/die set via hose [barbed hose outlets are indicated by asterisks in Figure 166, Chapter 3];
   Pump press slowly and release pressure 2-3 times before reaching ~6 tons value.
Disassemble the die/anvil set, promptly remove the pellet and place it into the instrument's pellet holder (for standard 13mm pellets), and insert the holder into the instrument compartment.

Step 3.
Record the solid-state FT-IR spectra of the Cr(III) *tris*-oxalato complexes using the following parameters: 64 repetitions (scans) in the range 400 – 4000cm^{-1} at 4cm^{-1} resolution, then subtract the previously recorded background with the same number of repetitions (scans) and resolution.

Step 4.
Print your data as a three-page printout. The first page is for a general (panoramic) view of the whole spectrum, while page two will be only for the 'fingerprint' region 400 – 1800cm^{-1}, and page three for the region of 2000 – 4000cm^{-1}. Page two should contain peak values to be analyzed and interpreted.

Step 5.
An example of spectrum of the complex is shown in Figure 218.

Step 6.
Perform bands' assignment using the 'functional groups frequencies' approach [**5**], and literature data for the initial compounds, such as oxalic acid hydrate (shown below, Figure 218), and potassium oxalate, displayed below, and handbook tables [**1**].

Bands for $K_2C_2O_4 \cdot 2H_2O$, cm^{-1}: 3273, 1599, 1407, 1319, 1312, 774, 721, 621, 528.

Explain observed shifts in positions of bands in your lab report.

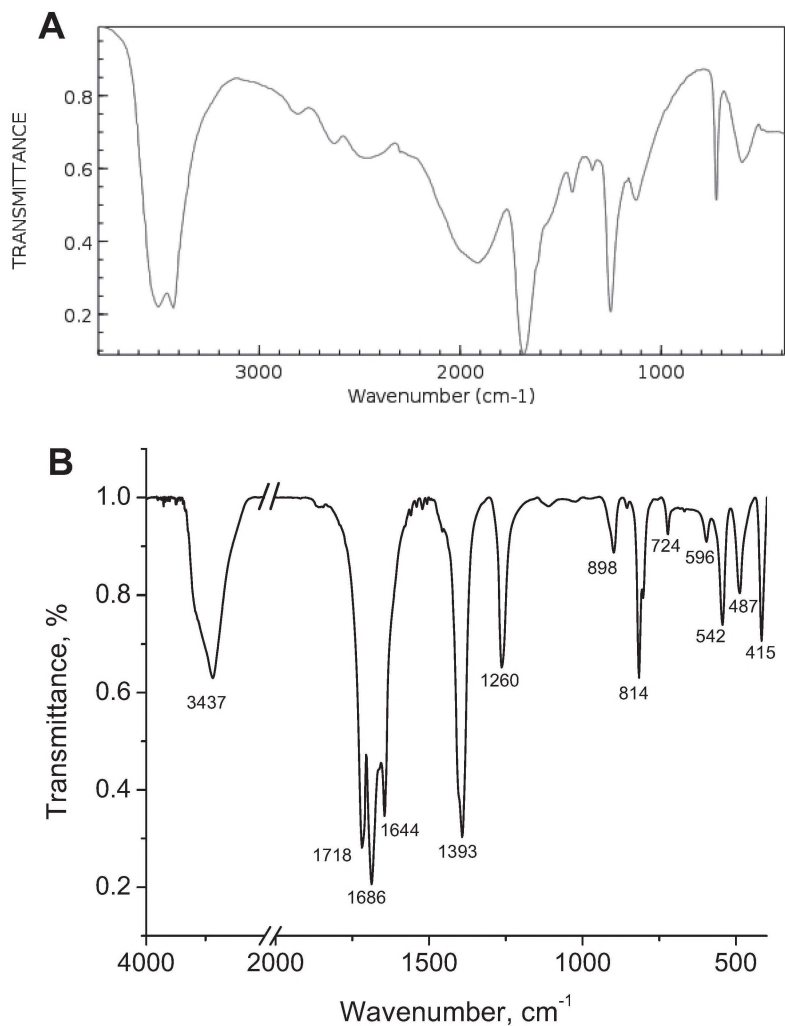**Figure 218.** Good quality FT IR-spectra of the oxalic acid dihydrate (**A**) and K$_3$[Cr(C$_2$O$_4$)$_3$]·3H$_2$O (**B**) in KBr pellets.

2.   Recording SDR (Spectrum of Diffusion Reflectance) of Cr-complex.
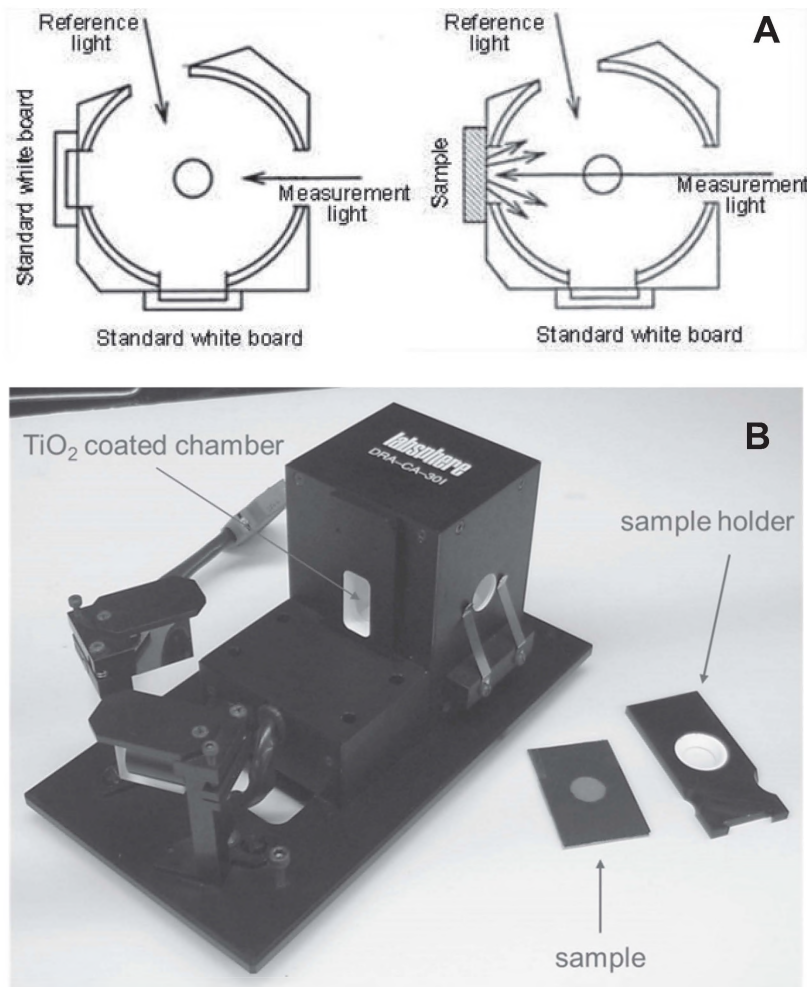

Figure 219.   Explanation for the principle of the light harvesting from solid samples (**A**), and actual integrating sphere used for recording SDR spectra of solid sample of *tris*-Cr(III) oxalate in our teaching laboratory (**B**). This piece is inserted in a spectrophotometer that has capability for such measurements.

Chemicals: Crystalline $K_3[Cr(C_2O_4)_3]\cdot 3H_2O$ made in previous lab.
Equipment and Materials:
                    Any available UV-visible spectrophotometer with solid
                    state capability;
                    White filter paper of small diameter: 3 – 6cm.

Step 1.
Place ~100-150mg of crystalline $K_3[Cr(C_2O_4)_3]\cdot 3H_2O$ complex into an
agate mortar and grind it with an agate pestle to a fine powder.

Step 2.
Take a small white round filter paper of ~5-6cm diameter, place it behind
the sample holder (Figure 219**B**), and attach the paper with the aid of
adhesive tape to the back of the holder.

Step 3.
Record its reflectance spectrum in *the absorbance mode,* and save it as a
background.

Step 4.
Detach the paper filter from the holder and place a small amount of
powdery complex on the middle part of it. Spread it gently to the area of
~2cm, and then tape it over with clear adhesive tape.

Step 5.
Record the reflectance spectrum of your complex in *the absorbance mode*.
Subtract the background and plot resulting spectrum. Measure the
wavelength of observed broad bands, and compare your solid-state
spectrum with the earlier recorded spectrum in solution. An example is
shown in Figure 220, below. You will need to attach the printout to your
lab report. Provide assignments of the observed transitions.

Step 6.
Make your conclusions and prepare this portion of the bigger lab report as
Part A.

NOTE:
The DRS are not quantitative method, and values of molar absorptivity or
reflectivity are not applicable for this type of electronic spectroscopy. This
is because of the experimental problems of the inability to prepare samples

of the same thickness, or occupying the same area, or of the same solid particle size, etc., that have to be examined, each time
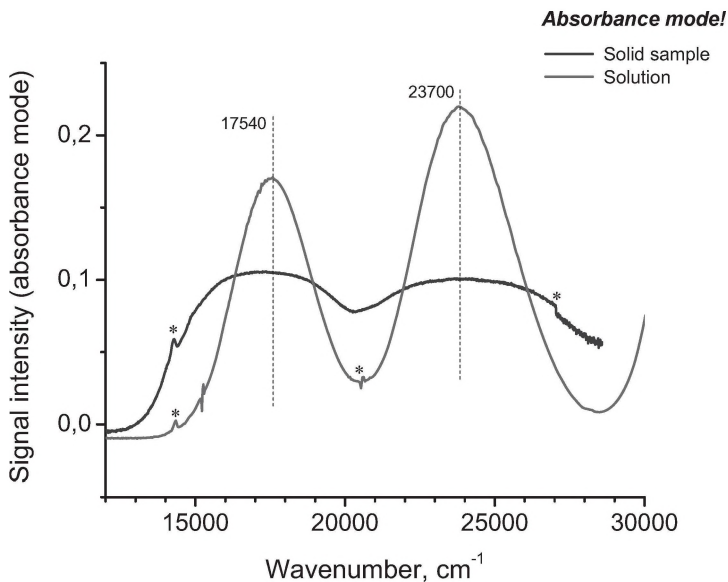

Figure 220. Overlaid for comparison electronic spectra of the $K_3[Cr(C_2O_4)_3]$ complex in solution (higher intensity peaks) and recorded in a solid state (broader peaks). Asterisks indicate instrumental artifacts.

3.   Magnetism of Solid $K_3[Cr(C_2O_4)_3] \cdot 3H_2O$: Experimental Measurements.

There is a variety of methods for measuring magnetic susceptibility. Normally in students' laboratories, Johnson-Matthew Gouy-type balances are used (Figure 221), which require a small 3mm inner diameter glass tube. The basic principle of the Gouy method is shown in Figure 221. It uses sensitive balances which are able to measure weight gain for a magnetic substance in the presence of magnetic field. The sample must take cylindrical shape of a sufficient length: long samples respond better to the field gradient, and display larger magnitude of the attractive force.
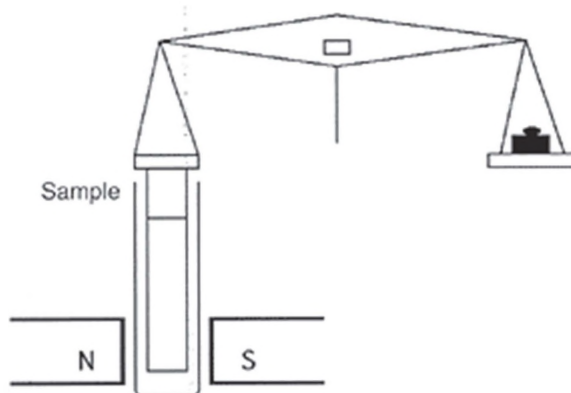
Figure 221. Principle of the Gouy method of measurements of χ_g: paramagnetic samples are attracted to the magnet, while diamagnetic substances are repelled.

Solid State Measurements Using the Johnson-Matthey Magnetic Susceptibility Balance (Figure 222): The balance must be leveled prior to use. Its readings are quite sensitive to this adjustment, so once the balance has been set up, it should not be moved at all.

Unfortunately, the measurements on this balance can only be performed at room temperature. Pack the tube with a ground powdery sample to at least 3-4cm in length, to produce accurate data. Compression of the sample inside the tube is accomplished with a Pyrex rod/compactor (Figure 222). Presence of air in a loose, not pressed, sample also skews the data.
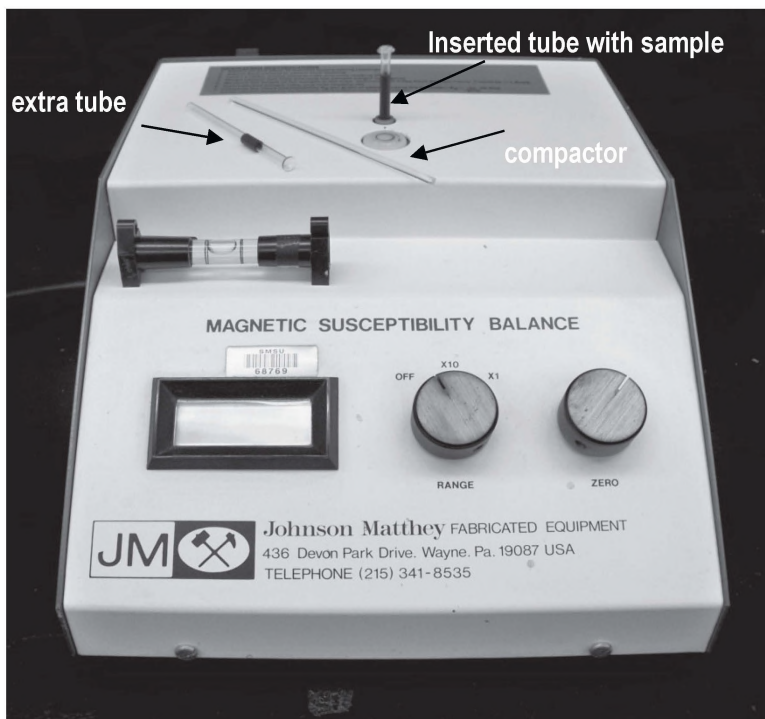
Figure 222. The Gouy balance operated at room temperature. Shown are an extra tube and a glass compactor for pressing the powdery sample inside the tube.

Step 1.
Turn the RANGE knob to the x1 scale and allow at least ten minutes warm-up time.

Step 2.
Adjust the zero knob until the display reads 000 (Figure 222).

Step 3.
Place an empty, pre-weighed, sample tube in the sample guide, and record the reading, R_o. *The sample tubes must be clean and dry.*

Step 4.
Grind the sample into a very fine powder, and pack it into the sample tube as evenly as possible. Note the mass of the sample in grams, and its length in centimeters. The length must be at least 1.5cm, preferably 2.5 - 3.5cm.

Step 5.
Place the packed tube into the tube guide and record the reading, R. A decrease in the reading (i.e. R - R_o negative) indicates that the sample is diamagnetic. If the reading goes off the scale, switch to the x 10 scale, re-zero (with the sample tube removed), and record the reading for the sample (note the x 10 scale).

Cleanup:
Empty the sample tubes, placing any waste in the sludge pan. Clean and dry the sample tubes.

1. Data Analysis

Solid State Measurements Using the Gouy Magnetometer (Figure 222). The magnetic susceptibility measured in the lab using this instrument represents the χ_g, susceptibility per gram, and is calculated using the following equation:

$$\chi_g = \frac{C(R - R_0)\ell}{m \times\ 10^9}$$

Where C is an instrument calibration constant (C = 0.972; may be different for different models), R and R_0 are the readings obtained, ℓ is the length of the sample in cm, and m is the mass of the sample in grams.

The χ_g is converted to molar magnetic susceptibility, χ_m (susceptibility per mole), by multiplying the mass susceptibility by the formula weight of the compound:

$$\chi_m = \chi_g \times\ formula \cdot\ weight.$$

Next, in order to calculate the magnetic susceptibility of the paramagnetic transition metal ion alone, χ^{para}, the diamagnetic contributions from other parts of the molecule must be subtracted from χ_m.

$$\chi^{para} = \chi_m - \chi^{dia}$$

Where χ^{dia} is the diamagnetic contributions from all atoms, χ^A, and bonds, χ^B, in the molecule. The diamagnetic contributions are calculated as the sum of the Pascal's constants for each atom and relevant bond. A set of Pascal's constants is provided in the Pascal Tables 1-5 at the end of this lab experiment.

The effective magnetic moment, μ_{eff}, and number of unpaired electrons, n, are then calculated as follows:

$$\mu_{eff} = 2.83\sqrt{\chi^{para}T} = \sqrt{n(n+2)}$$

where T is the temperature in K.

2. Sample Calculation

The following values were obtained for a standard compound - solid $CuSO_4 \cdot 5H_2O$ (F.W.= 249.7 g mol^{-1}):

$$R_0 = -33$$
$$R = 719 \ @ \ 20\,°C$$
$$m = 0.325 \ g$$
$$\ell = 2.62 \ cm$$

$$\chi_g = \frac{C(R - R_0)\ell}{m \times 10^9} \Rightarrow \frac{0.972(719 - (-33))(2.62)}{0.3250 \times 10^9} = +5.89 \times 10^{-6}$$

$$\chi_m = \chi_g \times formula - weight \Rightarrow 5.89 \times 10^{-6} \times 249.7$$
$$= 1.47 \times 10^{-3}$$

$$\chi^A = \sum Pascal's \ const. \ for \ atoms \Rightarrow \chi^A$$
$$= Cu^{2+} + SO_4^{2-} + 5 \times H_2O$$
$$\Rightarrow (-11 \times 10^{-6}) + (-40.1 \times 10^{-6}) + (5(-13 \times 10^{-6}) = -1.16 \times 10^{-4}$$

(commonly accepted numerical values of Pascal's constants are available from Tables 1- 4 below).

$\chi^B = 0$ because no constitutive (bond) corrections are needed. Thus,

$$\chi^{para} = \chi_m - \chi^A \Rightarrow \chi^{para} = 1.47 \times 10^{-3} - (-1.16 \times 10^{-4})$$
$$= 1.59 \times 10^{-3}$$

And,

$$\mu_{eff} = 2.83\sqrt{\chi^{para}T} = 2.83\sqrt{1.59 \times 10^{-3}(293)} = 1.93,$$

$$\mu_{eff} = \sqrt{n(n+2)} \Rightarrow 1.93 = \sqrt{n(n+2)} \Rightarrow n = \sqrt{(\mu_{eff})^2 + 1} - 1 \Rightarrow n$$
$$= \sqrt{1.93^2 + 1} - 1 = 1.17 \approx 1$$

which means Cu^{2+} has only one unpaired electron.

$$percent\ error = \frac{|theoretical - obtained|}{theoretical} \times 100 = \frac{|1 - 1.17|}{1} \times 100$$
$$= 17\%\ error$$

Pascal's Constants (Diamagnetic Corrections) for Ions and Neutral Molecules.

(from: John Berry in "*Journal of Chem. Educ.*" **2008**, *85* (4), pp. 532-536).

Pascal Table 1. Values of χDi (in $1 \cdot 10^{-6}$ emu mol^{-1}) for Atoms in Covalent Species.

Atom	χDi	Atom	χDi	Atom	χDi	Atom	χDi
Ag	−31.0	C (ring)	−6.24	Li	−4.2	S	−15.0
Al	−13.0	Ca	−15.9	Mg	−10.0	Sb(III)	−74.0
As(III)	−20.9	Cl	− 20.1	N (ring)	−4.61	Se	−23.0
As(V)	−43.0	F	−6.3	N (chain)	−5.57	Si	−13
B	−7.0	H	−2.93	Na	−9.2	Sn(IV)	−30
Bi	− 192.0	Hg(II)	−33.0	O	−4.6	Te	−37.3
Br	− 30.6	I	−44.6	P	−26.3	Tl(I)	−40.0
C	− 6.00	K	−18.5	Pb(II)	−46.0	Zn	−13.5

le 2. Values of λi (in $1 \cdot 10^{-6}$ emu mol^{-1}) for Specific Bond Types

	λi	Bond	λi	Bond	λi	Bond
	+5.5	Cl–CR$_2$CR$_2$–Cl	+4.3	Ar–Br	−3.5	Imidazole
	+0.8	R$_2$CCl$_2$	+1.44	Ar–Cl	−2.5	Isoxazole
	+10.6	RCHCl$_2$	+6.43	Ar–I	−3.5	Morpholine
r	+3.85	C–Br	+4.1	Ar–COOH	−1.5	Piperazine
				Ar–C(=O)NH$_2$	−1.5	Piperidine
H$_2$–	+4.5	Br–CR$_2$CR$_2$–Br	+6.24			
	+6.3	C–I	+4.1	R$_2$C=N–N=CR$_2$	+10.2	Pyrazine
	−5.0	Ar–OH	−1	RC≡C–C(=O)R	+0.8	Pyridine
	−5.0	Ar–NR$_2$	+1	Benzene	−1.4c	Pyrimidine
	−3.5	Ar–C(=O)R	−1.5	Cyclobutane	+7.2	α- or γ-Pyrone
	+1.85	Ar–COOR	−1.5	Cyclohexadiene	+10.56	Pyrrole
	+8.15	Ar–C=C	−1.00	Cyclohexane	+3.0	Pyrrolidine
	+0.8	Ar–C≡C	−1.5	Cyclohexene	+6.9	Tetrahydrofuran
	+0.0	Ar–OR	−1	Cyclopentane	+0.0	Thiazole
	+1.7	Ar–CHO	−1.5	Cyclopropane	+7.2	Thiophene
	−2.0	Ar–Ar	−0.5	Dioxane	+5.5	Triazine
	+3.1	Ar–NO$_2$	−0.5	Furan	−2.5	

Synthesis and Characterization of the Anionic Paramagnetic Complex

le 3. Values of χDi $(1 \times 10^{-6}$ emu mol$^{-1})$ for Anions

χDi	Anion	χDi	Anion	χDi	Anion	χDi
−51	$C_5H_5^-$	−65	NCO^-	−23	$S_2O_3^{2-}$	−46
−60	$C_6H_5COO^-$	−71	NCS^-	−31.0	$S_2O_8^{2-}$	−78
−37	CO_3^{2-}	−28.0	O^{2-}	−12.0	HSO_4^-	−35.0
−35	$C_2O_4^{2-}$	−34	OAc^-	−31.5	Se^{2-}	−48
−34.6	F^-	−9.1	OH^-	−12.0	SeO_3^{2-}	−44
−40	$HCOO^-$	−17	PO_3^{3-}	−42	SeO_4^{2-}	−51
−23.4	I^-	−50.6	$PtCl_6^{2-}$	−148	SiO_3^{2-}	−36
−30.2	IO_3^-	−51	S^{2-}	−30	Te^{2-}	−70
−32.0	IO_4^-	−51.9	SO_3^{2-}	−38	TeO_3^{2-}	−63
−13.0	NO_2^-	−10.0	SO_4^{2-}	−40.1	TeO_4^{2-}	−55
−18.9						

Pascal Table 4. Values of χDi (in 1×10^{-6} emu mol^{-1}) for Common Ligands

Ligand	χDi	Ligand	χDi
Acac–	–52	Ethylene	–15
Bipy	–105	Glycinate	–37
CO	–10	H$_2$O	–13
C$_5$H$_5$–	–65	Hyrdazine	–20
En	–46.5	Malonate	–45
NH3	–18	Pyrazine	–50
Phen	–128	Pyridine	–49
o-PBMA	–194	Salen2–	–182
Phthalocyanine	–442	Urea	–34

4.6. Experiment 13: Characterization of anionic potassium *tris*-oxalato{chromium(III)} in *solid state*

Part B

- Recording TG/DSC traces and identifying the phase transition region.
- Recording the powder XRD pattern for the final product – *tris*-oxalato-Cr-complex.
- Comparing recorded powder XRD patterns for the initial compounds (phase analysis).

It is important to recognize and emphasize the fact that solutions and solid-state properties might be different! For instance, upon dissolution, crystal lattice and crystal packing effects associated with it, and the complex's integrity may be violated due to *the dissociation*, or *solvation* effects, which may lead to a *change in metal center environment,* due to the solvent coordination. Thus, if UV-visible spectra of the complex in solid state and in solution look the same – then the metal environment is intact, and the inner sphere is unchanged.

The same is true about magnetism: in solid state, cooperative effects such as *ferro-* or *antiferro*-magnetic exchanges (due to close packing in the crystal lattice) may play an important role in electronic status of the complex. In solution, magnetism reflects only paramagnetic metal center and no cooperative effects. Therefore, in order to make sure that the description of geometry and electronic structure of a particular complex compound are correct, both types of studies are necessary - in solutions

and in solid state. In Part **B** of laboratory experiment **13,** we continue to study properties of solid complexes.

Thermal analysis.

Step 1.
Recording the TG/DSC traces for a sample of freshly prepared and dried $K_3[Cr(C_2O_4)_3]\cdot3H_2O$ complex using available thermoanalyzer. A sample of ~20mg is sufficient. Examples of recorded traces are shown in Figure 223.
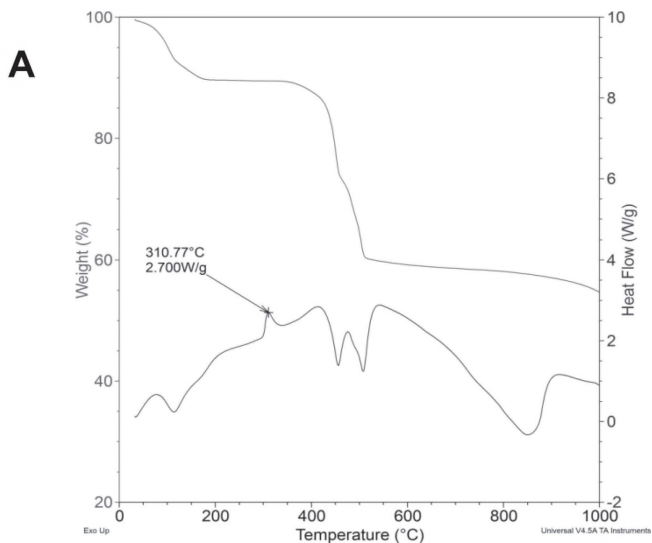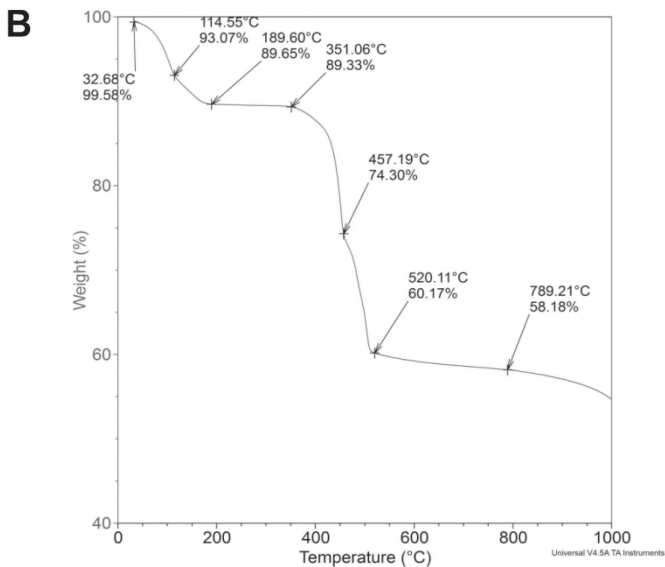
Figure 223. Results of TG/DSC analysis of K$_3$[Cr(C$_2$O$_4$)$_3$]·3H$_2$O sample: **A** – panoramic view showing the polymorphic phase transition at ~310°C; **B** – trace of the weight loss.

Perform thermogravimetric analysis of Cr(III) decomposition traces and complete the table below in a manner similar to that carried out in Chapter 2, during investigations of manganese nitrate and ferrous sulfate thermal decomposition processes (Tables 4 and 5 in this book).

Table 17. Results of thermal analysis studies of K$_3$[Cr(C$_2$O$_4$)$_3$]·3H$_2$O decomposition under pure N$_2$ atmosphere (Figures 223**A** and **B**).

Compound	Process*	Product	Weight losses, % calculated (*found*)	Error, %
K$_3$[Cr(C$_2$O$_4$)$_3$]·3H$_2$O		?	?	?

Powder diffraction data.

Step 1.
Use an already-ground sample of $K_3[Cr(C_2O_4)_3] \cdot 3H_2O$ (the same as the one that you used for the recording solid state reflectance spectrum) for recording the XRD pattern on the powder diffractometer. That can be done by placing a small amount of ground sample on a piece of cardboard and fixing it with clear adhesive tape. Then, that cardboard should be placed on a sample holder of the diffractometer and the powder pattern recorded, using the following parameters:

- two theta angles range from 6 to 60°;
- step of 0.02°;
- speed of the goniometer motion 0.1° per second.

Step 2.
Save the data in formats that will allow their processing outside the instrument, on another computer.

Step 3.
Repeat the previous step by recording powder XRD patterns for starting compounds $K_2C_2O_4 \, H_2O$, and $K_2Cr_2O_7$. This is important to investigate the purity of the final product - $K_3[Cr(C_2O_4)_3] \cdot 3H_2O$ – on presence of initial compounds. An example of contaminated product can be seen from the microscope photograph of one of the samples from the previous year's students' preparations (Figures 200 and 224).
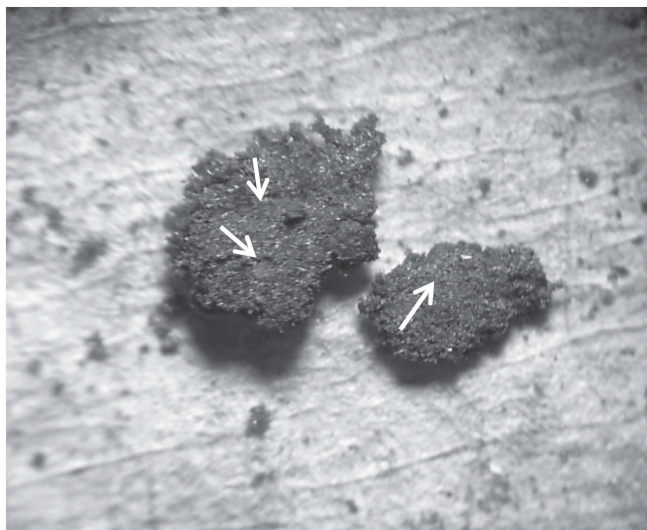
Figure 224. Optical microscope photograph at 20x magnification of the sample of $K_3[Cr(C_2O_4)_3]\cdot 3H_2O$ on a filter paper. Arrows indicate the visible presence of impurities of the starting orange $K_2Cr_2O_7$.

Step 4.
Make an overlaid plot of all three recorded XRD powder patterns for $K_3[Cr(C_2O_4)_3]\cdot 3H_2O$, $K_2C_2O_4$ H_2O, and $K_2Cr_2O_7$. Perform analysis by drawing vertical lines from the patterns of the starting compounds to the final product, in order to find the possible presence of peaks that correspond to them. An example of such analysis is shown in Figure 225. Write your observations and conclusions.

Finally, prepare a rather large lab report for **Part B,** which must contain your work, and observations of all the above parts of the study of the $K_3[Cr(C_2O_4)_3]$ complex in solid state: IR- and visible spectra, magnetism, thermal analysis, detection of polymorphic phase transition, and phase analysis. This lab report must be similar in scope and thoroughness to the previous one, describing the properties of an anionic Cr(III) complex in solutions. This time, however, it is all about the properties of solid $K_3[Cr(C_2O_4)_3]\cdot 3H_2O$. Again, this type of report is very typical of a real investigation in the area of modern coordination chemistry.
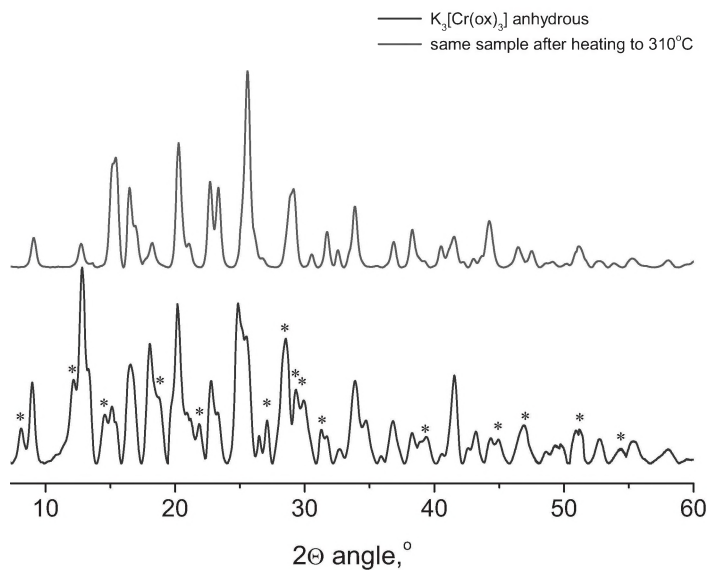
Figure 225. Comparison of two powder patterns for anhydrous complex before (bottom trace) and after polymorphic phase transition (top trace). Asterisks mark interplanar distances peaks that disappear during transition.

As the reader can see through this laboratory manual, the book provides a set of simple experiments, in grams quantities, and teaches students how to handle the obtained compounds. That includes their characterization, crystal growth, packaging, etc. All chemicals used are inexpensive, as opposed to many of those listed in the above laboratory manuals at the beginning of the Afterword.

The book also provides a variety of laboratory experiments with a good selection of what to learn, or synthesize, depending on the availability of instrumentation at a particular place. Thus, there is a choice for the lab instructor to adapt to existing laboratory conditions and supplies.

Finally, the biggest advantage of this laboratory manual is the explanation of physical methods, and in-depth interpretation of the NMR spectroscopy techniques and results using seemingly simple low molecular weight classic organic ligands – isomeric nitrosonaphtoles. That particular topic makes this book truly unique.

Your feedback, comments and suggestions are very welcome at NNGerasimchuk@MissouriState.edu, s.tyukhtenko@neu.edu, or via our phones: (417) 836-5165 and (860) 942-0255.

THE LIST OF CHEMICALS AND SOLVENTS USED IN EXPERIMENTS DESCRIBED IN THIS BOOK

_____

Experiment	Chemical or solvent	CAS number
Lab 1**A**:	$Mn(NO_3)_2xH_2O$, wet pink solid or viscous solution	17141-63-8
	HNO_3, conc.	7697-37-2
Lab 1**B**:	$KMnO_4$	7722-64-7
	$BaCl_2\ 2H_2O$	10326-27-9
	Elemental sulfur, S_8	7704-34-9
	Elemental phosphorous (red), $(P_4)_n$	7723-14-0
	Indicator: methyl orange	547-58-0
Lab 2**A**:	Iron filings *we used rusty tacks, small nails, but as chemical:*	7439-89-6
	H_2SO_4, conc.	7664-93-9
	KNCS	333-20-0
	Ethanol, 95%	64-17-5

Lab 2**B**:	$Cu(CH_3COO)_2 \, H_2O$		142-71-2
	Hydrazine hydrate, $N_2H_4 \, H_2O$		10217-52-4

Lab 3**A**,	*for PbTe*:	Elemental Te	13494-80-9
		HCl, conc.	7647-01-0
		HNO_3, conc.	7697-37-2
		Elemental lead, Pb	7439-91-1
		(or lead oxide, yellow PbO)	1317-36-8
		(or lead carbonate, $PbCO_3$)	598-63-0
		Hydrazine hydrate, $N_2H_4 \, H_2O$	10217-52-4
		Tartaric acid	526-83-0
		Ammonia solution, conc.	1336-21-6
	for PbSe:	Elemental Se	7782-49-2
		HCl, conc.	7647-01-0
		HNO_3, conc.	7697-37-2
		Elemental lead	7439-91-1
		(or lead oxide, yellow PbO)	1317-36-8
		(or lead carbonate, $PbCO_3$)	598-63-0
		Hydrazine hydrate, $N_2H_4 \, H_2O$	10217-52-4
		Tartaric acid,	526-83-0
		Ammonium hydroxide, NH_4OH, conc.	1336-21-6

Lab 3**B**:	Elemental cadmium		7440-43-9
	(or cadmium oxide, CdO)		1306-19-0
	Ammonium carbonate, $(NH_4)_2CO_3$		506-87-6
	Ammonium hydroxide, NH_4OH, conc.		1336-21-6

Lab 4**A**: *for NiCl₂*	NiCl₂ 6H₂O	7791-20-0
	SOCl₂	7719-09-7
for CoCl₂	CoCl₂ 6H₂O	7791-13-7
	SOCl₂	7719-09-7
Lab 4**B**:	SnCl₂ 2H₂O	10025-69-1
	Acetic anhydride, (CH₃CO)₂O	108-24-7
	Diethyl ether, (C₂H₅)₂O	60-29-7
Lab 5**A**:	CoCl₂ 6H₂O	7791-13-7
	1-Nitroso-2-naphtol	131-91-9
	Glacial acetic acid	64-19-7
	Methanol	67-56-1
Lab 5**B**:	CoCl₂ 6H₂O	7791-13-7
	2-Nitroso-1-naphtol	132-53-6
	Glacial acetic acid	64-19-7
	Methanol	67-56-1
Lab 6**A**:	Co(III) complexes from previous preparation	
	silicagel for column chromatography, 50-220 mesh	n/a
	CH₂Cl₂	75-09-2

Lab 6**B**:   Co(III) complexes from previous preparation
                   preparatory TLC plates   n/a
                   CH_2Cl_2 75-09-2
                   Toluene   108-88-3

Lab 7:   separated isomers of Co(III) complexes from previous lab
                   analytical Al-backed TLC plates, 20x20 cm
                   CH_2Cl_2 (or solvent mixture with toluene from above)

Lab 8:   separated isomers of Co(III) complexes from previous lab
                   Pure ligands: 1-Nitroso-2-naphtol   131-91-9
                   deuterated solvents:
                   $CDCl_3$ 865-49-6
                   CD_2Cl_2 1665-00-5
                   C_6D_6 1120-89-4

Lab 10:   potassium dichromate, $K_2Cr_2O_7$ 7778-50-9
                   Oxalic acid, $H_2C_2O_4\ 2H_2O$ 6153-56-6
                   Potassium oxalate, $K_2C_2O_4$ 6487-48-5

Lab 11: $K_3[Cr(C_2O_4)_3]3H_2O$ from previous preparation
                   Deuterated solvents for the Evans method:
                   D_2O 7789-20-0
                   CD_3OD 811-98-3

Many of listed here chemicals are used in several laboratory experiments.

The list of equipment used in experiments described in this book

Common laboratory glassware and small hardware as presented in Chapter 1

INSTRUMENTATION includes:

any available UV-visible spectrophotometer working in the range of 200 – 800 nm,
any available FT-IR spectrophotometer working in the range of 400 – 4000 cm^{-1},
derivatograph / thermal analyzer operational to ~1100ºC,
available X-ray diffractometers for powder and single crystal analysis,
electrical conductivity meter for solutions with the probe,
electrochemical setup for cyclic voltammetry measurements: potentiostat and electrodes,
available table top room temperature magnetic susceptibility measuring device,
any available FT-NMR spectrometer,
table top electrical centrifuge,
any available microscope.

AFTERWORD

It was assumed in this book that students have very limited laboratory experience, or none at all. This approach was justified. The assumption was based on many years of teaching the inorganic chemistry curriculum in two countries, with vastly different student populations.

There is a big void in instruction books, between primitive general chemistry manuals, and the chemical experimentation books by Woolins, Angelichi, Drezdon, Darensburg, etc., which assume a high level of comprehension and competency. This laboratory manual is designed to fill that void in part, showing students and any interested readers the properties of glass and joints, and the principles of operation of presented glassware pieces and commonly used lab equipment.

The level of practical exposure to actual laboratory glassware and instrumentation, and to physical and spectroscopic methods, is very minimal. As a result, when a student goes for the graduate degree (MS or Ph.D.), or for work in a synthetic chemistry laboratory in industry, his/her lab preparation is very, very limited. It takes a lot of time to properly train that person to perform common laboratory operations in a competent and safe manner. The main, striking, problem is that students simply are not familiar with many important concepts of glassware design and operations, or the principles of working with major lab equipment. One of the reasons is that students are not exposed to such instrumentation because of limitations existing in particular schools and universities. Of course, we are aware of expenses that many academic institutions face in maintaining their curriculum. That is why, at any opportunity throughout this book, we emphasize how to save on available resources, during the generation of small volumes of gases, for example, and so on.

Another reason is that the mainstream teaching labs shifted, over two decades ago, to *mini-scale preparations,* to cut cost. As a result, special *micro-kits* were designed and used in numerous laboratories. These are not typical glassware pieces which one will find later on in real research labs in the higher education institutions, or in kilo-labs or in the R&D labs in industry. The same is true with regard to the handling of a few milligrams of substances, which is way less typical than the common yields during normal scale syntheses carried out in other-than-teaching laboratories.
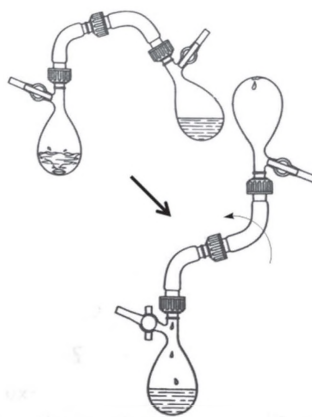
APPENDIX 1

AIR-FREE MANIPULATIONS DURING ANAEROBIC SYNTHESES

Mixing/addition of solutions:
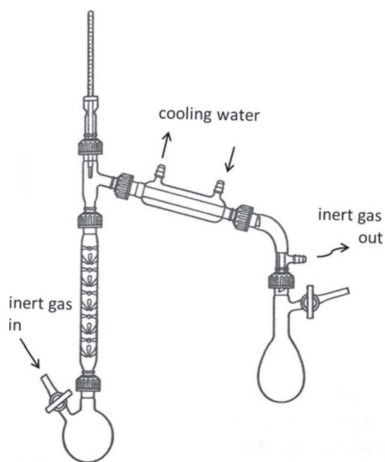

Assembly for *controlled* addition of solutions.
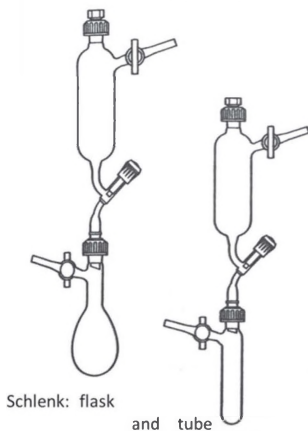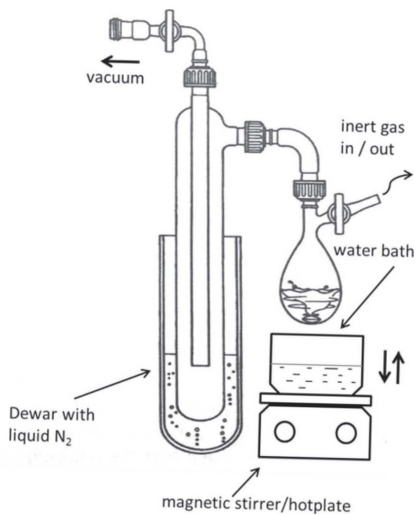
Two flasks assembly for rapid mixing of solutions.

Schlenk: flask and tube

Solvent removal:

Evaporation at room / elevated temperature under vacuum:

cooling water

inert gas
out

inert gas
in

**Evaporation at elevated temperatures
at ambient pressure.**

vacuum

inert gas
in / out

water bath

Dewar with
liquid N_2

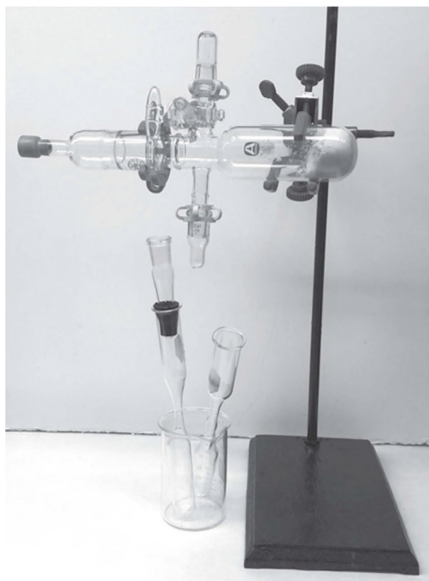magnetic stirrer/hotplate

Filtration using anaerobic filters of two types:
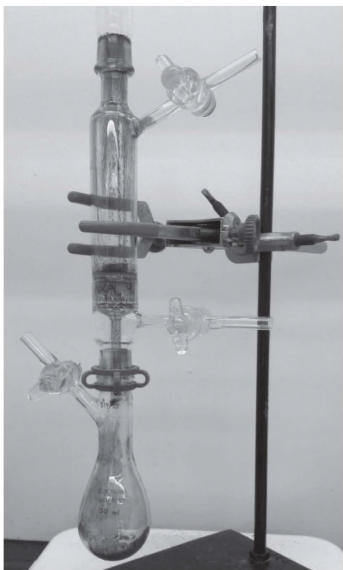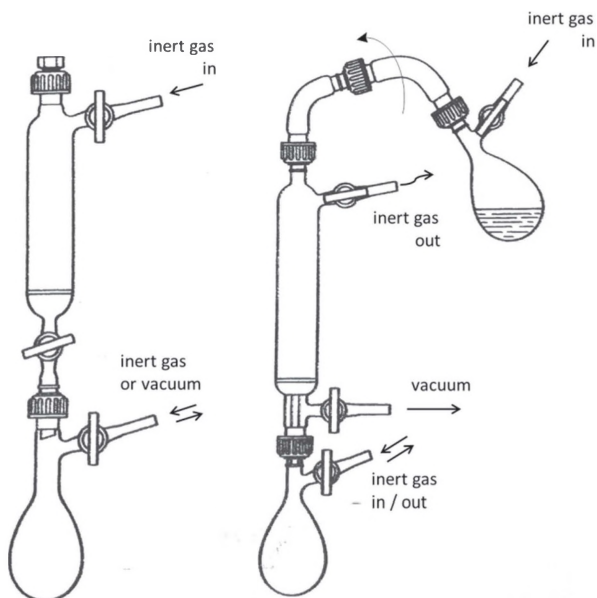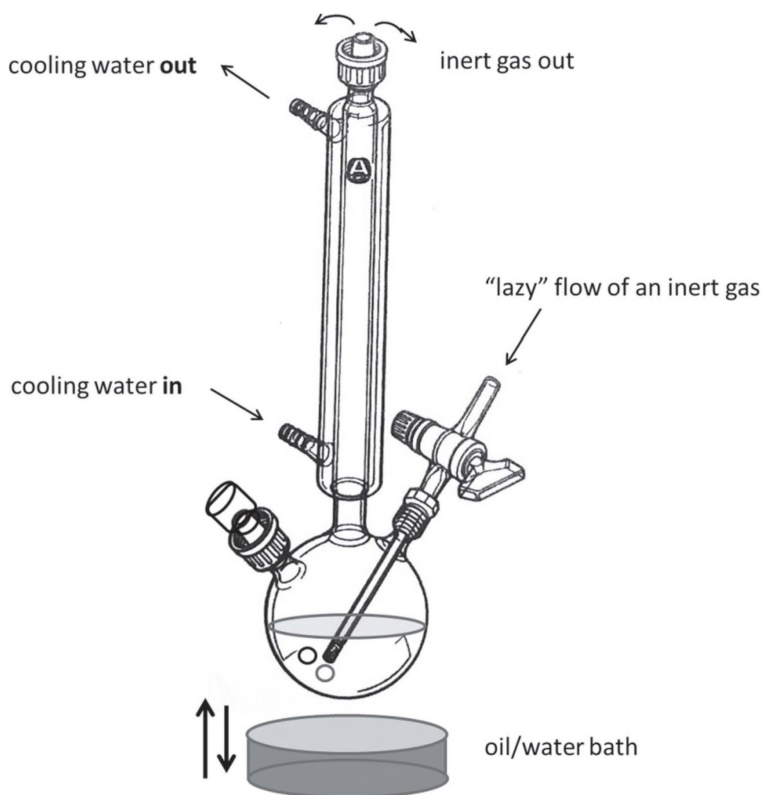

Filtered air-sensitive Fe(II) complex.

Two assemblies for crystallization:
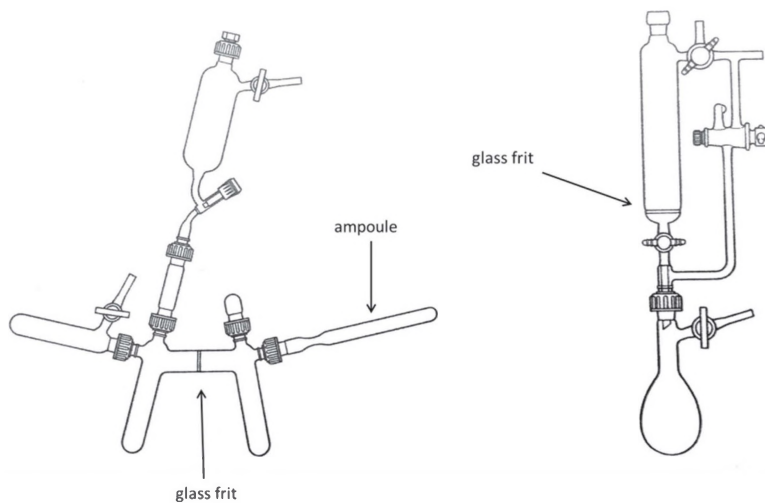
Air-sensitive solid is ready for packing in ampoules!

Solvent conditioning: degassing with an inert gas upon boiling.

cooling water **out**

inert gas out

"lazy" flow of an inert gas

cooling water **in**

oil/water bath

All pieces of glassware presented here are designed to work under small positive pressure of an inert gas when stopcocks and valves are opened.

APPENDIX 2

SOLUBILITY RULES (SOLUBILITY CHART)
FOR THE MOST COMMON SALTS OF IONIC COMPOUNDS

	NH_4^+	Li^+	Na^+	K^+	Mg^{2+}	Ca^{2+}	Sr^{2+}	Ba^{2+}	Al^{3+}	Zn^{2+}	Cu^{2+}	Fe^{2+}	Fe^{3+}	Pb^{2+}	Ag^+	Co^{2+}	Mn^{2+}	Hg^{2+}	Cd^{2+}
OH^-	S	S	S	S	N	N	S	S	N	N	N	N	N	N	-	N	N	-	N
F^-	S	S	S	S	N	N	N	N	N	S	S	S	-	S	S	S	S	N	S
Cl^-	S	S	S	S	S	S	S	S	S	S	S	S	S	N	N	S	S	N	S
Br^-	S	S	S	S	S	S	S	S	S	S	S	S	S	N	N	S	S	N	S
I^-	S	S	S	S	S	S	S	S	S	S	S	S	S	N	N	S	S	N	S
NO_3^-	S	S	S	S	S	S	S	S	S	S	S	S	S	S	S	S	S	S	S
S^{2-}	S	S	S	S	-	-	-	-	-	N	N	N	-	N	N	N	N	N	N
SO_4^{2-}	S	S	S	S	S	N	N	N	S	S	S	S	S	N	N	S	S	N	S
PO_4^{3-}	S	S	S	S	N	N	N	N	N	N	N	N	N	N	N	N	N	N	N
CO_3^{2-}	S	S	S	S	N	N	N	N	-	N	N	N	-	N	N	N	N	N	N
ace-tate	S	S	S	S	S	S	S	S	S	S	S	S	S	S	S	S	S	S	S

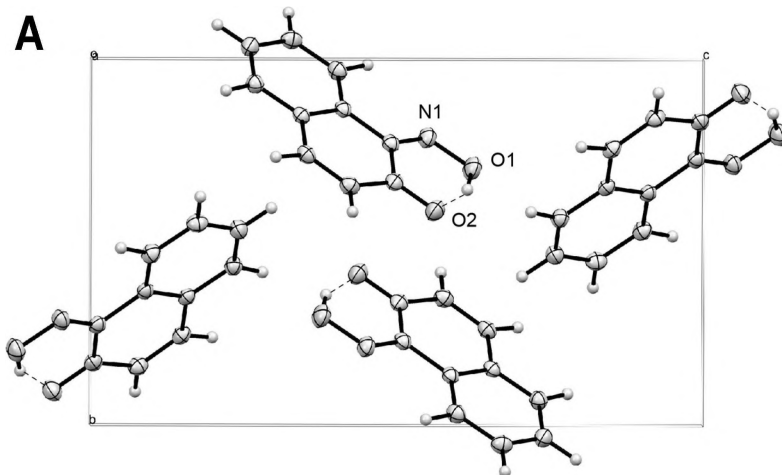**Meaning:**   **S** - soluble salt;   **N** - insoluble salt;   - does not exist in aqueous solutions

APPENDIX 3

CRYSTAL DATA AND STRUCTURES FOR ISOMERIC NITROSO-NAPHTOLS AND THEIR CO(III) COMPLEXES

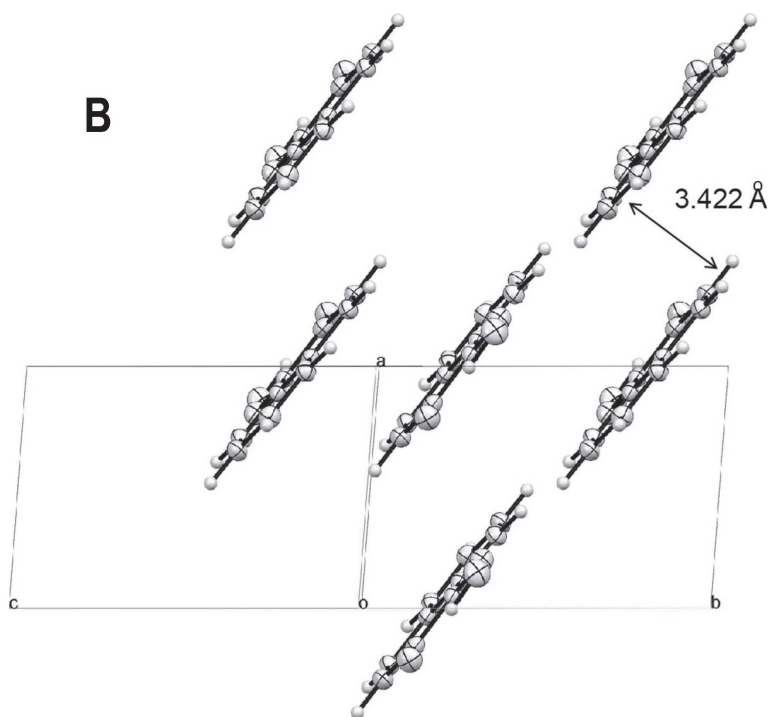**1-Nitroso-2-naphtol and its *fac*-Co(III) complex.**

Figure A3-1. The unit cells' content in the crystal structure of protonated free ligand – H(1NO-2OH). **A** – view along *a*-direction; **B** – view along [110] direction showing π–π stacking interactions between layers of compound.

Table A3-1.   Crystal data and structure refinement* for compounds in the 1-nitroso-2-naphtol system.

Parameter	H(1NO-1OH)[1]*	*fac*-Co(1NO-2OH)$_3$·DMSO[2]*
Empirical formula	$C_{10}H_7NO_2$	$C_{96}H_{72}Co_3N_9O_{24}S_3$
Formula weight	173.17	2008.60
Temperature	130(2)	120(2) K
Wavelength	0.71073 Å	0.71073 Å
Crystal system	Monoclinic	Rhombohedral
Space group	P 2$_1$/n	R-3
Unit cell dimensions	a = 5.4490(11) Å	a = 34.9521(18) Å
	b = 9.1287(18) Å	b = 34.9521(18) Å
	c = 15.462(3) Å	c = 13.0677(7) Å
	α= 90°	α= 90°
	β= 98.298(3)°	β = 90°
	γ= 90°	γ = 120°
Unit cell volume	761.1(3) Å^3	13825.3(12) Å^3
Z	4	6
Density (calculated)	1.511 Mg/m^3	1.447 Mg/m^3
Absorp. μ (mm^{-1})	0.107	0.683 mm^{-1}
F(000)	360	6192
Crystal size, mm	0.17·0.16·0.10	0.50·0.14 x 0.09
Reflections collected	9742	54207
Independent reflections	2044 [R(int)=0.04]	6281 [R(int)=0.059]
Structure solution	----- *Direct methods* ------	
Refinement method	---- *Full-matrix least-squares on F^2* ----	
Data/restraints/param.	2244 / 0 / 146	7558 / 6 / 388
Goodness-of-fit on F^2	1.054	1.043
Final R indices	R1=0.0452	R1=0.0789
R indices (all data)	R1=0.0783	R1=0.1090
Largest diff. peak/hole, e.Å^{-3}	0.327 / -0.211	2.426 / -2.137

* - crystal structures were submitted to the Cambridge Crystallographic Data Centre (CCDC);
[1]* - received CCDC # 917872; [2]* - received CCDC #917874
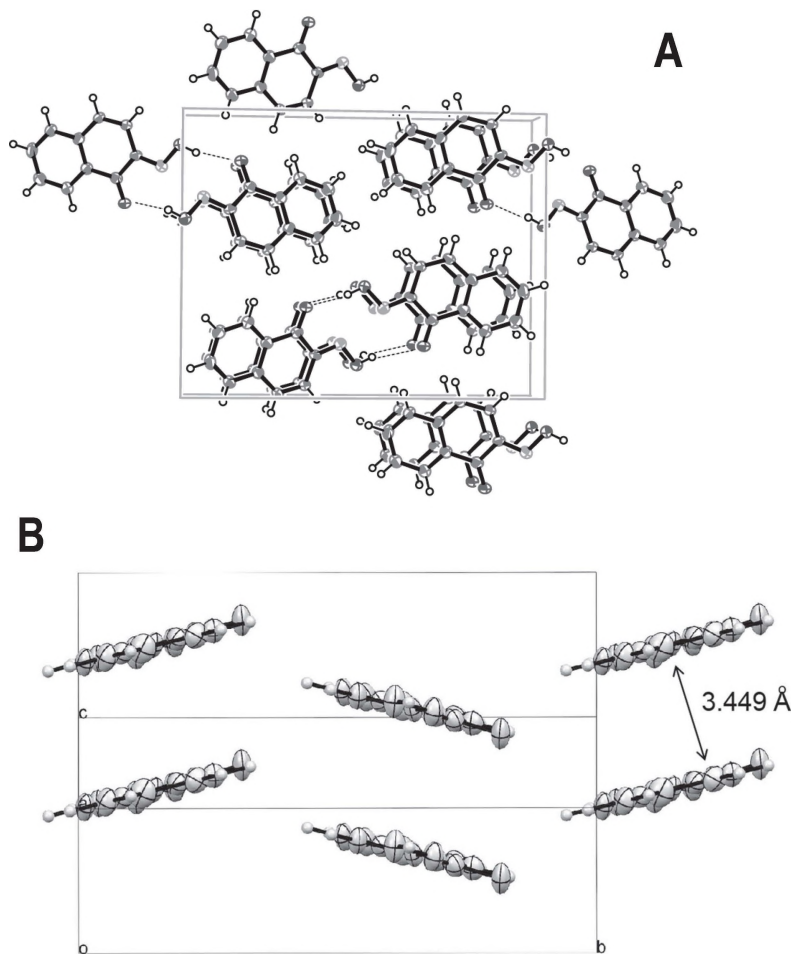
2-Nitroso-1-naphtol and its *mer*-Co(III) complex.

Figure A3-2. The unit cell content in the crystal structure of protonated free ligand – H(2NO-1OH). **A** – view along *a*-direction; **B** – perspective view showing π–π stacking interactions between layers of compound.

Table A3-2. Crystal data and structure refinement* for compounds in the 2-nitroso-1-naphtol system.

Parameter	H(2NO-1OH)[3*]	mer-Co(2NO-1OH)$_3$·CH$_2$Cl$_2$[4*]
Empirical formula	C$_{10}$H$_7$NO$_2$	C$_{31}$H$_{20}$Cl$_2$CoN$_3$O$_6$
Formula weight	173.17	660.33
Temperature, K	119(2)	120(2)
Wavelength	0.71073 Å	0.71073 Å
Crystal system	Orthorhombic	Monoclinic
Space group	P2$_1$2$_1$2$_1$	C2/c
Unit cell dimensions	a = 3.810(2) Å	a = 21.889(2) Å
	b = 12.743(8) Å	b = 21.094(2) Å
	c = 16.199(10) Å	c = 13.6387(14) Å
	α= 90°	α= 90°
	β= 90°	β= 119.6580(10)°
	γ= 90°	γ = 90°
Unit cell volume, Å^3	786.5(8)	5472.6(10)
Z	4	8
Density (calculated)	1.462 Mg/m^3	1.603 Mg/m^3
Absorp. μ (mm^{-1})	0.104	0.875
F(000)	360	2688
Crystal size, mm	0.10·0.05·0.05	0.10·0.06·0.04
Reflections collected	11129	34560
Independent reflections	2214 [R(int)=0.21]	6281 [R(int)=0.063]
Structure solution	----- Direct methods ------	
Refinement method	---- Full-matrix least-squares on F^2 ----	
Data/restraints/parameters	2214/0/119	6281/0/468
Goodness-of-fit on F^2	0.973	1.042
Final R indices	R1=0.0805	R1=0.0473
R indices (all data)	R1=0.2025	R1=0.0700
Largest diff. peak/hole, e.Å^{-3}	0.384/-0.378	0.793/-0.748

* - crystal structures were submitted to the Cambridge Crystallographic Data Centre (CCDC);
[3*] - received CCDC # 917873; [4*] - received CCDC #917875

APPENDIX 4

CRYSTAL DATA FOR POTASSIUM *TRIS*-OXALATO CR(III) COMPLEX

Table A4-1.   Crystal data and structure refinement* for Cr(III) complex.

Parameter	$K_3[Cr(C_2O_4)_3] \cdot 2H_2O \cdot CH_3OH$
Empirical formula	$C_7H_8CrK_3O_{15}$
Formula weight	501.43 g/mol
Temperature	120(2) K
Wavelength	0.71073 Å
Crystal system	Monoclinic
Space group	P 2_1/c
Unit cell dimensions	a = 7.6941(5) Å
	b = 19.6890(13) Å
	c = 10.2823(7) Å
	α = 90°
	β = 107.8260(10)°
	γ = 90°
Unit cell volume	1482.87(17) Å^3
Z	4
Density (calculated)	2.246 Mg/m^3
Absorp. μ (mm^{-1})	1.700
F(000)	1004
Crystal size, mm	0.240 x 0.262 x 0.394
Reflections collected	15015
Independent reflections	2598 [R(int) = 0.0227]
Structure solution	*Direct methods*
Refinement method	*Full-matrix least-squares on F^2*
Data / restraints / parameters	2598 / 5 / 248
Goodness-of-fit on F^2	1.072
Final R indices	R1 = 0.0455
R indices (all data)	R1 = 0.0476
Largest diff. peak/hole, e.Å^{-3}	1.446 / -1.241

* - crystal structure was submitted to the Cambridge Crystallographic Data Centre (CCDC) and received # 1839658

This book is designed to develop important practical skills for chemistry majors interested in synthetic chemistry. It will serve to teach students proper techniques for the preparation and handling of a variety of inorganic and coordination compounds. It shows them how to conduct thermal decomposition reactions; prepare moderately air-sensitive and moisture-sensitive compounds; and characterise obtained metal complexes using a variety of physical methods.

This volume is well-illustrated with colour photos, schemes and figures that allow safe, step-by-step work on assigned laboratory experiments. There are extensive pre-lab instructions for techniques, concepts and topics of experiments, and complete initial introductions to the methods used during the lab are also provided. Because of its clearly presented content with numerous practical examples, this book will be of great interest to chemistry professionals working in industry.

Nikolay Gerasimchuk obtained his first PhD in Inorganic Chemistry from Kiev State University, Ukraine, and his second in Bioinorganic Chemistry from the University of Kansas, USA. He is currently a Professor at Missouri State University, USA. His research interests are synthesis, spectroscopic characterization, and medical–biological applications of oxime-based ligands and their metal complexes. His publications include 118 papers, two book chapters, and two editorials in a special edition of *Current Inorganic Chemistry*.

Dr Sergiy Tyukhtenko is a Senior Research Scientist at the Center for Drug Discovery at Northeastern University, USA. He received his PhD in Physical Chemistry from National Taras Shevchenko University, Ukraine, in 1983. He is an expert in NMR spectroscopy applications for the structural elucidation of small molecules, peptides and proteins. His current research focuses on the structural biology and dynamics of endocannabinoid receptors, enzymes and transporters, with an emphasis on developing novel molecular probes and potential therapeutics.

9 781527 539204